

STRUCTURAL, BIOCHEMICAL AND PHYSIOLOGICAL ASPECTS
OF A SYSTEMIC VIRUS HOST INTERACTION

by

W.D. Boucher, B.Agr.Sc.(Hons.); Tas.

Submitted in partial fulfilment of the requirements
for the Degree of Doctor of Philosophy

University of Tasmania

Hobart

May, 1975.

This thesis contains no material which has been accepted for the award of any other degree or diploma in any University and to the best of my knowledge contains no copy or paraphrase of material previously published or written by any other person except where due reference is made in the text of the thesis.

W.D. Boucher

University of Tasmania,

Hobart.

May, 1975.

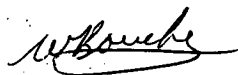
A handwritten signature in cursive script, appearing to read 'W.D. Boucher', with a horizontal line drawn underneath the name.

TABLE OF CONTENTS

	Page Number
<u>ACKNOWLEDGEMENTS</u> .. .	(i)
<u>SUMMARY</u> .. .	(ii)
<u>LITERATURE REVIEW</u>	
VIRUS-HOST BIOCHEMICAL INTERACTIONS.. .	1
A. ENZYMES AND SUBSTRATES OF CELLULAR METABOLISM. . .	1
1. Respiration Rates of Virus-Infected Tissues. . .	1
(a) Respiration rates following infection. . .	1
(b) Respiration rates in tissues systemically infected .. .	2
(c) Respiration rates of local necrotic lesion hosts .. .	4
2. Respiration Substrate Concentrations.. .	5
3. Carbohydrates. . .	5
4. Organic Acids. . .	7
5. Enzyme Systems Associated with "Dark" Respiration. . .	8
(a) Embden-Meyerhof-Parnas pathway and pentose phosphate pathway enzymes. . .	8
(b) Tricarboxylic acid cycle and enzymes associated with the mitochondrion. . .	10
6. Phosphorylated Compounds.. .	11
7. Host Nucleic Acid Synthesis.. .	13
8. Non-Protein Nitrogen .. .	15
9. Photosynthesis and other Functions Associated with Chloroplasts.. .	18
10. Enzymes of Photorespiration. . .	23
11. Polyphenol Oxidases and Peroxidases.. .	24
12. Acid Hydrolases. . .	27
13. Dehydrogenases and Miscellaneous Cellular Enzymes .. .	29
B. VIRUS-HOST HORMONAL INTERACTIONS.. .	30
1. Auxins.. .	31
2. Auxin-Scopoletin Interactions .. .	32
3. Gibberellins.. .	33
4. Cytokinins. . .	35
5. Abscissic Acid and other Growth Inhibiting Substances. . .	36
VIRUS-CELL ULTRASTRUCTURE INTERACTIONS.. .	37
1. Crystalline Inclusions. . .	38
2. X-Bodies .. .	39
3. The Nucleus .. .	42
4. Chloroplasts.. .	43
5. Mitochondria and other Cellular Components and Organelles	45
<u>GENERAL INTRODUCTION</u> .. .	47

SECTION I

VIRUS-HOST GROWTH AND PHYSIOLOGICAL INTERACTIONS

<u>INTRODUCTION</u> .. .	51
<u>MATERIALS AND METHODS</u> .. .	52
1. Virus concentration and tissue distribution in leaves showing well developed systemic symptoms .. .	52
(a) Virus concentration .. .	52
(b) Tissue distribution .. .	52
2. Trials to Determine the Effects of Virus Infection on Plant Growth .. .	53
(a) Plant height, internode length, leaf length, leaf number and root weight .. .	53
(b) Leaf growth during disease development .. .	54
3. Determination of Fresh Weight per Unit Leaf Area .. .	54
4. Estimation of Leaf Cell Numbers per Unit Leaf Area .. .	54
5. Leaf Tissue Preparation for Light Microscopy .. .	55
6. Trial to Determine the Effect of Virus Infection on Flowering Response .. .	55
<u>RESULTS AND OBSERVATIONS</u> .. .	57
1. Plant Size as Affected by Virus Infection .. .	57
2. Leaf Growth and Development Following Infection .. .	60
3. Effect of Infection on Leaf Cell Size .. .	64
4. Effect of Infection on Leaf Fresh Weight .. .	64
5. Leaf Tissue Age and Virus Concentration .. .	64
6. Virus distribution Within the Mosaic .. .	69
7. Observations on Flowering Response as Affected by Virus Infection .. .	69

SECTION II

VIRUS-HOST BIOCHEMICAL INTERACTIONS

A. ENZYMES AND REACTIONS OF CELLULAR METABOLISM

<u>INTRODUCTION</u> .. .	73
<u>MATERIALS AND METHODS</u> .. .	76
1. Crude Leaf-Tissue-Enzymes Preparation .. .	76
(a) Purification and Concentration by Acetone .. .	76
(b) Purification and Concentration by Dialysis .. .	77
2. Acrylamide Gel Electrophoresis .. .	77
3. Assays for Enzymes Separated by Electrophoresis .. .	80
(a) Acid phosphatase .. .	80
(b) Ribonuclease .. .	81
(c) α -amylase .. .	81
(d) Esterase .. .	81
(e) Leucine amino peptidase .. .	82
(f) Peroxidase .. .	82
(g) Catalase .. .	82

4. Direct Assays for Enzymes in Crude Tissue Extracts.	83
(a) Phosphoglucisomerase	83
(b) Glucose-6-phosphate dehydrogenase	83
(c) Alcohol dehydrogenase	84
(d) Cytochrome-C oxidase	84
(e) Glutamate dehydrogenase and NADH oxidase	85
(f) Ribulose 1,5-diphosphate carboxylase	86
5. Enzymes Assayed <u>In Situ</u>	87
(a) Nitrate reductase	87
6. Chlorophyll Determinations	87
<u>RESULTS</u>	89
1. Effect of Virus Infection on Enzymes of the Respiratory Chain and Mitochondria	89
(a) Cytochrome-C oxidase	89
(b) NADH oxidase	93
(c) Glutamate dehydrogenase	93
2. Effect of Infection on Enzymes Associated with Carbohydrate Metabolism	100
(a) Phosphoglucisomerase	100
(b) Glucose-6-phosphate dehydrogenase	100
(c) Alcohol dehydrogenase	104
3. Effect of Infection on the Photorespiratory Enzyme, Catalase	107
4. Peroxidase	107
5. Effect of Infection on the Host Photosynthetic Apparatus	111
(a) Ribulose 1,5-diphosphate carboxylase	111
(b) Chlorophyll "a"	111
(c) Chlorophyll a : chlorophyll b ratios	115
6. Effect of Infection on Nitrate Reductase Activity	117
7. Effect of Infection on the Acid Hydrolase Group of Enzymes	119
(a) Acid phosphatase	119
(b) Ribonuclease	122
(c) α -amylase	122
(d) Acid esterase	127
(e) Specific protease-leucine amino peptidase	127
B. ENDOGENOUS HOST HORMONES	
<u>INTRODUCTION</u>	130
<u>MATERIALS AND METHODS</u>	133
1. Extraction and Partial Purification of Endogenous Growth Regulators	133
(a) Gibberellic acid and abscisic acid	133
(b) Cytokinins	134
(c) Auxins	135
2. Separation of Growth Regulators by Thin Layer Chromatography	135
(a) Gibberellic acid and abscisic acid	135
(i) General conditions of chromatography	135
(ii) Chromatography of pure compounds and partially purified extracts	136

Table of Contents (cont.)

Page Number

(b) Cytokinins	137
(c) Auxins	137
3. Physiochemical Determinations of Growth Regulators	138
(a) Gibberellin A ₃	138
(b) Absciscic acid	138
(c) Indole acetic acid	138
4. Biochemical Assays of Growth Regulators	139
(a) Gibberellic acid	139
(i) Barley endosperm bioassay	139
(ii) Rumex leaf disc bioassay	140
(b) Absciscic acid	141
(c) Cytokinins	142
(i) Amaranthus-betacyanin production bioassay	142
(ii) Tobacco pith callus bioassay	143
(d) Auxins (Indole Acetic Acid)	144
<u>RESULTS</u>	146
1. Gibberellin A ₃ -like Activity in Extracts from Healthy and Virus-Infected Plant Tissues	148
(a) GA ₃ -like activity in extracts from young leaves and shoots	149
(b) GA ₃ -like activity in tissue extracts from mature leaves	149
2. ABA-like Activity in Mature Leaf Extracts from Healthy and Virus-Infected Plants	149
3. Cytokinin Activity in Extracts from Healthy and Virus- Infected Plant Tissues	157
(a) Cytokinin activity in young leaf and shoot extracts	158
(b) Cytokinin activity in mature leaf tissue extracts ..	162
(c) Cytokinin activity in root tissue extracts	165
4. The Effect of Virus Infection on the Concentration of an Indole Acetic Acid-like Component in Young Leaf and Shoot Tissue Extracts	170

SECTION III

VIRUS-HOST-CELL ULTRASTRUCTURAL INTERACTIONS

<u>INTRODUCTION</u>	174
<u>MATERIALS AND METHODS</u>	175
1. Tissue Preparation	175
(a) Araldite-embedded tissues	175
(b) Glycol methacrylate-embedded tissues	175
2. Sectioning and Post-Staining Techniques	176
<u>RESULTS AND OBSERVATIONS</u>	177
1. Chloroplast Structure and General Cellular Organization as a Function of Leaf Tissue Age	177
(a) Very young leaf tissues	177
(b) Immature leaf tissues	189

Table of Contents (cont.)	Page Number
(c) Mature leaf tissues.. .. .	196
(d) Senescing leaf tissues.. .. .	199
2. Some Miscellaneous Observations of Virus-Infected and Healthy Tobacco Leaf Cells.	202
<u>DISCUSSION</u>	205
<u>BIBLIOGRAPHY</u>	226
<u>APPENDICES</u>	

LIST OF PLATES

	Page Number
Plate 1 - Uninfected and TMV infected tobacco plants	58
Plate 2 - Mature leaves from uninfected and infected tobacco plants	62
Plate 3 - Mature leaves from uninfected and infected tobacco plants	62
Plate 4 - Young and immature leaves from uninfected and infected tobacco plants	63
Plate 5 - Section through leaf of uninfected tobacco plant	66
Plate 6 - Section through leaf of infected tobacco plant	66
Plate 7 - Section through border between light green island and dark green island tissue of infected tobacco leaf	66
Plate 8 - Apical meristem from virus infected tobacco plants, 12 weeks old	71
Plate 9 - Apical meristem from uninfected tobacco plant, 12 weeks old	71
Plate 10 - Apical meristem from an uninfected tobacco plant, 12 weeks old	71
Plate 11 - Uninfected tobacco plants, 15 weeks old	72
Plate 12 - Infected tobacco plants, 15 weeks old	72
Plate 13 - Electrophoresis power unit and buffer tank	78
Plate 14 - Electrophoresis gel mould	78
Plate 15 to 50 electronmicrographs of virus infected and uninfected tobacco leaf cells.	
Plate 15 - Virus infected leaf, 1 cm long	179
Plate 16 - Uninfected leaf, 1 cm long	180
Plate 17 - Young infected leaf, 2 cm long	181
Plate 18 - Virus inclusions in cells of young infected leaf, 2 cm long	182
Plate 19 - Plastids in virus-infected tobacco leaf cells, 2 cm long	183
Plate 20 - Epidermis of uninfected leaf, 2 cm long	183
Plate 21 - Cells of dark green island tissue in virus infected leaf, 2 cm long	184

List of Plates (cont.)

	Page Number
Plate 22 - Cells of uninfected leaf, 2 cm long	185
Plate 23 - Plastids in cells of uninfected leaf, 2 cm long	186
Plate 24 - Plastids in cells of infected tobacco leaf, 2 cm long	187
Plate 25 - Plastids in cells of uninfected tobacco leaf, 2 cm long	187
Plate 26 - X-body in cell of infected tobacco leaf, 2 cm long	188
Plate 27 - X-body in cell of tobacco leaf, 2 cm long	188
Plate 28 - Cells on the border between light green and dark green island of infected, immature leaf	190
Plate 29 - Cell wall boundary between cells of adjoining light green and dark green islands	191
Plate 30 - Plasmodesmata connections between cells of adjoining light green and dark green islands	191
Plate 31 - Cells of dark green island tissue of immature infected leaf	192
Plate 32 - Chloroplasts in cells of uninfected, immature leaf	193
Plate 33 - Chloroplasts in cells of uninfected, immature leaf	193
Plate 34 - Chloroplasts in cells of uninfected, immature leaf	194
Plate 35 - Chloroplasts in cells of dark green island tissue of infected, immature leaf	194
Plate 36 - Chloroplasts in cells of light green island tissue of infected, immature leaf	194
Plate 37 - X-body in cells of infected, immature leaf	195
Plate 38 - Cells of mature, virus-infected leaf	197
Plate 39 - Cells of mature, uninfected leaf	197
Plate 40 - Chloroplasts in cells of mature, virus-infected leaf	198
Plate 41 - Chloroplasts in cells of mature, uninfected leaf	198
Plate 42 - Chloroplasts in cells of senescing, virus-infected leaf	200

List of Plates (cont.)

	Page Number
Plate 43 - Chloroplasts in cells of senescing, virus-infected leaf	200
Plate 44 - Chloroplasts in cells of senescing, virus-infected leaf	201
Plate 45, Plate 46 - Chloroplasts in cells of senescing, uninfected leaf	201
Plate 47, Plate 48, Plate 49 - Single membrane-bound organelle containing crystalloid core	203
Plate 50 - Invagination in outer membrane of a chloroplast	204

ACKNOWLEDGEMENTS

I wish to express my gratitude to my supervisor, Professor G.C. Wade, Dean of the Faculty of Agricultural Science and Lecturer in Plant Pathology, for his guidance and constructive criticism throughout the course of this study.

I express my thanks to Professor K.C. Marshall, former Reader in Microbiology, for beneficial discussion and Dr. R.C. Menary, Senior Lecturer in Horticultural Science, for constructive criticism on the presentation of certain aspects of this study. I also wish to express my thanks to Mr. R. Cruickshank, Research Assistant to Professor G.C. Wade, for many relevant discussions on the content of this work and for technical advice and assistance.

Many other people contributed to the work of this thesis. In particular, I wish to thank Mr. R. Davies, former Electron Microscope Technician for the Department of Zoology and Mr. D. Munro, Plant Pathologist in the Tasmanian Department of Agriculture, for valuable technical assistance with respect to electron microscopy. I also wish to thank Mr. J. Groot, Glasshouse Technician, for his services in maintaining plants used during the course of this study and Mr. W. Peterson, Head of the Technical Staff, for his willingness to help at all times.

Finally, to my wife Robyn, I extend my special thanks for her support and assistance in the final presentation of this thesis.

SUMMARY

A susceptible tobacco variety infected with a mosaic-inducing strain of tobacco mosaic virus displayed certain alterations in normal growth patterns. This work confirmed that such plants, as a result of infection, were reduced in plant height, internode length and leaf size. Infected plants also had reduced root systems. The rate of leaf growth, that is the time taken for leaves to reach full expansion size, was similar for infected and virus-free plants although the number of leaves formed over a 6 week period following inoculation was slightly greater for virus-infected plants. Infection of young plants delayed both flower initiation and the appearance of inflorescences. A reduced rate of cell division in sub-apical regions appeared to be the major factor in reducing plant size.

The survival of plant supporting virus synthesis appeared to be related to certain metabolic changes. Specific enzymes associated with photorespiration and "dark" respiration had lower activities in virus-infected plants.

Enzymes indirectly associated with chloroplasts and photosynthetic pigments were also reduced in virus-containing tissues. To some extent, the reduced potential of carbon fixation by photosynthesis was offset by a reduced cellular demand from carbon utilized in photorespiration and "dark" respiration, this enabling cells to support a level of virus synthesis. Normal activity of an enzyme associated with the Embden-Meyerhof-Parnas pathway of carbohydrate metabolism higher activity of an enzyme associated with the pentose phosphate pathway and reduced activity of an enzyme associated with "dark" respiration suggested that most carbohydrates moving through the major pathways of metabolism are channelled towards virus synthesis through conversion to amino acids. The high activity of hydrolytic enzymes in virus-containing tissues suggested a high rate of metabolism of carbohydrates and nucleic acids that would be expected of cells supporting both virus synthesis and cellular metabolism.

Two features of virus infected plants ensure their survival: delayed onset of leaf senescence and the presence of virus-free tissues with leaf mosaics. Biochemical and ultrastructural studies revealed that over-mature leaves on virus-infected plants were metabolically active and composed of cells containing intact membrane systems. Most enzymes studied in similarly aged leaves from uninoculated plants had greatly reduced activities and cells in these tissues contained membrane components that showed signs of deterioration and disorganization. Virus-free areas of mosaic diseased leaves, referred to as dark green island tissues, were metabolically more active than comparably aged tissues from uninfected plants. Enzymes associated with photosynthesis and carbohydrate metabolism and photosynthetic pigments were at greatest levels in these tissues. Of the three tissue types compared, virus-containing and virus-free tissues from infected plants and leaf tissues from uninfected plants, dark green island tissues had the greatest potential for photosynthesis and carbohydrate metabolism.

Growth patterns of virus-infected plants, delayed flower initiation and onset of leaf senescence, the altered activities of enzymes associated with chloroplasts and carbohydrate metabolism and the stimulated activities of enzymes in dark green island tissues suggested that basic responses of plants to infection occurred through shifts in endogenous growth regulator levels. Bioassays of the major growth regulators revealed that although a gibberellin A₃-like compound was unaffected by infection, cytokinin-like compounds and an indole acetic acid-like compound were at higher levels in infected tissues and an abscisic acid-like compound was at a reduced level. The altered balance of the major growth stimulating and growth retarding hormones is sufficient to account for most of the measured and observed changes in diseased plants.

L I T E R A T U R E R E V I E W

VIRUS-HOST BIOCHEMICAL INTERACTIONS

Plants systemically infected with viruses generally undergo changes in pigment production, growth development or both. In some cases virus infections are lethal. It is well documented that infections of host plants with viruses produce disturbances in host-plant metabolism. However the nature of such disturbances is almost as varied as the number of virus/host plant combinations reported in the literature. Some attempts have been made to correlate symptom expression with disturbances to various metabolites, cellular enzyme activities, host physiological changes and the reflected morphological changes. The major problem associated with a review of this nature is that most reports in the literature concerning measurements on cellular biochemical functions have tried to relate concentrations of various metabolites or enzyme activities to host tissue resistance or susceptibility to infection.

The purpose of this review is to attempt to express the findings of these various reports in terms of host response to infection.

A. ENZYMES AND SUBSTRATES OF CELLULAR METABOLISM

1. The Respiration of Tissues Infected by Virus

Porter (1959) concluded that different viruses have different effects on respiration and that effects on respiration can vary between different hosts infected with the same virus. The physiological state of the tissue involved is so important that it requires a very strict definition of experimental conditions when evaluating the findings of such studies. However, provided some differentiation is made with respect to age of infection and type, some broad generalizations can be reached.

(a) Respiration rates following infection

For most host-plant-virus combinations resulting in a systemic infection, either unaltered respiration rate or an increase in respiration rate occurs over the period from inoculation to symptom appearance. A decrease in respiration over this period has not been observed from the literature.

Increased respiration rate occurs for inoculated tobacco leaves for three weeks following inoculation, whereas young leaves present at the time of inoculation showed no increase (Owen, 1956). Initial increases in respiration rate, following infection of tobacco epidermis with tobacco mosaic virus, have been reported by Yamaguchi and Takahashi (1964) and Takahashi and Hirai (1964). Burroughs, Goss and Sill (1966) measured increased respiration for barley following infection with brome-grass mosaic virus. They also reported a similar increase in respiration rate for mature barley leaves, seven days after infection with barley yellow dwarf virus. However, Jensen (1968) showed that respiration, of leaves not fully mature at the time of infection, was unaltered.

(b) Respiration rate of tissues systemically infected by virus

Many researchers have reported divergent and apparently contradictory results on this type of infection. Merrett and Bayley (1969) suggested that the greatest reason for this variation was the nature of expression of results, that is, whether final respiration rates were expressed on a dry or fresh weight basis or on protein-nitrogen, carbohydrate content or some other parameter. All of the preceding parameters can be secondarily changed as a result of infection. Owen (1955b) pointed out that infection could alter water content, dry-matter content and growth rate of infected leaves. The effect of virus on respiration would therefore depend on the basis used to express results.

There have been several reports of increased respiration of tissues systemically infected with virus. Borges (1953, as cited by Porter, 1959) reported increased respiration rate of Brassica chinensis infected with turnip yellow mosaic virus. Tobacco etch virus infection of tobacco caused a stimulation in respiration rate, which was maintained throughout the life of the plant (Owen, 1957). Both potato virus X and tobacco mosaic virus infection of N. glutinosa, increased rate of respiration by as much as thirty percent, once symptoms had appeared (Owen, 1958). Brome-grass mosaic virus infection of barley plants also resulted in increased respiration

(Burrough, Goss and Sill, 1966).

Unchanged respiration rates have been recorded for leaves and roots of cucumber infected with cucumber mosaic virus (Rubin and Zeleneva, 1964) and for barley leaves formed after infection of plants with barley yellow dwarf virus (Jensen, 1968).

For some virus/host combinations the initial increase in respiration, following inoculation, declined with time after infection. With maize dwarf mosaic virus on maize Tu and Ford (1968) found that respiration rate increased by 6% six days after inoculation. After nine days, the rate was 32% higher. At day eighteen the rate had declined but still remained higher compared with healthy tissue. However, the authors pointed out that much of the respiration increase was due to mechanical damage caused at the time of inoculation. A similar increase in respiration, followed by a decline was reported for N. rustica L. infected with alfalfa mosaic virus (Verhoyen, 1966; as cited by Merrett and Bayley, 1969).

In some cases, the decline in respiration rate with age of infection has proceeded until respiration rate had fallen to below that of comparable healthy tissues (Owen, 1956; Takahashi and Hirai, 1964). Although respiration rate of barley yellow dwarf virus-infected barley plants increased, following inoculation, it subsequently declined and from thirty five to sixty nine days after infection it was below that for comparable healthy tissues (Orlob and Army, 1961). Respiration rates of virus-infected tissues that are below rates for comparable healthy tissues have been recorded for young tobacco leaves that were formed after infection by tobacco mosaic virus and were showing systemic symptoms (Owen, 1955b; Owen, 1956). Respiration rate was lower in tomato stem tissue infected with tomato aucuba mosaic virus (Merrett, 1960).

Where respiration rate has been determined as carbon dioxide evolution it should be realized that such reports are a measure of both dark respiration and photosynthetic respiration. When respiration has been measured as oxygen uptake, only dark respiration has been measured. As the two

types of respiration could be affected differently by infection, the way in which respiration has been measured could also be a factor contributing to the conflicting reports concerning the effect of virus infection on respiration rate of tissues systemically infected by virus.

(c) Respiration rates of local necrotic lesion hosts

The investigation of several host-plant/virus combinations that resulted in local lesion formation has shown that at some stage in lesion development there is an enhancement of host-plant respiration (Merrett and Bayley, 1969). Increased oxygen consumption in leaves of Nicotiana sylvestris L. occurred following inoculation with tobacco mosaic virus (Parish, Zaitlin and Siegel, 1965). Similar increases in oxygen uptake, following tobacco mosaic infection have been recorded for the host plants N. glutinosa L. (Yamaguchi and Hirai, 1959), and N. tabacum L. Xanthi (Sunderland and Merrett, 1965). Increases in respiration rate have also been reported for Phaseolus vulgaris L. infected with southern bean mosaic virus (Chant, 1967) and for potato virus X-infected N. tabacum L. cv. White Burley (Owen, 1958). The rise in respiration appears to be more related to the development of disease symptoms than to an increase in virus concentration (Merrett and Bayley, 1969). This has been most conclusively demonstrated with those virus/host combinations where, under certain conditions, the combination does not produce a necrotic lesion. Under these circumstances the respiratory increase is small (Sunderland and Merrett, 1965; Parish, Zaitlin and Siegel, 1965). It has been suggested that the increased respiration rates of infected tissues was due to increased numbers of mitochondria (Weintraub, Ragetli and Dwurazna, 1964). However, more recent work by Pierpont (1968) failed to confirm this report.

A recent report by Simons and Ross (1971) suggests that respiratory increases following inoculation are not permanent. Tobacco mosaic virus infection, of the tobacco variety Samsun NN, resulted in increases in oxygen uptake and increased activity of several enzymes involved in

respiration. However, with older infections these increases and activities declined.

2. Respiration Substrate Concentration in Virus-Infected Tissues

Whitehead (1934) suggested that the higher respiration rate of potatoes, infected with potato leaf roll virus, was related to the amount of available substrate. He pointed out that the accumulation of starch in leaves of diseased plants occurred at a very early stage of development. Such accumulations could be delayed by exposing plants to continuous light of low intensity. Under these conditions the respiration of diseased tissues approximated to that of healthy ones.

Much work has been published since then concerning substrates which can be utilized in respiration for the ultimate release of carbon dioxide. As pointed out by Merrett and Bayley (1969) a major problem in correlating substrate concentration with respiration rate is determining which of the number of compounds present in the plant is providing the carbon ultimately released as carbon dioxide. Most polysaccharide reserves can be broken down to their constituent sugars which in turn can be converted to carbon dioxide via the Embden-Meyerhof-Parnas pathway, or the pentose, monophosphate shunt pathway, followed by the tricarboxylic acid cycle. Information on the concentration of intermediates in these pathways, particularly the sugar phosphates, would provide useful information. However, Merrett and Bayley (1969) pointed out that determinations of sugar phosphates, in plant tissues, is difficult because of their low concentrations. Proteins can be broken down to their constituent amino acids and their carbon skeletons released as carbon dioxide following deamination or transamination. Fats can ultimately be broken down to acetyl co-enzyme A which in turn can be fed into the tricarboxylic acid cycle.

3. Carbohydrates

In considering the effects that carbohydrates may have on respiration two other factors are important as they affect the concentration of

carbohydrates in the cell. Photosynthetic rate and translocation have a direct effect on carbohydrate concentration and both rates may be affected by virus infection (Merrett and Bayley, 1969).

Bowden (1964) observed that, with yellows diseases of plants, the carbohydrate/nitrogen ratio increased, whereas mosaic diseases often decreased the ratio. Whitehead (1934) reported increased starch in leaves of potato infected with potato leaf roll virus. A similar increase in carbohydrates was reported for sugar beet leaves infected with beet yellows virus (Watson and Watson, 1951). In barley, leaves infected with barley yellow dwarf virus, accumulation of starch and soluble carbohydrates, especially reducing sugars, occurs. Soluble carbohydrates were reduced in the roots of infected plants (Orlob and Arny, 1961). Diseases of the yellows type affect mostly the phloem of the host (Esau, 1967). It has been suggested that for these diseases, a virus-induced stimulation of respiration could be maintained in the leaf because of increased availability of substrate (Merrett and Bayley, 1969).

Wynd (1943) reported a decrease in carbohydrates for plants infected with mosaic virus diseases. However, he concluded that no definite conclusions could be reached concerning the general behaviour of the total carbohydrate fraction of plants to virus infections. Matthews (1973) concluded that turnip yellow mosaic virus infection of Chinese cabbage reduced sugars by diverting carbon fixed in the Calvin cycle from sugars to organic acids. Increased rate of carboxylation of phosphoenol pyruvate to form oxalacetate, resulted in higher levels of malate and aspartate being formed.

For local-lesion type infections, viruses have been reported to decrease both the synthesis and translocation of starch in the region of the lesion. During active photosynthesis the starch content was less compared with neighbouring non-infected tissues, while after a period of darkness, the starch content was greater (Diener, 1963). However, Weintraub and

Ragetli (1964) reported no differences in reducing sugars and sucrose in N. glutinosa L. plants infected with tobacco mosaic virus.

There are few reports concerning the effect of virus infection on pentose sugars. Dunlap (1931) found that healthy tobacco leaves contained 0.27% pentoses (expressed on a leaf fresh weight basis) while infected leaves contained 0.21%. Pentoses were reported to accumulate in areas surrounding local necrotic lesions caused by tobacco mosaic virus on tobacco (Farkas and Solymosy, 1962).

4. Organic Acids

The oxidation of organic acids in the tricarboxylic acid cycle and the associated coupling of this cycle to respiratory chain phosphorylation provides the main source of ATP for plants in the dark. Organic acids also provide carbon skeletons for amino acids.

Increases in organic acids following virus infection have been reported. Porter and Weinstein (1957) found more malic and citric acid in tobacco leaves seven days after inoculation by cucumber mosaic virus. This increase appeared to be correlated with a virus-induced stimulation of growth. When plants were exposed to $^{14}\text{CO}_2$ following inoculation, less isotope was incorporated into malic acid and about the same amount into citric acid compared with healthy leaves (Porter, 1959). For Physalis floridana, N. tabacum L. cv. White Burley and Lycopersicon esculentum systemically infected with potato virus X, potato virus Y and tobacco mosaic virus, increases in leaf oxalate, malate and citrate occurred (Venekamp, 1959). Similarly, Schuster (1964, as cited by Merrett and Bayley, 1969) reported increases in succinic, malic and citric acids in Nicotinia species infected with tobacco mosaic virus and Hyocyanus species infected with potato virus X.

Some reports suggest that virus multiplication is stimulated by organic acids. Tobacco mosaic virus multiplication increased in tobacco leaf discs floated on distilled water plus one of the organic acids, citrate, α -ketoglutarate, succinate or malate (Nour-Eldrin, 1955). Wiltshire

(1956a) found that the susceptibility of French beans to tobacco necrosis virus increased when the plants were kept in the dark. Dark treatment decreased the content of malic, fumaric, succinic and glycolic acids and increased citric acid without affecting oxalic and malonic acids. None of these acids had much effect on virus synthesis when infiltrated into leaves. Dark treatment of leaves of French bean and tobacco increased their susceptibility to tobacco necrosis virus and tomato aucuba mosaic virus respectively, but decreased the level of ascorbic acid. However, infiltration of leaves with ascorbic acid also increased their susceptibility to these viruses (Wiltshire, 1956b). Schlegel (1957, as cited by Porter, 1959) found that tobacco mosaic virus concentration increased 50% in tobacco leaf discs floated on solutions of organic acids. The effectiveness of organic acids was dependent on adequate nitrogen fertilization of plants prior to inoculation. It was not known whether the organic acids were effective indirectly as energy sources or directly as precursors in virus synthesis.

5. Enzyme Systems Associated with "Dark" Respiration

(a) Embden-Meyerhof-Parnas pathway and pentose phosphate pathway enzymes

Generally little change has been reported for the activities of enzymes of glycolysis, following virus infection. Boser (1958) looked at potato leaves and tubers systemically infected with potato leaf roll, streak virus, or mosaic virus and found that streak virus had no effect on phosphoglucumutase, hexokinase and enolase activities. Leaf roll and mosaic viruses caused slight increases in activity of hexokinase in tubers, and enolase in leaf tissues. The activities of phosphoglucumutase and enolase were reduced in leaf roll infected tubers.

In leaves of N. tabacum L. cv. White Burley locally infected with tobacco mosaic virus, the areas immediately surrounding lesions showed increased glucose-6-phosphate dehydrogenase and 6-phosphogluconate dehydrogenase activities. No change in activities occurred for phosphohexoisomerase, pentose phosphate isomerase and malic dehydrogenase. Pentose sugars

accumulated in these tissues and ribulose-5-phosphate, when added was only slowly metabolised. It was suggested that the later stages of the pentose phosphate pathway could not cope with strongly activated early stages (Farkas and Solymosy, 1962). For potato leaves systemically infected with potato leaf roll virus, decreased activity of glucose-6-phosphate dehydrogenase was found to occur (Boser, 1959). Takahashi (1971) found that in tobacco leaf epidermis, systemically infected with tobacco mosaic virus, the activities of glucose-6-phosphate dehydrogenase and 6-phosphogluconate dehydrogenase were unaltered. Reddy and Stahmann (1970) reported new isoenzymes for glucose-6-phosphate dehydrogenase in plants infected with pea wilt virus. No quantitative or qualitative changes in 6-phosphogluconate dehydrogenase were observed.

Some attention has been given to the relative roles of the Embden-Meyerhof-Parnas pathway and the pentose phosphate pathway in tissues infected with virus. Solymosy and Farkas (1963) reported that while key enzymes of the pentose phosphate pathway (G-6-P dehydrogenase, 6-phosphogluconate dehydrogenase) increased in activities, enzymes of the glycolytic pathway (hexokinase, glucose phosphate isomerase) showed unaltered activities in local-lesion hosts. The greatest increase in pentose phosphate pathway enzymes appeared to occur in tissues surrounding lesions.

Bell (1964) found that when lesions appeared on bean plants inoculated with southern bean mosaic virus, the C6/C1 ratio (ratio of sugars of the Embden-Meyerhof-Parnas pathway to sugars of the pentose phosphate pathway) decreased sharply, suggesting that more glucose was being metabolised via the pentose phosphate pathway. However, although Merrett and Sunderland (1967) reported increased release of $^{14}\text{CO}_2$ from glucose-6- ^{14}C and glucose-1- ^{14}C for a local-lesion tobacco host infected with tobacco mosaic virus, there was no change in the ratio C6/C1, with virus infection.

For systemic virus infections, Tien and Tang (1963, as cited by Merrett and Bayley, 1969) measured a decrease in the C6/C1 ratio during

the period of maximum virus increase for tobacco leaves infected with tobacco mosaic virus. Bell (1964), on the other hand, found that the C6/C1 ratio increased when beans were systemically invaded with southern bean mosaic virus. No change in the C6/C1 pathway ratio was reported by Baur et al. (1967), for the systemic infection of tobacco by tobacco mosaic virus. They found that approximately 80% of respiration was mediated via the Embden-Meyerhof-Parnas pathway and 20% via the pentose phosphate pathway. Merrett and Bayley (1969) concluded that sufficient evidence did not exist to support the hypothesis that there was a shift in respiratory metabolism from the Embden-Meyerhof-Parnas pathway to the pentose phosphate pathway.

(b) Tricarboxylic acid cycle and enzymes associated with the mitochondrion

Isolated mitochondria are capable of carrying out all the reactions of the tricarboxylic acid cycle. However, counterparts of several of the mitochondrial enzymes are present in the soluble fraction of the plant cell. Merrett and Bayley (1969) pointed out that in general the levels of a number of mitochondrial enzymes and carriers, such as cytochromes, succinate dehydrogenase, malate dehydrogenase, appeared to be present in constant relative proportions in mitochondria from widely different sources. They suggested that a virus-induced change in the total amount of one of the enzymes could result in a change in the amount of other enzymes, if the constant relative proportions of the enzymes was to be maintained.

Takahashi and Hirai (1966) pointed out that, although chloroplasts were the major site of ATP generation and amino acid synthesis in green leaves, mitochondria were also capable of amino acid synthesis and incorporation into proteins. In fact, in those tissues devoid of chloroplasts, mitochondria were the major source of amino acid synthesis.

There are conflicting reports concerning the effects of virus infection on the mitochondrial system. Contrary to some infections by obligate

fungal parasites, the tricarboxylic acid cycle appears to be operative in virus-infected tissues. Respiratory inhibitors which blocked the operation of this cycle suppressed synthesis of tobacco mosaic virus (Ryzhkov, 1957, as cited by Diener, 1963). Takahashi and Hirai (1966) reported that mitochondria of infected plants gave increased uptake of ^{14}C -leucine. The authors suggested that amino acid uptake represented increased protein synthesis by the mitochondria, although it was not known whether this increased protein was a bound, fixed mitochondrial type or a soluble type. No changes in mitochondrial protein-nitrogen were reported for N. glutinosa plants infected with tobacco mosaic virus (Pierpont, 1968). However, Nambier and Ramakrishnan (1970) found increases in mitochondrial-nitrogen and succinic oxidase activity for *Capsicum* and *Cucurbita* infected with tobacco mosaic virus and cucumber mosaic virus.

Martin (1958, as cited by Diener, 1963) observed an increase in cytochrome-oxidase in tobacco mosaic virus-infected tobacco leaves. Rubin and Ladygina (1972) found that for tobacco plants systemically infected with tobacco mosaic virus, cytochrome-C-oxidase activity decreased 24 hours after infection. For the local-lesion host N. glutinosa, cytochrome-C oxidase and succinic oxidase increased following inoculation. Pierpont (1968) on the other hand reported a slight decrease in cytochrome oxidase activity for N. glutinosa infected with tobacco mosaic virus.

6. Phosphorylated Compounds

Phosphorylated nucleotides provide the energy necessary for most cellular functions. In addition they constitute a nucleotide pool on which nucleic acid synthesis is dependent.

For virus-host interactions of the local-lesion type, an increase in ATP levels seems characteristic. Increased ATP following tobacco mosaic virus infection of resistant tobacco varieties has been reported by Sunderland and Merrett (1964; 1965 and 1967) and for tobacco etch virus infection of tobacco by Bayley and Merrett (1969). A decrease in levels

of ADP appeared to occur with increased levels of ATP (Sunderland and Merrett, 1967). Local lesion hosts treated with the oxidative phosphorylation uncoupler, 2,4-dinitrophenol (DNP), which increased respiration rate of uninfected tissues, characteristically showed no further increase in respiration rate following infection (Sunderland and Merrett, 1967). These authors suggested that virus infection brought about an uncoupling of respiration from oxidative phosphorylation, as reflected by a decreased ADP/ATP ratio. Merrett and Bayley (1969) proposed that in local lesion reactions, high respiration rate could be due to either ADP availability not being limiting or respiration proceeding without oxidative phosphorylation. Certain pathogenic fungi have been shown to produce toxins that have a similar uncoupling effect on respiration to DNP (Krupa, 1959). However, as Merrett and Bayley (1969) pointed out, no such uncoupling agents have been demonstrated in virus-infected tissues. It has been suggested that ATP concentration plays a role in viral resistance for local-lesion hosts. Bayley and Merrett (1969), in an investigation of the effects of tobacco etch virus on tobacco, found that addition of adenine increased the level of ATP in healthy tissues and increased tissue resistance to virus infection. No increase in respiration rate occurred following adenine treatment. Also, high ATP levels and viral resistance were characteristic of tissues surrounding local lesions. Rubin and Ladygina (1972) postulated that in resistant tobacco varieties, such as N. glutinosa, a maintenance or activation of energy conversion processes of mitochondria are characteristic, being associated with increased mitochondrial ATP content and a maintenance of inorganic-phosphorous uptake, 24 hours after infection. The chloroplasts in such diseases also displayed enhanced phosphorylation, ATP content and light-induced ATPase activity.

Both increases and decreases in ATP levels have been reported for tissues systemically infected with virus. Porter and Weinstein (1957, as cited by Porter, 1959) reported decreased levels of non-nucleic acid

organic phosphorous in tobacco leaves, 7 days following inoculation with cucumber mosaic virus. Decreases in ADP and ATP levels were also reported in tobacco callus cultures systemically infected with tobacco mosaic virus (Sunderland and Merrett, 1963b). Bozarth and Browning (1970) studied the diurnal fluctuations of the nucleotide pool of virus-infected and healthy bean leaves. The concentration of ATP varied in a similar manner for both infected and healthy tissues, with the lowest quantities occurring during the light and highest quantities during the dark periods. A higher concentration was found in diseased tissues at all times of sampling, 5 days after inoculation. No consistent differences were found in the nucleotide pool or phosphorylated nucleotides of guanosine, uridine, cytidine, AMP and ADP. Unlike local-lesion tissues, DNP has been shown to stimulate respiration in both healthy and systemically infected tobacco tissues (Takahashi and Hirai, 1965).

7. Host Nucleic Acid Synthesis

Most studies on host nucleic acid synthesis in virus-infected tissues have been concerned with changes that occurred immediately following inoculation. The earlier reports gave details on total extractable nucleic acids, which usually included viral nucleic acid. Consequently, increases in total nucleic acids were often reported. Both ribose nucleic acid and deoxyribosenucleic acid-phosphorous increased in tobacco leaves infected with cucumber mosaic virus (Porter and Weinstein, 1957, as cited by Diener, 1963). A similar increase in nucleic acid-phosphorous for tobacco mosaic virus-infected tobaccos was reported by Elbertzhagen (1958). Basler and Commoner (1956) divided the nucleic acids, extracted from TMV-infected tobaccos into buffer soluble and buffer insoluble at pH 7.0. Only the insoluble fraction was reported to be affected by infection. It was found that, prior to the appearance of detectable virus, the level of insoluble nucleic acids increased above that of healthy controls. The level declined during the period of maximum virus synthesis and finally established

at a level comparable with healthy tissues.

More recent reports suggest that the nucleic acid fractions most affected by systemic infections are associated with the chloroplasts. A decrease in this fraction has been widely reported. Mohamed and Randles (1971) investigated the effects of tomato spotted wilt virus infection on the chloroplast ribosomal nucleic acids (rRNA) of tobacco leaves. It was found that infection led to a reduction in chloroplast (70S) ribosomes. However, chloroplast rRNA still incorporated ^{32}P -orthophosphate while their concentration declined. Incorporation of radioactive label ceased 2 days after infection. It was concluded that for this virus and lettuce necrotic yellows virus infections some 70S degradation of 70S ribosomal RNA occurred. On the other hand, 12 hours after the appearance of TMV symptoms chloroplast ribosomes ceased to incorporate label. Although only small net losses of 70S rRNA occurred, synthesis of 70S rRNA was inhibited.

Hirai and Wildman (1969) showed that isolated chloroplasts, from TMV-infected tobaccos, had a reduced capacity for the incorporation of nucleoside triphosphates into RNA. They concluded that during the period of maximum virus synthesis, chloroplast rRNA and messenger RNA (mRNA) production from chloroplast DNA ceased. Oxfelt (1971) studied the effects of 2 strains of tobacco mosaic virus on the RNA type content of tobacco leaves. Both strains were reported to strongly inhibit chloroplast rRNA synthesis although inhibition was more complete in flavum-infected than in vulgare-infected leaves. Substantial degradation of chloroplast rRNA was shown to occur as a result of infection, with the amount of RNA degraded greatly exceeding the total amount of viral RNA synthesised. Cytoplasmic rRNA was not affected by infection, but the content of transfer RNA (tRNA) was slightly reduced.

Fraser (1971) concluded that the effects of tobacco mosaic virus infection on the RNA's of tobacco leaves, immediately following infection, depended on the age of the tissue when infection occurred. In young

leaves, virus reduced host RNA synthesis competition and in older leaves maintained RNA synthesis, which was necessary for viral protein synthesis. It was found, that once leaves had reached about $\frac{1}{3}$ of their final length, most parameters of growth were resistant to TMV infection, especially cytoplasmic rRNA and tRNA accumulations. Chloroplast rRNA was the only type to show a reduction with infection. There was some evidence that cytoplasmic rRNA was actually higher in older leaves following infection but this was thought to be due to an inhibiting effect on rRNA breakdown rather than a stimulating effect on synthesis.

In contrast to the above reports, Kato and Misawa (1971) suggested that cucumber mosaic virus infection of tobacco leaves suppressed nuclear DNA-dependent RNA synthesis in affected cells. It was found that cellular ribonucleic acid synthesis ceased following inoculation. They did not differentiate between cytoplasmic and organelle ribonucleic acids.

Few reports have appeared concerning types of nucleic acids other than ribosomal nucleic acids. Johnson and Young (1969) analysed for transfer RNA's (tRNA) in tobacco leaves, systemically infected with tobacco mosaic virus, for periods of up to 9 days following inoculation. In mature tissues, infection decreased the total tRNA level, while in young tissues no change in the total amount of tRNA was found. The only tRNA species to show a change in elution profile, following infection, was that for phenylalanine, in young tissues. However, with increasing time after inoculation, the elution profile for this tRNA tended to that which was typical for healthy tissue.

8. Non-Protein Nitrogen

There have been many reports concerning changes in non-protein nitrogen following virus infections. Most reports relate to changes in free amino acids and amides, which together with ammonia, are important constituents of the soluble nitrogen pool of the plant. Concentrations in this pool could affect protein synthesis and respiration rate.

Both increases and decreases in a range of nitrogenous compounds have been reported for a number of host-virus combinations. Andreae and Thompson (1950) demonstrated greatly reduced levels of tryptophane and tyrosine in leaf roll-infected potato tubers. Allison (1953) on the other hand suggested that the only consistent differences for a number of potato varieties infected with leaf roll, were increases in glutamine and glutamic acid. Results for tyrosine and tryptophane varied between potato varieties. Accumulation of pipercolic acid appeared to be a characteristic of Western-X diseased peach leaves (Diener and Dekker, 1954). Increases in free amino acids and amides, following infection, have been reported by Bozarth and Diener (1963) for *N. tabacum* systemically infected with either potato virus X, potato virus Y, or a combination of both. Studies on free amino acids and amides of intact tobacco plants after inoculation with tobacco mosaic virus, revealed net increases in serine, glutamine and asparagine, maximum concentrations being reached 48-120 hours after infection (Porter, 1959). Harpaz and Applebaun (1961) found increases in asparagine in maize seedlings infected with maize dwarf mosaic virus. Increases in asparagine and glutamine were also reported, for the first foliage leaves of tomato infected with tomato spotted wilt virus (Selman *et al.*, 1961). Higher levels of glutamic acid, glutamine and asparagine occurred in *N. glutinosa* one to two days after symptoms of lettuce necrotic yellows appeared (Randles, 1971). Decreases in ammonia, free amino acids and amides, during the period of tobacco mosaic virus synthesis, were reported by Commoner and Dietz (1952). This report was confirmed by Commoner and Nehari (1953) who described deficiencies in glutamine, glutamic acid, aspartic acid, asparagine and serine following infection with tobacco mosaic virus.

Many factors have been shown to influence the levels of nitrogenous compounds extractable from diseased tissues. Some of these modifying factors may account for the lack of consistency in results which have

appeared in the literature. The nitrogen status of plants prior to infection may have an important effect on whether virus synthesis occurs at the expense of host protein synthesis or concomitantly with it. Commoner and Nehari (1953) and Commoner et al. (1953) concluded that most nitrogen for tobacco mosaic virus synthesis comes from free ammonia within the cell and that changes in non-protein nitrogen, such as amides and amino acids, reflected the withdrawal of ammonia for tobacco mosaic virus synthesis. This further substantiated an earlier report by Wildman et al. (1949) who concluded from electrophoretic studies, that TMV was synthesised at the direct expense of a normal protein fraction. On the other hand, Holden and Tracey (1948) have shown that for well fertilized tobacco plants, the total nitrogen content of TMV-infected plants was higher than that of healthy plants. Non-protein nitrogen content has been shown to vary with the age of infection. Elbertzhagen (1958) found deficiencies of total-nitrogen and alcohol-soluble-nitrogen in TMV-infected and potato virus X-infected tobacco leaves during the early stages of infection. However, at later stages of infection total-nitrogen, protein-nitrogen and alcohol-soluble-nitrogen were higher in infected leaves. For tobacco plants infected with potato virus X, the concentrations of free amino acids and amides were lower at the time of rapid systemic spread of the virus. In symptomless leaves and leaves with older infections, these pools were higher than in comparable healthy leaves (Miczynski, 1961). Karaseck (1963) has shown that for tobacco systemically infected with tobacco mosaic virus, increases in free amino acids and amides occur immediately following inoculation, followed by decreases after 216 hours from inoculation.

The effect of virus infection on the measured levels of nitrogenous pools in the host can vary with the tissue type determined. In virus diseases of the yellows type, infection induced opposite effects on levels of nitrogenous compounds in roots and leaves. Sugar beet plants infected with beet yellows virus had lower levels of total-N, protein-N and

insoluble-N in leaves compared with healthy plant leaves. Infected *roots* on the other hand had higher levels of all classes of nitrogenous compounds, especially soluble-N (Diener, 1963). Orlob and Army (1961) reported similar findings for plants infected with barley yellow dwarf virus.

The severity of the infecting virus strain has also been shown to induce different host responses in terms of altered amino acid composition and inorganic nitrogen content. For maize infected with maize dwarf mosaic virus, twelve amino acids increased, three showed no consistent relationship, three decreased and all ammonium compounds and amides increased compared with healthy plants. A more severe strain of maize dwarf mosaic virus induced greater changes in amino acids than a milder strain (Ford and Tu, 1968).

Diener (1963) warned that the method of tissue extraction for amino acids and amides could introduce a further variability in reported results. There are several reports of both asparagine and glutamine accumulations in virus-infected tissues. However, glutamine is easily hydrolysed and since hot water or hot ethanol was used to extract amino acids and amides, in some of the studies where only asparagine accumulation was reported, these results for asparagine may be misleading.

9. Photosynthesis and Other Functions Associated with Chloroplasts

Chlorosis which is typical of many virus diseases, makes it obvious that either chlorophyll is not synthesized at the same rate as in healthy plants, or is destroyed (Diener, 1963). Reduced chlorophyll as a result of mosaic infection of tobacco has been reported by Dickson (1922, as cited by Peterson and McKinney, 1938), Elmer (1925, as cited by Peterson and McKinney, 1938), Dunlap (1928) and Peterson and McKinney (1938).

The effect of virus infection on the host pigment system can depend on the type of infection. Matthews (1973) investigated six leaf pigments in Chinese cabbage infected with turnip yellow mosaic virus. The effects of infection on the levels of chlorophyll "a" and "b" and the carotenoids,

β -carotene, lutein, violaxanthin and neoxanthin, depended on whether analyses were done on inoculated leaves or leaves systemically invaded by the virus. Eight days after inoculation, the concentration of pigments fell to 68-85 percent the levels in healthy tissues. This fall was attributed to a net loss of pigments. For leaves present at the time of inoculation but systemically invaded to induce vein-clearing symptoms, the six pigments remained unchanged until 10 days after inoculation. Beyond this period pigment production became less, compared with healthy tissues, due to a cessation in pigment synthesis. For tissues systemically infected and showing clearly defined mosaic symptoms of light green and dark green island tissues, dark green island tissue formed contributed to a renewed increase in chlorophyll, on a per plant basis. It was concluded that effects on leaf pigments were a secondary consequence of infection and not essential for virus replication. Kato and Misawa (1974) found, that for tobacco leaves systemically infected with cucumber mosaic virus, chlorophyll was reduced but carotenoids increased, 10 days following inoculation. An increase in carotene content and a decrease in chlorophyll was also reported for tobacco plants infected with TMV (Elmer, 1925, as cited by Bawden, 1956). Peterson and McKinney (1938) on the other hand reported that carotene content decreased following mosaic infections of tobacco.

The mechanism by which leaf pigments are reduced, following infection of a systemic nature, is probably also dependent on the type of infection and age of infection. Peterson and McKinney (1938) reported drops in chlorophyll, carotene and xanthophyll in mosaic diseased tobacco. Associated with reduced chlorophyll was a higher chlorophyllase activity. In healthy plants, however, the level of chlorophyllase activity was directly proportional to chlorophyll content.

Bailiss (1970a) investigated infections of cucumber cotyledons with cucumber mosaic virus. The development of chlorosis, following inoculation, was associated with increased chlorophyllase activity. As well as

catalysing the breakdown of chlorophyll to chlorophyllide and phytol it was also pointed out that this enzyme also probably catalyses the synthesis of chlorophyll during early leaf development. It was proposed that the enzyme was bound in the chloroplast lamellae and that virus infection resulted in a disruption of the chloroplast, releasing the bound enzyme for chlorophyll degradation. However, for cucumber mosaic virus induced yellowing of systemically infected tobacco leaves, Kato and Misawa (1974) suggested that the reduction in chlorophyll was not due to the action of the enzyme chlorophyllase. The amounts of chlorophyllides and pheophorbides were negligible in infected tissues. Infection also greatly reduced the activity of chlorophyllase. From their results it appeared that, in tobacco leaf tissues, chlorophyll was converted to pheophytin, a form lacking magnesium in chlorophyll. The appearance of pheophytin was preceded by a stimulated proteolytic activity which released chlorophyll from a protein-chlorophyll complex.

Virus infection is generally accompanied by a reduction in photosynthetic rate. Owen (1957) reported a 20 percent lowering of photosynthetic rate for tobacco plants infected with tobacco etch virus. Infection of tobacco by either potato virus X (systemic infection) or tobacco mosaic virus (local lesion infection) reduced photosynthetic rate by 20 percent, but only after the appearance of symptoms (Owen, 1957). Reductions in photosynthetic rate have also been reported for corn infected with maize dwarf mosaic virus (Tu and Ford, 1968) and barley infected with barley yellow dwarf virus (Orlob and Arny, 1961).

A possible consequence of infection is a reduced number of chloroplasts, rather than *impaired* chloroplast activity. Magyarosy et al. (1973) concluded that although squash mosaic virus infection resulted in fewer chloroplasts, isolated chloroplasts showed no differences with respect to products of photosynthetic CO₂ fixation, rates of cyclic and non cyclic phosphorylation and activities of phosphoenol pyruvate carboxylase,

ribulose 1,5-diphosphate carboxylase and malate dehydrogenase. However, most reports suggest that virus infection affects directly photosynthetic pigment content and/or rates of reactions associated with carbon dioxide fixation and ATP formation by the chloroplast.

Earlier work by Roberts *et al.* (1952) for potato virus X-infected potatoes and Spikes and Stout (1955) for chloroplasts isolated from sugar beets infected with beet yellows virus implied that reduced photosynthetic activity of infected tissues reflects more than reduced photosynthetic pigment. For tobacco infected with tobacco mosaic virus, the Hill reaction was reduced in chloroplasts isolated from diseased leaves (Zaitlin and Jagendorf, 1960). An instance of increased chloroplast activity as a result of virus infection has been reported by Goeffeau and Bove' (1965). The Hill reaction rate and both cyclic and non-cyclic phosphorylation increased, in Chinese cabbage infected with turnip yellow mosaic virus, during the period of rapid virus replication following inoculation. More recent work, reported by Matthews (1973) for turnip yellow mosaic virus infection of Chinese cabbage, has shown that in young, systemically infected leaf tissues, a stimulation of phosphoenol pyruvate carboxylase and aspartate amino transferase activity occurred. When infected plants were exposed to $^{14}\text{CO}_2$, more label entered organic and amino acids and less label entered sugars and sugar phosphates. However, it was also found that the following proteins and enzymes remained unaltered until virus concentration had reached its maximum, when they fell substantially: 68S ribosomes, Fraction I protein, ribulose diphosphate carboxylase and the overall rate of carbon fixation. Matthews (1973) also pointed out that these changes were shown to occur only in turnip yellow mosaic virus-infected Chinese cabbage. Increases in phosphoenolpyruvate carboxylase and aspartate amino transferase did not occur in tobacco mosaic virus-infected tobaccos.

Marked reductions in the concentration of CO_2 -fixing enzyme, ribulose-1,5-diphosphate carboxylase (Fraction I protein, 18S protein) have been

shown to occur as a result of systemic infection with some viruses. Pratt (1967) investigated chlorophyll content and CO_2 -fixing enzyme levels in healthy and virus-infected leaves of five plant species infected with six viruses. Reduced levels of chlorophyll in infected leaves were always accompanied by similar reductions in 18S protein. It was suggested that these reductions resulted from a partial repression of the genetic mechanism of the chloroplast and that the repression was not necessarily a function of virus concentration. A similar mechanism for the effect of virus infection on chloroplast function was suggested by Hirai and Wildman (1969) who concluded that ribosomal RNA and messenger RNA production, from chloroplast DNA, was switched off by unknown regulators during the period of grand TMV accumulation. The Flavum strain of tobacco mosaic virus strongly inhibited Fraction I protein synthesis in systemically infected tobacco while the Vulgare strain caused less inhibition (Oxefelt, 1971). Kato and Misawa (1974) found a reduction in Fraction I protein following infection of tobacco leaves with cucumber mosaic virus. They proposed that the reduction was due mainly to a suppression in synthesis of the smaller subunit of this protein, the smaller subunit being translated from nuclear DNA-dependent RNA.

Within leaves, chloroplasts are a prime site for ATP formation. The Hill reaction and cyclic and non-cyclic phosphorylation in leaves increased following the inoculation of Chinese cabbage with turnip yellow mosaic virus (Goeffeau and Bove', 1965). However, phosphorylation and the Hill reaction were decreased in isolated chloroplasts of tobacco mosaic virus-infected tobaccos (Zaitlin and Jagendorf, 1960). Rubin and Ladygina (1972) similarly found a reduction in the Hill reaction for up to 20 days, following inoculation of tobacco with tobacco mosaic virus. In order to more clearly elucidate the effect of infection, Rubin and Ladygina (1972) investigated the effects of various chloroplast phosphorylation inhibitors on uncoupling of photosynthetic phosphorylation and the interaction of such

uncoupling with virus-infection. They concluded that with a susceptible tobacco host, infection had its greatest effect on non-phosphorylation electron flow. That is, the long wavelength photochemical reaction concerned with light-induced electron transport and involving cytochromes "f" and "b₆", was inhibited.

10. Enzymes of Photorespiration

Photorespiration is a sequence of enzymatic reactions which converts the end product of photosynthetic CO₂ fixation, glycolate, to glycine (Kisaki and Tolbert, 1968; Vigil, 1973a; 1973b). These enzymatic reactions are compartmentalized, within leaf cells, in single membrane-bound organelles termed peroxisomes or microbodies (de Duve and Baudhuin, 1966; Kisaki and Tolbert, 1968; Frederick and Newcomb, 1969; Baker et al., 1973; Bibby and Dodge, 1973). The initial step of photorespiration is the oxidation of glycolate by glycolate oxidase, with the loss of carbon dioxide. This step is also responsible for the generation of hydrogen peroxide. Catalase, a major enzyme constituent of microbodies is involved in the breakdown of hydrogen peroxide (de Duve and Baudhuin, 1966; Tolbert et al., 1968; Feierabend and Beevers, 1971; Murry et al., 1972; Baker et al., 1973). For diseases of a systemic nature, some reduction in photorespiration appears to be associated with obvious symptom development.

Wynd (1942, 1943) found that catalase was greatly reduced in leaves of tobacco showing mosaic symptoms. Dark green leaves were found to have a greater catalase reaction than light green leaves, even though both were from healthy plants. Dark green areas of mosaic leaves contained more catalase than light green areas. Decreased catalase was also shown for virus-infected leaves of tomato and tobacco (Vager, 1955) and for barley yellow dwarf-infected barley plants (Orlob and Army, 1961). The activity of glycolic acid oxidase was markedly reduced in leaves of tobacco showing definite systemic symptoms as a result of infection with cucumber mosaic virus and in a variegated mutant of tobacco (Solymosy and Farkas,

1964). Healthy tissues and green, virus-free tissues of the mosaic had a higher enzyme activity. Virus-infected tissues and yellow tissues of the variegated mutant also had reduced levels of enzyme substrate and flavin mononucleotide (FMN). It was suggested that chloroplasts played an active role in the regulation of the level of glycolic acid oxidase. No changes in the isoenzyme pattern of catalases were detected in peas infected with pea wilt virus (Reddy and Stahmann, 1970).

For infections of the local lesion type, there is conflicting evidence for the effect of infection on photorespiration. Solymosy and Farkas (1964) found decreased activity of glycolate oxidase in the chlorotic halo around local-lesions resulting from infection of *N. tabacum* L. cv. "White Burley" with the para-strain of tobacco mosaic virus. Pierpont (1968) on the other hand, found no changes in activity of glycolate oxidase 40-68 hours after inoculation of leaves of *N. glutinosa* L. with tobacco mosaic virus. Measurement of enzyme activity coincided with the time of maximum synthesis of the virus. Although most respiratory enzymes increased then decreased, following infection of a local-lesion tobacco host with tobacco mosaic virus, catalase, together with peroxidase, remained higher in activity (Simons and Ross, 1971).

11. Polyphenol Oxidases and Peroxidases

These two enzyme systems have been extensively investigated in studies on metabolic changes resulting from virus infection. Polyphenol oxidases were once thought to be terminal respiratory oxidases, transferring electrons directly to oxygen. However, it has since been shown that this group of enzymes has a very low affinity for oxygen (Merrett and Bayley, 1969). Bonner (1957) suggested that phenol oxidases functioned by transferring electrons from phenols to a cytochrome.

There have been many reports of increases in phenol oxidases following infection of plant tissues with viruses, especially for the local lesion type of infection. Best (1937) reported that expressed sap from tomato and tobacco plants infected with tomato spotted wilt virus, contained higher

levels of an oxidase enzyme, tentatively identified as tyrosinase. This enzyme oxidized phenol, catechol, quinol and tyrosine in the presence of oxygen. A local lesion infection of Nicotiana tabacum L. cv. "White Burley" with tobacco mosaic virus resulted in increases in NADPH₂-dependent quinone oxidoreductase, NADPH₂ oxidase and O-diphenol oxidase activities (Farkas and Solymosy, 1962).

Reports of such increases following infection led to the early hypothesis that quinones, produced as a consequence of polyphenol oxidase activity, were responsible for the observed tissue necrosis (e.g. Solymosy et al., 1959). However, more recent evidence suggests that increases in polyphenol oxidases, following infection, are more a consequence of the hypersensitive reaction than the cause of it. Kikuchi and Yamaguchi (1960) demonstrated the appearance of increased O-diphenol oxidase activity one day after the first signs of visible lesion formation in N. glutinosa infected with tobacco mosaic virus. Van Kammen and Brouwer (1964) found that O-diphenol oxidase activity not only increased in the area of the necrotic lesion but increased throughout leaves of N. tabacum cv. "Samsun" locally infected with a strain of tobacco mosaic virus. Fritig and Hirth (1971) concluded from their studies on phenyl propanoids and coumarins in tobacco mosaic virus infected tobacco leaves showing a local lesion type reaction, that no significant changes in the biosynthesis of chlorogenic acid, umbelliferone, scopoletin and scopolin occurred until at least two days after infection. High increases in these compounds appeared after lesion formation. Van Loon and Geelen (1971) also concluded, from studies of tobacco mosaic virus infection of a local lesion tobacco cultivar, that changes in polyphenol oxidase activity did not precede lesion formation.

Enhanced O-diphenol oxidase activity has also been reported for tissues systemically infected with virus. Merrett (1962) reported a peak in O-diphenol oxidase activity eight days following inoculation of Lycopersicum esculentum cv. "Moneymaker" with tomato aucuba mosaic virus. Similarly Nye and Hampton (1966) reported increases in activity for this enzyme in leaves of N. tabacum L. cv. KY26 systemically infected with

tobacco etch virus. They recorded the greatest increase in the chloroplast fraction but suggested that infection resulted in the activation of inactive forms of the enzyme rather than new synthesis.

The other group of enzymes most reported in metabolic studies of virus-infected tissues is the peroxidases. Peroxidases catalyze the oxidation of various metabolites, especially phenolics, using hydrogen peroxide as the oxidizing agent. However, little is known of the importance of peroxidases in overall cellular metabolism. Their location is mainly in the cytoplasm with some activity in the chloroplast and mitochondrial fractions.

Increased peroxidase activity as a result of virus infection is well documented. Vager (1955) reported increased peroxidase activity for virus-infected leaves of tomato and tobacco. Orlob and Arny (1961) recorded similar increases for barley leaves infected with barley yellow dwarf virus. In addition to a general increase in peroxidase activity there are several reports of increases in the number of isoenzymes of peroxidases following infection. Two new isoenzymes appeared in young bean leaves infected with southern bean mosaic virus (Farkas and Stahmann, 1966). The number of isoenzymes of peroxidase, in Nicotiana glutinosa, increased from five to six with infections of tobacco mosaic virus and potato virus X (Bates and Chant, 1969; Chant and Bates, 1970). The number of positively charged isoenzymes of peroxidase increased in pea plants infected with pea wilt virus (Reddy and Stahmann, 1970). However, investigations of peroxidase isoenzyme changes with infection for tissues of various ages has led to the conclusion that no new isoenzymes are induced as a result of infection. Solymosy et al. (1967) stated that changes in isoenzyme patterns are a function of the host and not the virus. Novacky and Hampton (1968) investigated peroxidase isoenzymes from several virus/host-plant combinations and compared the patterns with those from young and senescent healthy tissues. Quantitative, but no qualitative changes in peroxidases were induced

by infection and senescence, although the changes induced by infection and senescence were not identical. They were unable to detect any new isoenzymes resulting from infection. Novacky and Hampton (1968) suggested, that in the report of Farkas and Solymosy (1966), the new isoenzymes, occurring as a result of virus infection, were present in young, healthy tissues, but at very low levels. Similarly, Esanu and Dumitrescu (1971) concluded that tobacco mosaic virus induced no new isoenzymes of peroxidases in tobaccos. Infection induced the earlier appearance of an isoenzyme that normally appeared towards leaf maturity.

Although peroxidases have been well reported, their role in infection and host reactions is little understood. Van Loon and Geelen (1971) suggested that peroxidases have a significant effect in limiting lesion enlargement in hypersensitive hosts. Treatment of a sensitive tobacco variety, infected with tobacco mosaic virus, with actinomycin D reduced lesion size and at the same time increased peroxidase activity by fifty percent. Such treatment had no effect on polyphenol oxidase activity.

12. Acid Hydrolases

Acid hydrolases mostly appear to be associated with single membrane-bound vacuoles in the cell cytoplasm called lysosomes. Matile et al. (1965) and Semadeni (1967) have shown that lysosomes of plants contain proteases, ribonucleases (RNAases), β -amylases, α -glucosidases, phosphatases, esterases, aryl sulphatases and NADH-diaphorases. Hall and Davie (1971) were able to show that vacuoles of maize roots contained naphthol AS-BI phosphatase, esterase, aryl sulphatase, glucuronidase and β -glycerophosphatase.

There have been few reports concerning the involvement of lysosomes and acid hydrolases in disease development. Kordova, Pottenroth and Wilt (1972) pointed to the importance that this class of enzymes may have in the development of a disease. During infection of mouse peritoneal phagocytes with rickettsiales, lysosomes retained their integrity and host

cells were not damaged. However, with infection of L-cells, early leakage of lysosomal acid phosphatase into the cytoplasm of macrophages induced a rapid, progressive and irreversible cell damage.

For tissues infected with plant viruses, some cases have been cited where hydrolase activity decreased with infection. Decreased protease activity was found in tobacco mosaic virus-infected tobaccos (Holden and Tracey, 1948). Phosphatase activity was reported to be lower in sugar beets infected with beet yellows virus (Sommer, 1957, as cited by Diener, 1963). Apart from these reports, most other reports suggest that some increase in acid hydrolase activity is associated with virus infection. In particular, ribonuclease activity is most consistently reported to increase following infection. Wolfgang and Keck (1958) found that the activity of phosphatase was higher in tobacco mosaic virus-infected leaves compared with healthy leaves. Increased RNAase activity was associated with tobacco leaves showing necrotic, local lesions (Reddi, 1959). Enzyme activity was highest in mature leaves and lowest in young leaves. It was concluded that the amount of tobacco mosaic virus synthesised and the number of lesions per leaf correlated with the RNAase activity of the tissue. Diener (1961) also reported higher RNAase activity in virus-inoculated leaves, but pointed out that other factors, distinct from virus infection, could lead to increased ribonuclease activity in leaves. Randles (1968) studied ribonuclease isoenzyme changes in Chinese cabbage systemically infected with turnip yellow mosaic virus. Infection maintained the intensity of one isoenzyme which, in healthy tissues, soon disappeared after cell division ceased. The other two isoenzymes, present in healthy tissues, increased in activity with infection. Virus-free areas in the mosaic of infected leaves were reported to have similar activities to healthy tissues. Although no qualitative or quantitative changes in isoenzymes of acid and alkaline phosphatase were detected for plants infected with pea wilt virus, the number of esterase isoenzymes increased and their mobility

and intensity were altered (Reddy and Stahmann, 1970).

13. Dehydrogenases and Miscellaneous Cellular Enzymes

Dehydrogenases participate in various energy transformation reactions through their association with nicotinamide adenine dinucleotides and dinucleotide phosphates (NAD, NADP).

Dehydrogenases have been reported to increase following virus infection (Yamaguchi and Hirai, 1956, as cited by Diener, 1963). Reddy and Stahmann (1970) reported no changes in isoenzymes of glutamate dehydrogenase for plants infected with pea wilt virus. However, new isoenzymes of NAD- and NADP-dependent malate dehydrogenase were reported for infected tissues. Both NAD/NADH_2 and $\text{NADP}/\text{NADPH}_2$ ratios were found to decrease in leaves of N. glutinosa showing necrotic local lesions as a result of tobacco mosaic virus inoculations (Sunderland and Merrett, 1963a). This decrease was shown to be due to accumulations of NADH_2 and NADPH_2 . However, for bean leaves with 5-day-old southern bean mosaic virus infections, no differences in the levels of NAD and NADP could be shown (Bozarth and Browning, 1970). Increased levels of all nicotinamide-adenine-dinucleotides were found in tobacco callus tissues systemically infected with tobacco mosaic virus (Sunderland and Merrett, 1963b).

Ascorbic acid oxidase has also been reported to increase following virus infection. Increases occurred in tomato infected with potato virus X or tobacco mosaic virus (Zachos, 1955, as cited by Diener, 1963) and in potato virus Y tolerant potato plants infected with potato virus X (Roberts et al., 1952).

A cytoplasmic protease, with a pH optimum of 5.5 increased in activity following inoculations of tobacco leaves with cucumber mosaic virus (Kato and Misawa, 1974).

Some evidence suggests that specific amino transferases increase following virus infection. Matthews (1973) found that aspartate amino transferase increased in activity in Chinese cabbage infected with turnip

yellow mosaic virus. Although glutamic acid-alanine transaminase increased in tobacco mosaic virus-infected tobacco leaves, the second day after inoculation, by the third day the activity had dropped to fifty percent of the normal level and remained at this level until symptoms appeared (Gubanski and Kurstak, 1960).

B. VIRUS-HOST HORMONAL INTERACTIONS

Many pathological and physiological diseases of plants have been reported to induce changes in the host plant hormonal system. A physiological disorder of tobaccos termed "frenching" was shown to be associated with reduced indole acetic acid (IAA) content of affected plants (Kefford, 1959; Woltz and Littrell, 1968). The disease was characterised by the development of numerous sword-shaped, narrow leaves, loss of apical dominance and a failure of internodes to elongate. Kefford (1959) found that severely "frenched" tips contained 2.16 μg IAA/kg fresh weight, while normal tissues contained 13.72 $\mu\text{g}/\text{kg}$.

Certain bacterial diseases have been shown to bring about an increase in IAA levels of their hosts. Crown gall, bacterial wilt and olive knot all bring about an increase in host IAA levels, partly due to their own contributions to the host IAA pool (Sequeira, 1973).

A feature of diseases caused by many obligate parasites, in particular rusts and mildews, is a stimulation of host metabolism in the area of infection. The secretion of cytokinins by plant pathogens, or by host cells in response to infection, has been frequently suggested to account for altered transport and accumulation of metabolites associated with such infections (Sequeira, 1973). Although cytokinin-like compounds are extractable from diseased tissues, most evidence suggests that the main cytokinin-like activity comes from increases in host cytokinins (Sequeira, 1973).

Literature on gibberellins, as natural growth regulators in plants, had its origin with the discovery that Gibberella fujikuroi produced

substances in culture that induced the exaggerated growth responses of rice plants infected by this pathogen (Stowe and Yamaki, 1957). Apart from a few species of Gibberella, gibberellin-like substances have also been detected in Agrobacterium tumefaciens and certain species of Rhizobium and Verticillium (Sequeira, 1973).

Growth inhibitor substances have been shown to be affected by some diseases. A correlation was shown between decreased tobacco stem internode elongation, maximum multiplication of Pseudomonas solanacearum and increased growth inhibitor content of stems, 4 to 12 days following inoculation of plants with this pathogen (Steadman and Sequeira, 1970). It was also shown that when pure abscisic acid was applied to roots, terminal buds or petioles, of tobacco plants, a reduction of internode length occurred, which lasted from 8-10 days following a single treatment. Tomato plants inoculated with Verticillium albo-atrum had a five-fold increase in abscisic acid from apical leaves (Pegg, unpublished, as cited by Sequeira, 1973).

Unlike many fungal and bacterial diseases, viruses make no unique contribution to the hormone pool of the host. Changes in levels of plant hormones as a result of virus infection reflect an altered host synthesis of endogenous growth regulators.

1. Auxins

The earliest reports of virus-induced, host hormone changes mostly related to auxins. Sequeira (1963) summarized the earlier reports by suggesting that although auxin levels could be reduced at advanced stages of infection by many viruses, there was no agreement as to the significance of this change and some reports even suggested that no decreases occurred at all.

Decreases in auxin-like substances following infection have been reported by Söding et al. (1941, 1943); Grieve (1943); Pavillard (1952, as cited by Porter, 1959); Pavillard (1954, as cited by Porter, 1959) and

Hirata (1954). Grieve (1943) determined auxin levels, by the Avena coleoptile curvature bioassay, for tomato plants infected with tomato spotted wilt virus. Auxins were defined as "non-diffusible, ether extractable material". It was suggested that the lower levels of auxins in infected leaves could be a result of increased degradation. Pavillard (1952, as cited by Porter, 1959) reported lower auxin levels in stunted, tobacco mosaic virus-infected tomatoes, while lower auxin levels were also found in potato plants infected with potato virus X plus virus Y, or potato leaf roll virus (Pavillard, 1954, as cited by Porter, 1959). Auxin levels were also lower in potato tubers from plants infected with leaf roll virus. Infected tissues not only had a lower auxin content, but a higher content of at least two growth inhibitors (Baumeister, 1951).

An increase in the level of auxins, for tomato plants infected with tomato spotted wilt, was reported by Jones (1956, as cited by Porter, 1959). Increased "acid promotor" was also reported from lupin pods, for plants infected with pea mosaic virus. The promotor was active in the wheat coleoptile straight growth bioassay and had a similar Rf value to IAA in paper chromatography. Infected lupin pods had three times the yield of promotor compared with healthy pods (van Steveninck, 1959).

A problem of some of the earlier auxin reports, was that only crude extraction procedures were employed which did not differentiate between the various growth regulators. As most bioassays are sensitive to two or more growth regulators, these results should be viewed with some reservation.

2. Auxin-Scopoletin Interactions

A fluorescent substance, present in plants and increasing in concentration following infection with many viruses, was described by Best (1936) and later identified as scopoletin (Best, 1944). The only clear evidence and complete agreement, from earlier reports, concerns increases in scopoletin in solanaceous hosts infected with several viruses. Diener (1963) suggested that scopoletin behaved as a growth inhibiting substance, which

under certain conditions could promote the destruction of auxins. However, work done by Goodwin and Taves (1950) established doubt as to the role of scopoletin as a growth inhibitor. Their work showed, that scopoletin, one of a number of coumarin derivatives, had only an initial inhibitory effect on Avena root growth rate, when applied at 10^{-3} M concentration. Roots recovered, and further treatment with scopoletin had no other effects on root growth. It was also pointed out by the above researchers, that scopoletin was normally present in infected tissues at a concentration of 5×10^{-5} M.

It has been suggested that the stunting effect of some viruses on their hosts is due to scopoletin inhibition of auxins (Bawden and Pirie, 1952). Pavillard and Beauchamp (1957, as cited by Diener, 1963) reported higher levels of scopoletin in tobacco mosaic virus-infected tobacco and suggested that this compound was responsible for the lower auxin levels in those plants. However, a report by Andreae (1952) suggested that rather than being inhibitory to IAA, scopoletin prolonged IAA activity in vitro by competitive inhibition with IAA-oxidase. It was further suggested that either, scopoletin and IAA were oxidized by a similar, but different enzyme, while competing for hydrogen peroxide, or the oxidizing enzymes were identical, with scopoletin being preferentially attacked.

3. Gibberellins

It is well recognized that a common effect of virus infection, on plant growth, is stunting. Some researchers have suggested that such stunting may be due to virus-induced alteration of hormone action (Goodman et al., 1967; Matthews, 1970). Diener (1963) concluded that it was likely that stunting of virus-diseased plants was in many cases caused by a virus-induced reduction of the effective concentration of gibberellin-like compounds.

The application of gibberellic acid to virus-infected plants has

been reported to reverse the stunting effect of infection. Such effective treatment was reported for severe etch virus-infected potato plants (Chessin, 1957, as cited by Steadman and Sequeira, 1970), ringspot and yellows infected Montmorency cherry trees (Hull and Koss, 1958, as cited by Steadman and Sequeira, 1970) and tobacco leaf curl infected plants (Nariani, 1963, as cited by Steadman and Sequeira, 1970). The stunting induced by 'corn stunt', 'aster yellows', and wound-tumor virus could also be reversed by the application of gibberellic acid to infected plants (Maramorosch, 1957). It should be noted however, that gibberellic acid treatment did not always completely overcome the stunting induced by infection and has not been reported to affect symptoms. Chessin (1957, as cited by Steadman and Sequeira, 1970) found that gibberellic acid treated plants failed to reach the final height of control plants. It would be unjustified to extrapolate on the results of these experiments to the situation within a host plant following infection. Many of these reports may simply represent a normal plant response to applied hormone, irrespective of the mode of action of virus infection on reducing plant growth. Severe etch virus-induced growth defects in tobacco were reduced by spraying plants with gibberellic acid (Stein, 1962). Infected plants typically showed depressed internode length and delayed flowering. Leaves present at the time of inoculation became smaller with infection, although leaves formed later were larger compared with healthy control plant tissues. Infection also increased the rate of leaf formation. As flowering was delayed, infected plants produced more leaves. Spraying with gibberellic acid restored, to some degree, elongation and brought about earlier flowering. Gibberellic acid treatment also reversed the reduction in leaf size caused by infection. However, it was also pointed out that spraying healthy plants with gibberellic acid also increased internode length, brought about earlier flowering and increased the rate of formation of leaves, though not affecting the number of leaves formed.

Endogenous plant gibberellins have been reported as either reduced following virus infection or unaffected. Some reports support the idea that virus-induced host stunting is associated with reduced levels of gibberellins. Reduction in endogenous gibberellins was associated with stunting of barley plants infected with barley yellow dwarf virus (Russell and Kimmins, 1971). Chromatographic separation of plant extracts suggested that gibberellin A₃ (GA₃) was the important gibberellin. However, it was pointed out that stunting was related more to reduced rate of cell division, which could also be affected by gibberellins. Bailiss (1973) found that early infection of cucumbers with cucumber mosaic virus reduced net assimilation rate, promoted the stunting of roots and reduced stem and leaf growth. Reduced levels of endogenous gibberellins (probably GA₁ and GA₃ as evidenced from paper and thin layer chromatography studies) were associated with infected plants. Budagyan *et al.* (1964) on the other hand, could find no differences in the levels of endogenous gibberellins between healthy and tobacco mosaic virus-infected Nicotiana glauca and Mamont tobacco leaves. Stunting is an important feature of tomato aspermy virus-infected tomato plants yet Bailiss (1970b) could find no differences in the levels of endogenous gibberellins between healthy and infected plants. It was found with this disease that reduced internode length was due mainly to reduced subapical mitotic activity. Applied, exogenous GA₃ could partly overcome this effect through increasing cell size, however, treated plants never attained the size of healthy controls.

Many of the investigations concerning endogenous gibberellin levels were conducted in ignorance of the antagonistic effects of the growth retarding hormone abscisic acid on both plant action of gibberellins and bioassay responses. Abscisic acid is extracted with gibberellins and can only be separated from them under certain conditions of chromatography.

4. Cytokinins

Most reports related to cytokinin-virus infection interactions

concern the effects of applying synthetic cytokinins to virus-infected plants and assessing the effects on virus synthesis. Kiraly et al. (1968) concluded that application of purine and non-purine cytokinins to tobacco and bean plants decreased their susceptibility to infection with tobacco mosaic virus and reduced the number of local lesions. Similarly, Nakagaki (1971) showed that applied kinetin decreased both susceptibility to and multiplication of tobacco mosaic virus in detached bean leaves. A reverse effect with applied cytokinins was reported by Milo and Sahai Srivastavia (1969), who found that the effects of applying various cytokinins to resistant and susceptible hosts, infected with tobacco mosaic virus, depended on the host and the type of cytokinin applied. Virus synthesis was stimulated by all cytokinins applied to N. glutinosa and N. tabacum.

5. Abscissic Acid and Other Plant Growth Inhibitors

Apart from the earlier reports, which implicated scopoletin as a growth inhibiting substance, very little has been published on the effects of virus infection on recognized growth inhibitory substances. Van Steveninck (1959) recorded three growth inhibitors as active constituents in healthy and pea mosaic virus-infected lupin pods. Plant material was extracted with ether, separated by paper chromatography in isopropanol: ammonia:water (8:1:1) and assayed for in the wheat coleoptile straight growth test. A weak, acid soluble inhibitor (Rf, 0.3-0.4) was detected in mature pods only. A neutral inhibitor (Rf, 0.9) gave a strong fluorescence under ultra violet light. However, the most potent inhibitor (Rf, 0.55-0.75) was present in both immature and mature pods. In immature infected pods, this inhibitor was present in amounts $\frac{2}{5}$ of that in healthy, immature pods. In mature pods, infection resulted in $2\frac{1}{2}$ times more inhibitor compared with healthy pods. This "potent" inhibitor appeared to be analogous with " β -inhibitor" previously reported in the literature.

Bennet-Clark and Kefford (1953) first described "inhibitor- β ". Ether-soluble extracts of bean shoots and stem, purified on paper

chromatograms developed in isopropanol:ammonia:water contained an inhibitor to the wheat coleoptile straight growth test and pea root expansion test (R_f , 0.6-0.7 from paper chromatograms). A similar inhibitor was also described in extracts from potato tubers (Hemberg and Larsson, 1961). Steadman and Sequeira (1969) reported that bacterial induced stunting of tobaccos was correlated with an increased content of an inhibitor with properties similar to those of "inhibitor- β complex". Milborrow (1967) and Steadman and Sequeira (1970) have both identified abscisic acid ((+) ABA) as the major component of the "inhibitor- β complex".

Ethylene production has been shown to be associated with local lesion formation. Ross and Williamson (1951) reported a stimulated production of a volatile, epinasty-inducing substance, from virus-induced local lesions. This material was assumed to be ethylene. Ethylene production was shown to be greatest in leaves inoculated with viruses that induced numerous, large, necrotic lesions. It was concluded that ethylene production was a consequence of necrosis and not the cause of it. Gáborjányi *et al.* (1971) also found increased ethylene evolution associated with local lesion formation. They suggested that local virus infection was associated with local senescence with an increased evolution of ethylene.

VIRUS-CELL ULTRA STRUCTURE INTERACTIONS

Most ultrastructural research on virus-infected tissues has concerned those diseases which produce obvious, visible symptoms. The mosaic-type diseases have been examined more closely. Ultrastructural changes, occurring following infection, vary depending on the particular host-virus combination. Apart from chloroplasts, alterations to other cellular organelles are usually specific for particular virus-host plant interactions. With most diseases, some disturbance in chloroplast structure can be seen, although again, the nature of the structural change is virus-host interaction dependent. The only unique structures described for virus-infected cells are virus crystalline inclusions and X-bodies. Neither of these two

types of structures have been observed in healthy tissue.

1. Crystalline Inclusions

A most obvious ultrastructure feature of virus-infected cells is the presence of virus particles. With some host-virus associations aggregation of virus particles occurs to produce a regular or amorphous crystalline structure. There have been many reports describing, with the aid of a light microscope, crystalline inclusions in virus-infected plants. Most descriptions are similar to that reported by Goldstein (1924) for mosaic virus-infected cells of tobacco.

With the aid of electron microscopy, crystalline inclusions of tobacco mosaic virus have been described in the cell cytoplasm of a number of host plants (Steere, 1957; Wehrmeyer, 1957, 1959, 1960; Shalla, 1959; Nakata and Hidaka, 1960, as cited by Matsui and Yamaguchi, 1966; Kolehmainen et al, 1965). Infections by other rod-shaped viruses have also been recorded to result in crystalline inclusions in the cytoplasm of infected cells. Crystalline inclusions have been recorded for petunia ringspot virus (Rubio-Huertos, 1962) and red-clover vein mosaic-like virus (Rubio-Huertos, 1964).

Purified preparations of tobacco ringspot virus, squash mosaic virus and turnip yellow mosaic virus all produced hexagonal virus crystals (Steere, 1957). For crystals of tobacco mosaic virus, rods of TMV were arranged parallel within each layer of the crystal with various layers orientated to produce a herringbone pattern (Steere, 1957).

There have been few reports of crystalline virus inclusions within cellular organelles. Intranuclear inclusions have been recorded for tobacco etch virus infections. Crystalline inclusions of tobacco etch virus (Riverside strain) occurred in the nucleus of infected leaf cells of Datura stramonium (Matsui and Yamaguchi, 1964a, b). Inclusions of tobacco severe etch virus have also been recorded in the nucleus of infected tobacco leaf cells (Rubio-Huertos and Hidalgo, 1964). Crystalline virus inclusions have been demonstrated within chloroplasts of sugar beet

infected with either beet yellows virus or Western yellows virus (Engelbrecht and Esau, 1963). Chloroplasts of Beta vulgaris infected with tomato ringspot virus (Engelbrecht and Weier, 1963, as cited by Matsui and Yamaguchi, 1966) and beets infected with beet mosaic virus (Fujisawa and Matsui, 1965, unpublished data cited by Matsui and Yamaguchi, 1966) also contained crystals of virus.

2. X-Bodies

The term X-body was first used by Goldstein (1924) to describe round, oval or amoeboid bodies present only in virus-infected cells. Such light microscope-visible structures were also reported by Goldstein (1926, 1927) and Sheffield (1931, 1934). Matsui and Yamaguchi (1966) described X-bodies as intracytoplasmic abnormal organelles encountered within virus-infected cells. They are generally considered to form as a host cell response to virus infection. Because of the generalized definition of X-bodies, descriptions of shape, structure and composition have varied greatly. Some confusion does arise concerning the term, "X-bodies". Whereas the term was used originally to describe light-microscope visible cellular abnormalities arising out of virus infection, the term has since been extended to include certain cytoplasmic abnormalities visible with the aid of an electron microscope. Through the broad use of this term, some structures, earlier designated as X-bodies, have been subsequently shown to be virus inclusion bodies.

Rubio (1956) and Rubio and van Slogteren (1956) described certain light microscope visible structures, associated with broad bean mottle and cabbage black ring virus infections, as X-bodies. When viewed with an electron microscope, these structures were found to be composed entirely of virus particles. However, the major shortcoming of this report, and indeed with most of the earlier reports, was that inadequate fixatives and embedding materials were used. For the reports of Rubio (1956) and Rubio and van Slogteren (1956), tissues were either unfixed or fixed in

alcohol-chloroform-acetic acid. "X-bodies", for viewing with an electron microscope, were removed from tissues by rupturing cells and allowing the cell contents to flow out into the surrounding water. Inclusions were transferred, by capillary pipettes, to electron microscope grids for viewing. Under these conditions, only virus particles appeared as distinct structures. Any other material appeared amorphous. Another earlier report by Matsui (1959) described X-bodies in tobacco leaf cells infected with tobacco mosaic virus, as either elliptical bodies composed of dense granules and lipid droplets or dense, granular peripheral zones enclosing a vacuolar-like space. Virus particles were rarely seen within these bodies.

The use of adequate fixatives and embedding procedures has revealed a greater structural detail associated with X-bodies. Shalla (1964a) and Hibino and Matsui (1965, as cited by Matsui and Yamaguchi, 1966) described a certain structure within the cytoplasm of leaf cells of Lycopersicon esculentum and Nicotiana tabacum infected with tobacco mosaic virus. This body appeared as a dense, filamentous aggregate, in the cytoplasm, composed mainly of a loose tangle of tubules. Some virus particles were scattered throughout these bodies, while virus inclusions were often detectable at their surface. Similar tubular structures in the cytoplasm of TMV-infected tobacco plants were reported by Kolehmainen et al. (1965). The most common structure was described as occurring in unordered groups or well oriented masses of tubes in the cytoplasm. The complex arrangement of tubules was interpreted as complex folding and extensive branching of the endoplasmic reticulum, with virus particles in its folds. For the same host-virus combination, Esau and Cronshaw (1967a) described X-bodies as membraneless assemblages of endoplasmic reticulum, ribosomes, virus particles and virus-related material in the form of wide filaments indistinctly resolvable as bundles of tubules. In a further paper (Esau and Cronshaw, 1967b) it was pointed out that these tubules bore some similarities in appearance and staining properties to tubular components of

sieve element protoplasm in tobacco. However, it was also noted that tubules of the X-component differed by the straight form of the tubules, the greater degree of order in the arrangement of the tubules in the aggregates, and to some extent, size. Kassanis and Turner (1972) suggested that X-bodies in TMV-infected tobacco may be predominantly coat protein.

A different type of X-body was described for N. tabacum leaf cells infected with tobacco severe etch virus. These bodies appeared to be enclosed by the tonoplast and contained cytoplasmic organelles such as mitochondria and chloroplasts, as well as scattered virus particles and rosette-like bundles of virus particles (Rubio-Huertos and Hidalgo, 1964). A similar type of body was described by Rubio-Huertos (1964, as cited by Matsui and Yamaguchi, 1966) in cells of Pisum sativum infected with a virus which had properties similar to red-clover vein mosaic-like virus.

Rubio-Huertos (1962) identified cytoplasmic areas, in bean leaf cells infected with petunia ringspot virus, as X-bodies. Although these structures were described as containing parallel arrangements of filamentous or doughnut-like structures, electron micrographs presented showed poor detail and no structural organization recognizable as cellular in origin. In a later publication by de Zoeten et al. (1974), these structures were re-examined. They often appeared adjacent to the nucleus and contained mitochondria and osmophilic globules. At higher magnifications, rays of vesicles could be seen to penetrate these structures, forming a kind of reticulum.

Amorphous inclusion bodies induced by potato virus X were shown to consist of collateral bundles of smooth or beaded sheets, usually interspersed with virus particles (Shalla and Shepard, 1972). These structures were destroyed when tissues were exposed to permanganate. They were also susceptible to breakdown by the proteolytic enzyme, subtilisin. Ferritin antibody labelling revealed that these structures were antigenically unrelated to potato virus X or its depolymerized structural protein.

Cow pea cells infected with the spherical virus, cow pea mosaic virus, contained structures, visible with a light microscope, known as "cytopathological structures". Van der Scheer and Groenewegen (1971) studied these structures with an electron microscope. The inclusion bodies, which were usually in close association with nuclei, were composed of membranous structures and tubules with virus-like particles surrounded by an outer sheath. The nuclei of infected cells were also observed to contain membranous structures similar to those of the cytoplasmic inclusions. Similar inclusions were reported in cells of a number of host plants infected with the spherical virus, Brazilian eggplant mosaic virus (Kitajima and Costa, 1974). As well as being composed of membrane-bound vesicles and tubules, these cytoplasmic inclusions included mitochondria, dictyosomes, endoplasmic reticulum, lipid droplets and peroxisome-like structures.

Not all X-bodies have been described as fairly complex cytoplasmic structures. Spinach leaf cells, infected with sugar beet mosaic virus, were reported to contain X-bodies which were simply described as vesicular profiles of the cytoplasm (Fujisawa and Matsui, 1965, as cited by Matsui and Yamaguchi, 1966).

3. The Nucleus

From the bulk of evidence to date, it can be concluded that very few viruses are consistently associated with the nucleus. Only tobacco etch virus has been consistently demonstrated to occur within the host cell nucleus (Rubio-Huertos and Hidalgo, 1964; Matsui and Yamaguchi, 1964a, 1964b).

There have been some reports of tobacco mosaic virus association with the nucleus. Goldin and Fedotina (1962, as cited by Matsui and Yamaguchi, 1966) found crystalline inclusions of TMV in both the nucleus and cytoplasm. However, Matsui and Yamaguchi (1966) pointed out that the methods of fixation and embedding, in the above report, were inadequate. Tobacco mosaic virus particles were also observed, within the nucleus of tobacco

cells, by Reddi (1964). However, in this report, nuclei were isolated from plant cells, disrupted and their contents examined on a grid, following negative staining. Some virus particles were demonstrated by this technique. Esau and Cronshaw (1967b) detected aggregates of TMV particles in the nucleus of systemically infected leaf cells of tobacco.

Hibino and Matsui (1965, unpublished data as cited by Matsui and Yamaguchi, 1966) have demonstrated an intranuclear space for nuclei of tobacco cells. This space was shown to be an extension of the cytoplasm into the nucleus. Virus particles were observed within this space. Virus synthesis in cells undergoing mitosis could also account for some virus particles being entrapped by nuclei. Cells in differentiating mesophyll tissue of N. tabacum L., systemically infected with TMV, divided in the presence of large accumulations of the virus. During mitosis, virus particles and aggregates of particles were seen scattered among the chromosomes and continued to be associated with them until the later stages of mitosis. When the new daughter nuclei became enclosed with nuclear envelopes, virus particles were usually left outside (Esau and Gill, 1969).

For tobacco mosaic virus, isolated reports of virus associations with nuclei can usually be attributed to artifacts of fixation and embedding, artifacts associated with thin sections or chance encapture of virus particles by dividing cell nuclei. Apart from an occasional association with virus particles, there have been no reports of other structural abnormalities of nuclei in TMV-infected host cells.

4. Chloroplasts

The earliest conclusion drawn from electron micrographs of tobacco mosaic virus-infected tobacco leaf cells was that chloroplasts were fully disintegrated and virus particles were associated with the fragments (Scotland et al., 1955). However, in the light of recent knowledge concerning fixatives it is now known that the above observed effects were due to improper fixation and embedding techniques.

Generally, most reports concerning the mosaic induced by tobacco mosaic virus have failed to detect virus particles in the chloroplast (Matsui, 1958; Nakata and Hidaka, 1961, as cited by Matsui and Yamaguchi, 1966; Gerola et al., 1960a, 1960b). Matsui (1958) concluded that there was no real evidence for an association of TMV particles with chloroplasts. However, Boardman and Zaitlin (1958a,b) found tobacco mosaic virus associated with a chloroplast fraction isolated from infected leaves. This fraction contained 0.6-4.2 percent of the total cell virus. Esau and Cronshaw (1967a) observed small aggregates of tobacco mosaic virus in chloroplasts of systemically infected tobacco plants. The lack of a membrane surrounding these particles, and the use of orthodox fixation and embedding procedures suggests that this was a real case of TMV-association with chloroplasts. Shalla (1964) has observed vacuoles or vesicles in the chloroplast stroma for tomato leaves infected with TMV. As these vesicles contained mitochondria as well as virus particles it was concluded that they represented projections of the chloroplast, enclosing cytoplasm. It was suggested that such vacuoles would account for the report of Boardman and Zaitlin (1958a, b).

Generally, in tobacco leaves showing very mild mosaic symptoms, chloroplasts appeared normal in structure. For leaves showing more severe symptoms, chloroplasts showed some disorganization of the stroma lamellae and grana, disappearance of the grana and starch accumulation, although full disintegration of chloroplasts was rarely encountered (Matsui and Yamaguchi, 1966). In young leaves which had developed a systemic infection, chloroplasts could have reduced grana lamellae or a total absence of grana (Gerola et al., 1960a, 1960b).

Similar chloroplast abnormalities have been reported for other virus-host combinations. Maize chloroplasts in plants infected with maize mosaic virus I, were characterized by disintegration of the stroma and grana lamellae and a lack of osmophilic granules (Herold et al., 1960). In

cucumber plants infected with cucumber virus 4, chloroplasts exhibited fat degradation, disintegration of grana and stroma lamellae and the appearance of elliptical granules (Hršel, 1962, as cited by Matsui and Yamaguchi, 1966). Disintegration of grana and stroma lamellae and the appearance of oil droplets has also been reported for chloroplasts of wheat leaves infected with wheat striate mosaic virus (Lee, 1964).

There has been only one well documented case of chloroplasts being the site for synthesis of the invading virus. Ushiyama and Matthews (1971) studied chloroplast abnormalities in Chinese cabbage infected with turnip yellow mosaic virus. They concluded that chloroplasts in infected cells always contained small, double-membrane-bound, peripheral vesicles. Other chloroplast abnormalities such as reduction in size and number of grana and increases in phytoferritin and the number of osmophilic globules were considered secondary effects of infection since they were not typical of all infected cells and they were not present at the very early stages of infection. Staining properties of these vesicles and more recent evidence (Matthews, 1973) points to the vesicles as sites of replication for the virus.

5. Mitochondria and Other Cellular Components and Organelles

Knowledge concerning structural changes of mitochondria, with infection, is sparse to date. It can be stated however, that at present no virus particles have been observed within mitochondria.

Gerola et al. (1960a, b) observed that mitochondria were hardly recognizable in cells within yellow areas of the mosaic induced in tobacco by tobacco mosaic virus. Giant mitochondria (6-10 times normal size) were observed within X-bodies associated with tobacco severe etch virus infections (Rubio-Huertos and Hidalgo, 1964).

The only virus-induced change to cellular organelles, in cucumber plants infected with cucumber green mottle mosaic virus, was the presence of strikingly enlarged and degenerate mitochondria (Hatta et al., 1971).

Such mitochondria contained small vesicles which were bordered by a unit membrane. Most of the vesicles were reported to occupy the space between the outer and inner mitochondrial membranes. From the staining reaction of these vesicles, it was felt that they represented sites of synthesis of viral nucleic acid within the cell. If this surmise is correct this would be the first reported case of mitochondria being directly involved with virus synthesis. Vacuolised mitochondria in cucumber plants infected with cucumber virus 4, had been previously reported by Hršel (1962, as cited by Matsui and Yamaguchi, 1966).

Virus-induced alterations of other cellular membrane systems have been rarely reported. Vesicles and osmophilic granules were found associated with the golgi apparatus of cells of cucumber leaves infected with cucumber virus 4 (Hršel, 1962, as cited by Matsui and Yamaguchi, 1966). Ultrastructural disorganization of cellular membrane systems has been observed for certain other diseases in plants. Goodman and Plurad (1971) found widespread damage to membranes and particulate cellular components in tissues showing a hypersensitive reaction induced by bacterial infections. The plasmalemma, tonoplast and membrane of microbodies was profoundly damaged within 7 hours of infection. Israel and Ross (1967) reported that a common feature in leaf cells of tobacco plants infected with a local-lesion inducing strain of tobacco mosaic virus, was the presence of single-membrane-bound "spherosomes" containing a single crystalline body. The crystalline bodies were present in mesophyll cells in the zone periferal to a necrotic lesion. Kitajima and Costa (1974) observed that peroxisome-like bodies (microbodies?) usually accumulated around or within Brazilian eggplant mosaic virus-induced inclusions. These crystalline contents were reported to have undergone some dissolution processes. It was suggested that the change in internal structure of the peroxisome-like bodies indicated mobilization of associated enzymes and that this mobilization was reflected in the increased metabolic activity of infected cells.

GENERAL INTRODUCTION

In most biochemical and physiological studies of host responses to diseases, the major problem has been to differentiate between host biosynthetic systems and those of the pathogen. Virus diseases of plants offer an opportunity to study host responses during the development of a disease. Apart from the contributions that viruses make to the biosynthetic pathways of nucleic acid and protein synthesis, most other aspects of cellular metabolism, that are measurable, can be fairly confidently assumed to be of host origin.

Virus diseases represent competition between virus synthesis and host cell homeostasis. The manner in which host plants respond to infections by viruses is variable and complex. Reports from the literature have shown that many aspects of tissue metabolism can be affected during the course of development of a virus infection. Of the numerous virus/host combinations, reported in the literature, infection has been shown to affect such cell functions as photosynthesis, respiration, carbohydrate and protein synthesis, energy transformations and many other lesser biosynthetic pathways. There is also some evidence for altered plant hormone synthesis following infection.

Some generalizations from reported metabolic and ultrastructural disturbances in diseased tissues have been attempted in the literature review. However, such generalizations are made difficult by the wide range of host/virus combinations that have been studied. Even for the much reported tobacco mosaic virus, a wide range of host plants, virus strains, tissue ages and stages of infection have been investigated. The situation has been further complicated by the use of different parameters which have been used, particularly biochemical and physiological data.

It is intended, in this report, to investigate as fully as possible, the biochemical and ultrastructural changes which accompany a well established systemic disease and relate these changes to the patterns of growth and symptom development typical of the disease. In this study, the

mosaic disease induced by tobacco mosaic virus in a susceptible tobacco host was the system investigated.

Diseases of the mosaic type have certain characteristics which distinguish them from other systemic plant virus diseases. Primarily they are diseases of the photosynthetic organs of the host. As with most systemic diseases three separate phases are recognisable in the development of the disease.

1. Inoculation and development of the disease in inoculated tissues. This earliest stage of disease development is usually accompanied by general tissue yellowing.

2. Translocation to and systemic infection of tissues already present at the time of inoculation. Infected leaf tissue typically develops vein-clearing and diffuse mottle patterns.

3. Invasion and infection of meristem tissues. Leaves infected while at or near the apical meristem develop the characteristic symptoms of the disease, such as leaf distortions, leaf colour patterns and general growth responses.

The relative importance of each stage of disease development on ultimate plant growth and reproduction will depend on the age of the plant when infection occurs. Plants which develop the characteristic symptoms of the disease are usually infected while young.

With some mosaic diseases, the leaf patterns of yellow-green and dark green areas have been shown to be composed of infected and virus-free cells respectively (Reid and Matthews, 1966; Chalcroft and Matthews, 1967; Atkinson and Matthews, 1970). For the mosaic induced by turnip yellow mosaic virus in Chinese cabbage, only those leaves less than 1.0 centimeter long at the time they became systemically infected, developed the characteristic mosaic pattern (Reid and Matthews, 1966). It has been suggested that mosaic patterns did not develop if leaves had passed the cell division stage (Doke, 1971). Reid and Matthews (1966) considered that

the mosaic pattern was determined by events taking place in leaves in which cell division was taking place and that each distinct island of tissue in the mosaic represented the progeny of a single cell. The mosaic disease of tobacco is also characterised by the development of highly abnormal leaves. Tepfer and Chessin (1959) suggested that the "shoe-string" leaves of tobacco resulted directly from the absence of, or reduced activity of the marginal meristems of the leaf primordia. Retarded shoot and leaf growth of young, infected tobacco plants has also been reported as typical of the disease (Takahashi, 1972).

For this report of a study of host biochemical and ultrastructural changes arising from a systemic infection of the mosaic type, the specific aims are as follows:

1. To reaffirm previous reports as to the distribution of virus within the leaf mosaic.
2. To determine the effects of the disease on certain host growth parameters.
3. To establish the biochemical and ultrastructural characteristics of diseased tissues by comparison between healthy and infected tissues of the same age for a range of tissue ages.
4. From comparisons between healthy tissues and virus-free and virus-infected tissues within the leaf mosaic, to determine which host responses are a direct consequence of virus synthesis/host cell competition and which responses form part of a more general response or adaption to the disease.
5. To establish the major biochemical and ultrastructural changes responsible for the characteristic macrosymptoms of the disease.

General Conditions of Virus Inoculation and Plant Growth

Nicotiana tabacum L. var. Hickory Prior was used as the susceptible host plant through this work. Tobacco mosaic virus (U1 strain supplied by Dr. Richard Francki, Waite Research Institute, Adelaide, S.A.) was chosen as the disease agent because of the well defined leaf mosaic patterns this virus induces in N. tabacum.

Plants were grown in a U-C potting mix and received a weekly nutrient supplement of Hoagland's solution. Both healthy and infected plants were grown under fluorescent, "Grow Lux" tubes, providing 14 hours continuous lighting. All virus inoculations were performed on plants at the 5-8 leaf stage of growth. Infected and healthy plants, although grown together on the same bench and under the same bank of lights, were separated from each other by buffer rows of the virus resistant tobacco species Nicotiana glutinosa L.

SECTION I

VIRUS-HOST GROWTH &
PHYSIOLOGICAL INTERACTIONS

INTRODUCTION

The purpose of this section is to define and confirm the physical characteristics of the disease. General stunting has been reported for susceptible tobacco varieties infected with tobacco mosaic virus. It is important, in considering the development of the disease, to establish what degree of growth retardation occurs and whether this retardation is a manifestation of reduced cell size, reduced cell numbers or combinations of these effects.

MATERIALS & METHODS

1. Virus Concentration and Tissue Distribution in Leaves Showing Well Developed Systemic Symptoms

(a) Virus concentration

A trial was designed to measure the tissue age/virus concentration profile for plants on which leaves were showing well developed mosaic patterns. Virus concentration was measured by the infectivity of leaf extracts in inducing local necrotic lesions on the resistant host plant Nicotiana glutinosa L. Inoculum was prepared by grinding pre-weighed dissected leaf tissues into 10 ml of 0.05 M boric acid/borate buffer, pH 8.0. Wherever possible, virus infected, yellow/green tissues, were dissected from the leaf mosaic pattern. For tissues of the meristem and at leaf position 1 from the apex, dissection was not possible. Ten fold dilutions were prepared from each extract to give a dilution series of 10^{-1} , 10^{-2} , 10^{-3} and a total of 21 treatments. Ten millilitres of each dilution extract were transferred to 2.5 cm x 5.0 cm glass vials. Half leaves of N. glutinosa were inoculated. All but 2-3 leaves were trimmed from each plant, with all remaining leaves being about the same size and colour. Plants were grouped into 6 blocks of 4 plants each, with a total of 22 half leaves per block. Each half leaf was assigned, at random, a number from 1 to 21 to correspond with the number of treatments and dilutions. Half leaves were dusted with carborundum (400 mesh), a 6 cm x 2 cm plant label dipped into the inoculum was drawn over the upper surface of the leaf. A new label was used for each treatment dilution. Each treatment dilution and each leaf age was replicated 6 times on half leaves in each block. Lesions were counted, per half leaf, 3-4 days later.

(b) Tissue distribution

Leaves, at leaf position 8 from the stem apex, were removed from healthy and virus-infected tobacco plants. Half gram fresh weights of the three tissue types, healthy, yellow-green island tissue and dark green

island tissue, were dissected from the leaves and each type ground in 10 ml 0.05 M borate buffer, pH 8.0. A 10-fold dilution series was prepared for each extract to give final dilutions of 10^{-1} , 10^{-2} , 10^{-3} .

Nicotiana glutinosa plants were trimmed to 2-3 leaves per plant and arranged into 6 blocks of 2 plants. Inoculations of treatment dilutions to half leaves ~~were~~ as previously described. Lesions were counted 3-4 days later.

2. Trials to Determine the Effects of Virus Infection on Plant Growth

(a) Plant height, internode length, leaf length, leaf number and root weight

A trial was designed to test the effect of virus infection on the above parameters of plant growth. The two treatments were virus-free and virus-infected plants. The trial was designed with five replications of each treatment in three blocks giving a total of fifteen replications per treatment. Plants were arranged in blocks according to initial plant size so that any influence of initial size on the results was avoided. Plants were inoculated with tobacco mosaic virus (TMV) at the 6-8 leaf stage of development. As it was intended to count the number of leaves at the end of the trial, and as blocks contained plants with different leaf numbers prior to inoculation, the fourth leaf from the apex of each plant, at the time of inoculation, was designated as leaf number one. Inoculum was prepared from virus-infected leaves by macerating tissues in distilled water. Leaf number one, on each plant, was inoculated. During the period of plant growth (6 weeks), leaf number one and the later formed leaves, numbers 5 and 9, were marked with paint spots with a different colour for each leaf position. This ensured that when leaf length measurements were taken, leaves of the same age formed after infection were compared. After 6 weeks, a number of measurements were taken from each plant. Plant height was recorded from the soil level in each pot to the stem apex. Leaves were counted between leaf number 1 and the youngest visible leaf

near the meristem. The youngest developed leaf was usually 0.5 cm long. The length of leaves at leaf numbers 5, 8 and 10 were recorded together with the internode length between leaf numbers 5 and 6.

Root weights were determined by removing all plants from pots and carefully washing the sand/peat mixture from the roots. Root balls were cut from stems, blotted dry and the total fresh weight of root material, for virus-infected and healthy plants, recorded.

(b) Leaf growth during disease development

A trial was set up to measure leaf growth during the course of development of the disease. Leaf growth was estimated from the leaf area approximation of leaf length multiplied by leaf width. There were 9 replications of infected and non-infected plants. Prior to inoculation plants were chosen for uniformity of size and leaf number. Infected plants were inoculated with virus at the 7-8 leaf stage of development. At the time of inoculation leaf number 4, from the base of each plant, was marked with a paint spot. During the course of the trial, every third leaf formed along the shoot was marked with a paint spot of a particular colour to ensure that comparisons were made between leaves of the same age. At weekly intervals, measurements of length and width were taken from marked leaves and converted to leaf area approximations.

3. Determination of Fresh Weight per Unit Leaf Area

Discs of leaf tissue were punched from healthy and virus-infected leaves at the same leaf position from the apex of each plant. For leaves of the same age, 10 discs were punched from each leaf with a cork borer, 0.55 cm internal diameter. Discs of tissue were also selected from the different tissue types of the mosaic.

4. Estimation of Leaf Cell Number per Unit Leaf Area

Three 0.55 cm diameter discs were punched from healthy and infected tobacco leaves of the same age. Leaves at similar positions from the apex were chosen. For infected leaves, discs were also removed from the

different tissue types. Sets of discs were sliced into 1 mm wide strips, immersed in 6 ml of cell separating medium and infiltrated under vacuum. Cell separating medium consisted of 0.5 percent Aspergillus pectinase in 0.05 M citrate buffer, pH 6.0. Strips were incubated for 2 days at 28°C with occasional vigorous shaking to encourage cell separation. Cell numbers were estimated from cell counts in 4 microlitre droplets. All procedures were duplicated. All counts were converted to cell numbers per unit leaf area.

5. Leaf Tissue Preparation for Light Microscopy

Leaf sections, 5 mm x 5 mm, were dissected from leaves and sliced into 1 mm strips at one edge to give a "comb" effect. Tissues were vacuum infiltrated and fixed in 1 percent aqueous osmium tetroxide for 1 hour. After washing with 3-4 changes of distilled water, tissues were dehydrated in a graded alcohol series. Following two changes in epoxy propane, tissues were infiltrated with a 1:1 (V/V) mixture of epoxy propane and araldite for 24 hours. The epoxy propane was evaporated off and sections transferred to a fresh araldite mixture and left at room temperature for two days. Sections were set in araldite by holding at 60°C for 24 hours. One micron thick sections were cut on an LKB ultramicrotome, sections stained with methylene blue and examined with a Leitz light microscope. For composition of araldite, see Appendix 50.

6. Trial to Determine the Effect of Virus Infection on Flowering Response

A photographic record was made on the extent of inflorescence formation of virus-infected and healthy plants of the same age. The time of flower initiation was determined on dissected meristems by observing the structure and shape of the apical meristem and associated initials. Plants for this purpose were grown under 14 hours of continuous light with supplemental lighting being provided from banks of "Gro-Lux" fluorescent tubes. Infected plants were inoculated at the 5 leaf stage of

development. Meristems were dissected from both healthy and infected plants at the intervals 3, 6 and 9 weeks following inoculation of virus-infected plants.

RESULTS AND OBSERVATIONS

1. Plant Size as Affected by Virus Infection

Stunting was a general characteristic of tobacco plants infected with the U1 strain of tobacco mosaic virus and was most pronounced for plants that were young when infected (see Plate 1). Plants with 5-6 week old infections attained heights 55 percent of that for healthy control plants (Figure 2). Paralleling the reduction in plant height was a reduction of internode length. The internode between leaves at nodes 5 and 6, numbered from the original inoculated leaf near the base of each plant, was reduced to an average of 60 percent for virus-infected plants compared with uninoculated control plants (Figure 2). The number of leaves formed per plant was little affected by virus infection. Infected plants averaged 12 leaves per plant, formed above the original inoculated leaves, compared with 11 leaves per plant for healthy control plants. The extra leaf formed per infected plant during the 5-6 weeks following inoculation was statistically significant at the 1 percent level of probability (see Appendix 6). It would seem therefore that virus infection stimulated the rate of formation of leaf primordia and hence the rate of apical mitotic cell division.

Reductions in plant height and internode length with virus infection were accompanied by reductions in leaf size as assessed by leaf length. The difference in leaf length between leaves of the same age from healthy and infected plants, became more pronounced with leaf age (see Figure 1). Leaf length reductions of 20 percent were typical of mature and immature leaves from infected plants. These reductions were statistically significant at the 1 percent level of probability (see Appendices 1 and 2 respectively). The slight reduction in length of young leaves, (node 10 from the original inoculated leaf), was not statistically significant (see Appendix 3).

As well as retarding the size of the aerial portions of tobacco




Plate 1

Healthy and virus-infected tobacco plants (foreground) photographed 4 weeks after inoculation. Leaves marked with the same coloured paint spot occur at the same leaf node above the original inoculated leaf (leaf node 4 from the plant base).

Figure 1

Relationship between leaf length and leaf node position from plant base. The effect of virus infection on reducing leaf length is statistically significant at the 1 percent level of probability for leaves at node positions 5 and 8 above the original inoculated leaf (see Appendices 1 and 2 respectively).

 Virus-infected



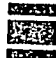
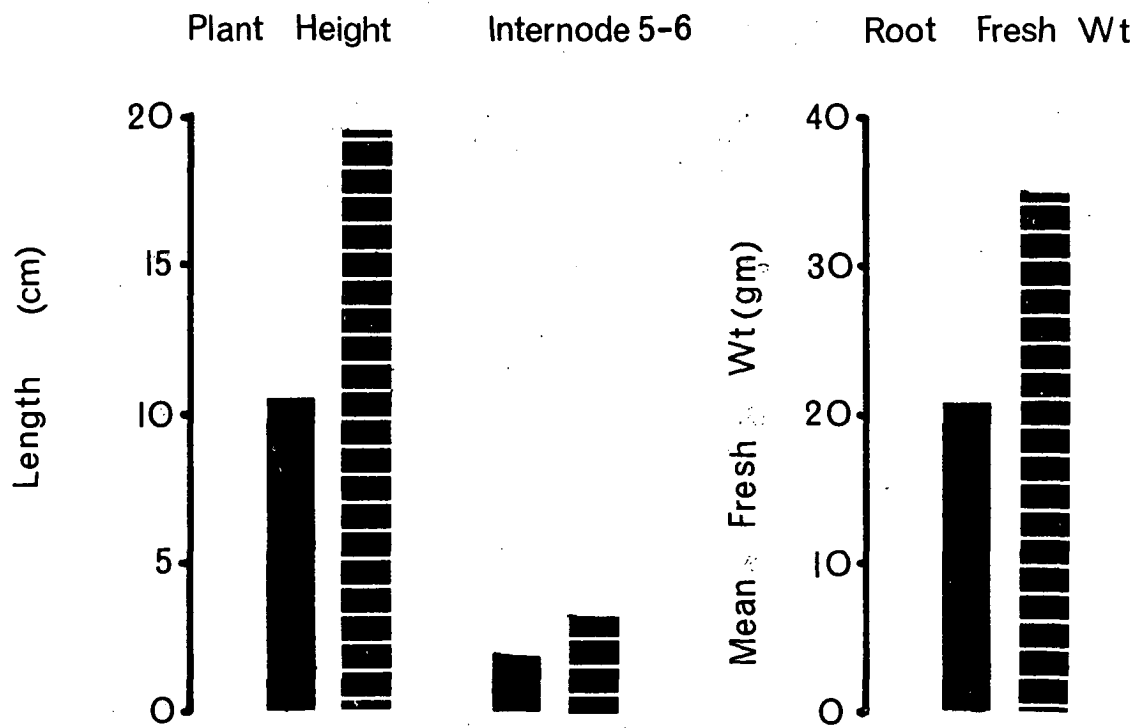
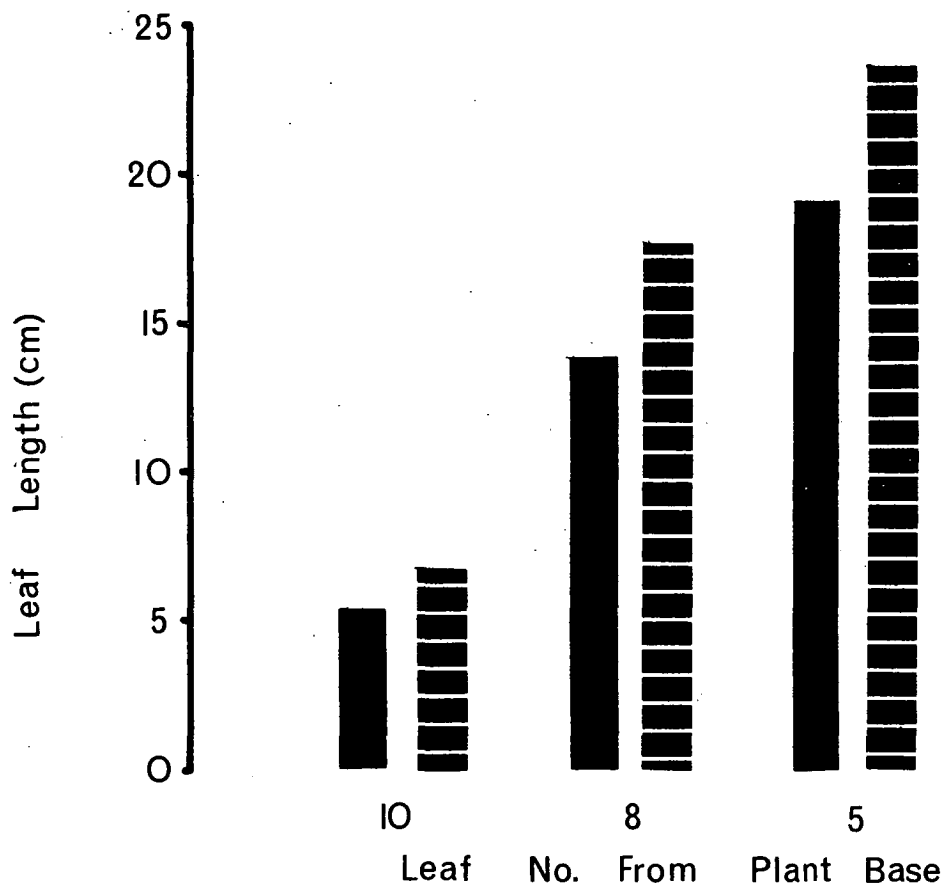
 Healthy control

Figure 2

The effect of virus infection on plant height (left), internode length (centre) and root fresh weight (right). Measurements on plant heights are presented in Appendix 4. The reduction in plant height following virus infection is significant at the 1 percent level of probability (see Appendix 4). Measurements on the length of internode 5/6 are presented in Appendix 5. Reduction in internode length of virus-infected plants is significant at the 1 percent level of probability (see Appendix 5).

 Virus-infected

 Healthy control



plants, virus infection also reduced root size (Figure 2). The fresh weight of roots harvested from infected plants was 40 percent less compared with healthy plants.

Statistical analyses of the measured parameters of plant growth revealed a significant initial plant size interaction with subsequent growth retarding effects of virus infection on plant height (Appendix 4), internode length (Appendix 5) and leaf length (Appendices 1, 2). Plants were arranged in blocks, prior to inoculation, according to size. Parameters of growth from blocks containing plants of greatest initial size were least affected by infection.

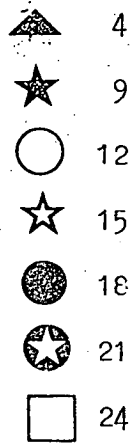
2. Leaf Growth and Development Following Infection

The extent of reduction in leaf size caused by virus infection was related to the age of the leaf with respect to the time of inoculation (see Figure 3). Leaves that were well formed at the time of inoculation (leaves at nodes, numbered from the plant base upwards) were little affected, in terms of leaf area approximation, by infection. Leaves at nodes 8-11 from the plant base, all of which would have been present as leaf primordia at the time of inoculation, showed the greatest reductions in leaf area following infection with up to 64 percent reductions being measured.

These leaves, on development, were typified by greatly reduced leaf laminae and general distortion (see Plates 2, 3). Leaves which developed from primordia formed subsequent to infection (leaves at nodes 12-24 for the trial plants) were generally less affected by infection with reductions in leaf area approximations of 25-30 percent being recorded. Although later formed leaves showed some distortions and reduced lamina growth they were generally more normal in shape (Plate 4). From all leaf measurements taken, differences in growth between healthy and infected leaves of the same age did not become apparent until after leaves had attained lengths greater than 5 cm. The effects of virus infection on

Figure 3

Relationship between leaf growth and time after inoculation. The actual figures plotted are presented in Appendix 7 and represent the means from measurements on 9 plants each for both virus-infected and healthy controls. The following key indicates the node position, from the base of healthy and infected plants, occupied by leaves on which measurements were taken. Infected plants were inoculated on the leaf at node position 4 from the plant base.



(——) Leaves from uninfected plants

(-----) Leaves from virus-infected plants

Leaf Area (sq cm x 100)

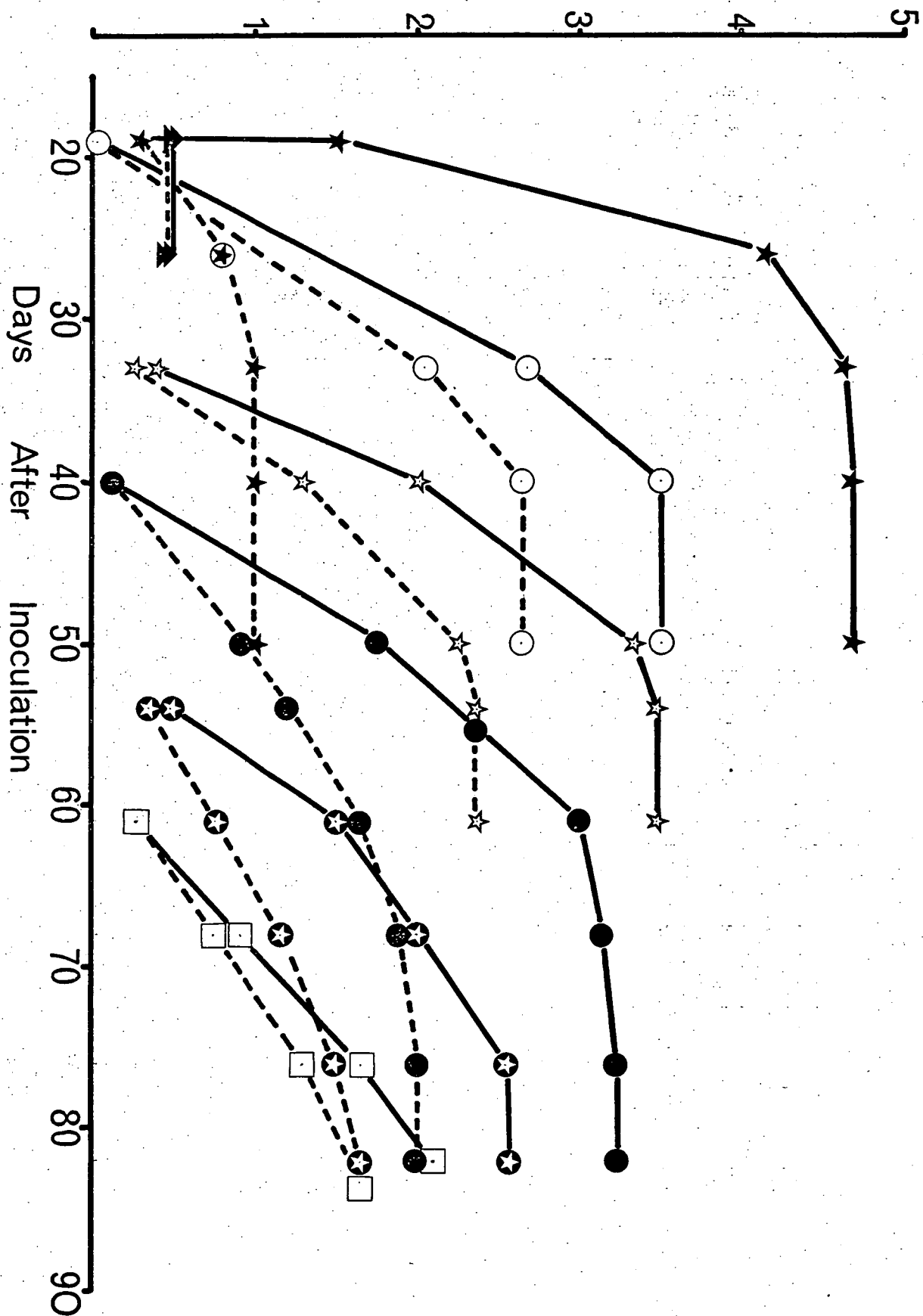




Plate 2

Leaves at nodes 8 and 9 from the plant base. Leaves at node 9 are marked with a yellow paint spot. The upper leaves are from virus-infected plants and the lower two leaves are from healthy control plants.

Photographed 4 weeks following inoculation.



Plate 3

Leaves at nodes 10 and 11 from the plant base. Leaves at node 11 are marked with a blue paint spot. The upper two leaves are from virus-infected plants and the lower two from healthy control plants.

Photographed 5 weeks following inoculation.



Plate 4

Leaves at nodes 15, 16, 17 and 18 from the plant base, photographed 6 weeks following inoculations. The upper leaves are from a virus infected plant and the lower leaves from a healthy control plant.

leaf area were therefore most pronounced during the phase of growth associated with cell enlargement.

3. Effect of Infection on Leaf Cell Size

Reductions in leaf growth became most obvious during the growth phase associated with cell enlargement and therefore some effect of infection on cell enlargement was expected. However, for most leaf ages studied, the number of cells per unit leaf area remained fairly constant within the comparison of healthy versus infected light green and dark green island tissue (Figure 4). Only for very young leaf tissues was there a significant difference in the number of isolated cells from healthy and infected tissues. For these leaves, infected tissues seemed to be more resistant to enzymatic disruption which may have reflected differences in the structure of cell wall pectins.

Sections through healthy and infected leaf material revealed that infection had its greatest effect on the height of palisade mesophyll cells. Palisade cells of light green island tissues were short and blocky (Plate 6) compared with cells of dark green island tissues (Plate 7) and similarly aged healthy tissues (Plate 5).

4. Effect of Infection on Leaf Fresh Weight

Virus infection resulted in a higher fresh weight per unit leaf area for both light green and dark green island tissues of the mosaic compared with healthy control tissue (Figure 5). The greatest difference in fresh weight between leaves from healthy and infected plants occurred with very young tissues with a 50 percent increase in unit leaf area fresh weight resulting from virus infection. For older tissue ages compared, the increase in fresh weight per unit leaf area, as a result of infection, varied from 6 to 12 percent.

5. Leaf Tissue Age and Virus Concentration

Virus concentration reached a maximum soon after leaves passed the cell division stage (Figure 6). For leaves older than leaf position 3

Figure 4

The relationship between leaf cell numbers per unit leaf area and leaf age. All points plotted on the graph represent the mean of two independent estimations.

Figure 4 Key

- (●——●) Leaves from healthy control plants
- (□-----□) Light green island tissue of leaves from infected plants
- (▲-.-.-▲) Dark green island tissue of leaves from infected plants

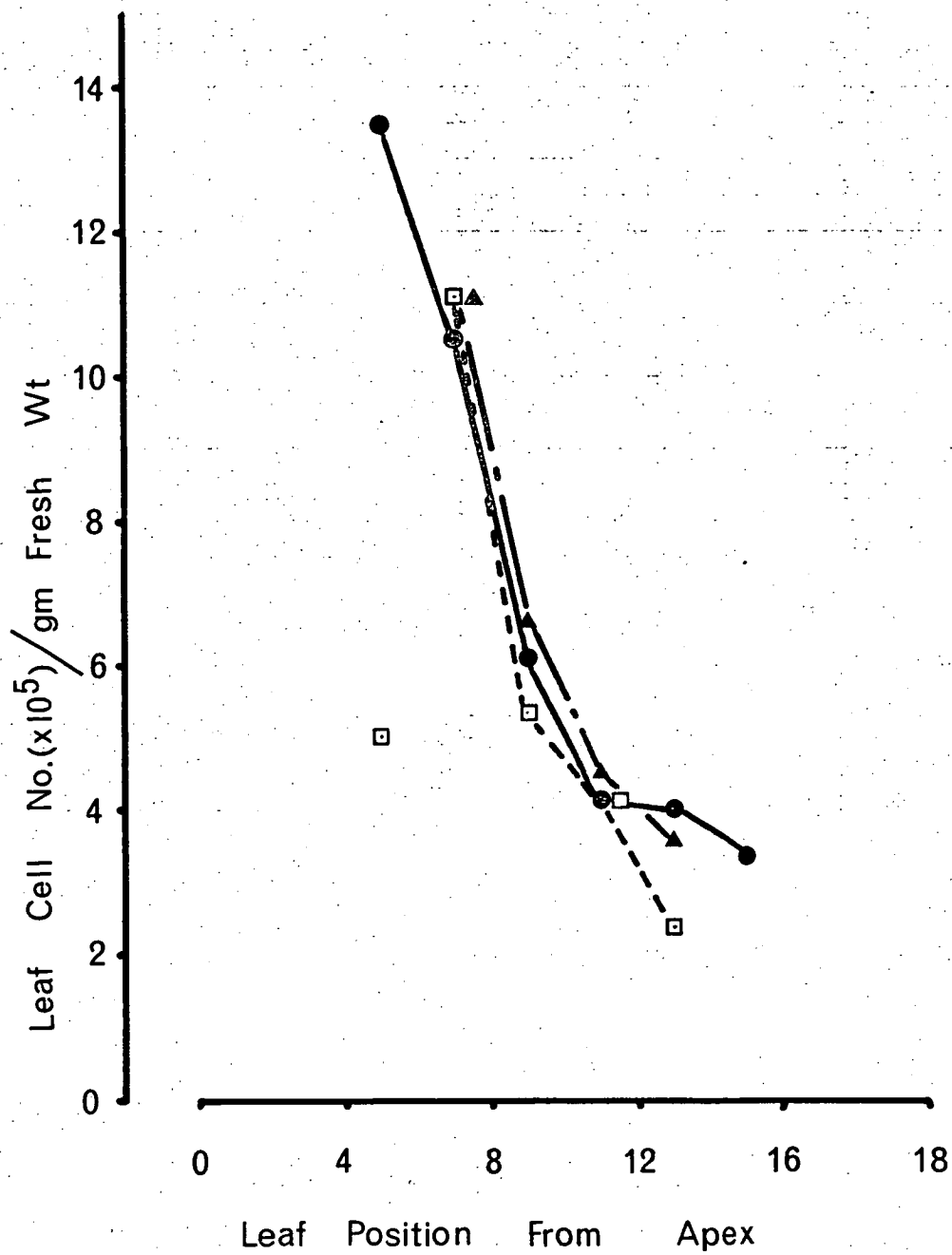


Plate 5

Transverse section through an immature healthy tobacco leaf. Note the columnar appearance of the mesophyll palisade cells beneath the upper leaf epidermis.

(Magnification 800 X)

Plate 6

Transverse section through an immature leaf from a virus-infected tobacco plant. Note the blocky appearance of the mesophyll palisade cells.

(Magnification 800 X)

Plate 7

Transverse section across the border between light green/dark green island tissues of an immature leaf from a virus-infected tobacco plant. Note the transition in shape of mesophyll palisade cells on either side of the border. The cells of the light green island are blocky in appearance (right hand side) compared with the columnar shaped cells of the dark green island tissue (left hand side).

(Magnification 800 X)

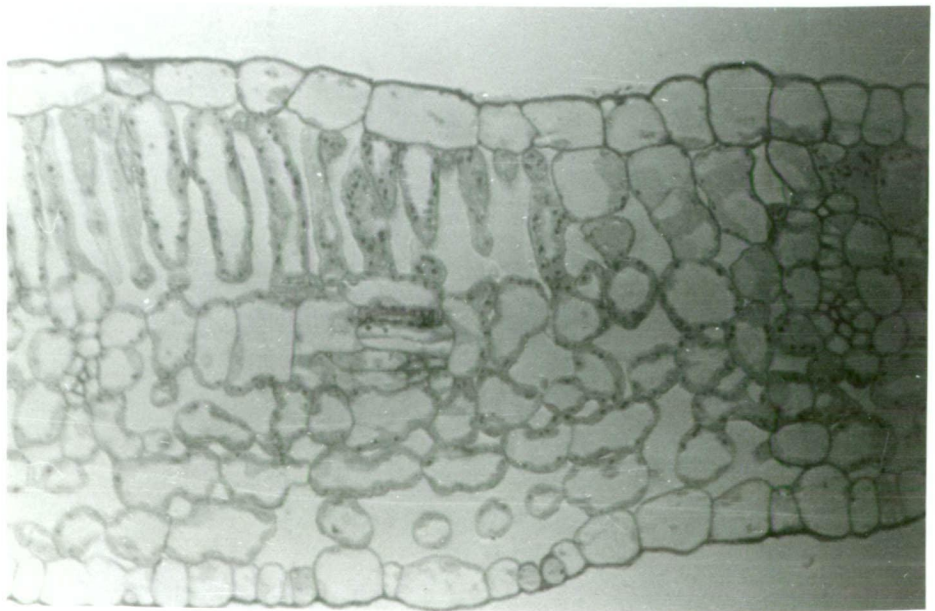
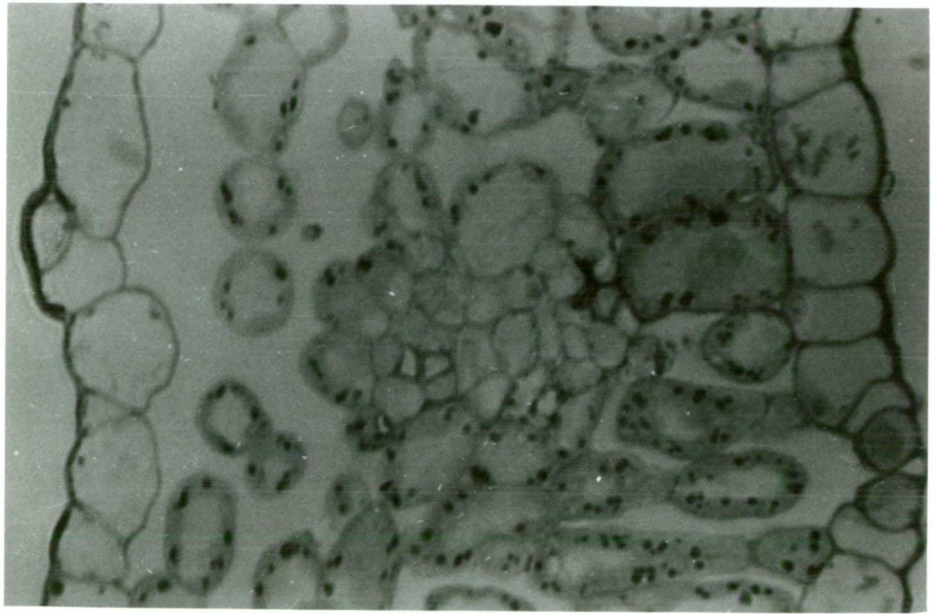
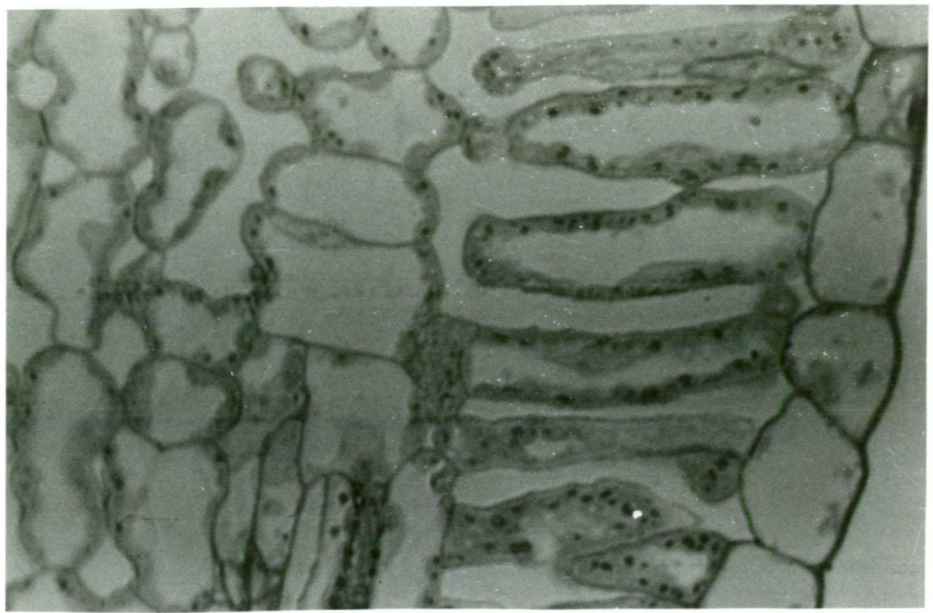


Figure 5

Relation of leaf tissue fresh weight per unit leaf area to leaf age for tissues from healthy control leaves (●—●), light green island tissues (□—□) and dark green island tissues (▲—▲).

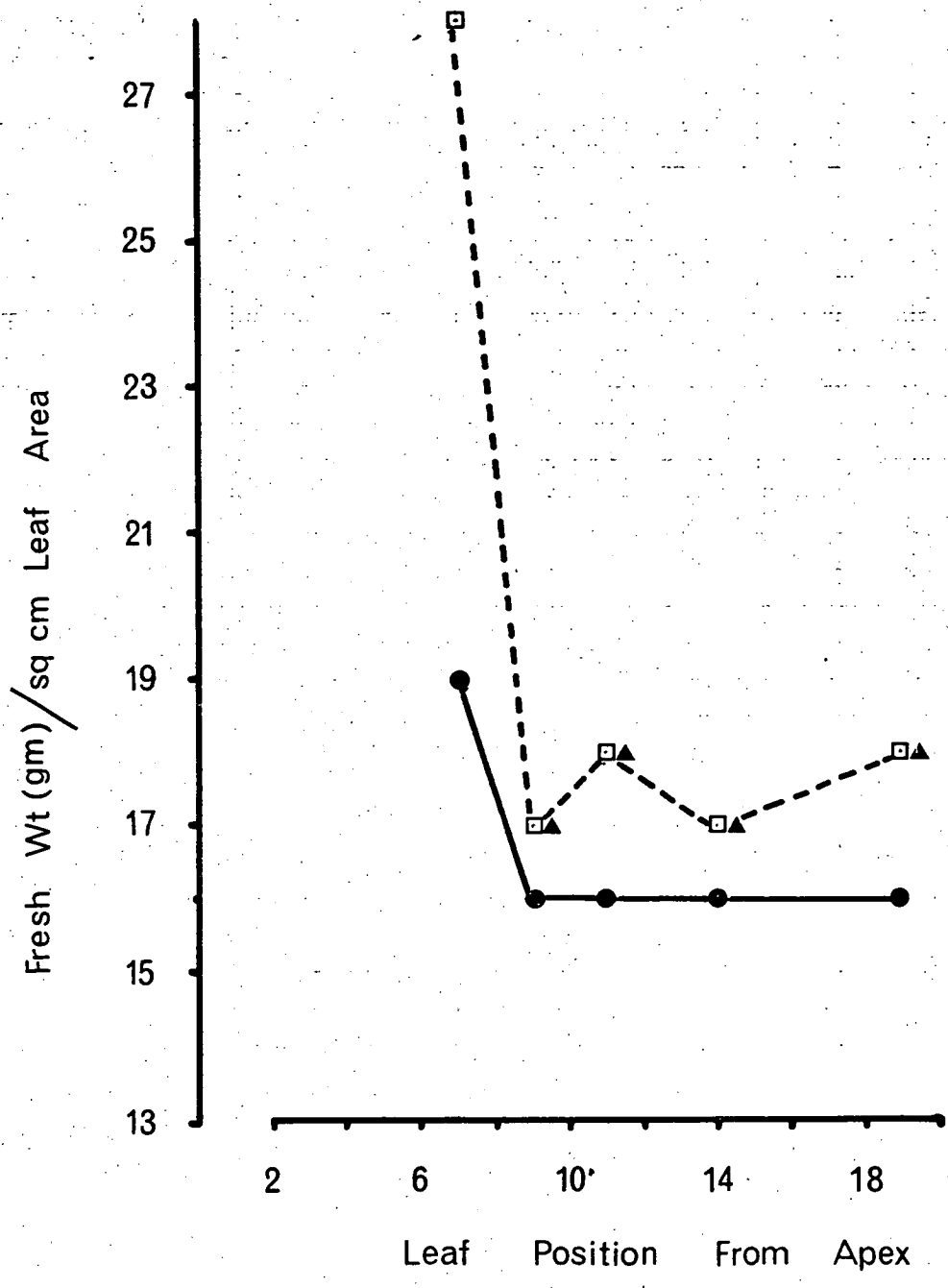
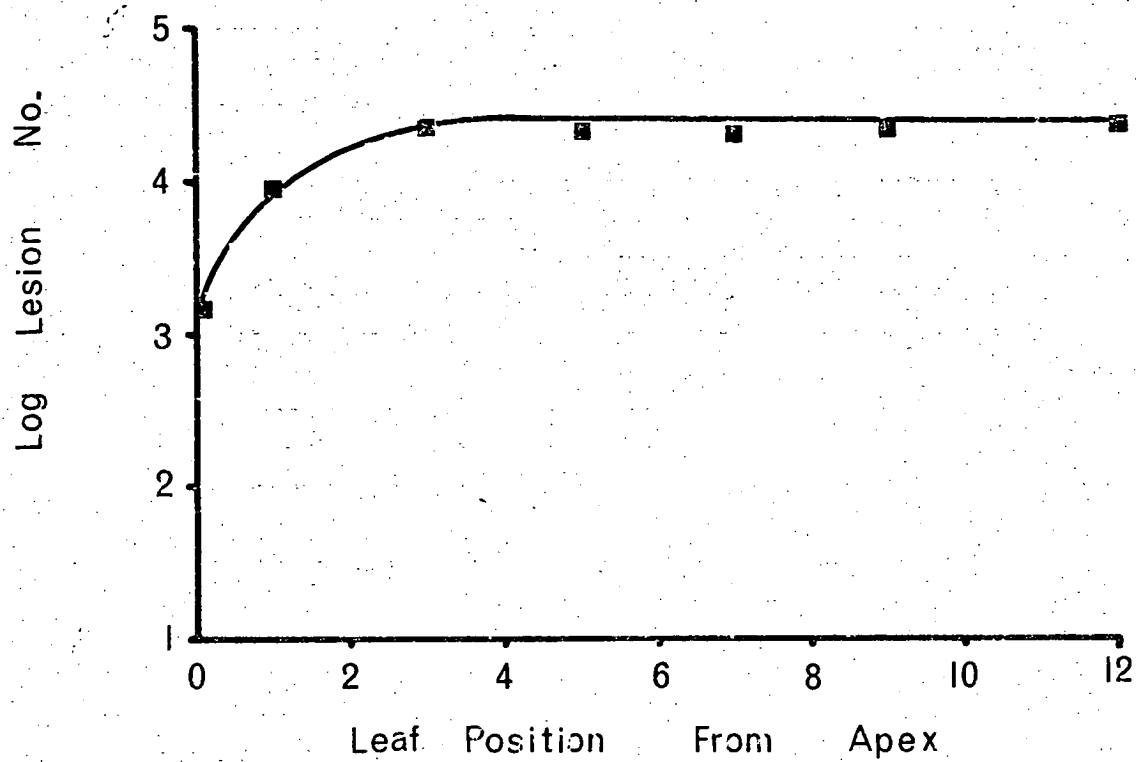


Figure 6

Relation of virus concentration to leaf tissue age for plants showing well developed mosaic leaf patterns. Virus concentration was assessed from the local lesion score on $\frac{1}{2}$ leaves of Nicotiana glutinosa following inoculation with leaf tissue extracts from virus-infected plants (see Appendix 8).



from the stem apex virus concentration, expressed on a tissue fresh weight basis, remained fairly constant. The period of maximum virus increase appeared to be associated with those tissues between the meristem and leaf position 3 from the apex. Virus concentrations determined for the meristem and leaf position 1 were probably underestimated as it was not possible to separate the light green tissues from the mosaic. To enable a more direct comparison with other results, virus concentration was expressed on a tissue fresh weight basis. For a quantitative estimation of virus concentration in tissues of different ages, virus levels could have been more appropriately expressed on a per cell basis to take into account the decrease in cell numbers per gram of leaf tissue as leaves enlarge towards maturity. The period of constant virus concentration occurring in tissues older than leaf position 3 from the apex would then become a period of linear increase in concentration as the number of cells per unit fresh weight of leaf tissue declined with leaf expansion. However, irrespective of the basis used to express the results, the period of maximum virus increase would still be restricted to those leaves between the meristem and leaf position 3 from the stem apex.

6. Virus Distribution Within the Mosaic

Dark green island tissue dissected from a well defined leaf mosaic pattern contained about 6 percent of the apparent concentration of virus extracted from light green island tissues (see Appendix 9). About 5 percent of the virus level associated with dark green island tissues could be attributed to non-specific lesion formation and a function of the inoculating technique. With greater care in dissecting dark green island tissues from light-green island tissues the virus level associated with this tissue type could be much further reduced.

7. Observations on Flowering Response as Affected by Infection

Trial plants used for determining the effects of virus infection on plant growth were not immediately discarded following final measurements

but left on benches in the glasshouse for several weeks. It soon became apparent that healthy control plants flowered well ahead of virus-infected plants.

To further investigate the effect of infection on flower initiation, meristems were dissected from healthy and diseased plants, 3, 6 and 9 weeks following inoculation. Three weeks after inoculation the meristems of both infected and healthy plants were in the vegetative phase. A vegetative meristem was recorded when the apical zone was domed and surrounded by leaf primordia. Six weeks after inoculation the meristems of healthy plants had undergone floral initiation (Plates 9, 10) while the meristems of infected plants were still vegetative (Plate 8). Nine weeks following inoculation, healthy plants had produced obvious inflorescences (Plate 11) whereas infected plants still appeared to be in a state of vegetative growth (Plate 12).

Plate 8

Dissected apical meristem from a tobacco plant with a 6 week-old virus infection. Plants were about 12 weeks old from the date that seeds were sown. Note the leaf primordia about the domed apical meristem.

Plate 9

Dissected apical meristem from an uninfected tobacco plant about 12 weeks old from the date that seeds were sown. Note the flower primordia surrounding the central meristem.

Plate 10

Dissected apical meristem from an uninfected tobacco plant 12 weeks old from the date that seeds were sown. Note the advanced development of flower primordia surrounding the meristem.

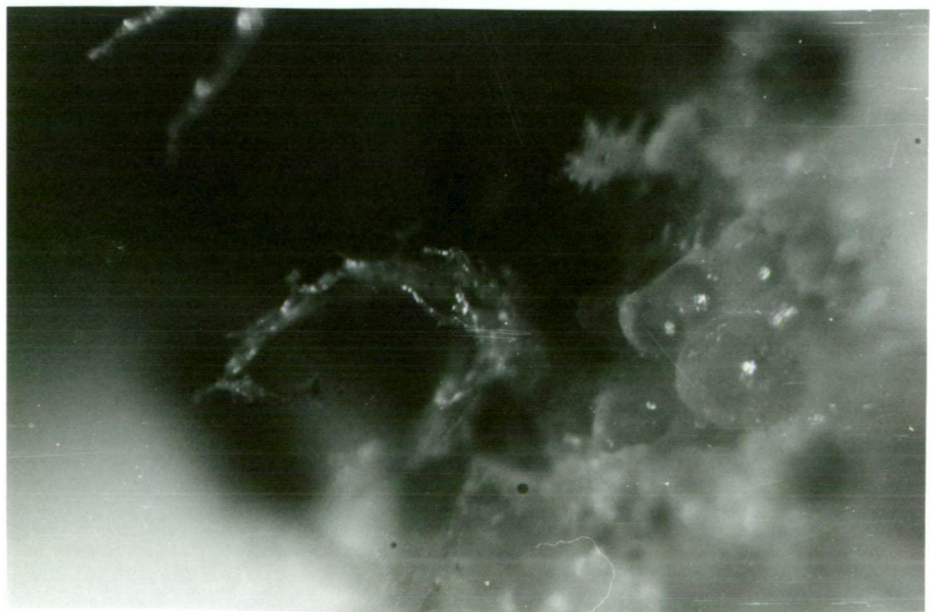
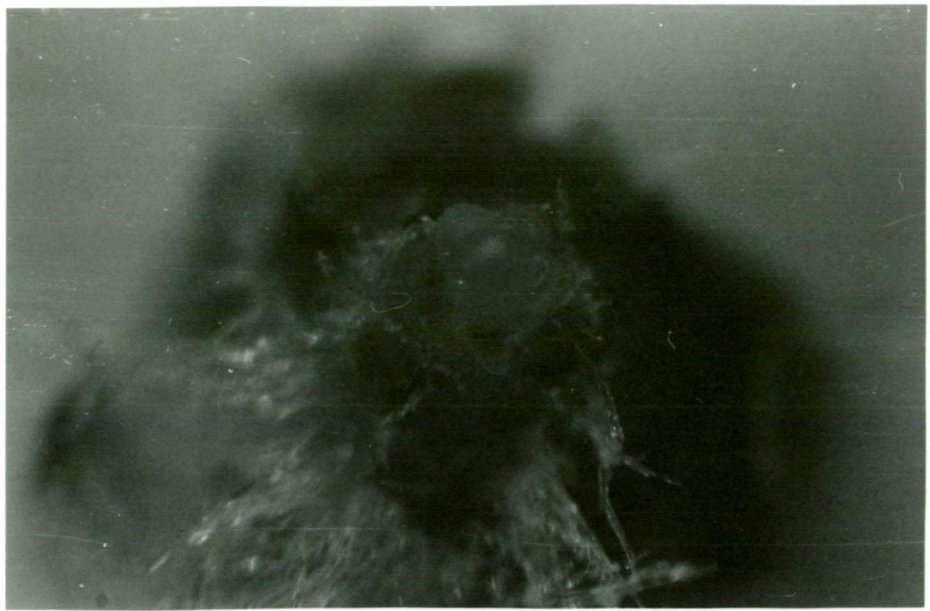




Plate 11

Healthy tobacco plants, 15 weeks old from the date that seeds were sown. Note the well developed inflorescences.



Plate 12

Tobacco plants, 15 weeks old from the date that seeds were sown and infected with virus for 9 weeks. Note the absence of inflorescences.

SECTION II

VIRUS-HOST BIOCHEMICAL INTERACTIONS

A. ENZYMES & REACTIONS OF CELLULAR METABOLISM

INTRODUCTION

A number of enzyme systems were chosen to represent the major metabolic pathways in tobacco leaf cells. The following is a brief analysis of the relative importance of these enzyme systems in cellular metabolism.

The hydrolase group of enzymes including phosphatases, esterases, amylases, ribonucleases and specific proteases, has been shown to be chiefly associated with lysosomes. These enzymes were chosen for study because they are important in the metabolism of carbohydrates, nucleic acids, nucleotides and phosphoproteins. In addition to the breakdown of these compounds, hydrolases also participate in condensation reactions, in which ester linkages are synthesised. They are also involved in transphosphorylation and transesterification reactions. Hydrolases are generally involved in breakdown and restructuring reactions essential for the recycling of metabolites in metabolically active cells.

Photosynthesis in plants has two major functions. The photo-system, comprising of a number of cytochromes and photosynthetic pigments, is involved in the conversion of light energy to chemical energy by the formation of high energy phosphates. The other major contribution of photosynthesis and chloroplasts to the cell is the production of basic carbon skeletons from gaseous carbon dioxide. This reaction is dependent on pyridine nucleotides and the Calvin cycle enzymes. The first enzymatic sequence of carbon dioxide fixation is controlled by ribulose 1, 5-diphosphate carboxylase.

Respiration on the other hand can be viewed as competing with cellular biosynthesis for carbon compounds produced by photosynthesis. Two distinct types of respiration are now recognized, mitochondrial or dark respiration and photorespiration. The breakdown of fats, carbohydrates and proteins yields products, which when fed into the Krebs cycle, can be coupled to oxidative phosphorylation with the ultimate production of high energy phosphates. The terminal chain of electron transfer is

mediated by the cytochromes and their associated oxidases. Mitochondrial integrity and hence respiration potential, can also be estimated from the activity of other enzymes normally associated with this organelle. Glutamate dehydrogenase and reduced pyridine nucleotide oxidase are localized in mitochondria (Matsumoto *et al.*, 1971). Photorespiration competes more directly for products of photosynthesis and involves a reaction sequence from glycolate to glycine, during which hydrogen peroxide is produced as a by-product. Reactions of photorespiration take place within microbodies (see literature review). Catalase, a major enzyme constituent of microbodies, is involved in the detoxification of hydrogen peroxide. The two major pathways of carbohydrate metabolism, in the cell, are the hexos-phosphate pathway and the pentose phosphate pathway. Two major enzymes in these pathways are phosphoglucoisomerase and glucose-6-phosphate dehydrogenase. Alcohol dehydrogenase represents the terminal reaction in the breakdown of carbohydrates (glycolysis).

Reduced ferridoxin is formed as the terminal reaction of photosystem electron flow during photosynthesis. Oxidation of ferridoxin is accomplished through carbon dioxide fixation and conversion of nitrate to ammonium. Although nitrate reductase is located outside the chloroplast, its activity is indirectly dependent on photosynthesis by its direct association with the chloroplast-bound nitrite reductase reaction.

The role of peroxidases in cellular metabolism is still little understood. A measure of the activity of this enzyme does allow comparisons between the system under investigation and the many reports concerning this enzyme in virus-infected tissues.

A major problem in this section was the choosing of suitable units for expressing enzyme activities when comparing healthy and virus-infected tissues of the same chronological age. Enzyme activities for quantitative studies are usually quoted as units of substrate consumed or units of reaction product formed per unit reaction time per unit tissue fresh weight,

dry weight, total soluble protein content or carbohydrate content. Tracey (1948) has shown that tobacco mosaic virus infection affected both fresh and dry weights of tobacco plants. Total soluble protein and carbohydrate content have also been shown to be affected by virus infection. In this section it was decided to express all enzyme activities on a unit tissue fresh weight basis, bearing in mind that this parameter is affected by infection, particularly in very young tissues.

For quantitative work, enzyme activities should obviously be expressed in terms of substrate or reaction product conversion. However, relative activities rather than absolute activities are more usefully reported here, as the most meaningful interpretations concern comparisons between tissues of the same age. Expressing activities as absorption per unit fresh weight of leaf tissue is adequate for relative comparisons.

For those enzymes separated and assayed for in acrylamide gels, a measure of relative activity of various isoenzymes has been estimated by rating the colour intensity, produced in the enzyme assay, on a scale between zero and five where five represents bands with highest colour development. Although inadequate for quantitative assays, a reasonable estimate of relative enzyme activity, within tissues of the same age, can be made.

MATERIALS & METHODS

1. Crude Leaf-Tissue-Enzymes Preparation

A major problem with crude tobacco leaf tissue enzyme preparations was the inactivating action of phenolics on enzymes during the concentration of extracts. This problem was partly overcome by incorporating specific phenolics inhibitors in the extracting buffer. Most phenolics were removed during the course of acetone precipitation of proteins. Although acetone is useful in concentrating and removing phenolics from crude extracts, its use is limited to those enzymes whose activities are little affected by acetone dehydration. Acid hydrolases and enzymes of carbohydrate metabolism were concentrated from crude extracts by acetone precipitation. For the other enzymes assayed for, concentration was achieved by dialysis.

Comparisons between healthy and infected leaf tissues were made on a similar age basis. Leaves of the same age were harvested according to their position from the apex of the plant. The first visible leaf, usually 0.5 to 1.0 cm long, was designated as leaf position 1. The first fully expanded leaf, or mature leaf, usually occurred at leaf positions 10 to 12. Senescing tissues corresponded to leaves on uninfected plants that showed signs of chlorosis. For comparisons of tissues within the leaf mosaic, islands of tissue were dissected out using a scalpel.

(a) Purification and concentration by acetone

Leaf tissue, (0.5 gm fresh weight), less midribs and larger veins, was ground with a mortar and pestle, to a slurry with 2 ml of extracting buffer. The buffer used was a tris-citrate buffer, pH 8.7, containing 0.1 mM 2-mercaptoethanol (2-ME) and 0.1 mM sodium diethyldithiocarbamate (DIECA) (for buffer composition see Appendix 10). Extracting buffer was stored at 4°C prior to being used. Two volumes of chilled acetone (-15°C) were added to the freshly ground leaf tissue slurry

and the extracts were stored in polythene centrifuge tubes held in crushed ice, till centrifuging. Acetone-insoluble protein was recovered by centrifuging at 5000 g for 10-15 minutes at 0°C. All centrifugations were performed in an "MSE High Speed 18" refrigerated centrifuge. The protein pellet was redissolved in 1 ml of extracting buffer by standing at 4°C for at least 2 hours. For some experiments 1 percent Triton X-100 was included in the extracting buffer to ensure complete disruption of lysosomes and other cellular organelles. However, extracting in non-isotonic solutions was in itself satisfactory for disrupting membrane-bound organelles. Resuspended extracts were centrifuged at 25,000 g for 20 minutes at 0°C to remove undissolved residues. Final concentration of extracts was achieved by a further acetone precipitation (2 volumes of chilled acetone), centrifugation at 5,000 g for 15 minutes at 0°C and resuspension of the pellet in 0.05 ml of extracting buffer.

(b) Purification and concentration by dialysis

Dissected leaf tissue was ground with 5 ml of extracting buffer (as used in the previous method) to a slurry and stored in centrifuge tubes held in crushed ice, till centrifuging. Extracts were clarified by centrifuging for 30 minutes at 38,000 g at 0°C. Supernatants were loaded into a Minicon-B Concentrator dialysis apparatus (5 ml capacity per well, 15,000 MW cut-off, 0.05 ml final volume, manufactured by Amicon Corporation) and allowed to concentrate overnight at 0°C. Final volumes were adjusted to 0.2 ml with extracting buffer prior to removal from the dialysis apparatus.

2. Acrylamide Gel Electrophoresis

The power unit (Plate 13) delivered either constant current or constant voltage (0-50 mA, 0-300 V, respectively). The electrode vessel apparatus (Plate 13) was constructed of perspex and the cathode and anode compartments each contained platinum electrodes. The general technique used was that essentially reported by Raymond and Weintroub (1959) for horizontal-slab electrophoresis using a discontinuous buffer system as

Plate 13

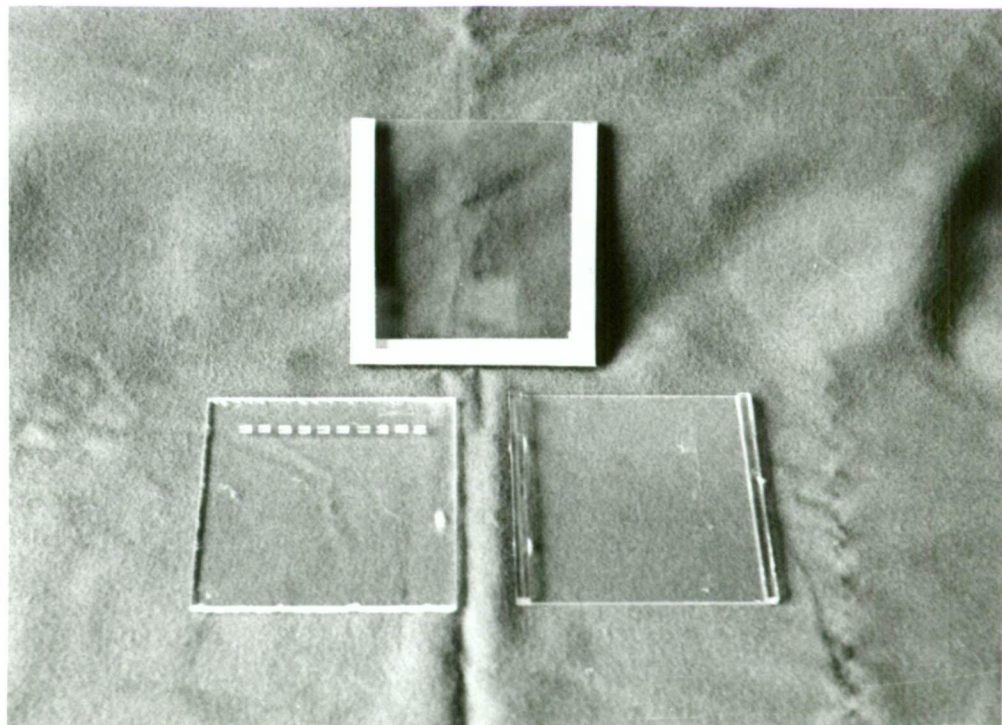
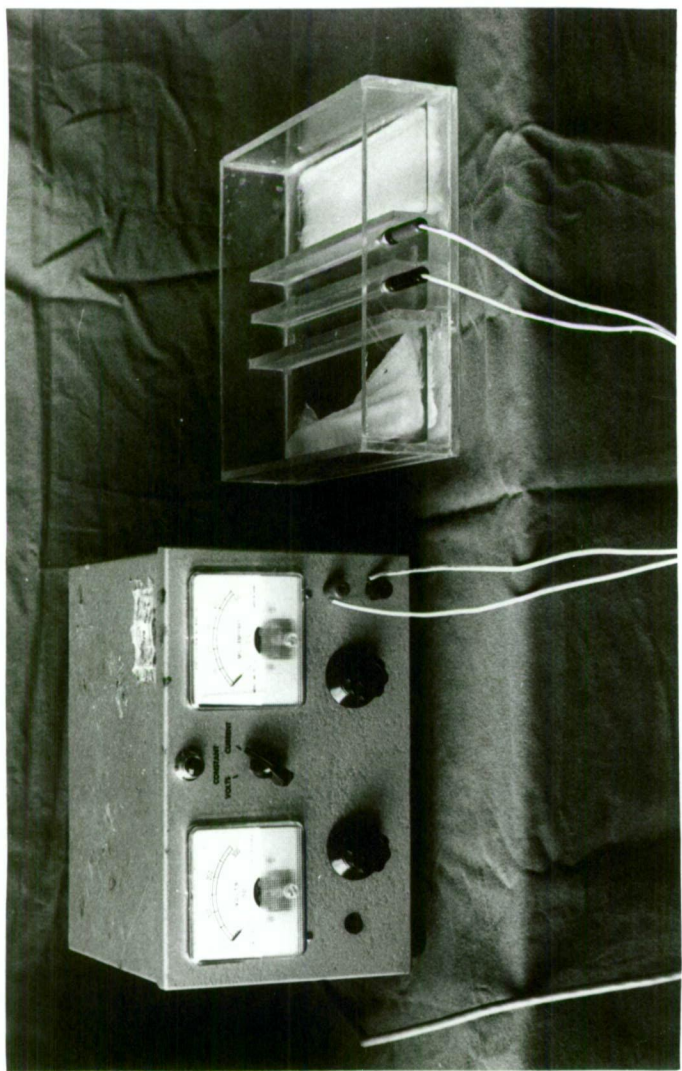
Electrophoresis power unit on the left, with either constant current or constant voltage control. Electrophoresis tank unit on the right, constructed from perspex and partitioned into two buffer compartments, each with a platinum electrode.

(Magnification $\times \frac{1}{5}$)

Plate 14

Gel mould constructed (above) and disassembled (below). Plate with well formers constructed of perspex and other components of glass.

(Magnification $\times \frac{1}{5}$)



reported by Ornstein (1964). The mould used to construct gels (Plate 14) was made up of glass and perspex components. The assembled mould was held together with adhesive tape, along three edges, leaving the top of the mould open. Well formers (1.5 mm wide, 4.0 mm long and 2.5 mm deep) were aligned 15 mm from the top edge of the perspex plate. The final gel dimensions were 72 mm wide, 80 mm long and 3.5 mm thick. Gels were removed from their moulds by removing the adhesive tapes and dissassembling the moulds. Gels were supported on a glass slab during electrophoresis.

Clear acrylamide gels were prepared from the basic chemical constituents of acrylamide, NN-methylene bisacrylamide, NN,N',N'-tetramethyl ethylene diamine and ammonium persulphate, dissolved into gel buffer (see Appendix 10). For the proportions of the above constituents to construct 7.5, 8.0 and 10 percent acrylamide gels see Appendix 11. Gel components were made up in tris-citrate buffer (see Appendix 10). The first three constituents can be mixed without polymerization occurring. Prior to pouring the unpolymerized gel into a mould, ammonium persulphate crystals were added and stirred to dissolve. Gels polymerized in 10-15 minutes, depending on laboratory temperatures.

For electrophoresis of crude enzyme preparations, polymerized gels were removed from their moulds and placed on a flat glass plate in the electrode or tank vessel, with the gel wells nearest the cathode compartment. The electrode compartments of the tank vessel were supplied with fresh tank buffer (see Appendix 10). Contact between the electrode compartments and the gel was established through tank-buffer-saturated muslin wicks, dipping into each compartment and butting to the leading and tailing edges of the gel. It was important that no air bubbles were present along the zone of contact between wick and gel. Gel wells were filled with gel buffer with the aid of a finely drawn out micropipette to avoid surface spread of the buffer. Gels were pre-electrophoresed until the tank buffer had reached the gel wells (usually about 10 minutes). Wells

to which crude enzyme extracts were to be added were blotted dry with fine strips of filter paper and extracts loaded as described previously. At least one well for each gel was filled with a dilute solution of bromothymol blue in gel buffer. This dye acted as a marker dye for the boundary between tank and gel buffer in the gel and thus served to indicate the buffer front from which Rf values were calculated. For both pre-electrophoresis and sample electrophoresis a constant current of 15 mA was used for a single gel. This coincided with a starting voltage of 60. If two gels were run simultaneously the 60 volt starting voltage was achieved by a current setting of 25 mA. A run was concluded when the tracker dye had moved about 5.0 cm from the wells. Prior to specific enzyme localization, gels were usually sliced horizontally into two or three thin slabs. This allowed for at least three different enzyme determinations per gel run. The apparatus used for gel slicing was a Gradipore gel slicer, model 342.000/4.

3. Assays for Enzymes Separated by Electrophoresis

All tissue extracts were prepared by the acetone precipitation method.

(a) Acid phosphatase

Gel slices were washed for 10 minutes in 0.1 M acetate buffer, pH 5.2. Slices were then incubated in a solution of 100 mls 0.1 M acetate buffer, pH 5.2 containing 20 mg α -naphthol acid phosphate (potassium salt), 20 mg magnesium chloride and 50 mg naphthanyl Diazo Blue B. Gels were stained for a minimum of 60 minutes at 28°C. Areas of phosphatase activity appeared as red-purple bands. The distance of each band from the origin was recorded together with an intensity rating for each band. Intensities from very faint (rating of 0.25) to the maximum staining intensity (rating of 5.0) were recorded for each gel. All comparisons were run in the one gel. Values of Rf for each band were determined from the ratio of distance of migration of a particular band to the distance of

the tracker dye from the well.

(b) Ribonuclease (RNAase)

The method used was essentially that reported by Randles (1968). For RNAase localization in gels, 10 percent acrylamide gels were made up containing 0.3 mg per ml of high molecular weight, wheat germ ribosomal RNA. Following electrophoresis, gel slices were washed in 0.1 M sodium acetate buffer, pH 5.4, for 15 minutes. Strips were then incubated in buffer for 2-3 hours at 37°C. Gels were stained in a solution of 0.02 percent Toluidine Blue for 30 minutes and destained overnight, in water. Zones of RNAase activity appeared as clear bands against a blue-staining background. Bands were recorded by their Rf values and staining intensities.

(c) α -Amylase

Acrylamide gels were prepared containing 0.2 percent soluble starch. Gel slices were washed in 0.05 M phosphate buffer, pH 6.4 for 15 minutes. Slices were then incubated for 30-60 minutes, in fresh buffer solution, at 28°C. Following incubation, the buffer was replaced by a solution containing 0.005 percent iodine and 1.5 percent potassium iodide (W/V) and allowed to stain until the background colour of the gel was blue-black. Areas of α -amylase activity appeared as clear zones against the dark background. Bands were recorded by their Rf values and intensity ratings.

(d) Esterase

Gels were washed for 15 minutes in 0.05 M phosphate buffer, pH 6.4 then incubated for 15 minutes in a 0.1 percent solution of α -naphthol acetate in phosphate buffer. This solution was prepared by dissolving 5 mg α -naphthol acetate in 0.25 ml acetone, then adding dropwise, with constant stirring, to 25 ml of water. The final volume was made up to 50 ml with the phosphate buffer. Following incubation (28°C) gels were transferred to a staining solution of naphthanyl Diazo Blue B (50 mg in 50 ml distilled water) for 10-20 minutes. Zones of esterase activity

appeared as red to purple bands. Bands were recorded by their Rf values and intensity ratings.

(e) Leucine amino peptidase

Gels were washed for 15 minutes in 0.1 M sodium acetate buffer, pH 5.2. Slices were then incubated for 60 minutes, at 37°C, in a solution of 1-leucyl- β -naphthylamide (40 mg in 100 ml of buffer). The substrate was then replaced with fresh medium containing 50 mg per 100 ml of Black-K-Salt (Koch-Light) and gels incubated for a further 60 minutes at 37°C. Zones of enzyme activity appeared as purplish bands, which were recorded by their Rf values and intensity ratings.

(f) Peroxidase

Gels were washed for 15 minutes in citrate-phosphate buffer, pH 4.4. Slices were then incubated, for 15 minutes at room temperature, in a solution of 1 percent hydrogen peroxide and 0.06 percent guaiacol in citrate-phosphate buffer. When preparing the incubation medium, guaiacol was first dissolved in a minimum volume of alcohol then added drop wise, with vigorous swirling, to the buffer. Zones of peroxidase activity appeared as blue bands, which were recorded by their Rf values and intensity ratings.

(g) Catalase

Acrylamide gels were prepared containing 0.2 percent soluble starch. Following electrophoresis, gels were washed for 15 minutes in citrate-phosphate buffer, pH 4.4. Catalase was localized in gel slices by incubating slices in buffer containing 1 percent hydrogen peroxide (V/V of 100 volume) for 15-30 minutes then transferring the slices to a 0.5 percent solution of potassium iodide. Isoenzymes were located as clear zones against a blue-black background of stained starch. Recordings of Rf values and band rating intensities had to be made within 10 minutes of transferring the gel slices to the potassium iodide solution. After this time, bands began to fade.

4. Direct Assays for Enzymes in Crude Tissue Extracts

(a) Phosphoglucoisomerase (adapted from a method reported by Buell et al., 1958 and Nelson and Lynn Wakefield, 1972).

Crude leaf enzyme extract was prepared by the acetone precipitation method from 1.0 gm fresh leaf material with a final extract volume of 0.1 ml. Enzyme substrate of 46 mM 2-sodium glucose-6-phosphate, 1 ml of 0.05 M tris buffer, pH 7.6 was incubated with 0.05 ml of crude enzyme preparation for 45 minutes at 38°C. A control consisting of 1 ml of enzyme substrate and 0.05 ml of distilled water was incubated along with the leaf tissue extracts. Enzyme activity was determined by measuring the amount of fructose-6-phosphate formed from the substrate. A 0.1 ml aliquot of incubate was mixed with 1 ml of fresh reagent comprising 40 volumes of 20 N sulphuric acid and 1 volume of glacial acetic acid containing 0.4 percent resorcinol and 1 percent thiourea. After heating in a water bath at 60°C for 20 minutes, solutions were cooled and diluted to 5 ml with water. Fructose-6-phosphate produced was determined as absorbance at 500 nm against a substrate blank. Fructose standards (10, 7.5, 5.0, 2.5, 1.0 and 0.5 mg/ml) were also assayed for in the above colour developing reaction and a fructose concentration against absorbance standard curve constructed.

(b) Glucose-6-phosphate dehydrogenase (after the method of Schnarrenberger et al. (1972)

Crude leaf extract was prepared by the acetone precipitation method from 1.0 gm fresh weight of leaf material with a final extract volume of 1.0 ml. The substrate medium composition, in 0.05 M tris buffer, pH 8.8, was as follows:

7.5 mM wrt magnesium chloride

250 μ M wrt NAD

2 mM wrt glucose-6-phosphate (sodium salt)

Enzyme activity was followed spectrophotometrically in a Hitachi UV

Spectrophotometer. Three ml of assay mixture were pipetted into a quartz curvette and the percentage transmittance at 340 nm adjusted to read 100. The reaction was started by adding 0.5 ml of crude leaf extract to the curvette, stirring for 1 minute then following the change in absorbance by taking readings at 1 minute intervals for 5 minutes. Leaf tissue extracts awaiting assay were stored in crushed ice containers. Ideally, the percentage transmittance at time zero should be between 40 and 50.

(c) Alcohol dehydrogenase

Leaf enzyme extracts were prepared as for glucose-6-phosphate dehydrogenase determination. Enzyme activity was followed spectrophotometrically at 340 nm wavelength setting. The assay mixture in 0.05 M tris buffer, pH 7.6 was as follows:

Ethanol - 0.002 ml per 1 ml buffer
 NAD - 5 μ Moles per 1 ml buffer
 magnesium chloride - 1 μ Mole per 1 ml buffer

Three millilitres of assay mixture were pipetted into a quartz curvette and percentage transmittance adjusted to read 100. The reaction was started by adding 0.5 ml of crude leaf extract and thoroughly stirring for 1 minute. Absorbance readings were taken at 1 minute intervals for 5 minutes.

(d) Cytochrome-C oxidase (essentially after the method of Matsumoto et al., 1971)

Crude enzyme extract was prepared from leaf homogenates by the dialysis concentration method. One gram fresh weight of starting material was reduced to a final volume of 0.2 ml. Enzyme activity was followed spectrophotometrically by the oxidation of reduced cytochrome-C. Reduced cytochrome-C was prepared by the method of Horie and Morrison (1963). To prepare 10 ml of 1×10^{-4} M reduced cytochrome-C, 5 ml of a 1×10^{-4} M solution of cytochrome-C was treated with 5.0 mg of solid sodium dithionite. The reduced cytochrome-C was then passed through a column, 2 cm in

diameter and 4 cm high containing Dowex 1 resin in the acetate form, and washed through the resin with distilled water. This treatment removed excess dithionite and products of dithionite oxidation. The final solution of cytochrome-C contained acetate ions and had a pH of about 5.7. The assay mixture, at a final volume of 3 ml in a curvette was as follows:

1.5 ml 0.1 M potassium phosphate buffer, pH 7.0

1.5 ml 1×10^{-4} M reduced cytochrome-C

Prior to addition of enzyme, percentage transmittance at 550 nm was adjusted to read 30. The reaction was started by adding 0.05 ml of crude leaf enzyme and thoroughly mixing for 30 seconds. Spectrophotometer readings were then taken at 30 second intervals for up to 5 minutes.

(e) Glutamate dehydrogenase and NADH oxidase (after the method of Matsumoto et al., 1971)

Crude leaf enzyme extracts were prepared from 1.0 gm fresh weight of leaf material by the dialysis concentration method. Final extract volumes were 0.2 ml. Enzyme reactions were followed by absorbance changes at 340 nm wavelength. Transmittance was adjusted to read 100 percent for 3 ml of assay mixture. Crude enzyme was added with thorough stirring for one minute to allow for temperature equilibration. Spectrophotometer readings were taken at 30 second intervals for periods of up to 5 minutes. The assay solution for glutamate dehydrogenase was composed of the following, in 10 ml of 0.05 M tris-HCl-buffer, pH 7.6:

5 mg α -ketoglutaric acid

0.5 mg NADH

53.5 mg ammonium chloride

The reaction was started by adding 0.05 ml of crude leaf enzyme. The assay solution for NADH oxidase was made up as follows:

0.5 ml of 0.1 M phosphate buffer, pH 7.2

0.2 ml of 1 mM NADH

0.5 ml of 1.2 M sucrose

1.8 ml of distilled water

The reaction was started by adding 0.1 ml of crude leaf enzyme.

(f) Ribulose 1,5-diphosphate carboxylase (assay method after Chen, McMahon and Borgorad, 1967)

Crude leaf enzyme was prepared from 1.0 gm fresh weight of leaf material by the dialysis concentration method. The final extract volume was adjusted to 0.2 ml. Enzyme reactions were carried out in 2 ml glass vials with the following assay solution composition per 10 ml of 0.05 M tris-HCl buffer, pH 7.6:

0.00391 gm Ribulose diphosphate
 0.0024 gm Sodium EDTA
 0.046 gm Glutathione
 0.051 gm Magnesium chloride ($6H_2O$)

To 0.2 ml of assay solution was added 0.05 ml of crude leaf enzyme. The reaction was started by adding 0.2 ml of ^{14}C -sodium bicarbonate (100 μg per ml, specific activity of 10 μCi per ml). After a 5.0 minute incubation at $28^{\circ}C$, the reaction was stopped and unreacted bicarbonate removed by adding 0.2 ml of 5 N hydrochloric acid per vial. The residual radioactivity in each vial was counted in a Unilux liquid scintillation counter by transferring 0.1 ml of reaction product to 10 ml of DIOTOL liquid scintillation fluid. Vials with scintillator were left in the counter overnight to eliminate light-stimulated emissions. Samples were counted for 1 minute and enzyme activity expressed as counts per minute, following a correction for a zero blank. The zero blank was made up of assay solution with distilled water replacing crude leaf enzyme extract. The composition of DIOTOL liquid scintillator used, was as follows:

500 ml Toluene
 500 ml Dioxane
 300 ml Methanol
 104 gm Naphthalene

6.5 gm PPO (2,5-diphenyloxazole)

130 gm (POPOP) 1,4-di(2-(5-phenyloxazolyl))-benzene

5. Enzymes Assayed In Situ

(a) Nitrate reductase (after the method of Randall, 1969)

Tissue discs were removed from tobacco leaves of a specific age by punching out 10 discs with a cork borer, 4 mm inside diameter. The ten discs were weighed and their fresh weight recorded. The discs were infiltrated with nitrate substrate by transferring 10 discs to five millilitres of nitrate substrate (0.1 M potassium nitrate in 0.05 M phosphate buffer, pH 7.0) and forming and releasing a vacuum 4-5 times. Tubes containing discs and substrate were stoppered and incubated in the dark at 28°C for 60 minutes. Nitrite released was measured by adding to each tube the following reagents:

(i) 2.5 ml 1 percent sulphanilamide ($\frac{W}{V}$) in 25 percent hydrochloric acid

(ii) 2.5 ml 0.02 percent N-(1-naphthyl)-ethylene diamine-2HCl

The colour produced was measured in a spectrophotometer set at 550 nm.

Enzyme activity was expressed as nMoles Nitrite/gm fresh weight of leaf tissue/hour and was estimated by the following equation:

$$\frac{\text{ppm Nitrite} \times 217.4}{\text{fresh weight tissue (gm)}} \times \frac{60}{\text{Incubation time (mins.)}}$$

Where ppm Nitrite = Absorbance 550 nm x 0.82 (0.82 was the slope of a plot of nitrite concentration against absorbance 550 nm).

6. Chlorophyll Determinations

Leaf chlorophylls were extracted from 10 discs, each 4 mm diameter, punched from leaves of various ages. Discs were weighed and extracted in 5 ml of absolute ethanol overnight at 4°C. Extracts were scanned in a Unicam SP.800 Ultraviolet Spectrophotometer between wavelengths 850 nm and 430 nm. Chlorophylls "a" and "b" were determined from the recorded

traces and expressed as absorption per gram fresh weight of leaf tissue. Chlorophyll "a" was measured from its peak of absorption at 660 nm and chlorophyll "b" from its peak at 430 nm.

RESULTS

1. Effect of Virus Infection on Enzymes of the Respiratory Chain and Mitochondria

(a) Cytochrome-C oxidase

Enzyme activities for the comparisons healthy versus infected light green and dark green island tissues are presented graphically in Figures 7, 8, 9 and 10. From immature tissue comparisons (Figures 7 and 8) the greatest enzyme activity was associated with tissue extracts from uninfected plants. Activities in infected dark green island tissues were less compared with healthy tissues of the same chronological age but greater than the activities in light green island tissues from the same leaf. As leaves matured, enzyme activities in infected light green island tissues exceeded the activities in comparably aged healthy tissues (Figures 9, 10).

A profile for enzyme reaction rates versus leaf tissue age (leaf position from the stem apex) was constructed using reaction rates derived from the slope of individual enzyme activity profiles (Figures 7, 8, 9 and 10) for the comparisons healthy versus infected light green and dark green island tissues (see Figure 11). In uninfected tobacco leaves, cytochrome-C oxidase activity reaches a peak just prior to maturity or full leaf expansion and thereafter declines rapidly with the onset of senescence. Reaction rates in extracts of infected, dark green island tissues, although less than in comparably aged uninfected tissues, tended to follow more closely the profile of healthy tissue extracts. The sharp rise in enzyme activity as healthy leaves approach maturity may be analogous to the climacteric rise in respiration rates of many fruits as they approach maturity. No sharp rise in enzyme activity occurred in infected, light green island tissues. Reaction rates in light green island tissues remained fairly constant in extracts from over-mature leaves (leaves that had reached full expansion size) and displayed no decline as was typical for over-mature uninfected leaves.

Figure 7

Cytochrome-C oxidase activity (Abs. 550 nm/gm fresh weight of leaf tissue) versus reaction time for young leaf tissue extracts (leaf position 6 from the stem apex). For points plotted see Appendix 12.

(○——○) - Healthy tissue

(□-----□) - Light green island tissue

Figure 8

Cytochrome-C oxidase activity (Abs. 550 nm/gm fresh weight of leaf tissue) versus reaction time (minutes) for immature leaf tissue extracts (leaf position 9 from the stem apex). SE of points plotted = 0.028. (See Appendix 13)

(○——○) - Healthy tissue

(□-----□) - Light green island tissue

(Δ---Δ) - Dark green island tissue

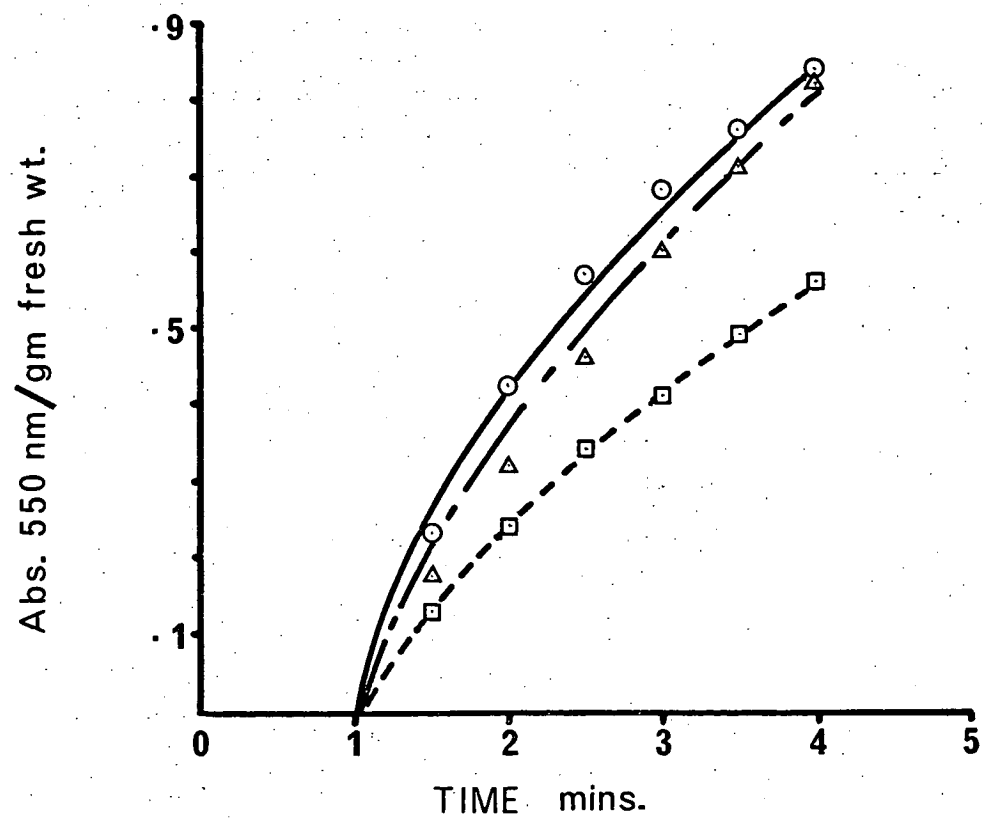
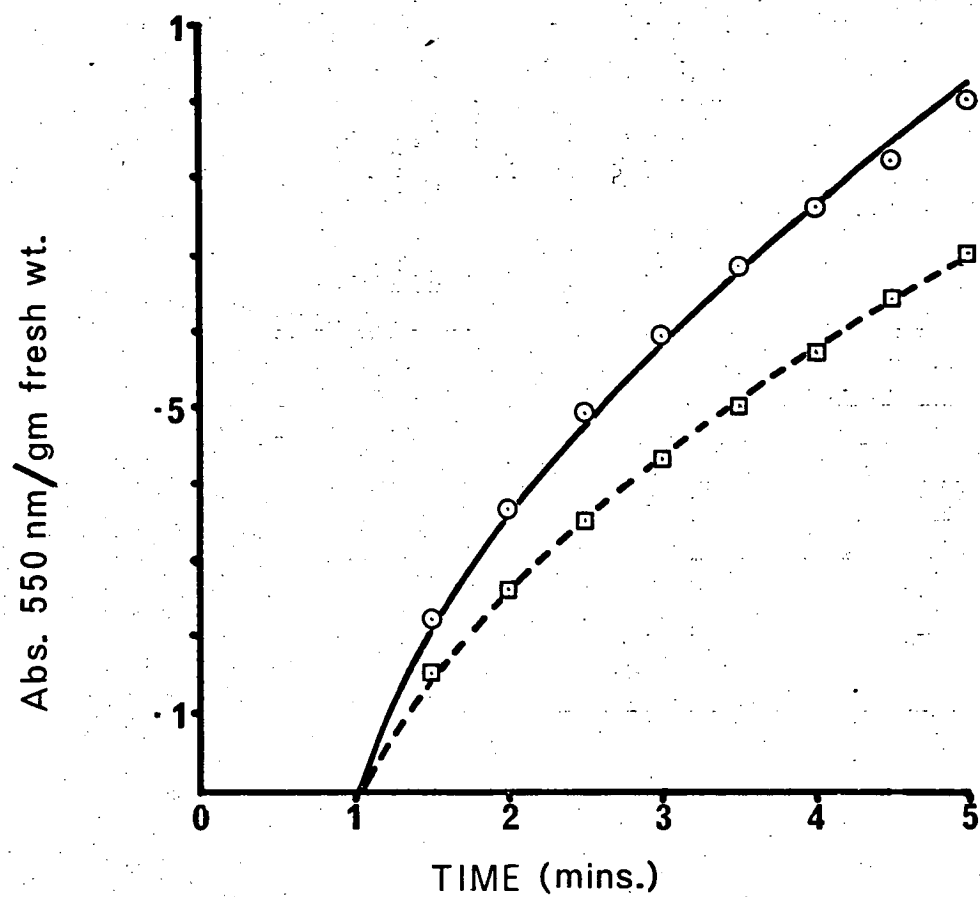


Figure 9

Cytochrome-C oxidase activity (Abs. 550 nm/gm fresh weight of leaf tissue) versus reaction time (minutes) for mature leaf tissue extracts (leaf position 10 from the stem apex). SE for points plotted = 0.0128 (see Appendix 14).

- (○——○) - Healthy tissue
- (□-----□) - Light green island tissue
- (Δ— — —Δ) - Dark green island tissue

Figure 10

Cytochrome-C oxidase activity (Abs. 550 nm/gm fresh weight of leaf tissue) versus reaction time (minutes) for senescing leaf tissue extracts (leaf position 11, 12 from the stem apex). SE for points plotted = 0.0317 (see Appendix 15).

- (○——○) - Healthy tissues
- (□-----□) - Light green island tissues

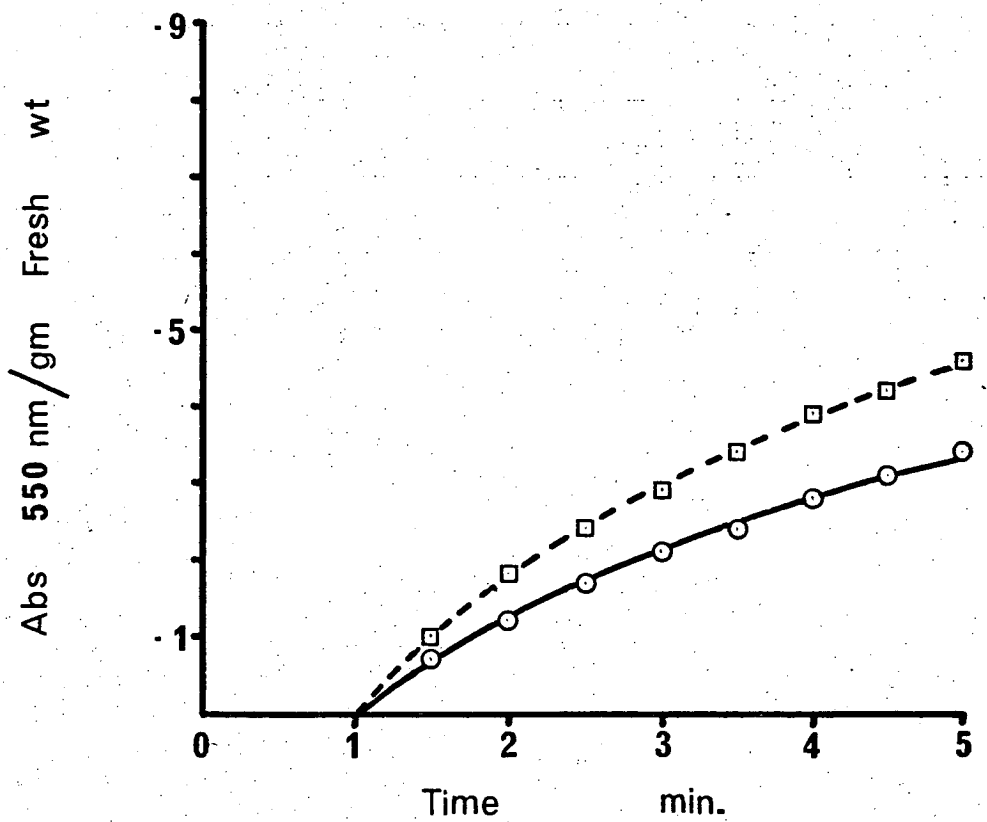
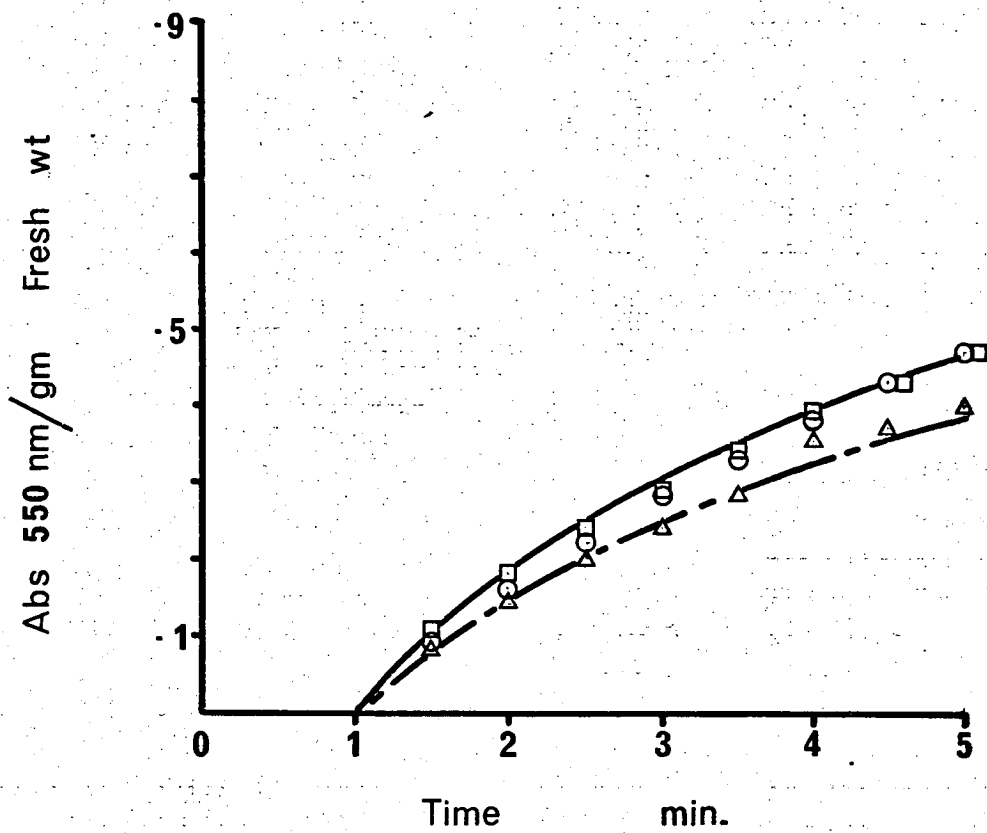
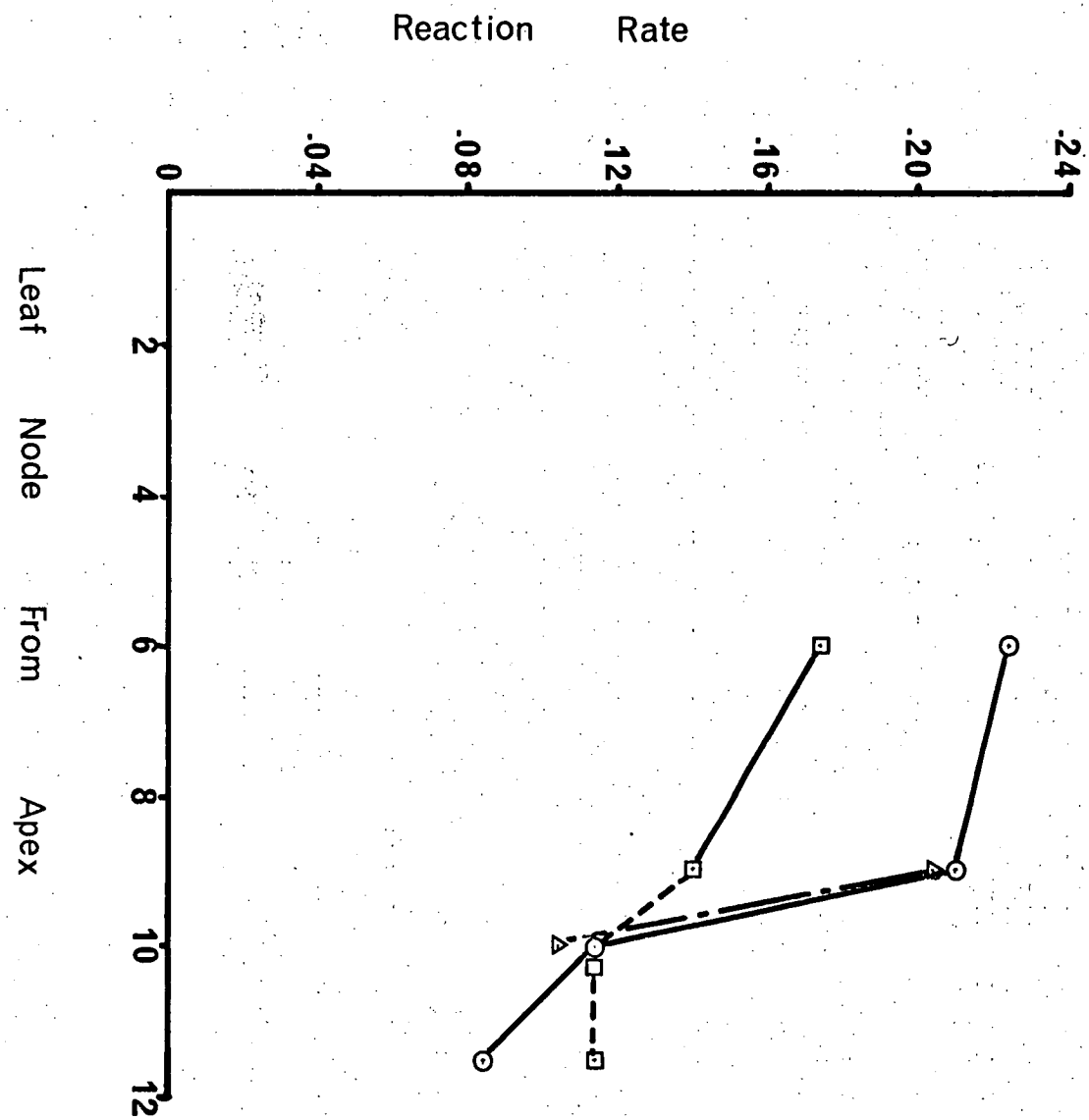


Figure 11.

Relation between cytochrome-C oxidase reaction rate (change in Abs. 550 nm/minute/gm fresh weight of leaf tissue) and leaf tissue age (leaf position from the stem apex).

- (O———O) - Healthy tissues
- (□-----□) - Light green island tissues
- (Δ—...—Δ) - Dark green island tissues



(b) NADH oxidase

Enzyme activity in immature (leaf position 6 from the stem apex) and mature leaves (leaf position 10 from the stem apex) was reduced with virus infection. The activity of NADH oxidase was less in both light green and dark green island tissues from infected leaves compared with similarly aged healthy leaves (Figures 12 and 13). In over-mature leaf tissues, however, enzyme activity was greater in light green island tissue compared with leaf tissue of the same chronological age from healthy plants (Figure 14). Enzyme activities in light green and dark green island tissues of mature infected leaves were similar.

Reaction rates, as estimated from the slope of individual enzyme reaction curves (Figures 12, 13 and 14), for each comparison are presented in Figure 15. Enzyme activities in uninfected leaf tissues declined rapidly once leaves reached maturity. No fall in activity was measured for infected over-mature light green island tissue.

(c) Glutamate dehydrogenase

The ratio of enzyme activity in light green island tissues to activity in similarly aged leaves from uninfected plants varied with chronological age of the leaves. Enzyme activity was less in young, infected light green island tissues than in healthy leaf tissue of the same age (Figure 16). However, for immature, mature and over-mature comparisons, activity was greater in infected, light green island leaf tissue (Figures 17, 18 and 19). Enzyme activity in dark green islands from immature and mature infected leaves was less compared with light green island tissues from the same leaves and similar to activities in healthy leaves of a comparable age (Figures 17 and 18).

Reaction rates, constructed from the slopes of individual enzyme reaction graphs (Figures 16, 17, 18 and 19), for healthy and virus-infected tissue comparisons, varied with leaf tissue age (Figure 20). Enzyme activity in healthy leaf tissues increased as leaves matured but

Figure 12

NADH oxidase activity (Abs. 340 nm/gm fresh weight of leaf tissue) versus reaction time (minutes) for young leaf tissue extracts (leaf position 6 from the stem apex). For actual values of points plotted see Appendix 16.

(O———O) - Healthy tissues
 (□-----□) - Light green island tissues

Figure 13

NADH oxidase activity (Abs. 340 nm/gm fresh weight of leaf tissue) versus reaction time (minutes) for immature leaf tissue extracts (leaf position 9 from the stem apex). For actual values of points plotted see Appendix 16.

(O———O) - Healthy tissues
 (□-----□) - Light green island tissues
 (Δ-----Δ) - Dark green island tissues

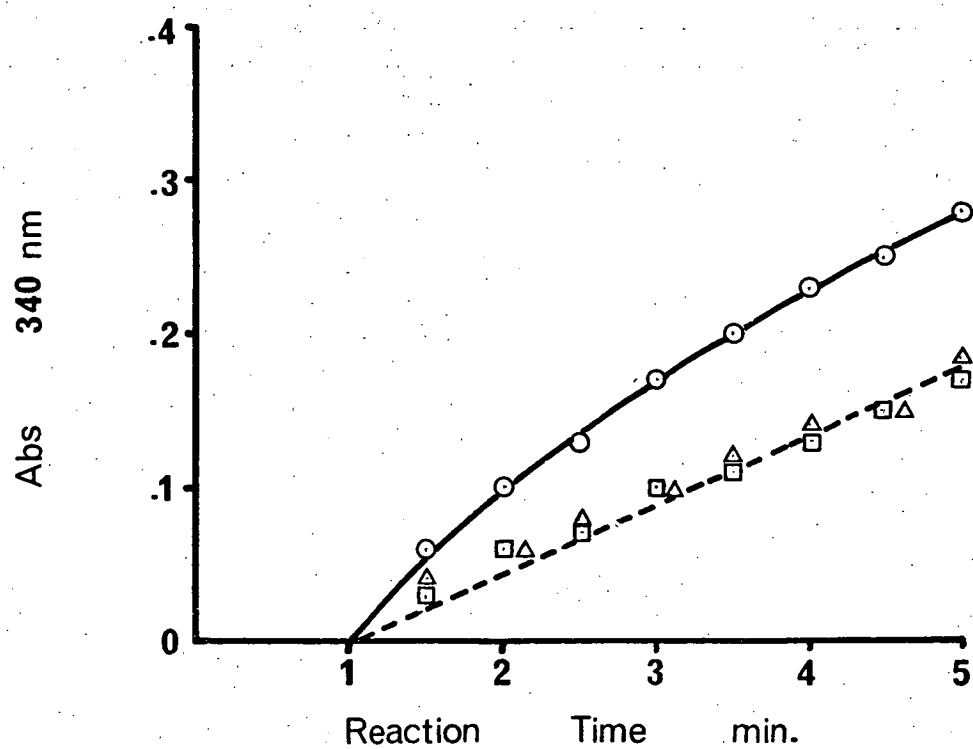
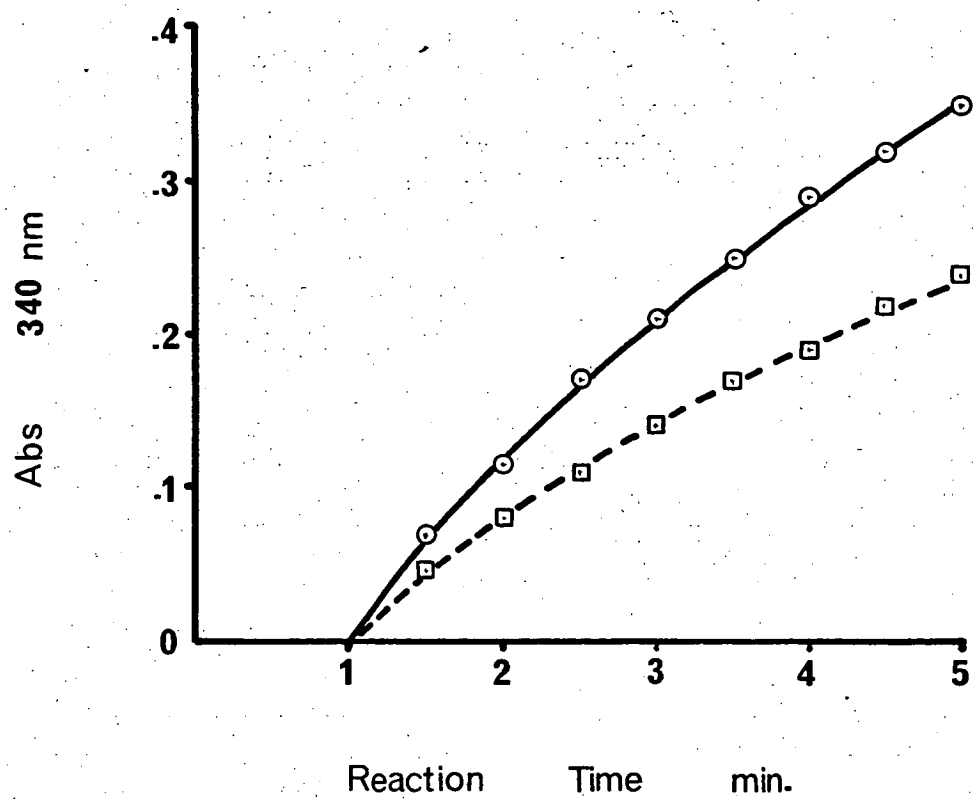


Figure 14

NADH oxidase activity (Abs. 340 nm/gm fresh weight of leaf tissue) versus reaction time (minutes) for mature-senescent leaf tissue extracts (leaf position 11 from the stem apex). For actual values of points plotted see Appendix 16.

(○——○) - Healthy tissues

(□-----□) - Light green island tissues

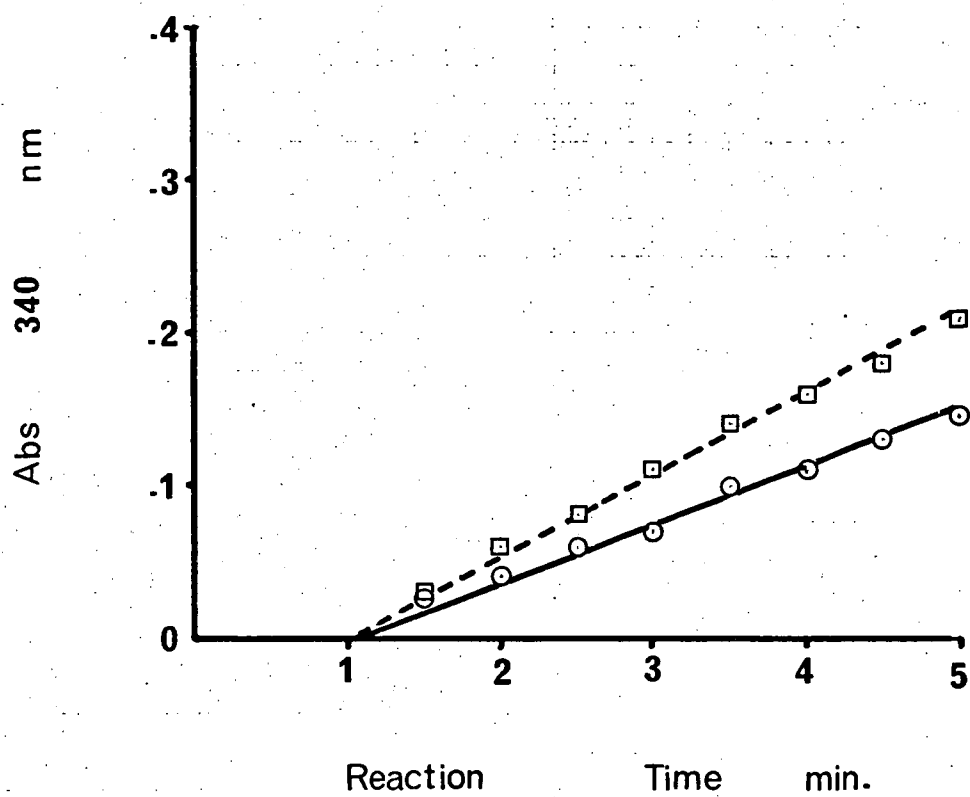


Figure 15

Relation between NADH reaction rate (change Abs. 340 nm/minute/gm fresh weight of leaf tissue) and leaf tissue age (leaf position from the stem apex).

- (○——○) - Healthy tissue
- (□-----□) - Light green island tissue
- (▲) - Dark green island tissue

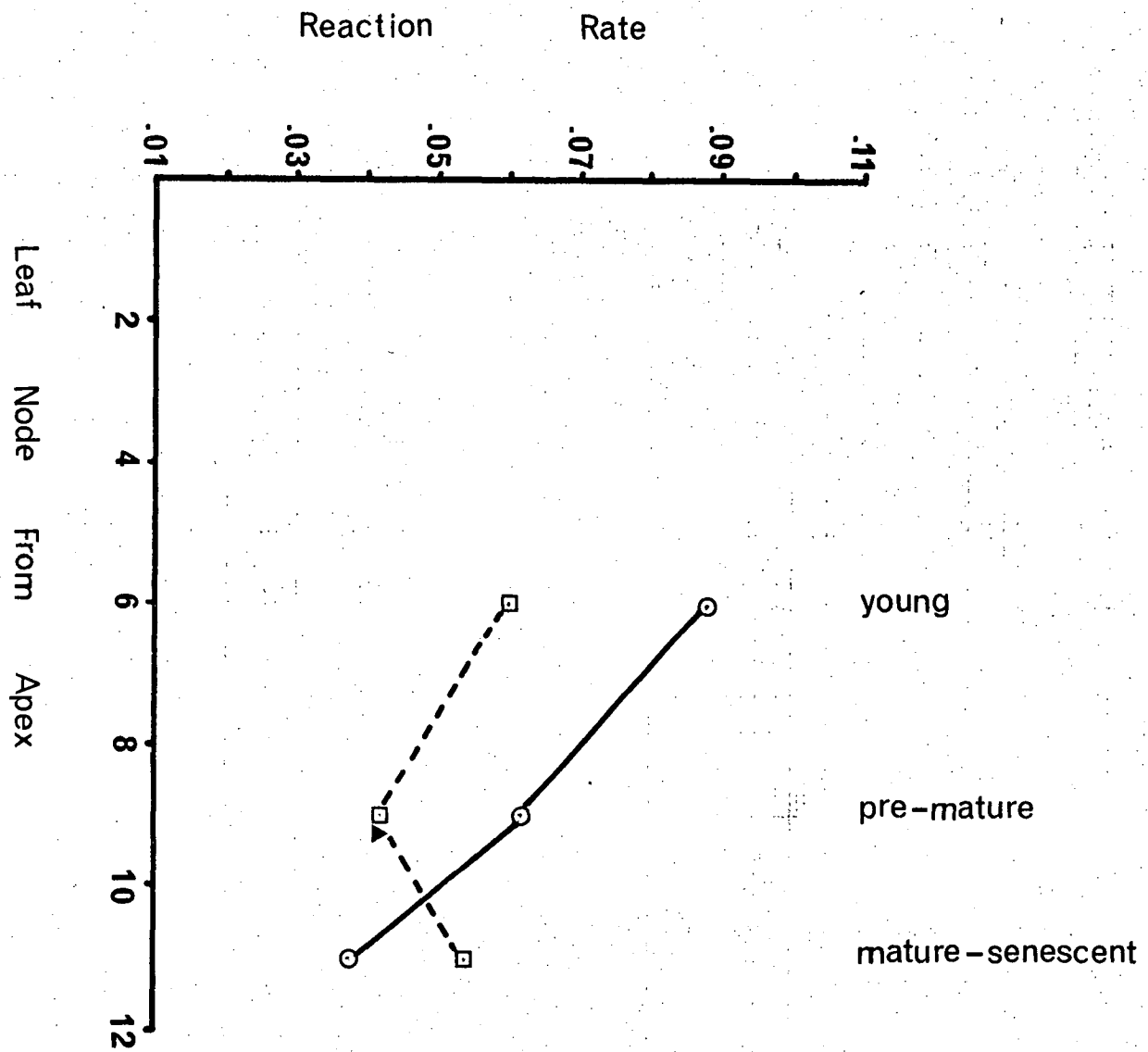


Figure 16

Glutamate dehydrogenase activity (Abs. 340 nm/gm fresh weight of leaf tissue) versus reaction time (minutes) for young leaf tissue extracts (leaf position 6 from the stem apex). For values of plotted points see Appendix 17.

(○——○) - Healthy tissues

(□-----□) - Light green island tissue

Figure 17

Glutamate dehydrogenase activity (Abs. 340 nm/gm fresh weight of leaf tissue) versus reaction time (minutes) for immature leaf tissue extracts (leaf position 9 from the stem apex). SE of points plotted = 0.053 (see Appendix 18).

(○——○) - Healthy tissue

(□-----□) - Light green island tissue

(△---△) - Dark green island tissue

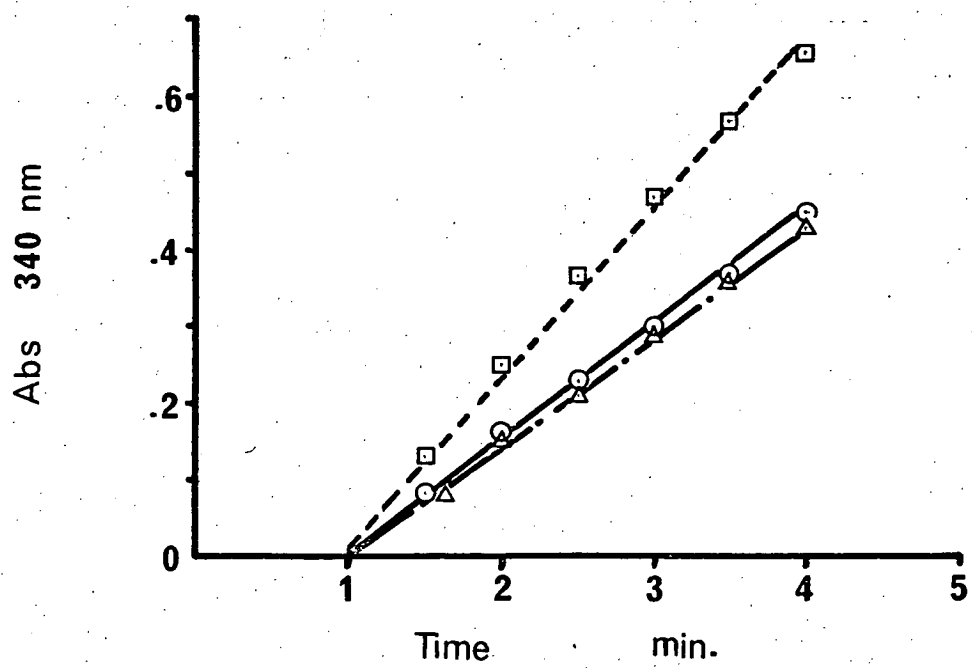
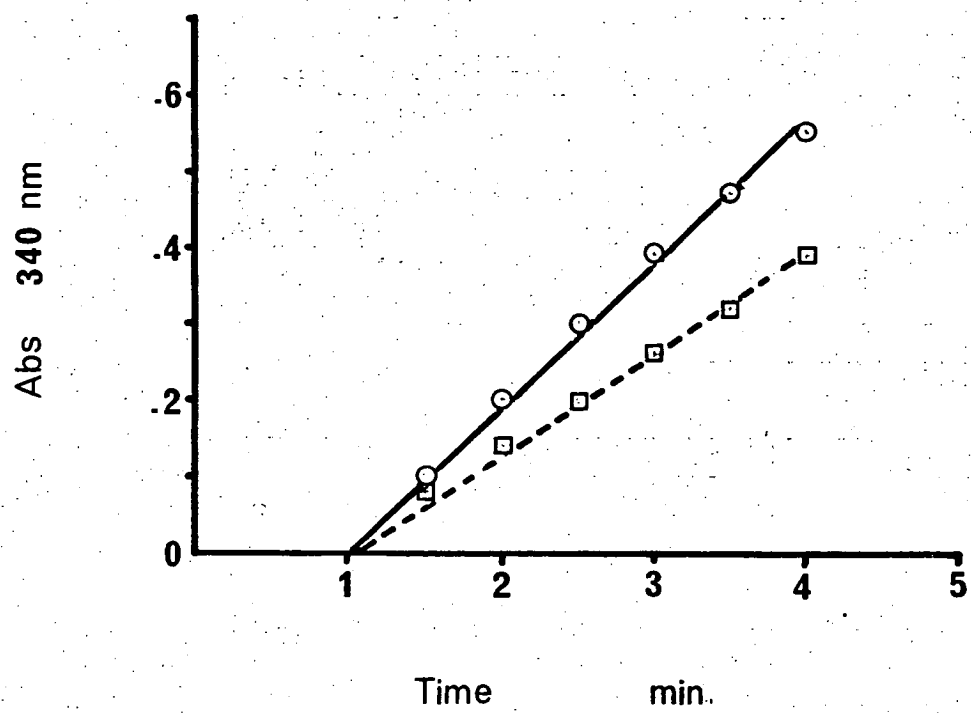


Figure 18

Glutamate dehydrogenase activity (Abs. 340 nm/gm fresh weight of leaf tissue) versus reaction time (minutes) for mature leaf tissue extracts (leaf position 10 from the stem apex). SE of points plotted = 0.076 (see Appendix 19).

(○——○) - Healthy tissue

(□-----□) - Light green island tissue

Figure 19

Glutamate dehydrogenase activity (Abs. 340 nm/gm fresh weight of leaf tissue) versus reaction time (minutes) for senescent leaf tissue extracts (leaf positions 11, 12 from the stem apex). For value of points plotted see Appendix 17).

(○——○) - Healthy tissues

(□-----□) - Light green island tissues

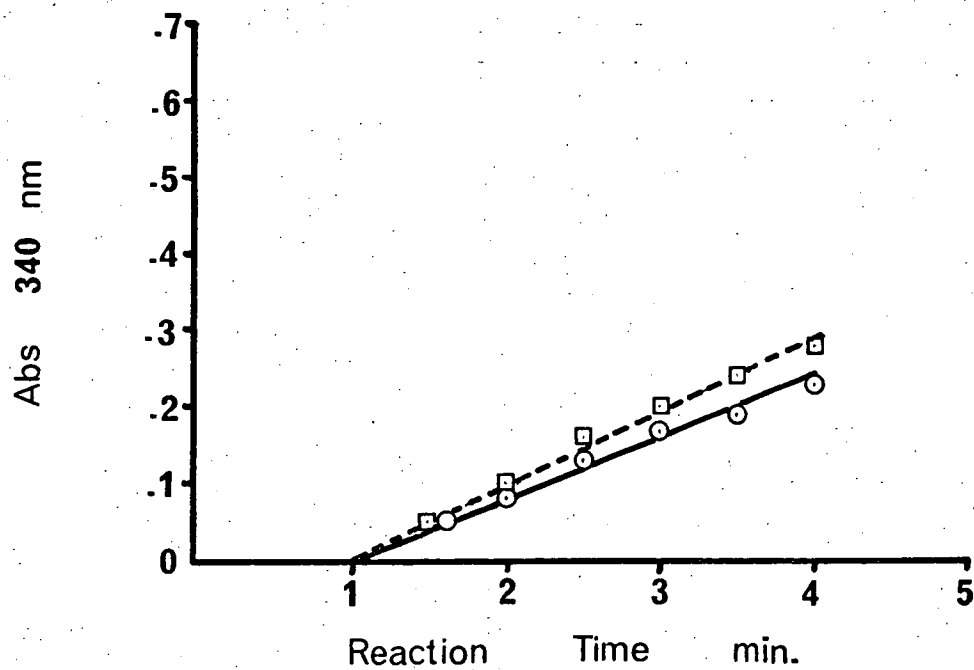
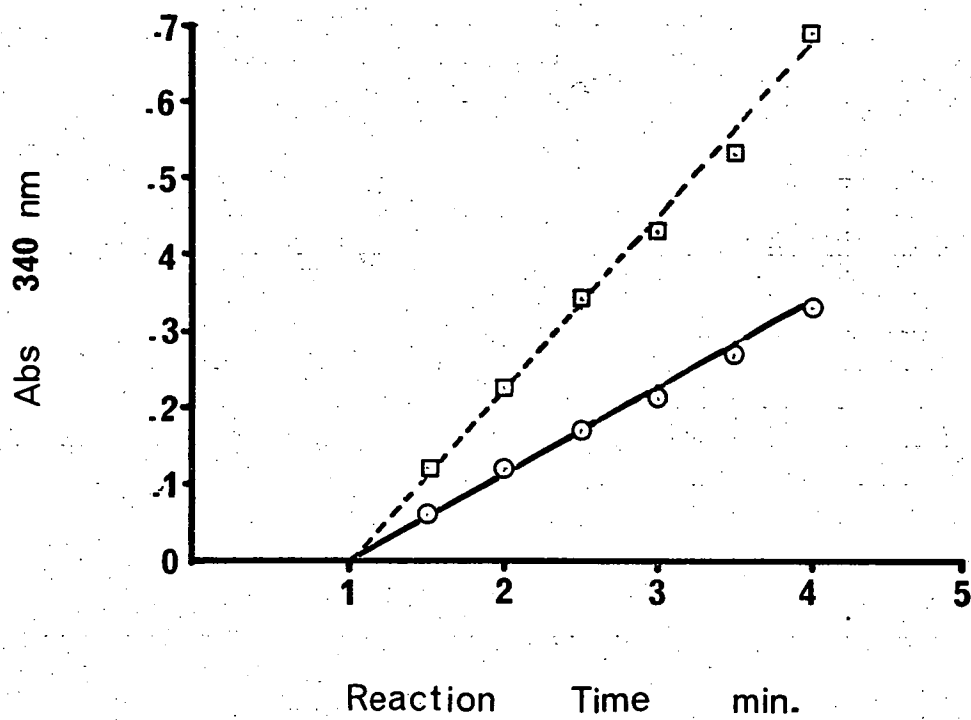


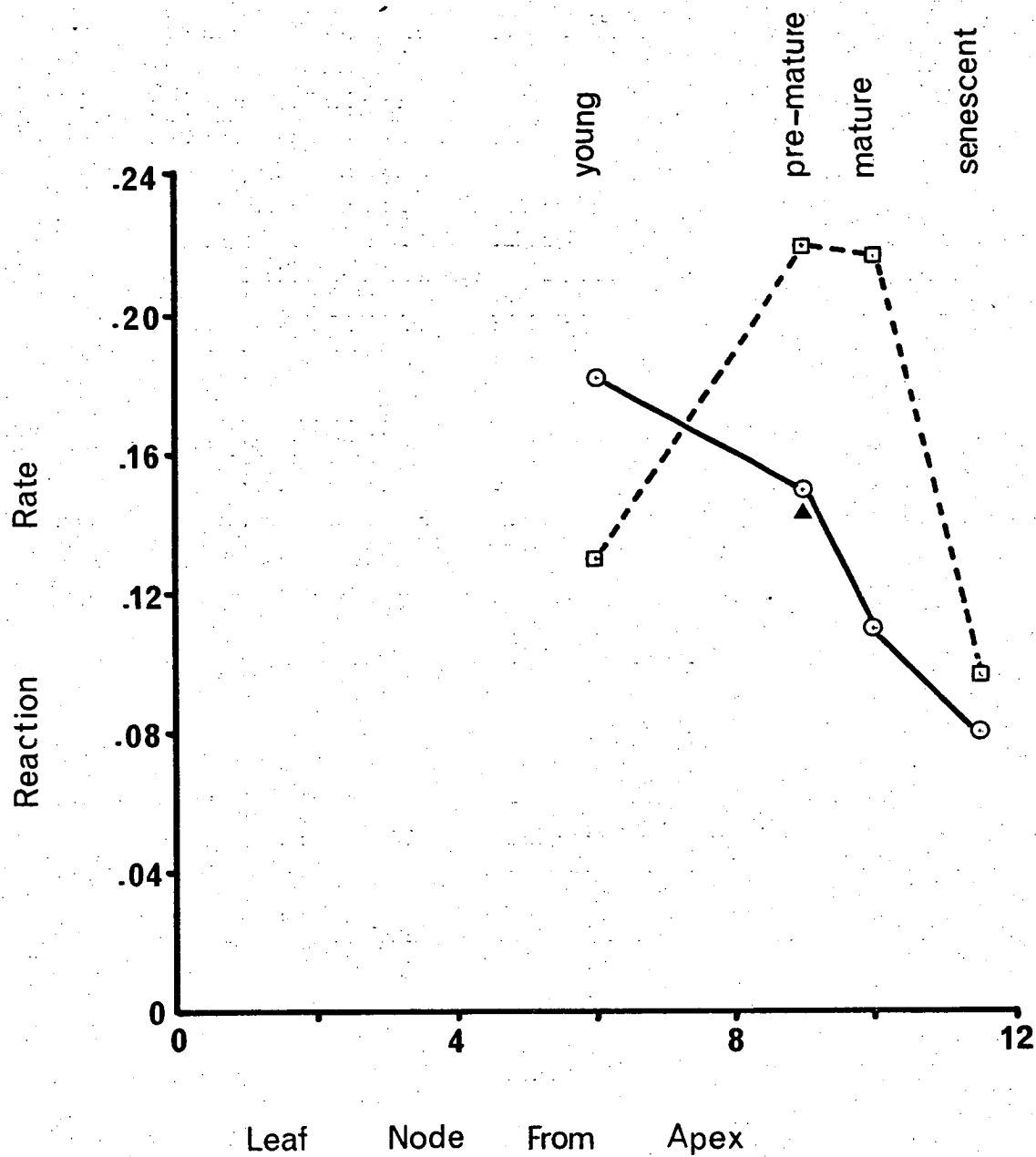
Figure 20

Relation between glutamate dehydrogenase reaction rate (change in Abs. 340 nm/minute/gm fresh weight of leaf tissue) and leaf tissue age (leaf position from the stem apex).

(○——○) - Healthy tissue

(□-----□) - Light green island tissue

(▲) - Dark green island tissue



declined in over-mature leaves. In light green island tissues from virus-infected leaves, reaction rates increased sharply as leaves matured and remained constant in over-mature leaves.

The relationship between virus-infected, light green island leaf tissue and leaf tissue from uninfected tobacco plants was similar for all mitochondrial enzymes studied. Enzyme activities were less in young infected leaves than in young healthy leaves, but were greater in mature, infected leaves than in mature healthy leaves. While the activities of all enzymes declined in over-mature healthy leaves, activities remained constant in leaves of a similar chronological age, from virus-infected plants.

2. Effect of Infection on Enzymes Associated with Carbohydrate Metabolism

(a) Phosphoglucoisomerase

Reaction rates for the Embden-Meyerhof-Parnas pathway enzyme, phosphoglucoisomerase, as presented in Figure 21, were recorded as mgm equivalents of fructose produced during a 45 minute incubation period. Absorbance 500 nm data for the comparisons healthy versus infected light green and dark green island tissues was converted to fructose equivalents using a standard curve of fructose concentration plotted against absorbance 500 nm (see Appendix 21).

Within each tissue-age comparison, enzyme activity was similar for healthy and infected light green and dark green island leaf tissue. Enzyme activities were compared in young tissues (leaf position 4 from the stem apex) and mature leaves (leaf position 8 from the stem apex). Enzyme activity, expressed on a tissue fresh weight basis, increased with leaf age but declined in over-mature tissue.

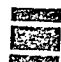


(b) Glucose-6-phosphate dehydrogenase (G-6-PDH)

Enzyme activities for individual treatments are presented in Figures 22 and 23 and summarized as reaction rates in Figure 24. Enzyme activity

Figure 21

Phosphoglucoisomerase reaction rate (mgm Equivalents of fructose produced in 45 minutes reaction time/gm fresh weight of leaf tissue) for extracts of leaf tissues of different ages (leaf position from stem apex).

SE of points plotted = 0.418 (see Appendix 20).

-  Healthy tissue
-  Light green island tissue
-  Dark green island tissue

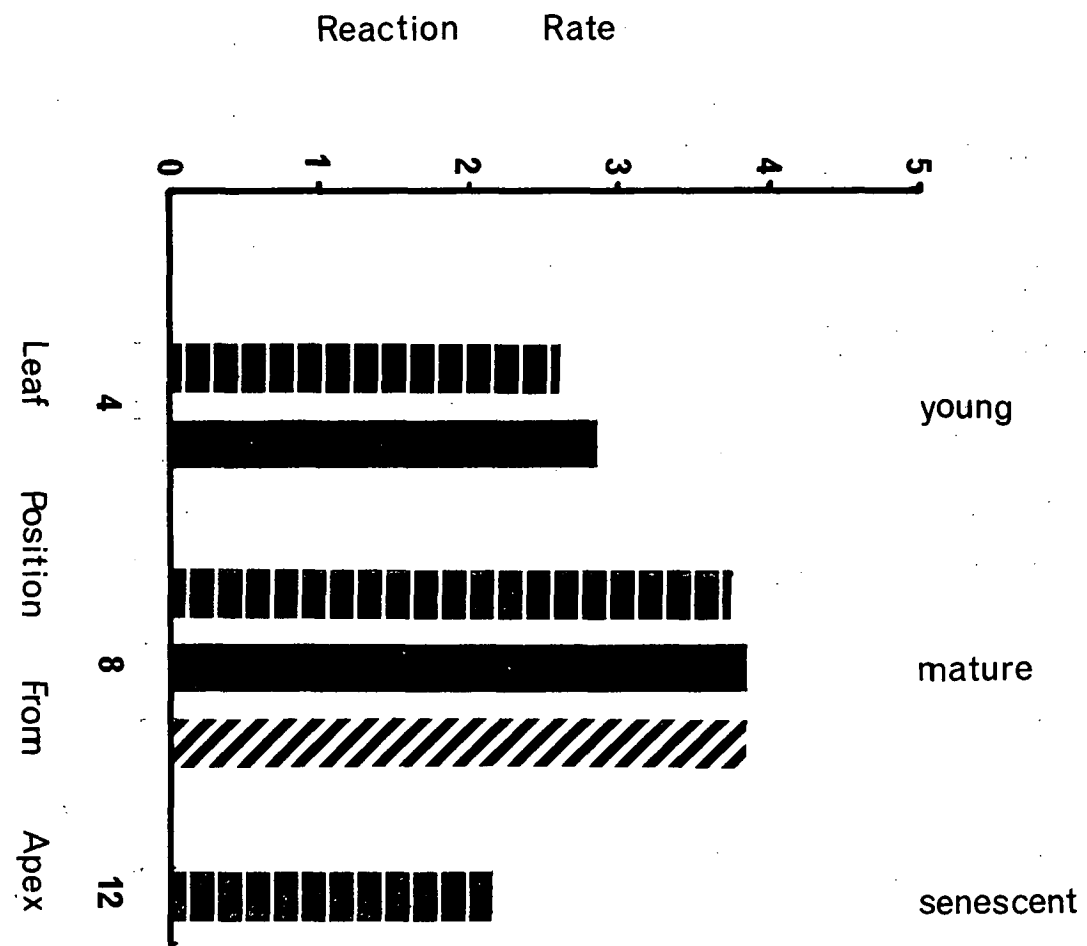


Figure 22

Glucose-6-phosphate dehydrogenase activity (Abs. 340 nm/gm fresh weight leaf tissue) versus reaction time (minutes) for young leaf tissue extracts (leaf position 6 from the stem apex).

SE of points plotted = 0.0075 (see Appendix 22).

- (○——○) - Healthy tissue
- (□-----□) - Light green island tissue
- (△—·—·△) - Dark green island tissue

Figure 23

Glucose-6-phosphate dehydrogenase activity (Abs. 340 nm/gm fresh weight leaf tissue) versus reaction time (minutes) for mature leaf tissue extracts (leaf position 9 from the stem apex).

SE of points plotted = 0.0111 (see Appendix 23).

- (○——○) - Healthy tissue
- (□-----□) - Light green island tissue
- (△—·—·△) - Dark green island tissue

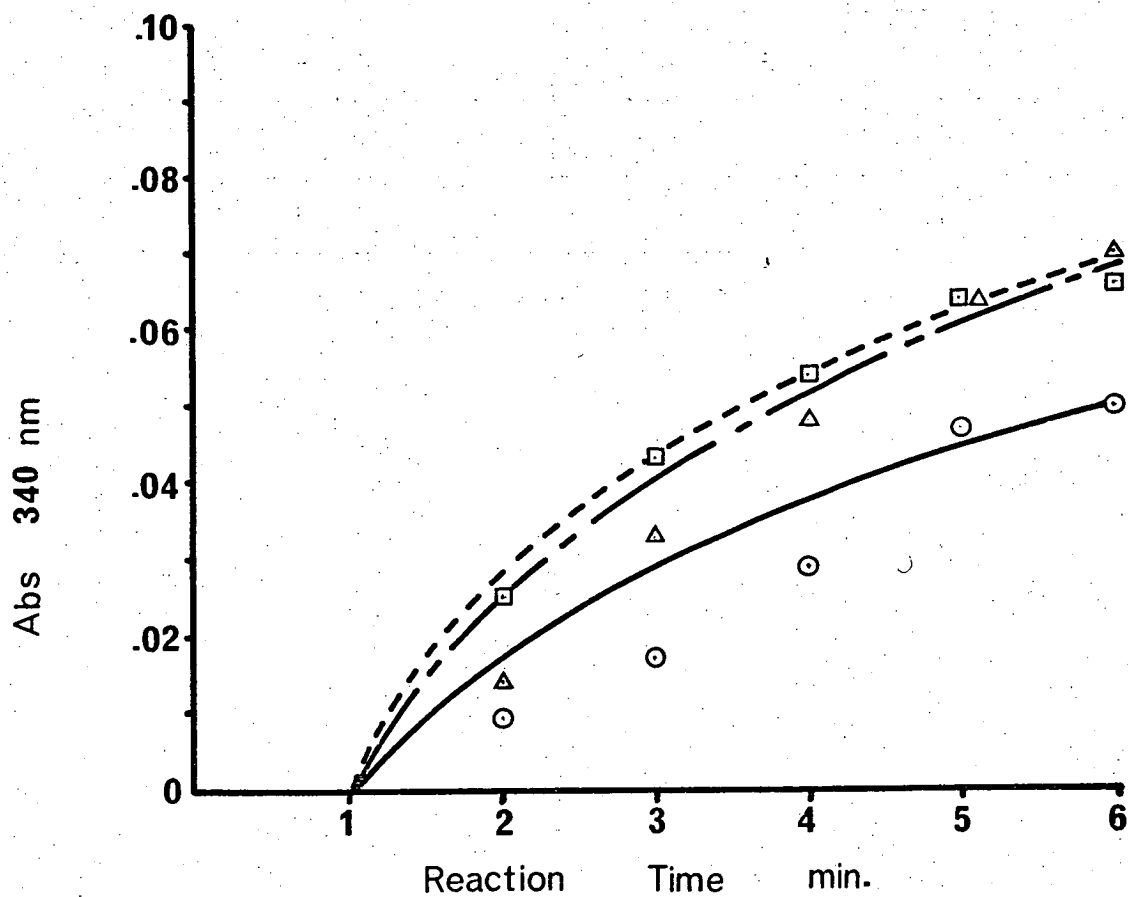
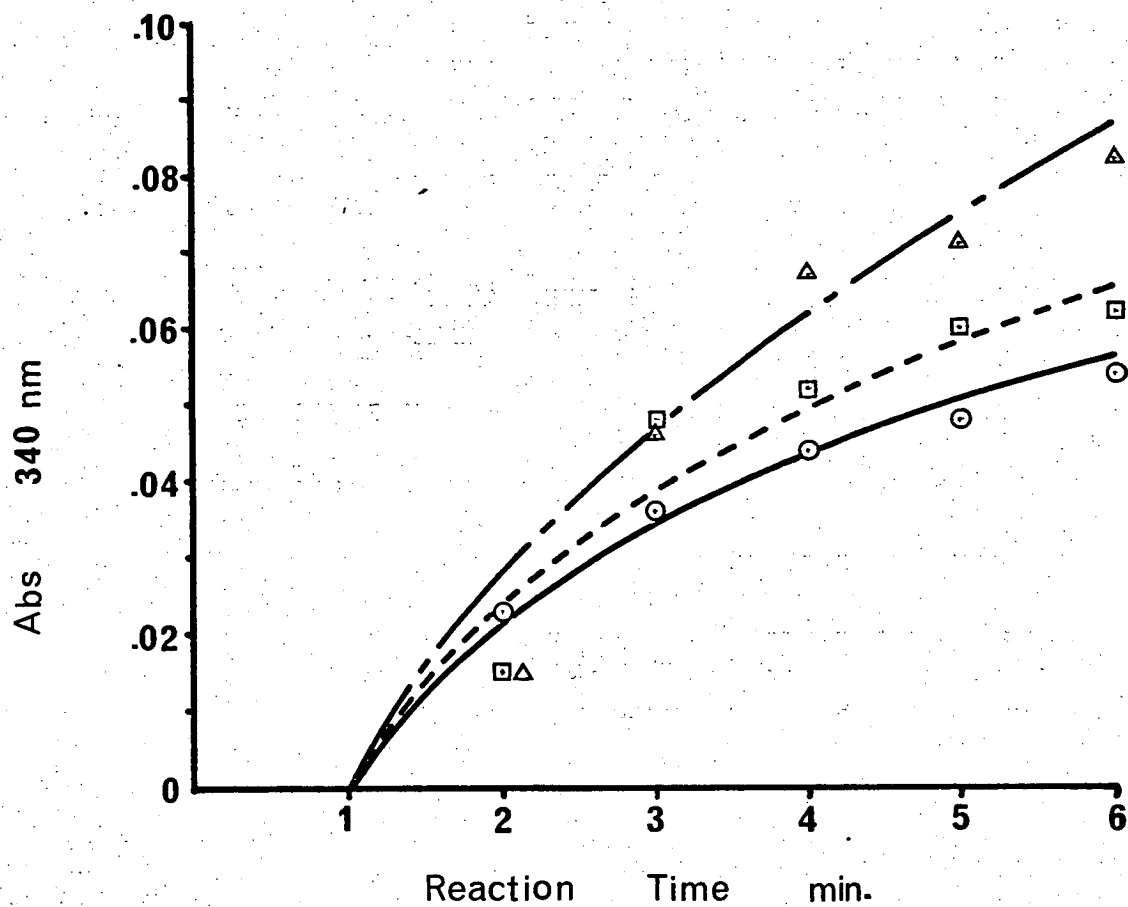
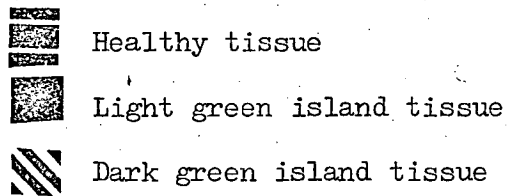
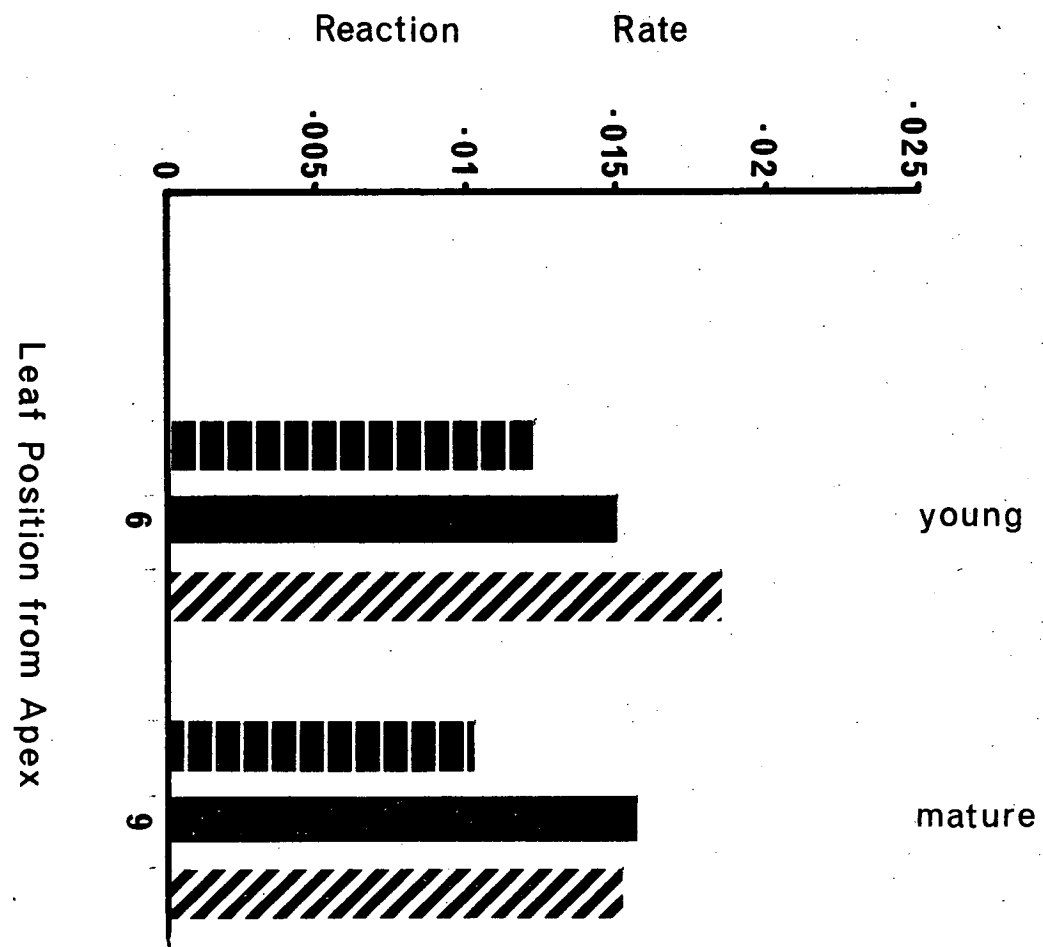


Figure 24

Relation between glucose-6-phosphate dehydrogenase reaction rate (change Abs. 340 nm/minute/gm fresh weight of leaf tissue) and leaf tissue age (leaf position from stem apex).





was greater in young leaf tissues from virus-infected plants when compared with similarly aged tissue from healthy plants (Figures 22 and 24). For the comparison of light green versus dark green island tissue from the same leaf, enzyme activity was higher in dark green island tissue. Enzyme activity relationships between mature healthy and virus-infected leaves were similar to those in young leaves, except for the comparison light green island versus dark green island tissues from the same leaf, where activities were the same (Figures 23 and 24).

(c) Alcohol dehydrogenase

Enzyme activities for the comparisons healthy versus infected light green and dark green island leaf tissues are presented in Figure 25 (young tissues at leaf position 6 from the stem apex) and Figure 26 (mature tissues at leaf position 9 from the stem apex). All activities are summarized as reaction rates (Figure 27) from the changes of absorbance 340 nm during a 5 min. reaction interval.

The effects of infection on enzyme activity depended on the age of leaf supporting virus synthesis. For the comparison immature healthy versus immature infected light green and dark green island tissues, enzyme activity was reduced in leaves from infected plants (Figures 25 and 27). In a comparison of tissue types from mature tobacco leaves, enzyme activity was higher in leaves from infected plants (Figures 25 and 27). For the comparison light green island versus dark green island leaf tissue, enzyme activity in dark green islands was greater compared with light green islands from the same leaf for both young and mature leaves from infected plants (Figures 25, 26 and 27).

Enzymes of carbohydrate metabolism, in particular the pentose phosphate pathway enzyme, glucose-6-phosphate dehydrogenase and the terminal enzyme of glycolysis, alcohol dehydrogenase, were more active in extracts of mature leaves from virus-infected plants than similarly aged leaves from healthy plants. Within leaves from virus-infected plants,

Figure 25

Alcohol dehydrogenase activity (Abs. 340 nm/gm fresh weight leaf tissue) versus reaction time (minutes) for young leaf tissue extracts (leaf position 6 from the stem apex).

SE of points plotted = 0.00394 (see Appendix 24).

(○——○) - Healthy tissue

(□-----□) - Light green island tissue

(Δ—·—·Δ) - Dark green island tissue

Figure 26

Alcohol dehydrogenase activity (Abs. 340 nm/gm fresh weight leaf tissue) versus reaction time (minutes) for mature leaf tissue extracts (leaf position 9 from the stem apex).

SE of points plotted = 0.011 (see Appendix 25).

(○——○) - Healthy tissue

(□-----□) - Light green island tissue

(Δ—·—·Δ) - Dark green island tissue

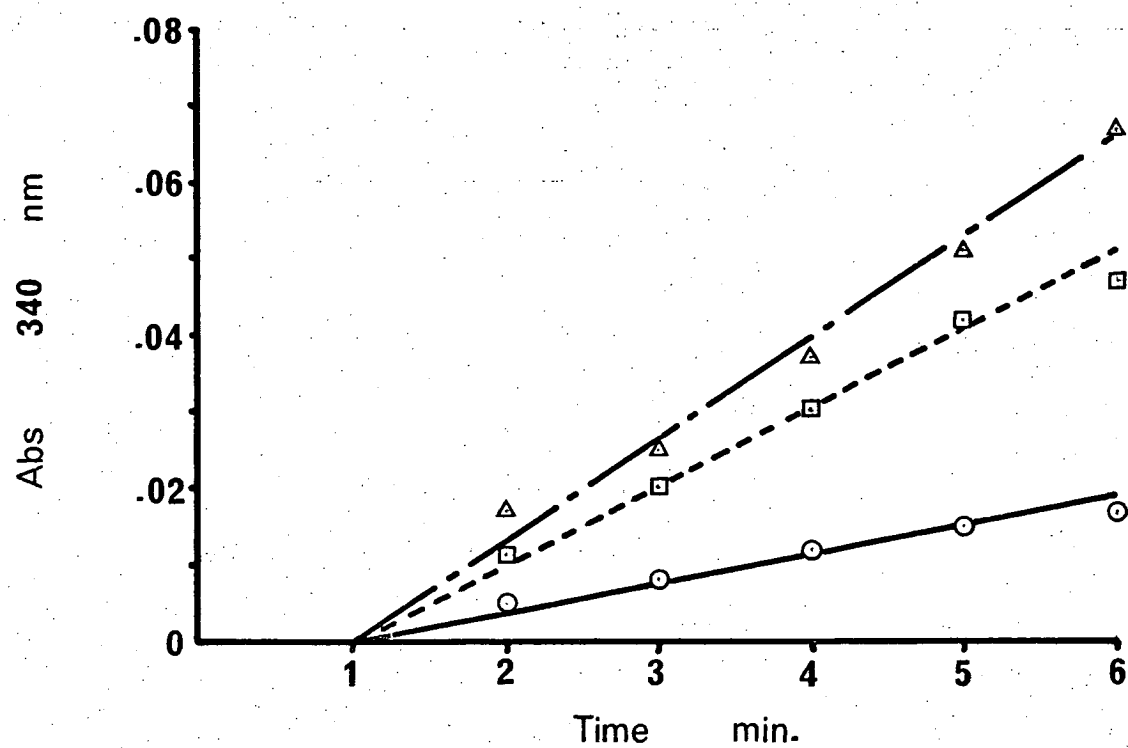
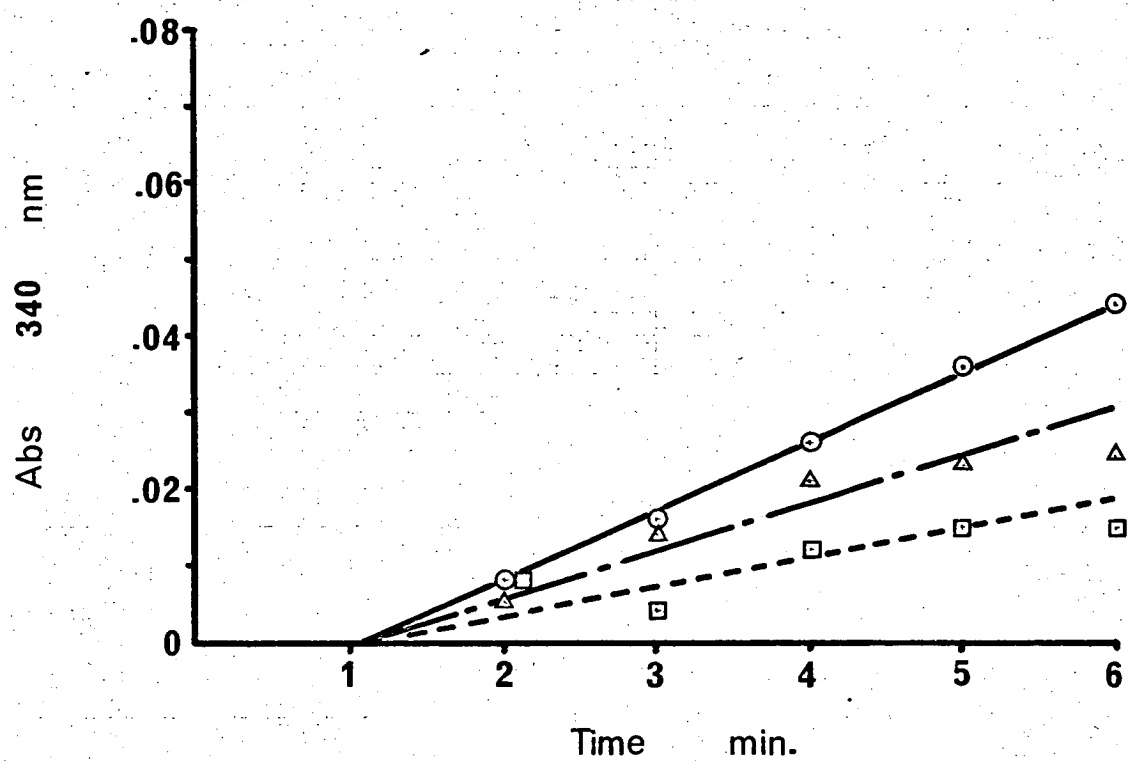
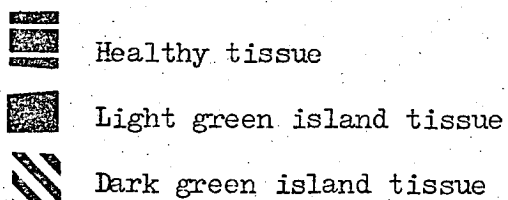
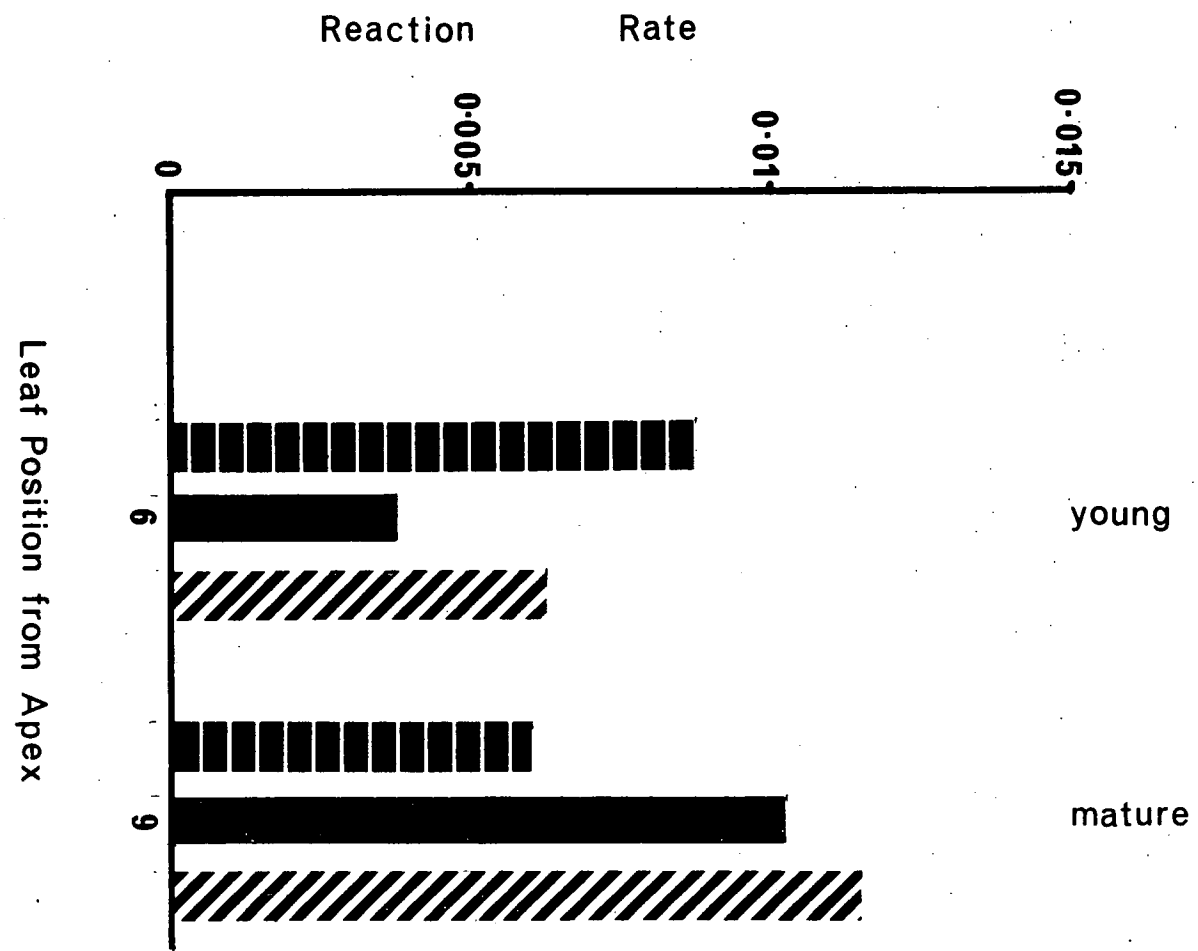


Figure 27

Relation between alcohol dehydrogenase reaction rate (change in Abs. 340 nm/minute/gm fresh weight of leaf material) and leaf tissue age (leaf position from stem apex).





all enzyme activities were higher in dark green island tissues compared with adjoining light green island tissues.

3. Effect of Infection on the Photorespiratory Enzyme, Catalase

Virus infection did not induce new and specific isoenzymes of catalase (Figure 28). However, infection did reduce the number of isoenzymes of catalase normally present in immature and mature leaves. For healthy control plants there were two isoenzymes of catalase in immature and mature leaves (leaf position 7 and 10 from the apex respectively). Only the slower migrating isoenzyme was present in young and senescing leaf tissues. With virus infection the number of isoenzymes, in immature and mature leaf extracts, was reduced to one fast-migrating band for light green islands. The isoenzyme pattern for catalase was similar in healthy leaves and dark green island tissues from virus-infected leaves. Total catalase activity, representing a summation of isoenzyme intensities, for each leaf tissue type/age combination is presented in Figure 29. Catalase activity was much reduced in light green island tissues of all ages compared with both healthy and virus-infected dark green island tissues. The catalase activity/leaf age profile for healthy and dark green island tissues was similar. Catalase activity in young leaves from infected plants represents combined activities in light green and dark green islands as leaves were too small for tissue dissection. The higher level of catalase in young, infected leaves is probably due to the contribution from dark green island tissues.

4. Peroxidase

Patterns of individual isoenzymes of peroxidase, separated and characterized in acrylamide, are presented in Figure 30. Tobacco plants did not produce a specific isoenzyme of peroxidase in response to infection. However, in both immature and mature leaves from virus-infected plants, infection induced a fast, negative migrating isoenzyme that was absent from comparably aged leaves from uninfected plants but present in young

Figure 28

Zymogram of catalase isoenzymes in tobacco leaf tissue extracts, separated in 7.5% acrylamide gels. Intensity ratings of gel staining reactions are presented in Appendix 26.

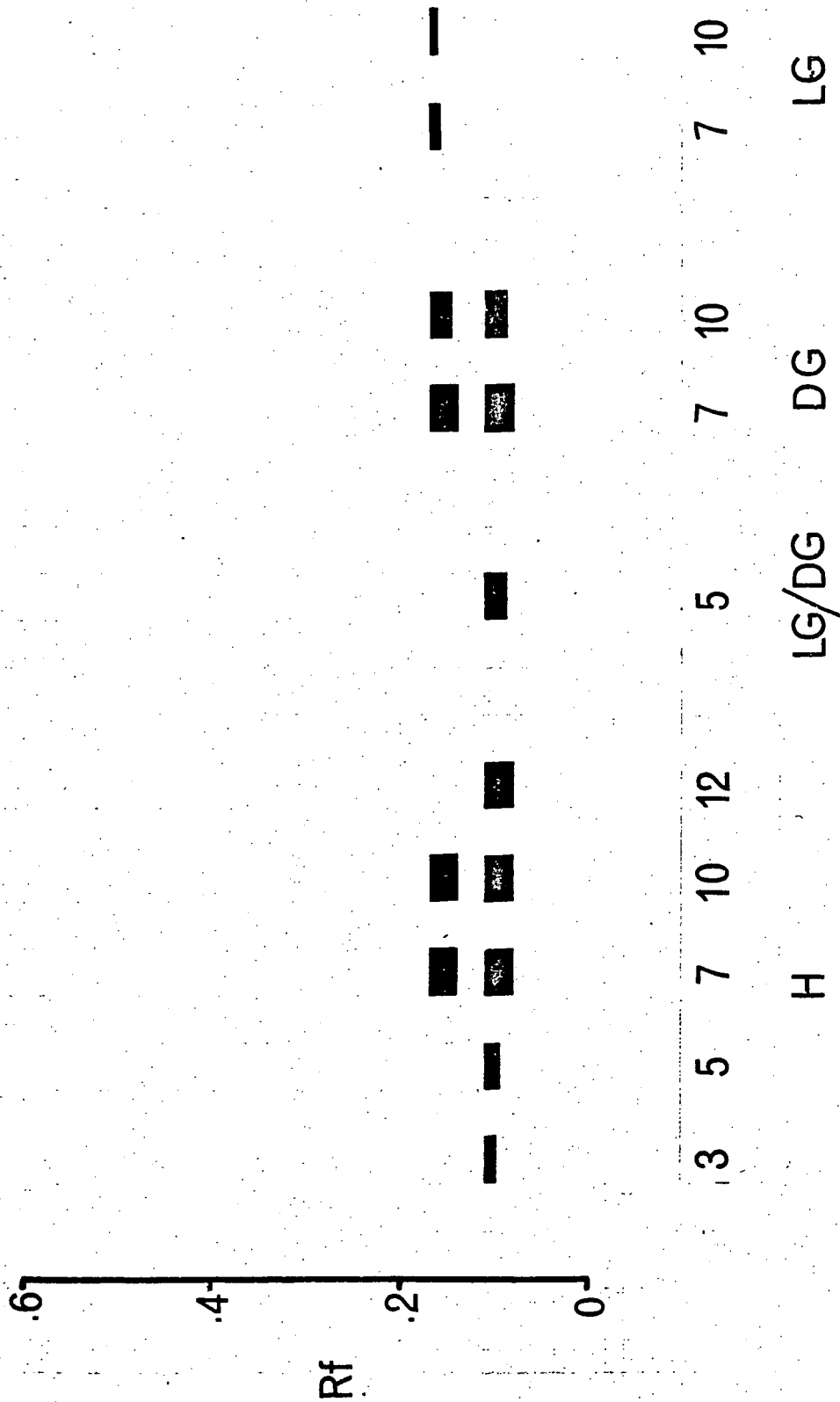


Figure 29

Relation between total catalase activity (summation of zymogram intensity ratings, see Appendix 26) and leaf tissue age (leaf position from stem apex).

(○——○) - Healthy tissue

(□-----□) - Light green island tissue

(△-.-.-△) - Dark green island tissue

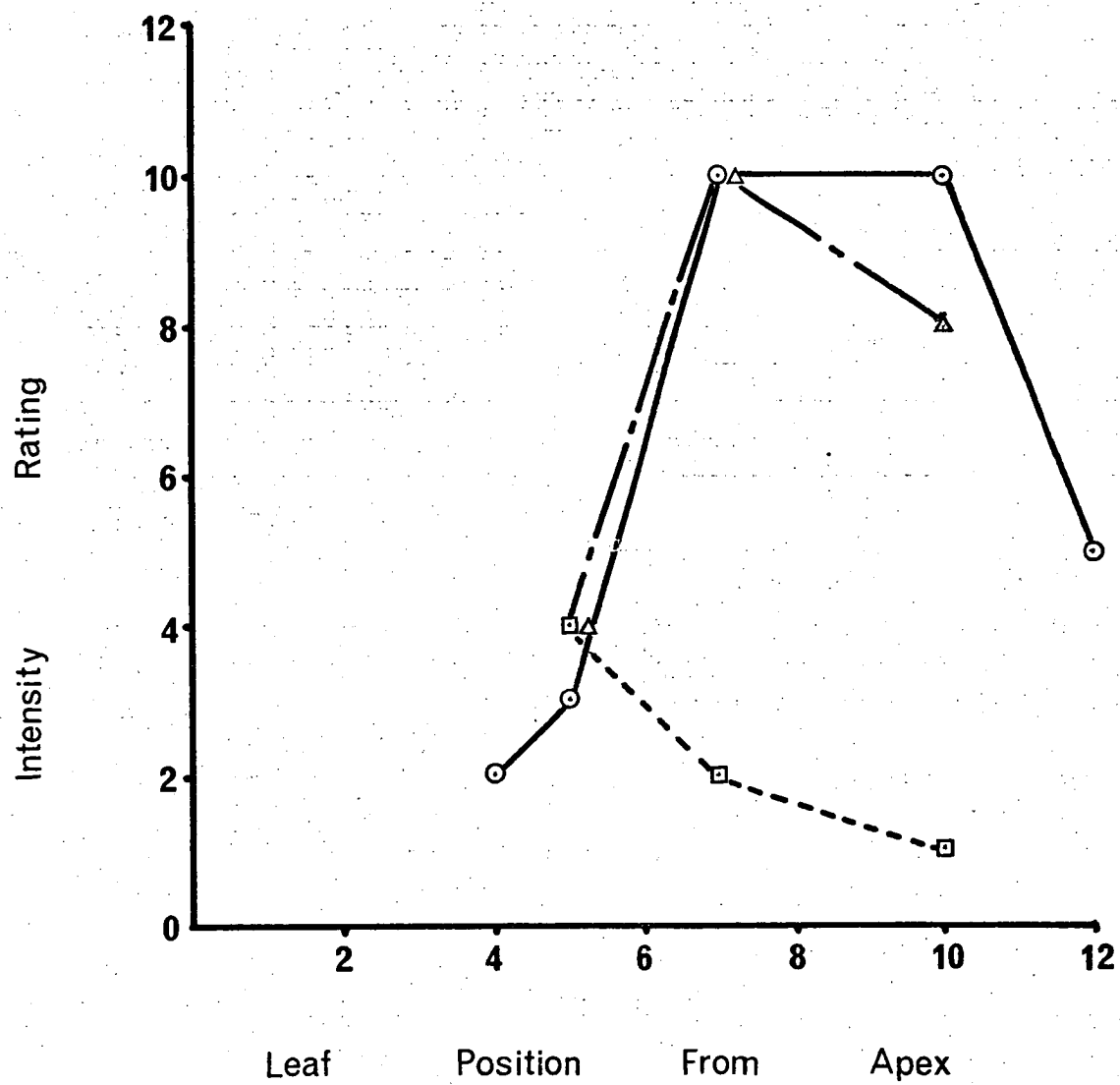
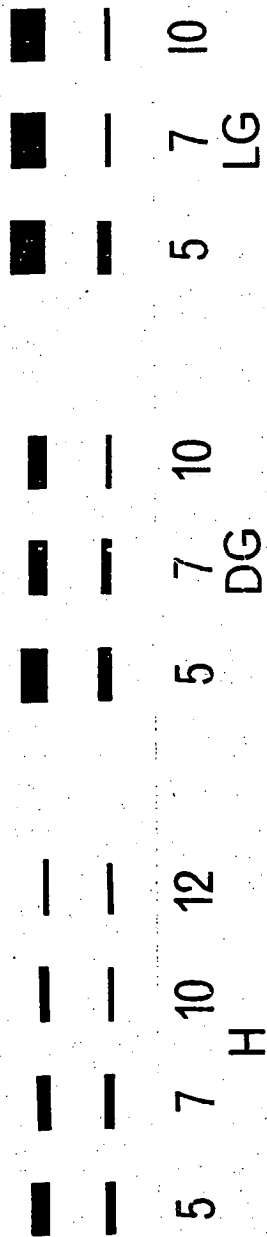


Figure 30

Zymogram of peroxidase isoenzymes in tobacco leaf tissue extracts, separated in 7.5% acrylamide gels.

Rf

.8
.6
.4
.2
0
.2



5 7 10 12 H

5 7 10 LG

5 7 10 DG

and senescing leaves from healthy plants. This fast-migrating isoenzyme (Rf 0.55) was present in both light green and dark green island tissues of infected leaves. The pattern of slow, positive migrating isoenzymes was similar for all tissue ages irrespective of their virus status.

The summation of individual isoenzyme intensity ratings to give a total peroxidase estimation for each tissue type/leaf age is presented in Figure 31. Peroxidase activity was higher, for all leaf tissue age comparisons, in extracts from virus-infected leaves compared with leaves from virus-free plants. Within infected leaves, peroxidase activity was greatest in light green island tissues compared with adjoining dark green islands.

5. Effect of Infection on the Host Photosynthetic Apparatus

(a) Ribulose 1,5-diphosphate carboxylase (RuDP carboxylase)

Enzyme activities for the leaf tissue comparisons healthy versus infected light green and dark green islands are presented in Figure 32. Enzyme activities were greater in leaf extracts from virus-infected plants compared with similarly aged leaves from uninfected plants. Within mature leaves from infected plants, enzyme activity was higher in dark green islands compared with adjoining light green island tissues.

(b) Chlorophyll "a"

The level of chlorophyll "a" reached a maximum in immature and mature leaves on uninfected plants (Figure 33). In light green island tissues of virus-infected leaves the highest level of chlorophyll occurred at leaf position 9 from the stem apex which corresponded to senescing leaves at the same leaf position on healthy plants. The greatest amounts of chlorophyll were extracted from dark green island tissues of infected leaves. Chlorophyll "a" levels remained low and constant in light green island tissues of young leaves from infected plants, whereas chlorophyll increased in comparably aged leaves from uninfected plants. This lag period or period of zero chlorophyll "a" synthesis was associated with

Figure 31

Relation between total peroxidase activity in leaf tissue extracts (summation of intensity ratings of isoenzyme staining reactions in gels—see Appendix 27) and leaf tissue age (leaf position from stem apex).

(○——○) - Healthy tissue

(□-----□) - Light green island tissue

(△-.-.-△) - Dark green island tissue

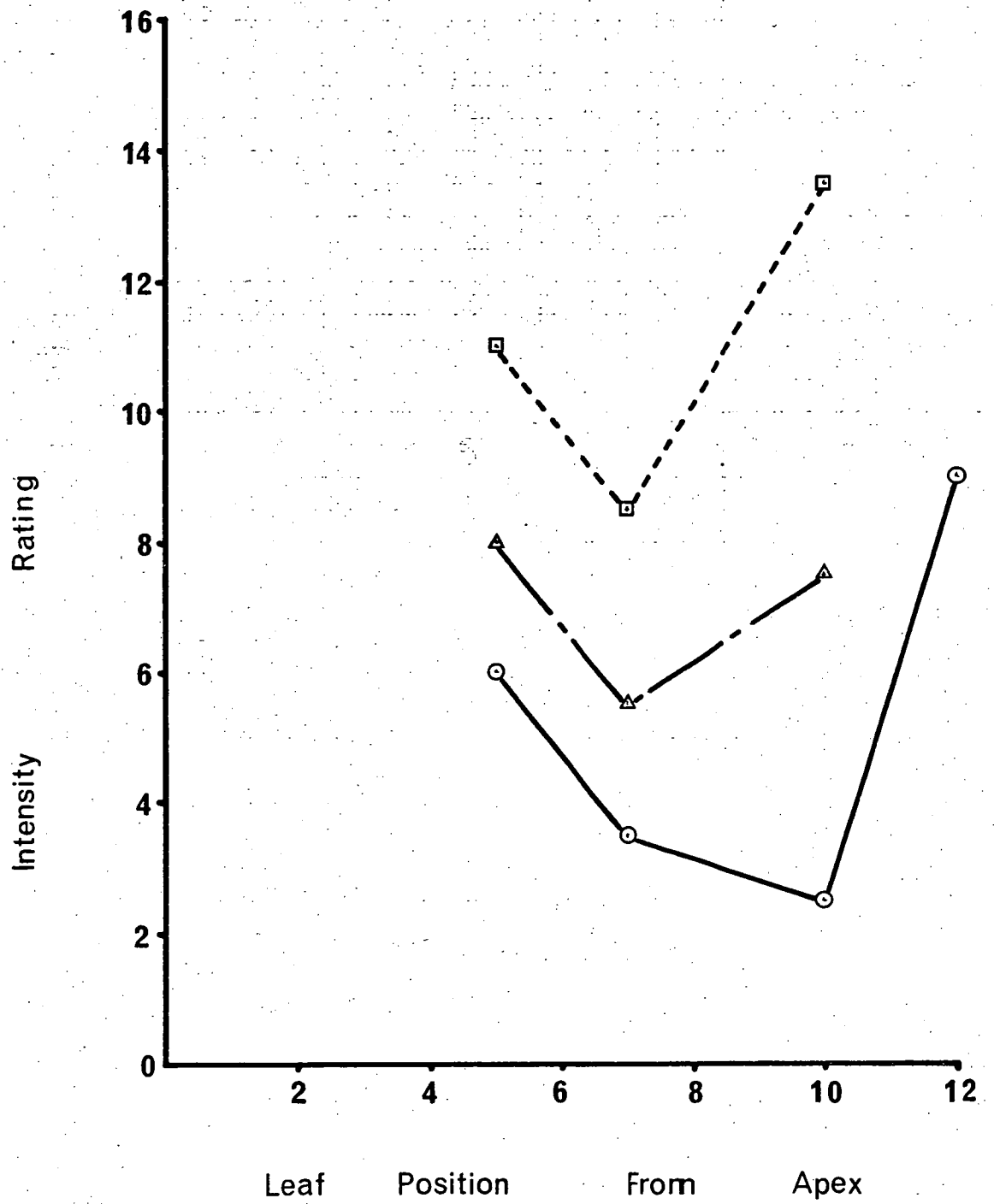


Figure 32

Ribulose 1,5-diphosphate carboxylase activity (radioactive counts/minute $\times 10^4$ /gm fresh weight of leaf tissue) versus leaf tissue age (leaf position from stem apex).

(○——○) - Healthy tissue

(□-----□) - Light green island tissue

(△---△) - Dark green island tissue

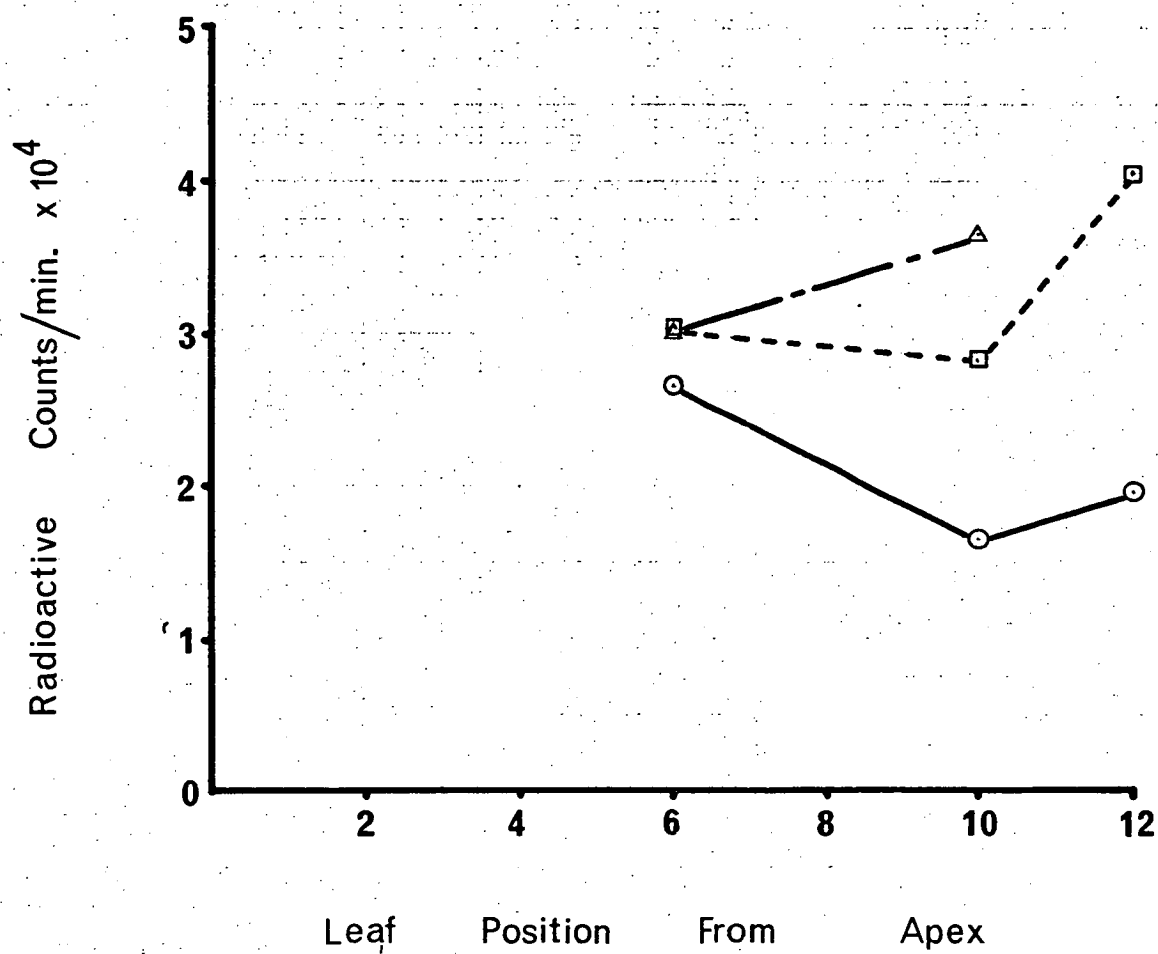


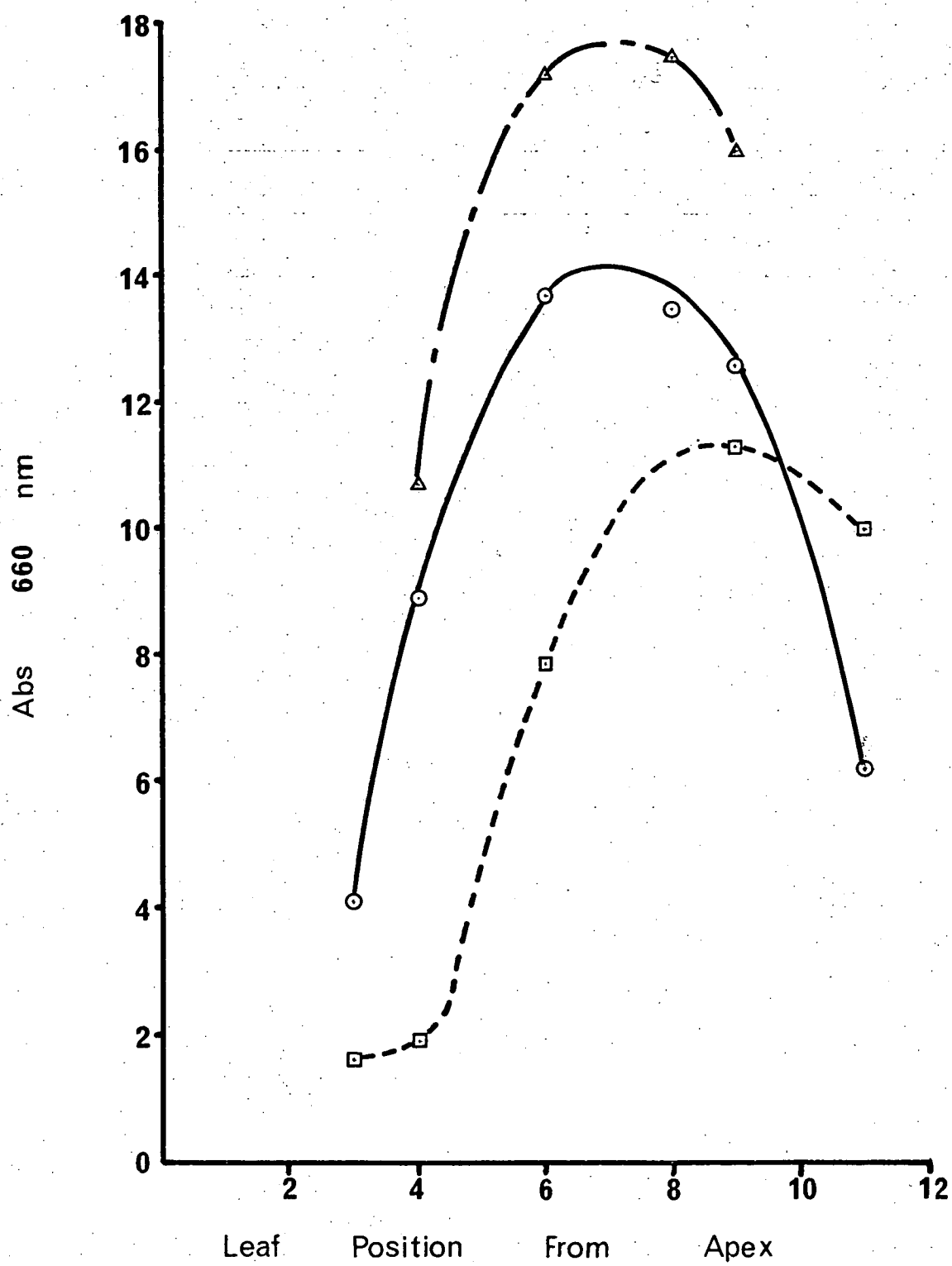
Figure 33

Chlorophyll "a" levels (expressed as Abs. 660 nm/gm fresh weight leaf tissue) as a function of leaf tissue age (leaf position from stem apex).

(○——○) - Healthy tissue

(□-----□) - Light green island tissue

(Δ-.-.-Δ) - Dark green island tissue



leaves from infected plants up to leaf position 4 from the stem apex. However, the initial lag period in chlorophyll "a" build up was compensated for to some extent by the extended leaf age when chlorophyll "a" reached a maximum compared with healthy plants.

Extractable chlorophyll "a" levels fell rapidly in over-mature leaves from healthy plants (leaves occurring below position 8 from the stem apex). The rate of decline of chlorophyll "a" in over-mature leaves from infected plants was much less in light green island tissues compared with similarly aged tissues from healthy leaves.

(c) Chlorophyll "a" : chlorophyll "b" ratios

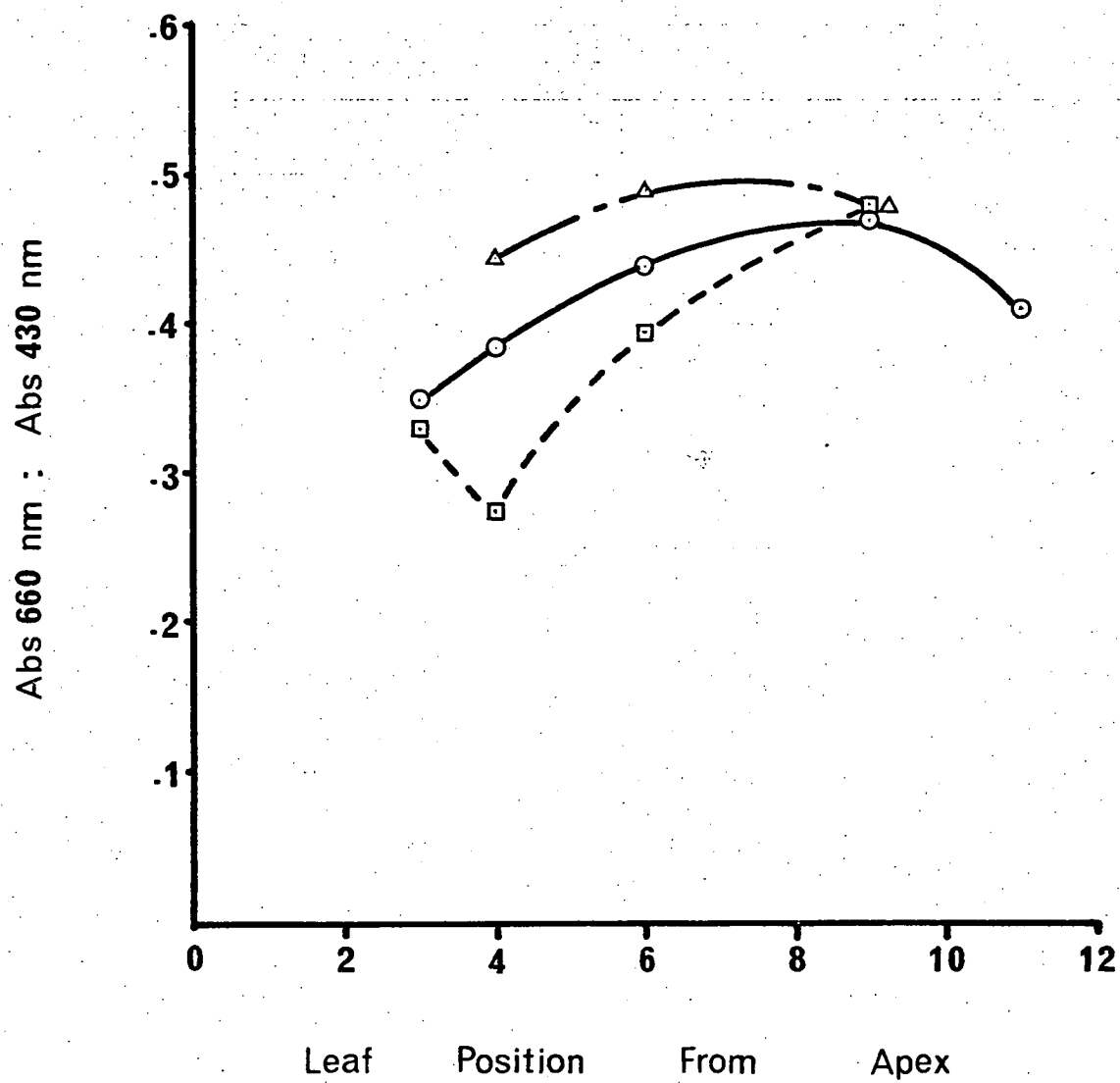
Chlorophyll "a" has two absorbance peaks, the maximum one at 660 nm. Chlorophyll "b" has absorbance maximas at 642 nm and 430 nm. Chlorophyll a:b ratios were constructed from the chlorophyll "a" peak at 660 nm and the chlorophyll "b" peak at 430 nm (Figure 34).

Ratios plotted against leaf age for the tissue comparisons healthy versus infected light green and dark green islands show a similar relationship to the chlorophyll "a"/tissue age profile (Figure 33). Different profiles for healthy, light green island and dark green island tissues would be expected if chlorophyll "b" synthesis was little affected in tissues from virus-infected plants. Chlorophyll "a" level has already been shown to be affected by infection (Figure 33). If both pigment systems had been similarly affected by virus infection, ratios within a single leaf age comparison would be the same for healthy and infected tissues. Chlorophyll a:b ratios for healthy leaves and infected, dark green island leaf tissues reached a peak in immature leaves (leaf position 8 from the stem apex) and both profiles were bimodal in shape. In contrast the chlorophyll ratios for infected, light green island leaf tissues reached a maximum in leaves that corresponded to mature-senescent leaves at the same leaf position on healthy plants. Chlorophyll ratios also

Figure 34

Chlorophyll a:b ratio (ratio of Abs. 660 nm to Abs. 430 nm) as a function of leaf tissue age (leaf position from stem apex).

- (○——○) - Healthy tissue
- (□-----□) - Light green island tissue
- (△-----△) - Dark green island tissue



declined in young infected leaf tissues further suggesting that chlorophyll "a" synthesis was being suppressed. The decline in chlorophyll a:b ratio for young, light green island tissues coincided with the lag period in chlorophyll "a" synthesis for these tissues. The chlorophyll ratio was highest in infected, dark green island tissues suggesting that either chlorophyll "b" synthesis was suppressed or chlorophyll "a" synthesis was stimulated.

Overall, virus infection induced an increase in the activity of the carbon dioxide fixing enzyme, ribulose 1,5-diphosphate carboxylase. Highest enzyme activity was associated with infected, dark green island tissues. Light green island tissues had reduced enzyme activity compared with dark green island tissues from the same leaf. Chlorophyll "a" levels and chlorophyll a:b ratios were less in infected, light green island leaf tissues compared with dark green islands and similarly aged leaves from healthy plants. Chlorophyll "a" levels and chlorophyll a:b ratios were higher in infected, dark green island tissues compared with healthy leaves of similar chronological ages. There was a lag in increase of chlorophyll "a" level in light green island tissues from young infected leaves but the maximal level of chlorophyll "a" in light green islands was associated with older leaves on infected plants than the leaf age for maximum chlorophyll "a" content for healthy plants. Chlorophyll "b" levels did not appear to be much affected by infection.

6. Effect of Infection on Nitrate Reductase Activity

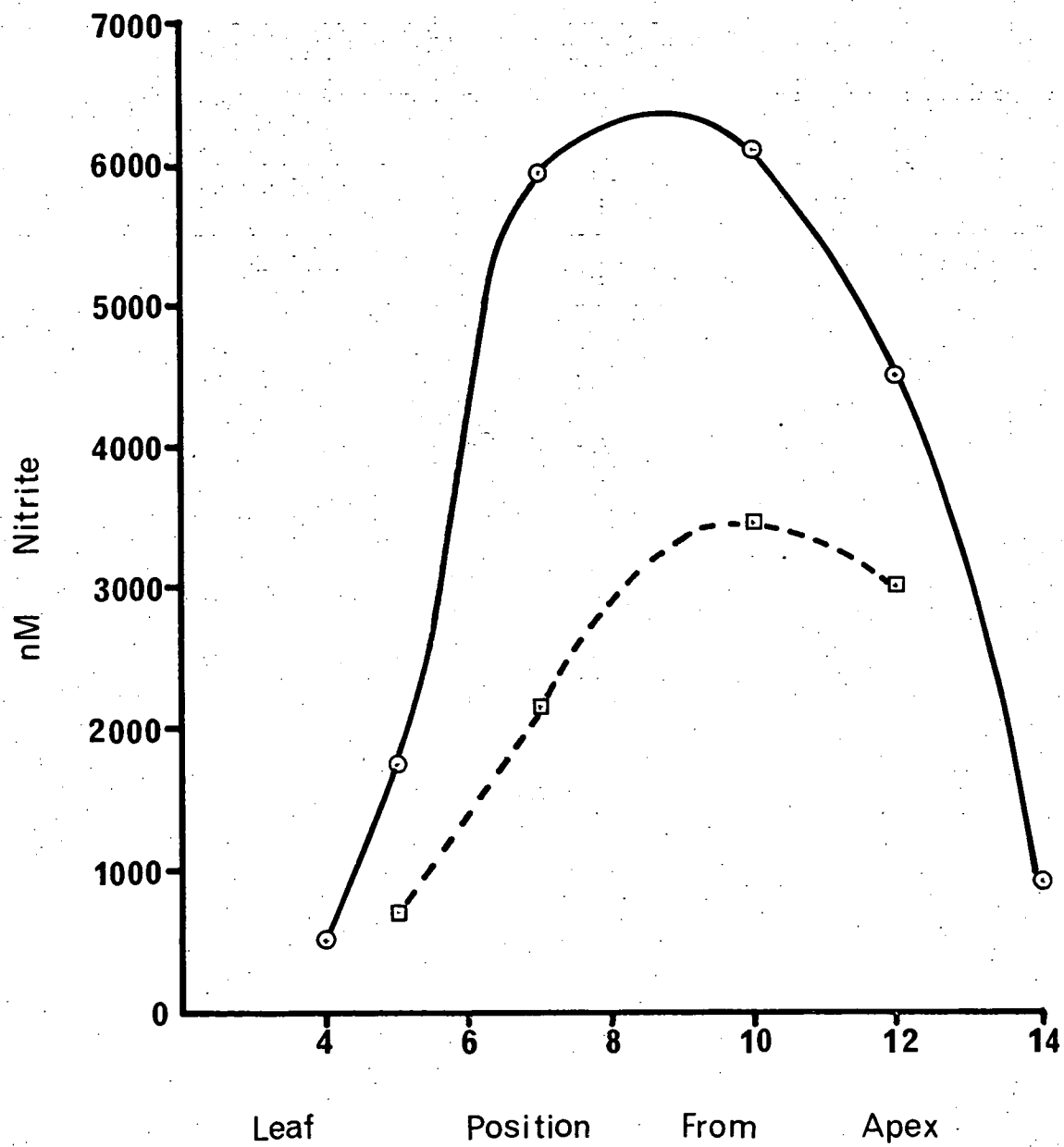
Nitrate reductase activities, determined for healthy and light green island tissues from infected plants, are presented in Figure 35. Leaf tissue age/enzyme activity profiles for nitrate reductase closely paralleled the chlorophyll "a" level/leaf age profiles for healthy and light green island tissues. Enzyme activities were highest in leaves from healthy plants and reached a maximum in immature to mature leaves (leaf position 8-9 from the stem apex).

Figure 35

Relation between nitrate reductase reaction rate (nMoles nitrite/
gm fresh weight leaf tissue/hour) and leaf tissue age (leaf position
from stem apex).

(○——○) - Healthy tissue

(□-----□) - Light green island tissue



In general, enzyme activity was lower in light green island tissues from infected plants. Highest activity for light green island was associated with tissues from leaves at leaf position 10 from the stem apex, whereas the activity in leaves at the same position on healthy plants was declining.

7. Effect of Infection on the Acid Hydrolase Group of Enzymes

The gel patterns of isoenzymes for specific hydrolytic enzymes are presented as zymograms. The thickness of bands in the zymograms are proportional to the colour staining intensities of bands in gels. According to their staining intensities in acrylamide gels, isoenzymes were rated from 1 to 5 on an intensity rating scale with rating 5 being assigned to isoenzymes giving the most intense staining reaction and rating 1 the least intense but easily discernable reaction. Two other ratings were also used to record bands which gave only faint reactions, "vf" for very faint and barely discernable bands and "f" for faint bands. On an intensity rating scale, "vf" has a value of 0.25 and "f" a value of 0.5.

Total enzyme activity for specific enzymes is a summation of individual isoenzyme intensity ratings.

(a) Acid phosphatase

One isoenzyme of acid phosphatase (R_f 0.07), present in extracts from virus-infected leaves of various ages was absent from healthy tissues (see Figure 36). It is possible that this particular isoenzyme is present in healthy tissues younger than those assayed for here and so it cannot be proposed with any certainty that virus infection induced the appearance of a new and specific isoenzyme of acid phosphatase. Some isoenzymes, present in young leaf tissue extracts from healthy plants, disappeared as leaves aged, however the full complement of isoenzymes was maintained in similarly aged leaves from virus-infected plants (Figure 36).

Total acid phosphatase activity for each tissue age comparison is presented in Figure 37. Phosphatase activity was greatest in extracts

Figure 36

Zymogram of acid phosphatase isoenzymes from tobacco leaf tissue extracts, separated in 7.5% acrylamide gels.

Rf

0.8
0.6
0.4
0.2
0

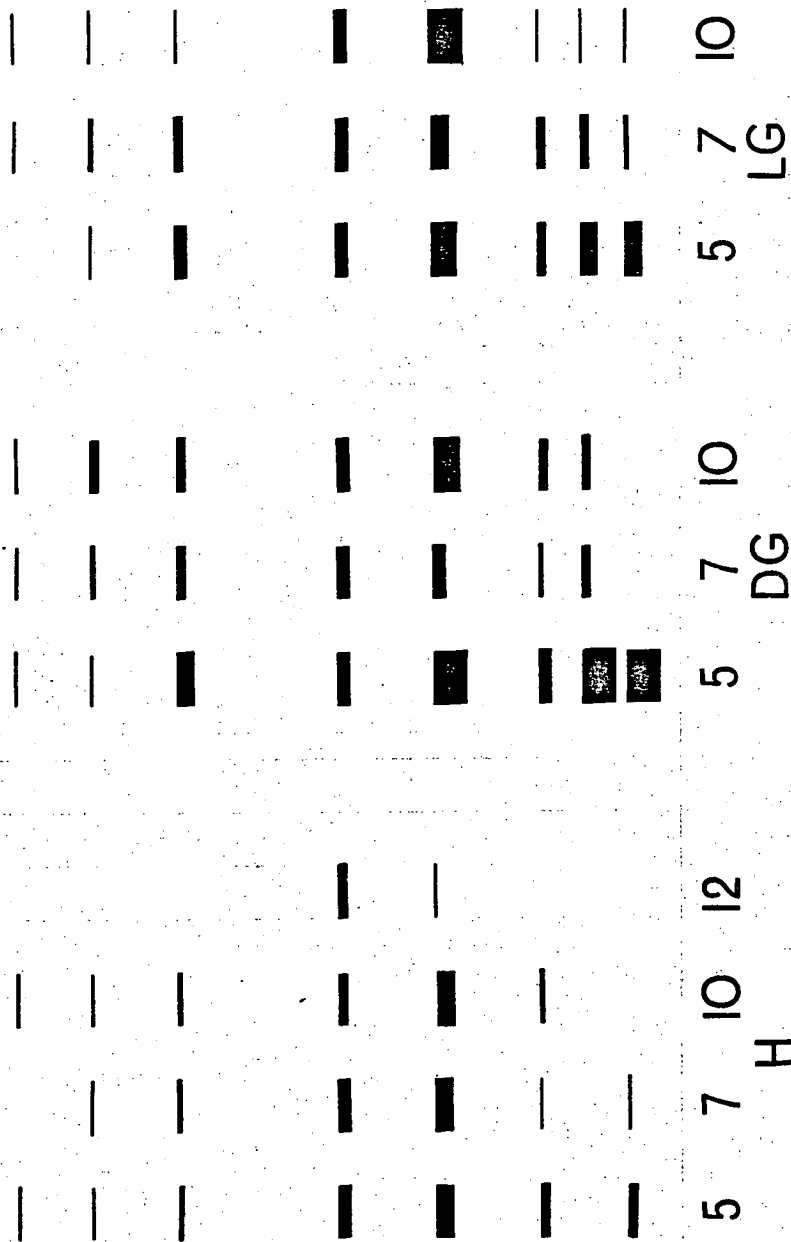
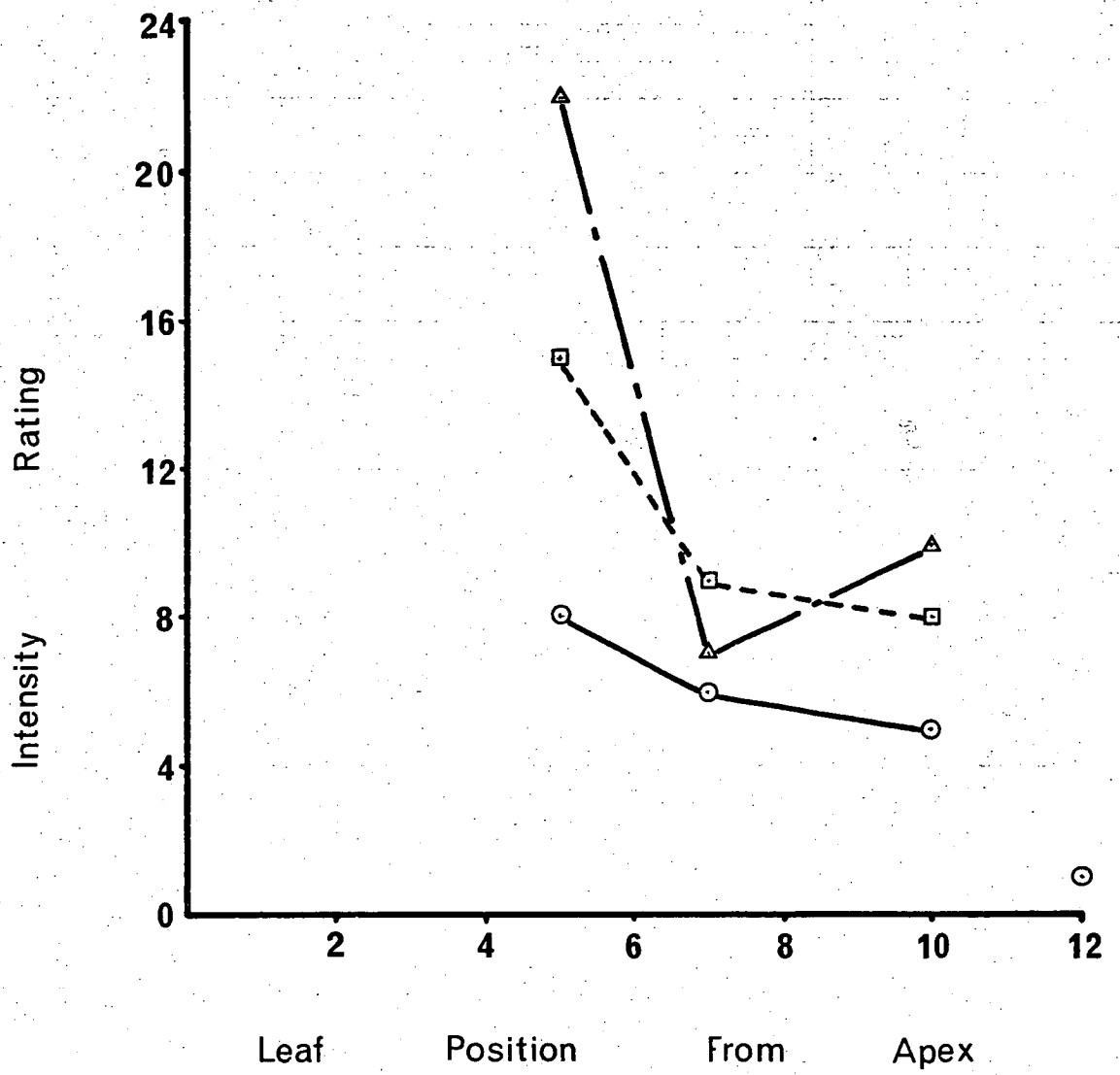


Figure 37

Relation between total acid phosphatase activity in leaf tissue extracts (summation of intensity ratings of isoenzyme staining reaction in gels - see Appendix 28) and leaf tissue age (leaf position from stem apex).

- (○———○) - Healthy tissue
- (□-----□) - Light green island tissue
- (△---△) - Dark green island tissue



from infected leaves compared with healthy leaves of the same chronological age. Within infected leaves, total phosphatase activity was greater in light green island tissues than in adjoining dark green islands.

(b) Ribonuclease (RNAase)

Two primary isoenzymes of RNAase, one at Rf 0.2 and the other at Rf 0.87, were present in tobacco leaf tissues of various ages (Figure 38). The staining intensities of both major bands were greater for light green and dark green island tissues from infected leaves than for comparably aged leaf tissues from uninfected plants.

Total RNAase activities, as presented in Figure 39, were highest in leaf tissues from infected plants compared with leaves at the same position from the stem apex from healthy plants. Activities in light green island tissues exceeded activities in adjoining dark green islands of infected leaves.

(c) α -amylase

Infection delayed the disappearance of a slow, negative-migrating isoenzyme of α -amylase (Rf 0.08) as leaves matured (see Figure 40). This isoenzyme, present in extracts of young leaves from uninfected plants (leaf position 5 from the stem apex) was absent from immature, mature and senescing leaves from the same plants (leaf positions 7, 10 and 12 from the stem apex respectively). In extracts from infected leaves, the slow-migrating isoenzymes were present in light green and dark green islands of immature leaves. All three major isoenzymes of amylase (Rf's 0.08, 0.23, 0.49) gave more intense staining reactions for extracts from infected leaves compared with similarly aged leaves from healthy plants. Leaves from infected plants were more active with respect to total amylase activity than leaves of a similar age from healthy plants (see Figure 41). Light green island tissues from infected leaves had greater amylase activity than adjoining dark green island tissues.

Figure 38

Zymogram of ribonuclease (RNAase) isoenzymes from tobacco leaf extracts separated in 10% acrylamide gels.

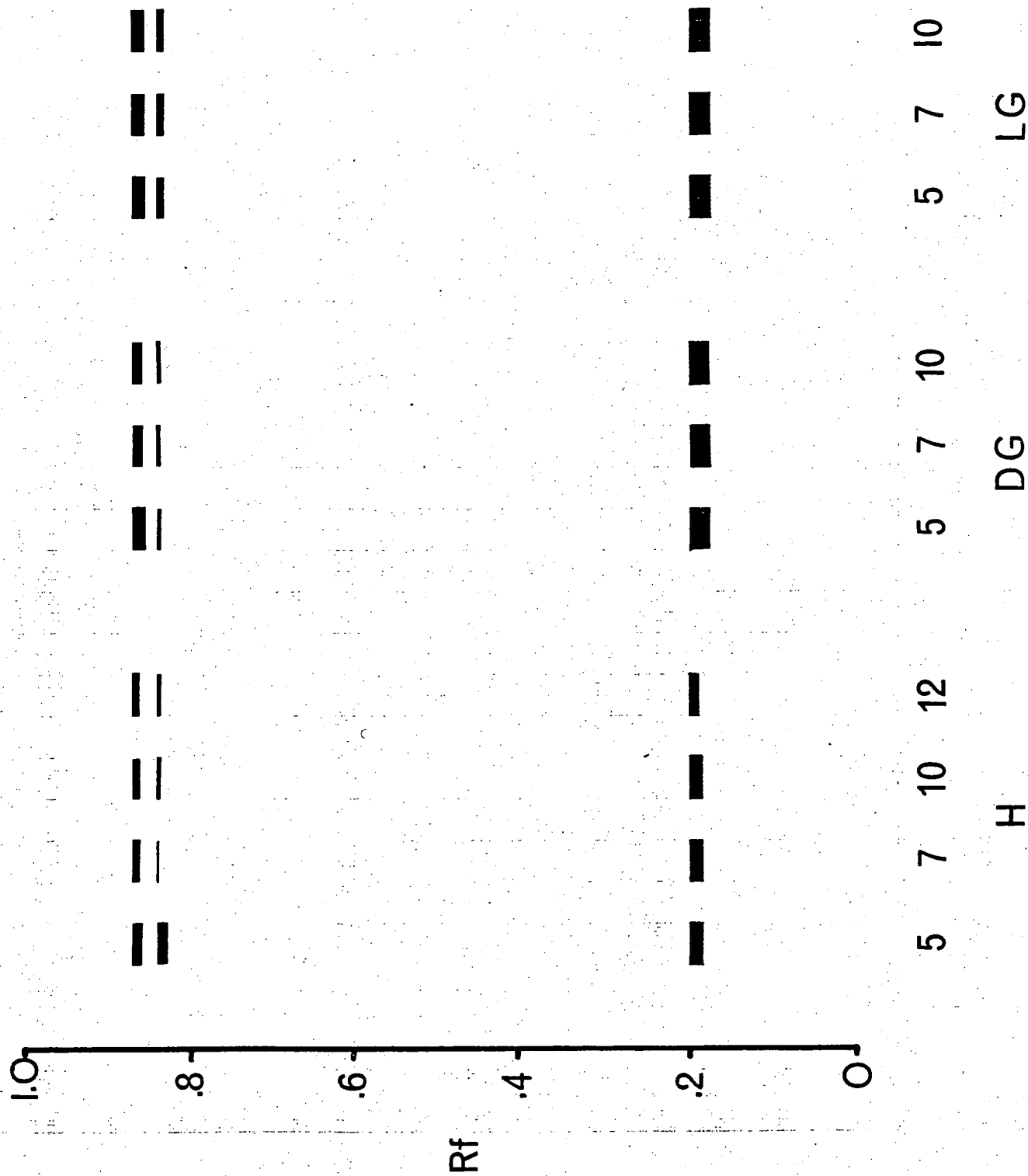


Figure 39

Relation between total RNAase activity in leaf tissue extracts (summation of intensity ratings of isoenzymes staining reactions in gels - see Appendix 29) and leaf tissue age (leaf position from stem apex).

- (O———O) - Healthy tissue
- (□-----□) - Light green island tissue
- (Δ—·—·Δ) - Dark green island tissue

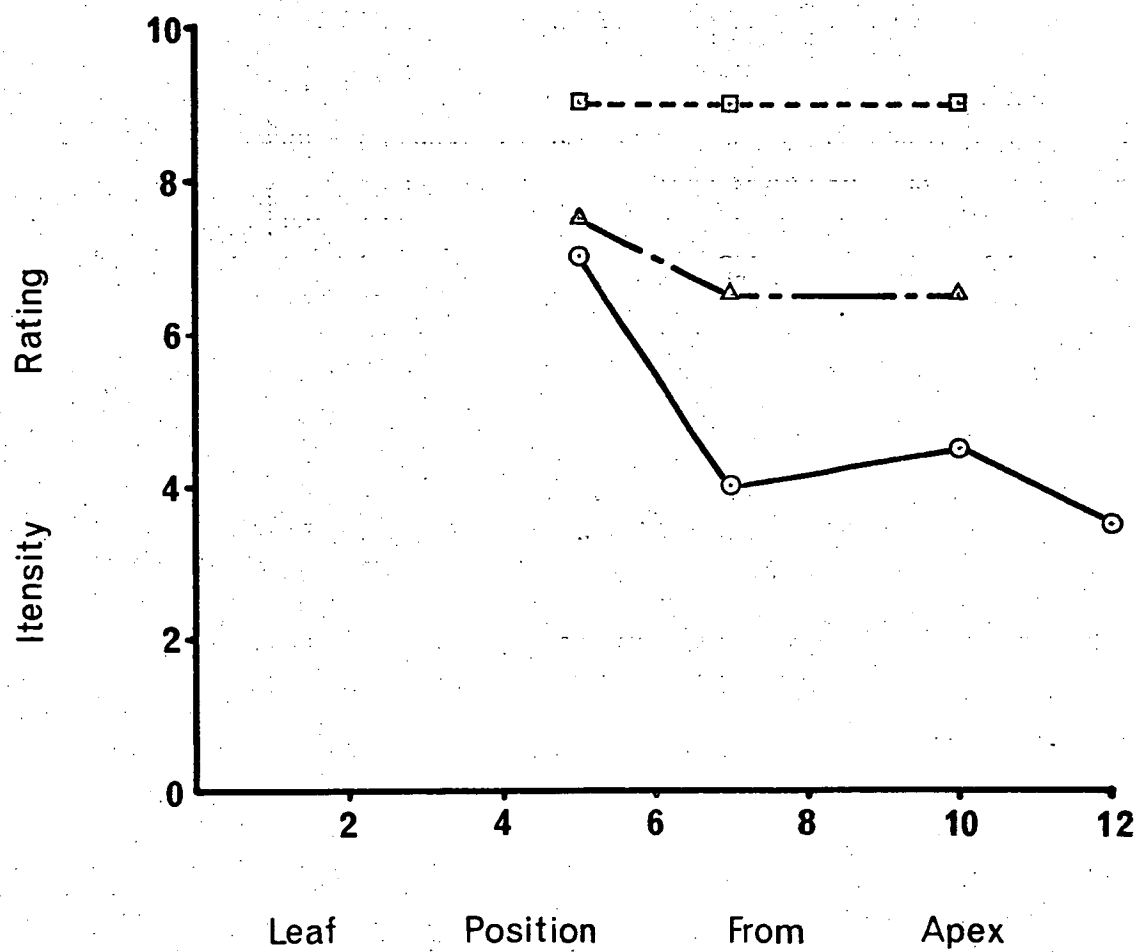


Figure 40

Zymogram of α -amylase isoenzymes from tobacco leaf tissue extracts separated in 7.5% acrylamide gels.

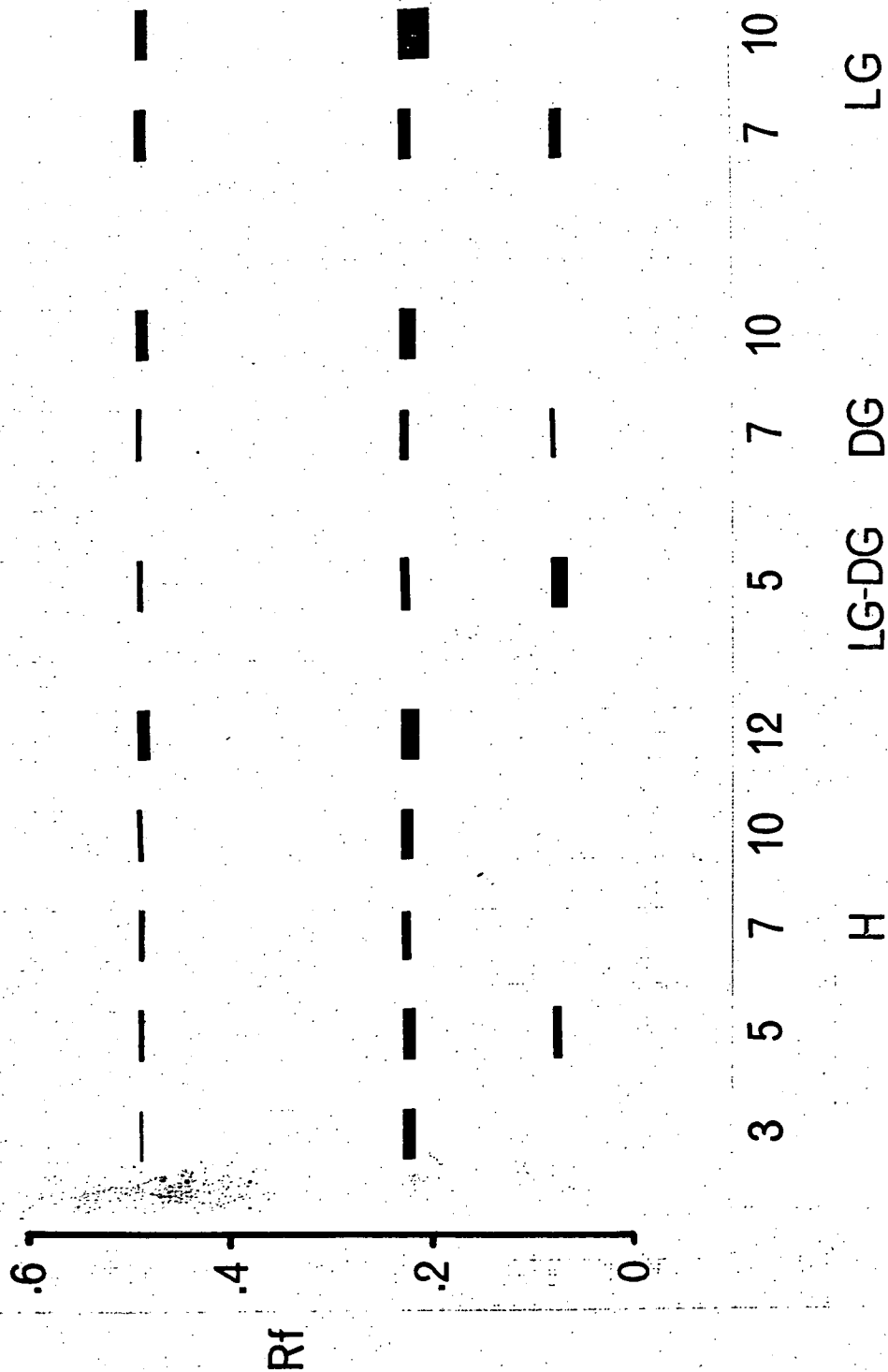
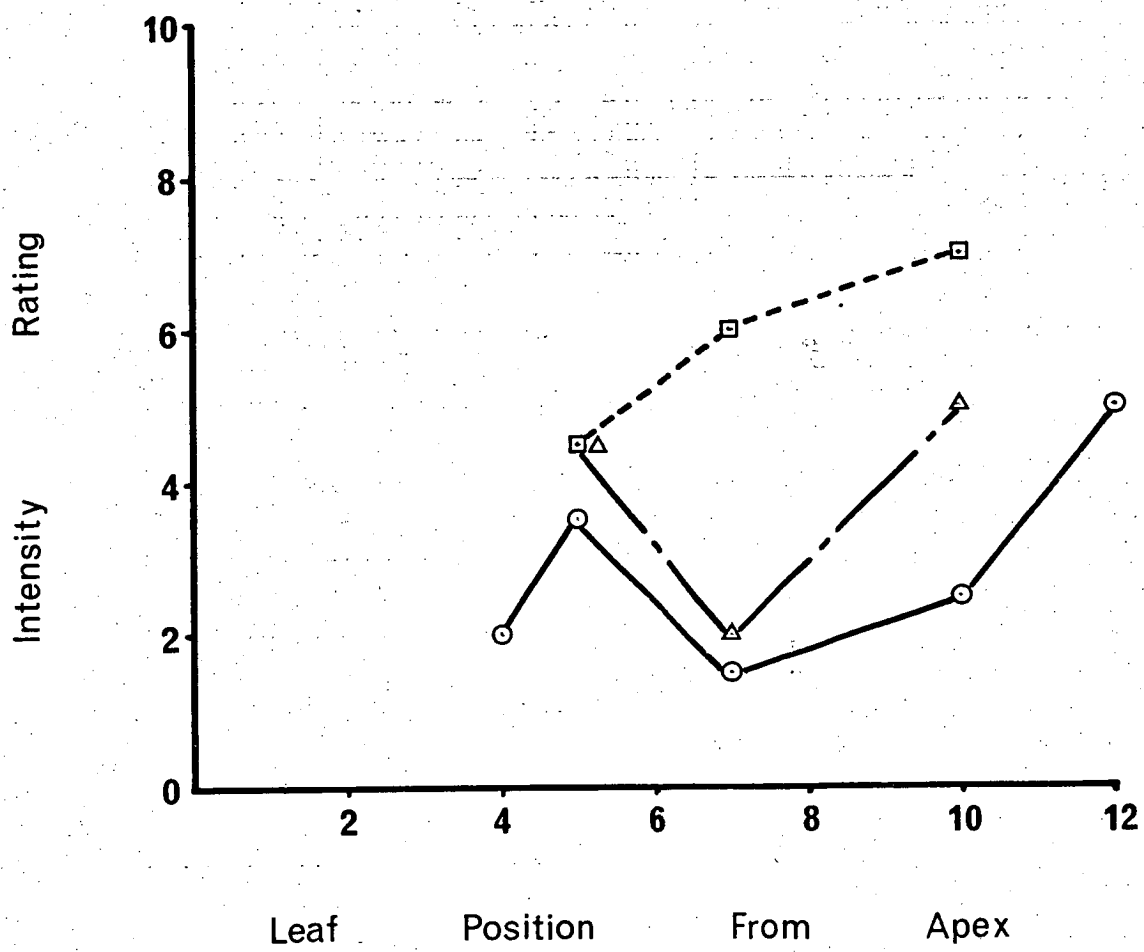


Figure 41

Relation between total α -amylase activity in leaf tissue extracts (summation of intensity ratings of isoenzyme staining reactions in gels - see Appendix 30) and leaf tissue age (leaf position from stem apex).

- (○——○) - Healthy tissue
- (□-----□) - Light green island tissue
- (△—...—△) - Dark green island tissue



(d) Acid esterase

Thirteen isoenzymes of esterase were detected in extracts of tobacco leaves and all thirteen isoenzymes were present in extracts of light green and dark green islands from infected leaves (see Figure 42). Isoenzymes that migrated towards the anode (R_f 's 0.05, 0.16, 0.28, 0.37, 0.50, 0.68) were more active in mature tissue extracts of light green and dark green islands from infected leaves than in extracts from healthy leaves of the same chronological age. Isoenzymes that migrated towards the cathode, during electrophoresis, were more active in young tissue extracts from healthy plants compared with extracts of light green and dark green islands from infected leaves.

(e) Specific protease - leucine amino peptidase

Isoenzymes were only detected in extracts of young and immature leaves from uninfected plants (see Figure 43). Enzyme activity was greatest in the younger leaf tissues.

Except for the specific protease, leucine amino peptidase, activities of the acid hydrolase group of enzymes were generally higher in leaves from virus-infected plants compared with leaves of a similar age from uninfected plants. Within leaves from infected plants, enzyme activities were greater in light green islands than in adjoining dark green islands. Generally, no virus-specific isoenzymes could be clearly demonstrated in extracts from infected plants. The greater numbers of isoenzymes, for specific hydrolytic enzymes, in tissue extracts from mature, virus-infected leaves compared with mature healthy leaves could be attributed to the maintenance of specific isoenzymes, present in young healthy tissues but absent from mature healthy tissues.

Figure 42

Zymogram of acid esterase isoenzymes from tobacco leaf extracts separated in 7.5% acrylamide gels. For the value of intensity ratings see Appendix 31).

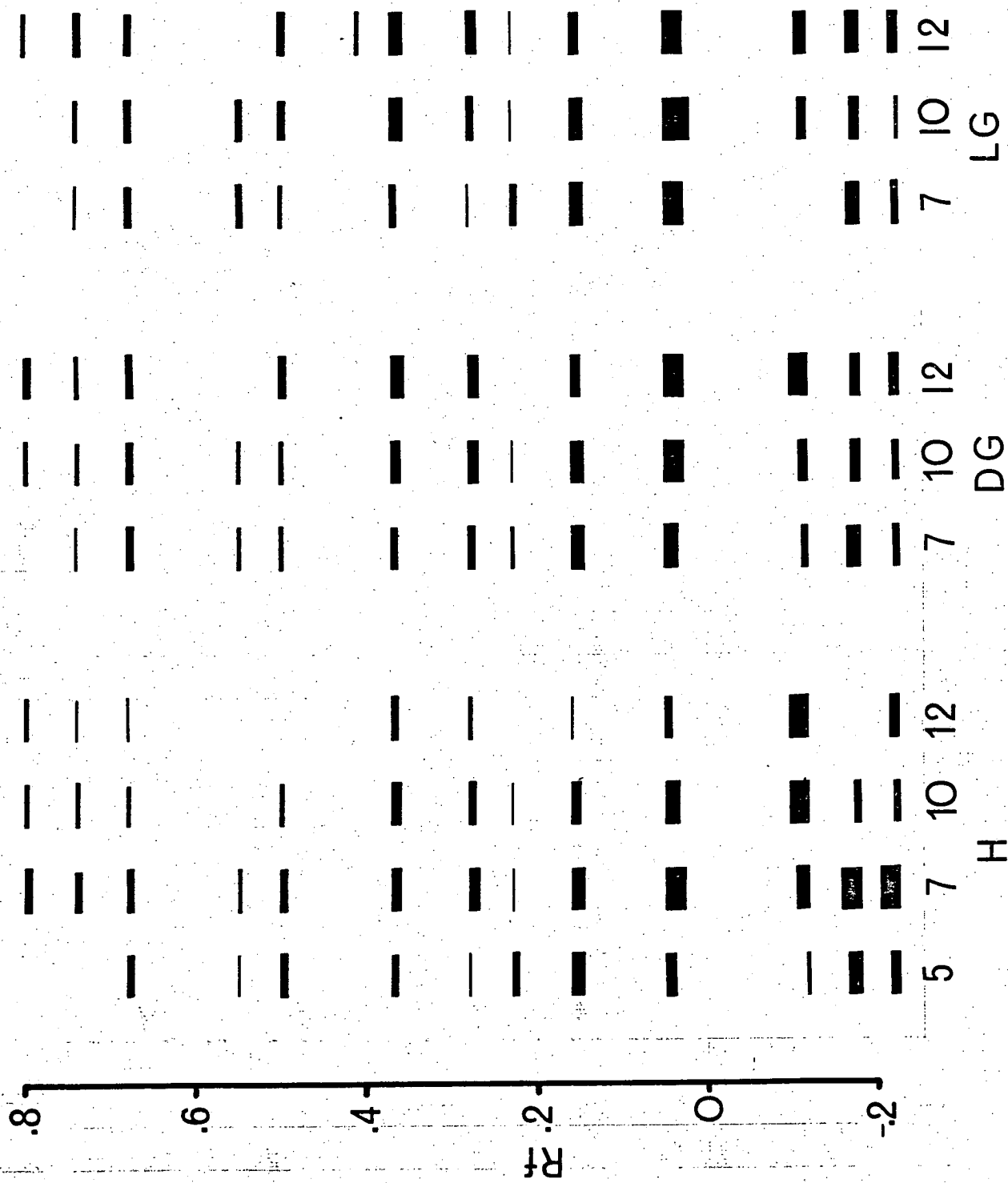
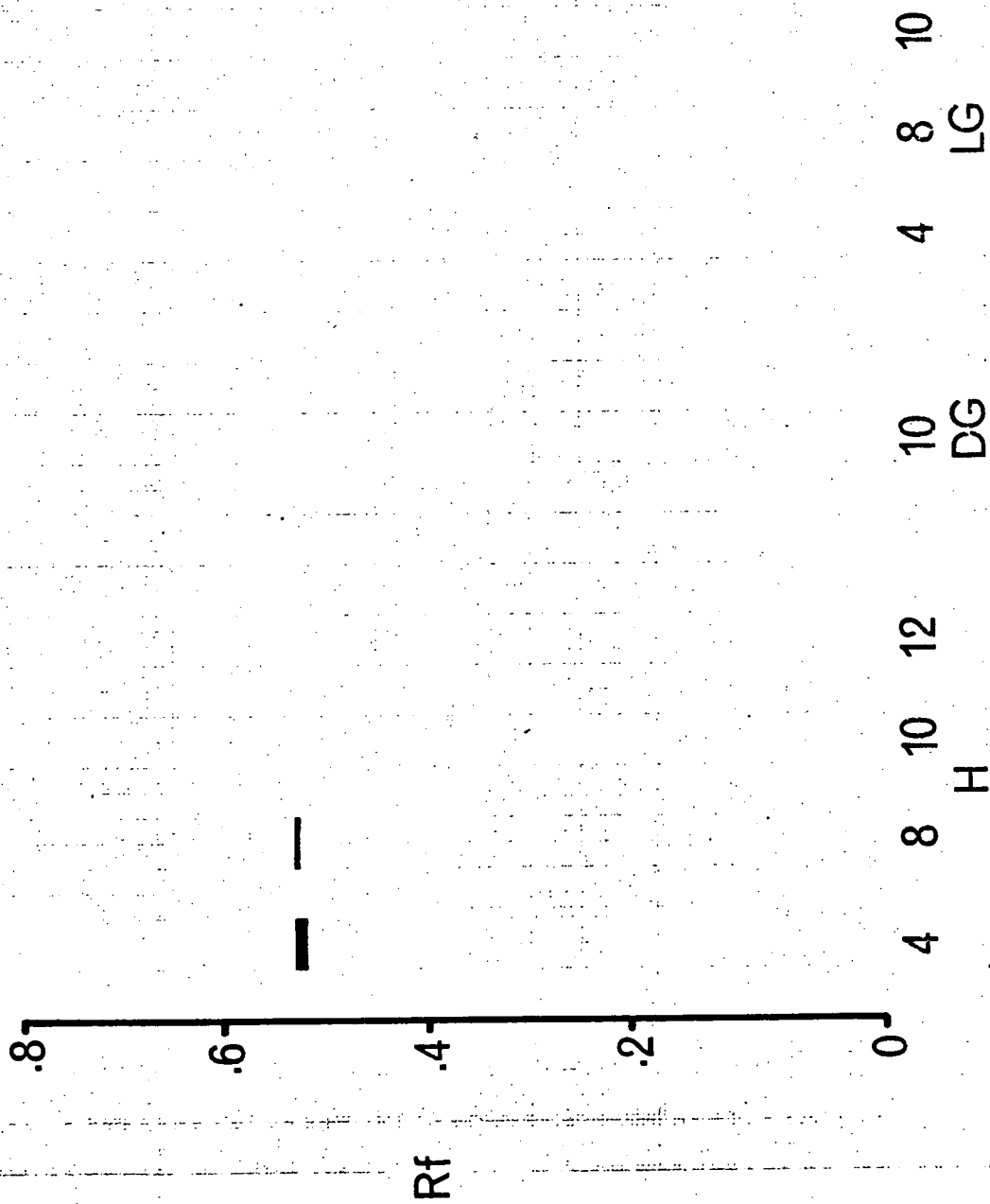


Figure 43

Zymogram of leucine amino peptidase isoenzymes from tobacco leaf extracts separated in 10% acrylamide gels.



SECTION II

VIRUS-HOST BIOCHEMICAL INTERACTIONS

B. ENDOGENOUS HOST HORMONES

INTRODUCTION

The growth response of virus diseased plants and the biochemical activities of both tissues supporting virus synthesis and virus-free tissues adjoining virus-containing tissues, suggests that many host responses to infection are the result of altered hormone activity.

At present, four classes of compounds are recognized as plant hormones. These are:- auxins, gibberellins, cytokinins and abscisic acid. Although each group of compounds has some unique actions within the plant, many of their roles overlap. In many instances, a specific action of one hormone can be antagonized by one or more of the other hormones. The interactions between hormones complicate both the interpretation of results and the bioassays of specific compounds. Generally, plant hormones fall into two broad categories, those promoting growth and those inhibiting growth and enhancing senescence. Auxins, gibberellins and cytokinins fall into the first category while abscisic acid constitutes a growth inhibitor.

The auxin, indole acetic acid (IAA) has been reported present in tobacco (Kefford, 1959) together with the gibberellins A1 and A3 (Sembdner and Schreiber, 1965) and abscisic acid (Steadman and Sequeira, 1970). Little information has been reported concerning the identity of tobacco cytokinins.

Plant hormones can be estimated in tissue extracts by biological assays or physical and chemical methods. Physical and chemical methods provide the most precise information as to identity and concentration. However, such determinations are restricted to those compounds that have been chemically identified and whose properties have been accurately documented. Abscisic acid auxins and some gibberellins can be accurately assayed for by such methods (e.g. gas-liquid chromatography). A major problem in using physical and chemical assay procedures is that prior knowledge of the chemical identities of specific growth substances from particular hosts is required. In many instances the specific identity of

hormones from a host plant are unknown. Other problems arising from the use of physical and chemical assays are the higher degree of purity of tissue extracts required and the lower sensitivity of such assays compared with biological assays.

For all major groups of growth regulators a number of bioassays have been developed. Bioassays vary in their suitability for a particular compound. This especially applies for bioassays of gibberellins. Bioassays also vary in their sensitivities to a group of compounds, their incubation periods and the degree of purity of plant extracts required for a good response. Where ever possible, more than one bioassay was used, or tested, for each type of plant hormone. Bioassays for the four major groups of plant hormones are included here.

Earlier reports concerning the biological assays of plant hormones were often misleading due to a failure to appreciate that extraction procedures employed did not give separation of auxins, gibberellins and abscisic acid. This problem has been largely overcome since the introduction of chromatographic techniques. Biological assays for auxins, gibberellins and abscisic acid, reported here, involved the removal of zones from thin layer chromatography plates corresponding to the Rf values of IAA, gibberellin A₃ and abscisic acid. A number of thin layer chromatography support media and solvent systems were tested for maximum separation of these three compounds.

The concentrations of hormones in partially purified or chromatographically separated plant extracts as determined by a bioassay, are most accurately estimated from dose/response curves. That is, the bioassay response to a dilution series of the extracts. Concentration is determined from parallelism between responses to known growth regulators and unknown potential growth regulators. This concept assumes that the identity of a particular hormone in the extract is known. Even in situations where the specific identity of a particular hormone is in doubt, a dilution series

of the extract should still be tested in the bioassay. This ensures that a dose/response curve of some order will be obtained and that any inhibitors to the particular bioassay, whether of plant, solvent or chromatography support medium origin, will be diluted out beyond the range of sensitivity of the bioassay.

MATERIALS & METHODS1. Extraction and Partial Purification of Endogenous Growth Regulators(a) Gibberellic acid and abscisic acid

Both young and mature leaf tissue were removed from healthy and virus-infected plants and extracted for growth hormones. Young tissues were harvested from plants with 30 day old infections while mature tissues were harvested from plants infected for 40 days. Leaves at leaf positions 10, 11 and 12 from the shoot apex were harvested for mature tissue extractions. Young tissues included the terminal shoot, apex and upper 5 leaves.

One hundred grams fresh weight of leaf tissue was deep frozen. Frozen material was broken up by hand and freeze-dried. Freeze-dried leaf material was homogenized in 250 ml of pre-chilled, 80 percent methanol (-15°C) and shaken overnight at 10°C in stoppered flasks. Insoluble leaf material was removed by vacuum filtration and the filtrate reduced to the aqueous phase on a rotary evaporator, at 35°C . Evaporation was stopped when all methanol had been removed. This point was recognized when condensation appeared in the neck of the evaporating flask. Evaporation beyond this point can result in substantial losses of gibberellins and abscisic acid. The pH of the aqueous phase was adjusted to 2.5 with 10 N hydrochloric acid and the extract partitioned three times with 50 ml volumes of re-distilled ethyl acetate. Phase separations were performed in phase separating flasks. To the combined ethyl acetate fraction, half a volume of 5 percent sodium bicarbonate was added, the phases thoroughly shaken and separated. The ethyl acetate fraction was discarded. The bicarbonate fraction was partitioned a further three times with 50 ml volumes of re-distilled ethyl acetate, discarding the ethyl acetate. The pH of the bicarbonate phase was then adjusted to 2.5 with 10 N hydrochloric acid, and partitioned three times with ethyl acetate. The ethyl

acetate fractions were retained, pooled, and evaporated to dryness on a rotary evaporator at 35°C. The residue was taken up in 3 ml of re-distilled methanol and stored at 4°C to be further purified by thin layer chromatography.

(b) Cytokinins

Young and mature leaf tissues were harvested from plants with 30 day old infections. All leaf material had well defined mosaic patterns. For mature leaf tissues, 150 gm fresh weight of tissues, at leaf positions 10, 11 and 12 from the apex, were harvested, deep frozen and freeze-dried. One hundred gm fresh weight of young tissue, including the uppermost 5 leaves and meristem was similarly prepared. Root material was harvested from pot-grown plants by removing the plants carefully and thoroughly washing the roots. Root material was deep-frozen and freeze-dried and 10 gm freeze-dried weight used in subsequent solvent extractions.

The extraction procedure employed was essentially that reported by van Staden, Webb and Wareing (1971). Freeze-dried material was homogenized in 200-300 ml of pre-chilled, 80 percent methanol, shaken overnight at 10°C and filtered to remove insoluble residues. The pH of the filtrate was adjusted to 2.5 with 10 N hydrochloric acid and the aqueous fraction partitioned three times against 50 ml volumes of re-distilled ethyl acetate, discarding the ethyl acetate. The pH of the aqueous fraction was then adjusted to 7.0, with 10 N sodium hydroxide and the aqueous fraction partitioned twice with 50 ml volumes of water-saturated, re-distilled n-butanol. The pooled n-butanol fractions constituted the "butanol-soluble-fraction". Tris-HCl buffer (pH 8.2) was added to the aqueous phase to a final concentration of 0.1 M. Magnesium chloride (0.01 M) and alkaline phosphatase (1 mg per 10 ml extract) were added to the aqueous extract and the solution incubated for 24 hours at 30°C. Following partitioning with two 50 ml volumes of water-saturated n-butanol, the butanol fractions were pooled to constitute the "water-soluble-fraction". Butanol

phases were evaporated to dryness, on a rotary evaporator at 35°C and the residues taken up in 2.5-3.0 ml of re-distilled methanol and stored at 4°C.

(c) Auxins

Young tissues, including the upper shoot, meristem and leaves to leaf position 5 from the stem apex, were harvested from plants with 40-day-old infections.

One hundred and twenty grams fresh weight of tissue was homogenized with 200 ml of ethyl acetate at 2°C for 2 minutes. The resulting slurry was shaken at 10°C for at least 12 hours. Insoluble residue was removed by filtering and the filtrate washed with a further 100 ml of ethyl acetate. The ethyl acetate fractions were pooled and partitioned against 100 ml of 5 percent sodium bicarbonate. After separating the two phases in a separating funnel, the ethyl acetate fraction was discarded. The pH of the bicarbonate fraction was adjusted to 3.0 with 20 percent phosphoric acid and the acidified extract phase-separated against two 50 ml volumes of re-distilled ethyl acetate. The ethyl acetate fractions were retained, combined and stored at -15°C overnight. Ice crystals which formed were separated from the ethyl acetate by filtering. The ethyl acetate fraction was evaporated to dryness under reduced pressure at 35°C, the residue redissolved in 3 ml of redistilled ethanol and stored in stoppered glass tubes at 4°C.

2. Separation of Growth Regulators by Thin Layer Chromatography (TLC)

(a) Gibberellic acid and abscisic acid

(i) General conditions of chromatography

A number of TLC support media and solvent systems were tested to determine the optimum combination for greatest separation of gibberellic acid and abscisic acid. Support media of cellulose CC41, Kieselgel G type 60 and Kieselgel GF254 were spread over thoroughly washed glass plates (20 cm x 20 cm) to a depth of 400 microns. Pure compounds or partially purified

extracts were layered onto plates with a Rodder Streaker, delivering 0.5-1.0 ml per plate. Solvent systems employed were; isopropanol:ammonia (s.g. 0.88):water (10:1:1); toluene:ethyl acetate:acetic acid (40:5:2); ethyl acetate:chloroform:acetic acid (15:5:1). All plates were run until the solvent front reached a pre-scribed line, 14 cm from the origin.

(ii) Chromatography of pure compounds and partially purified extracts

Chromatography of partially purified extracts was achieved by streaking 0.5-1.0 ml of final methanol extract on TLC plates of Kieselgel GF254. As well as preparing plates for healthy plant extract and infected plant tissue extract, a third plate was prepared with a 1.0 ml mixture of GA₃, (+)ABA and some plant extract for determining the R_f values of pure compounds relative to any major bands from the plant extracts. This allowed for a more accurate estimation of the position of these compounds on plates streaked with partially purified extracts. Plates were run together in ethyl acetate:chloroform:acetic acid solvent for GA₃ isolation and toluene:ethyl acetate:acetic acid for ABA isolation until the solvent fronts had migrated 14.0 cm from the origin. Plates were removed from the chromatography tank and dried for 30-60 minutes beneath a warm air blower.

The R_f values of GA₃ and (+)ABA were determined by physiochemical methods and their positions, relative to major plant zones giving strong fluorescence under long wave length ultraviolet light, estimated. The positions were then marked onto the plates streaked with tissue extracts and a 2.0-3.0 cm wide zone scraped from each plate about the theoretical positions of the pure compounds. Each zone was scraped into a 25 ml glass test tube and stored under vacuum in a desiccator for 24 hours, to ensure complete evaporation of chromatography solvents.

Plate zones to be assayed for GA₃ activity, were taken up in 5.0 ml of 0.005 M citrate buffer, pH 6.0, 24 hours prior to setting up a bioassay and tubes stored at 4°C. Plate zones to be assayed for ABA activity, were

taken up in 3.0 ml of 0.005 M citrate buffer, pH 6.0.

In order to further verify the identity of an ABA-like compound, tissue extracts were chromatographed in two distinct solvent systems. The appropriate zone from an ethyl acetate:chloroform:acetic acid solvent run plate was scraped off and extracted with three lots of methanol. The methanol extract was evaporated to dryness and the residue redissolved in 1.0 ml of methanol. This extract was streaked onto a fresh TLC plate of Kieselgel GF254 and run two times in toluene:ethyl acetate:acetic acid solvent system. A plate streaked with pure ABA was treated similarly to plates streaked with plant tissue extracts and used for the purpose of locating the position, on TLC plates, of abscisic acid.

A 3.0 cm wide zone, about the R_f position of pure ABA, was scraped from each plate and taken up in 3.0 ml 0.005 M citrate buffer, pH 6.0, overnight at 4°C.

(b) Cytokinins

The conditions of chromatography were similar to those used for gibberellins and abscisic acid purification. For cytokinins in tissue extracts, 0.5 ml of final methanol soluble extract was streaked onto TLC plates layered with Kieselgel G type 60. Plates were run in an isopropanol:ammonia:water solvent system. The solvent run of 14.0 cm was divided into 10 equal width zones, from the origin to the solvent front and each zone carefully scraped off into a glass test tube. Tubes were stored under vacuum in a desiccator for 24 hours. Twenty four hours prior to setting up a bioassay, each zone was taken up in 5.0 ml ^M/₇₅ phosphate buffer, pH 6.1, containing 1 mg per ml of tyrosine.

(c) Auxins

One ml of ethanol soluble, final plant extract was streaked onto a TLC plate of Kieselgel G type 60 and run in isopropanol:ammonia:water solvent. A 3.0 cm wide zone was scraped from each plate, corresponding to a region about the R_f of indole acetic acid (IAA). The R_f of IAA was

determined by running a TLC plate, streaked with 0.5 ml of IAA (100 ppm in ethanol) and 0.5 ml of partially purified tissue extract, together with plates streaked with tissue extract alone. The positions of any major bands fluorescing under long wave length ultraviolet light, were marked on the plate and the zone of IAA developed by physiochemical methods. From the position of bands of plant origin on plates streaked with plant tissue extracts and the relative position of IAA from the control plate, a line corresponding to the theoretical position of IAA was marked on each plate. A plate zone was scraped off from around this line. Following vacuum desiccation, plate zones were suspended in 10 ml of 0.05 M citrate-phosphate buffer, pH 5.0, containing 2 percent sucrose and stored, in the dark, at 4°C.

3. Physiochemical Determinations of Growth Regulators

(a) Gibberellin A₃

Water:conc. sulphuric acid (30:70, $\frac{V}{V}$) was sprayed over a TLC plate. Gibberellin A₃ gave a yellow-green fluorescence under long wave length ultraviolet light.

(b) Abscissic acid

Abscissic acid strongly absorbs short wave length ultraviolet light. On ultraviolet light sensitive plates of Kieselgel GF254, ABA appeared as a purple band against a fluorescing background.

(c) Indole acetic acid

Colour development of indole acetic acid was achieved with Ehrlich's reagent. Chromatograms were sprayed with 10.0 ml of a solution of 1.0 gm p-dimethylamino benzaldehyde dissolved into 50 ml of 24 percent hydrochloric acid plus 50 ml of 96 percent ethanol. Plates were warmed to 50°C for 20 minutes then exposed to vapours of aqua regia. Indole acetic acid appeared as a deep blue band.

4. Biological Assays of Growth Regulators

(a) Gibberellic acid

(i) Barley endosperm bioassay

Gibberellins stimulate α -amylase production in barley aleurone layers. Amylase activity is determined from the concentration of free sugars in the reactant, following the incubation of barley endosperm pieces in dilute solutions of gibberellic acid. The amount of sugars released from starch is proportional to the concentration of gibberellic acid in the test solution. The method used was essentially that described by Coombe, Cohen and Paleg (1966a, 1966b). Seeds of a commercial, awned, brewers barley were graded for uniformity of size. Cracked and diseased seeds were discarded. An excess of seeds required for an assay were counted out and soaked in 50 percent sulphuric acid (V/V) at 25°C for 3 hours to remove husks and sterilize seeds. Acid was decanted off and seeds were shaken vigorously for 30 seconds in autoclaved, distilled water and decanted quickly. Seeds were washed in several changes of water until the pH of the surrounding solution was stable. Seeds were then soaked in sterile water for 24 hours at 0-2°C.

All subsequent operations were carried out in sterile conditions in a laminar air flow unit. All vials, implements and solutions (except gibberellin stock solutions) were sterilized. Seeds were cut transversely, 4 mm from their distal ends, discarding the embryo portion of each seed. Endosperm portions were transferred to a petri dish of distilled water until enough segments had been cut for a complete bioassay. Endosperm pieces were then rinsed in distilled water and spread over a moistened filter paper disc within a petri dish. Two endosperm pieces were transferred to each vial (2 inch x 1 inch glass vials) along with 1.0 ml of solution for testing. Vials were capped and incubated, in the dark, at 28°C for 24 hours. Following incubation vials were stored at -20°C. Sugar levels in the 1.0 ml incubates were determined by the Anthrone reagent method as described by de Bruyn *et al.* (1968).

Anthrone reagent was prepared by dissolving 0.1 gm of anthrone per 100 ml of 76 percent (V/V) sulphuric acid, heating in a boiling water bath for 15 minutes followed by rapid cooling. Fresh reagent was prepared for each bioassay and was used 3-24 hours after preparing. Frozen vials, containing 1.0 ml of reactant, were thawed at room temperature and diluted to 10 ml with distilled water. Filter paper cups, made by forming 9.0 cm Whatman No.1 filter paper discs over the end of a 25 ml glass test tube, were inserted into each vial. One millilitre of solution was withdrawn from each cup and transferred to 25 ml glass test tubes. Nine millilitres of anthrone reagent were pipetted into each tube, the contents thoroughly stirred and heated in a boiling water bath for 8 minutes. After cooling, the colour of each tube was measured by the absorbance at 625 nm wavelength against a blank prepared from water plus reagent.

A standard curve for assay response to gibberellin A3 concentration was determined for each separate assay. Dilutions of a stock solution of GA3 (10^{-6} gm per ml) were prepared in 0.005 M citrate buffer, pH 6.0, to give final concentrations of 0, 10^{-7} , 10^{-8} , 10^{-9} , 10^{-10} , 10^{-11} gm per ml. For chromatography zones suspended in 5 ml of buffer, dilution series, in buffer, were prepared to give dilutions of 1, $1/5$, $1/25$, $1/125$. Each complete bioassay comprised of a dilution series of healthy and infected tissue extracts purified by thin layer chromatography and GA3 standards. Each tissue extract dilution and GA3 standard was replicated four times.

(ii) *Rumex* leaf disc bioassay

This bioassay relies on a gibberellin-induced inhibition of chlorophyll breakdown, in the dark, in leaf discs from *Rumex obtusifolius* L. The method was first reported by Whyte and Luckwill (1966) and the method reported here is a modification of the original method as used by Hoad (personal communication).

Bioassays were performed in 5 cm plastic petri dishes on 5 cm discs of Whatman No.1 filter paper. One millilitre of test solution or GA3

standard was pipetted onto each filter paper disc. Test solution dilutions and GA₃ standards were prepared in distilled water. Discs of leaf tissue were removed from mature Rumex leaves, with a 6.5 mm diameter cork borer, and floated on distilled water. Mature leaves from near the base of a plant were chosen and all discs were punched from one leaf. Eight to ten discs were transferred to each petri dish, with the upper leaf surface up and tissues incubated in the dark at 28°C for 7 days, or until discs incubated with water had just turned yellow. Chlorophyll was estimated by extracting each set of leaf discs with 10 ml of methanol overnight at 4°C and measuring the absorbance, spectrophotometrically at 665 nm wavelength. Chlorophyll loss was expressed as the ratio of absorbance of leaf discs after an incubation period, to the absorbance of leaf discs prior to the assay being set up.

For the bioassay of plant extracts, 3.0 cm wide zones, corresponding to the R_f of GA₃, were scraped from each TLC plate and suspended in 3.0 ml distilled water. A two-fold dilution series was made up from each plate zone suspension.

(b) Absciscic acid

The stimulation of α -amylase in barley aleurone layers by gibberellic acid is inhibited by absciscic acid. The extent of inhibition is dependent upon the concentrations of gibberellic acid and absciscic acid (Chrispeels and Varner, 1966a, 1966b, 1967). The basis of this interaction was used as an assay method for ABA by Barton et al. (1973). The method reported here is a modification of the above technique which essentially employs the barley endosperm bioassay for gibberellins as reported by Coombe, Cohen and Paleg (1966a, 1966b). Conditions for the bioassay and setting up procedures were as reported for the barley endosperm bioassay for gibberellins. However, all 1.0 ml incubates included 2.5×10^{-8} gm per ml GA₃. Dilution series of TLC plate zones and absciscic acid standards were prepared in 0.005 M citrate buffer, pH 6.0. To each dilution

was added a half volume of buffer and a half volume of 10^{-7} gm per ml GA3 to give final gibberellic acid concentrations of 2.5×10^{-8} gm per ml. A 5-fold dilution series of abscisic acid was prepared to give final concentrations of 2×10^{-6} , 4×10^{-7} , 8×10^{-8} , 1.6×10^{-8} , 3.2×10^{-9} , 6.4×10^{-10} and 1.28×10^{-10} gm per ml. Reactants for bioassay included, in addition to plate zone dilutions and pure abscisic acid, a zero control and a GA3 control (2.5×10^{-8} gm per ml.).

(c) Cytokinins

(i) *Amaranthus*-betacyanin production bioassay

The *Amaranthus* assay is based on the cytokinin-induced formation of betacyanins in cotyledons and hypocotyls from *A. caudatus* seedlings, incubated in the dark in the presence of tyrosine. The method used was that developed by Biddington and Thomas (1973). This technique was finally adopted for all cytokinin results reported here.

Seeds of *Amaranthus caudatus* L. were sown on moistened filter paper discs in 9.0 cm glass petri dishes and allowed to germinate in darkness at 22°C for 96 hours. All subsequent bioassay procedures were carried out under safe green light. After 3 days germination, seedlings were sprayed with distilled water to facilitate seed coat removal. On day 4 the seed coats were removed and explants, consisting of the upper portion of the hypocotyl plus the cotyledons, were cut from the seedlings. Explants were used as the bioassay sections, sets of ten being transferred to 5.0 cm plastic petri dishes. Each dish contained three layers of 5.0 cm Whatman No.1 filter paper discs moistened with 2.0 ml of $M/75$ phosphate buffer, pH 6.1, containing 1 mg/ml tyrosine and the cytokinin to be assayed for. Dishes were incubated in the dark at 22°C for 18 hours, after which the explants were transferred to 3 ml of distilled water. Betacyanin was extracted by two cycles of freezing and thawing and the optical densities at 542 nm and 620 nm determined.

A cytokinin standard response curve was obtained from dilutions of

kinetin (6-furfurylamino purine). The final concentrations of kinetin included were 2×10^{-6} , 2×10^{-7} , 2×10^{-8} , 2×10^{-9} gm per ml.

A blank using solvent only was also run in each assay. Both n-butanol soluble and water soluble cytokinins were chromatographed, the plate divided into 10 equal zones each of which was assayed.

Total cytokinin-like activity of partially purified extracts was determined on the final methanol soluble fractions for n-butanol soluble and water soluble cytokinins. As these extracts contained many other concentrated plant compounds, a dilution series of each extract was prepared in buffered tyrosine. One ml of methanol extract was evaporated to dryness and taken up in 5 ml of $M/75$ phosphate buffer containing tyrosine. For the assay a five-fold dilution series of each extract was prepared plus a buffer-tyrosine control.

(ii) Tobacco pith callus bioassay

The growth of tobacco pith calluses is extremely sensitive to cytokinin concentration. At low concentrations, growth is stimulated while at high concentrations growth is retarded.

Callus tissue for cytokinin assays was derived from pith cells of Nicotiana tabacum L. var. "Hickory Prior". Stem segments from tobacco were surface sterilized by swabbing with alcohol and flaming. The ends were cut off to expose fresh pith tissue and the pith was removed with a small, sterile cork borer. Cores were cut into discs 3-5 mm thick and transferred to plastic petri dishes containing sterile culture medium. Dishes were sealed with parafilm, to minimise moisture loss and incubated at 68°F under continuous white light. Callus growth culture medium was essentially that reported by Nagata and Takebe (1971) and contained 0.2 ppm kinetin and 0.2 ppm naphthalene acetic acid. (For complete composition see Appendix 32). Calluses were maintained by regular, monthly sub-culturing to this basic medium. The same medium, but without kinetin, was used to assay for cytokinins in extracts. In the bioassay, ten

callus pieces, each 3-5 mg fresh weight, were transferred to a petri dish containing 20 ml of sterile culture medium plus cytokinin. Dishes were incubated for 3 weeks under the previously mentioned conditions. Callus pieces were weighed and their fresh weights recorded. All bioassays were carried out in duplicate.

Callus response to kinetin was determined by adding kinetin to the incomplete growth medium to give final concentrations of 2.0, 0.2, 0.1, 0.02, 0.01 and 0.002 mg per ml. For bioassay of partially purified tissue extracts, 1.0 ml of methanol extract was evaporated to dryness and the residue taken up in 2 ml distilled water. A 10-fold dilution series was prepared for each extract.

(d) Auxins (indole acetic acid)

Auxins promote cell elongation in both roots and shoots. The coleoptile straight growth test bioassay is a development of this property. The method used here was originally reported by Bentley and Housley (1954) and modified by Hancock et al. (1964). Barley seeds, of a commercial brewing variety, were soaked in distilled water overnight. Seeds were sown in plastic trays on layers of wet tissue paper and incubated in the dark at 22°C for 4 days. All subsequent steps involving the germinated seed were carried out under a Kodak safe red light. When coleoptiles were about 2.0 cm long, a 1.0 cm section, excluding the apical 3 mm, was cut from each. Coleoptiles were chosen for uniformity of size and lack of curvature. One centimetre long sections were cut with a device incorporating two razor blades separated from each other and joined to a 1 cm wide block of perspex. This ensured that all sections were cut to the same length. For the bioassay, 5 cm plastic petri dishes were used, each containing 4 ml of test solution. The assay medium was composed of indole acetic acid dilution or TIC plate zone dilution in 0.05 M citrate/phosphate buffer, pH 5.0. Ten coleoptile segments were transferred to each dish and carefully floated on the 4 ml of solution. Dishes were placed in

plastic trays on moistened tissue paper and incubated for 18-20 hours at 22°C in the dark. The lengths of coleoptile segments were measured with the aid of a photographic enlarger.

A bioassay response curve to auxins was set up using a final concentration range for indole acetic acid of 0, 10^{-8} , 10^{-7} , 10^{-6} , 10^{-5} gm/ml. A 5-fold dilution series was prepared for each TLC plate zone. The above buffer system plus 2 percent sucrose was used for all dilutions and each treatment was duplicated.

RESULTS

Results from bioassays on plant hormones are commonly expressed in terms of a known standard and presented as "standard hormone equivalents". Presentation of results in this manner is only really justified when parallelism has been demonstrated for the dose/response curve of an unknown and the standard (Bailiss and Hill, 1971). Quoting absolute values of hormone levels in plant tissues is only justified if losses incurred during extraction and chromatography are determined. It was not considered necessary, in this work, to present final results as absolute concentrations. More interest lies in the relative changes in hormone levels rather than absolute levels. For this reason, final results in this section are expressed as ratios of hormone levels between healthy and infected tissues of a similar age. Assuming that losses of hormone during extraction are the same for healthy and infected tissues, given the same initial weights prior to extraction, hormone levels in virus-infected tissues, relative to levels in healthy tissues, gives an adequate assessment of the effects of virus infection on host hormone metabolism.

The preliminary extraction procedures employed allowed for no separation between auxins, gibberellins and abscisic acid. Final separation was dependent on thin layer chromatography (TLC) using a suitable solvent system. The R_f values for pure compounds of gibberellin A₃, indole acetic acid (IAA) and abscisic acid (ABA), on TLC plates run in various solvent systems is presented in Table 1. The most suitable solvent system for the isolation of a GA₃-like compound and its separation from major plant fluorescent bands was ethyl acetate:chloroform:acetic acid (ECA). Absciscic acid on the other hand was best isolated from other major plant hormones and fluorescent bands of plant origin in a toluene:ethyl acetate:acetic acid solvent system (TEA). Indole acetic acid and cytokinins were isolated on TLC plates developed in isopropanol:ammonia:water (IAW).

TABLE I

Rf values of GA3, ABA and IAA on thin layer plates coated with Kieselgel GF254 or Kieselgel G60.

Solvent System	Rf ABA	Rf GA3	Rf IAA
Isopropanol:Ammonia:Water (10:1:1)	0.72	0.64	0.66
Toluene:Ethyl acetate:Acetic acid (40:5:2)	0.13	0	-
Ethyl acetate:Chloroform:Acetic acid (15:5:1)	0.87	0.50	-

1. Gibberellin A3-like Activity in Extracts from Healthy and Virus-Infected Plant Tissues

It has been previously established that the major gibberellins in tobacco are gibberellin A1 and A3. These gibberellins are difficult to separate and with the extraction and purification procedures employed here, would almost certainly be together in the final extract. Both gibberellins give good responses in the barley endosperm bioassay and the Rumex senescing leaf disc bioassay. Although the lower sensitivity range of the Rumex leaf disc bioassay was suitable for the tobacco leaf extracts tested, certain other characteristics of the bioassay made its use unsuitable. The long incubation time of the assay (at least 7 days under the conditions employed) allowed for fungal growths in the bioassay dishes. This could only have been avoided by employing aseptic extracting, purifying and bioassaying techniques or purifying the final extracts to exclude most other plant constituents. Fungal growths were only a problem for tissue extracts tested and never occurred when pure compounds were bioassayed. The nature of the bioassay response, retardation of leaf disc senescence, is not specific but a general metabolic reaction. Senescence is associated with many biochemical changes in the cell, any of which could be affected by normal plant constituents concentrated during the extraction procedures. This was in fact suggested from the bioassay results for tissue extracts. Some component(s) in the extracts were toxic to the leaf discs.

The Rumex leaf disc bioassay for gibberellins was not suited to the conditions of tissue extraction and degree of extract purification reported here and was abandoned in favour of the barley endosperm bioassay.

The barley endosperm bioassay for gibberellins has the advantages of a short incubation time (24 hours) and a more specific mechanism of response (induced α -amylase synthesis in aleurone layers). The problem of toxic plant constituents in tissue extracts was therefore minimized.

Asceptic techniques were used in setting up each bioassay and this, together with the short incubation time ensured minimal contamination of incubates. The only disadvantages of the barley endosperm bioassay were its sensitivity to other plant hormones and the time involved in setting up the bioassay. Sensitivity to abscisic acid required adequate separation of the gibberellins from abscisic acid by thin layer chromatography. The time involved in setting up the bioassay imposed a limit to the number of extracts and extract dilutions that could be tested at any one time by the one person. A standard curve for the response of the barley endosperm bioassay to a concentration range of GA₃ is presented in Figure 44. The response curve for the bioassay represents the average response over six independent bioassays, performed at different times (see Appendix 33).

(a) GA₃-like activity in extracts from young leaves and shoots

The barley endosperm bioassay response to a five-fold dilution series of TLC purified plant extracts is presented in Figure 45. Dilution curves for both healthy and infected tissue extracts had a similar shape and were parallel with the dose/response curve for GA₃ over the upper dilution range (see Figure 44). Both healthy and virus-infected tissue extract curves are superimposed and there appears to be no effect of virus infection on GA₃-like activity in young tissue extracts.

(b) GA₃-like activity in tissue extracts from mature leaves

No measurable GA₃-like activity was detected from relevant TLC plate zones of healthy and infected leaf tissue extracts. Dose/response curves for both extracts gave no responses in the barley endosperm bioassay over the five-fold dilution series of each tested (Figure 46).

2. ABA-like Activity in Mature Leaf Extracts from Healthy and Virus-Infected Plants

Abscisic acid inhibition of the barley endosperm bioassay for gibberellins is demonstrated in the dose/response curve of ABA concentrations

Figure 44

Relation between \log_{10} gibberellin A3 concentration (gm/ml) and induced α -amylase activity in barley endosperm pieces (free sugars produced by amylase developed photocolrimetrically with anthrone reagent and measured at 625 nm wavelength).

Standard error of plotted points = 0.0526 (see Appendix 33)

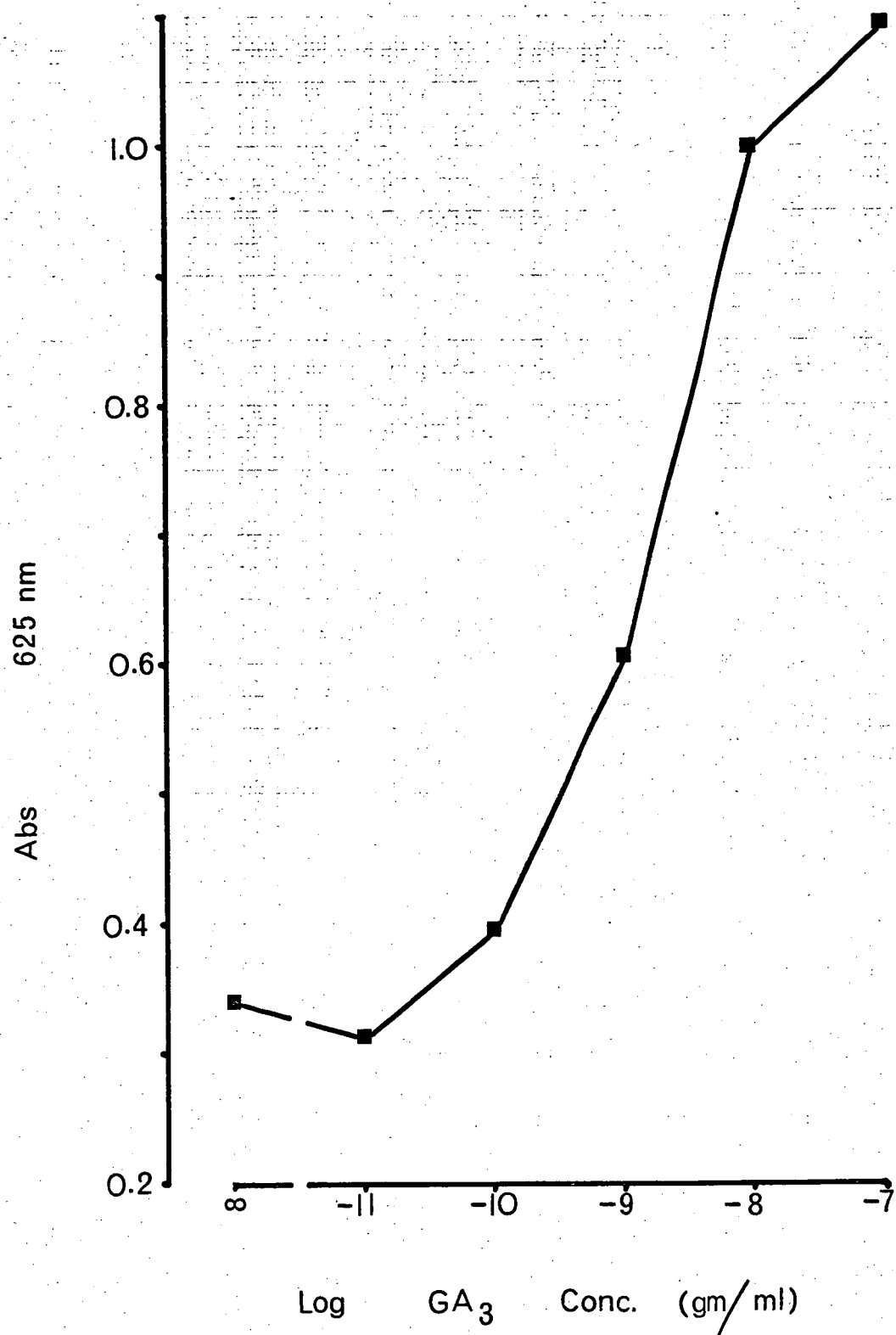


Figure 45

Relation between gibberellin A₃-like activity in young tobacco tissue extracts (plotted \log_{10} of purified extract dilutions) and induced α -amylase activity in barley endosperm pieces (free sugars liberated developed in anthrone reagent and measured at 625 nm wavelength).

Standard error of plotted points = 0.0338 (see Appendix 34)

(O———O) - Extracts from healthy tobacco plants

(□-----□) - Extracts from virus-infected plants

(▲) - Sterile water control

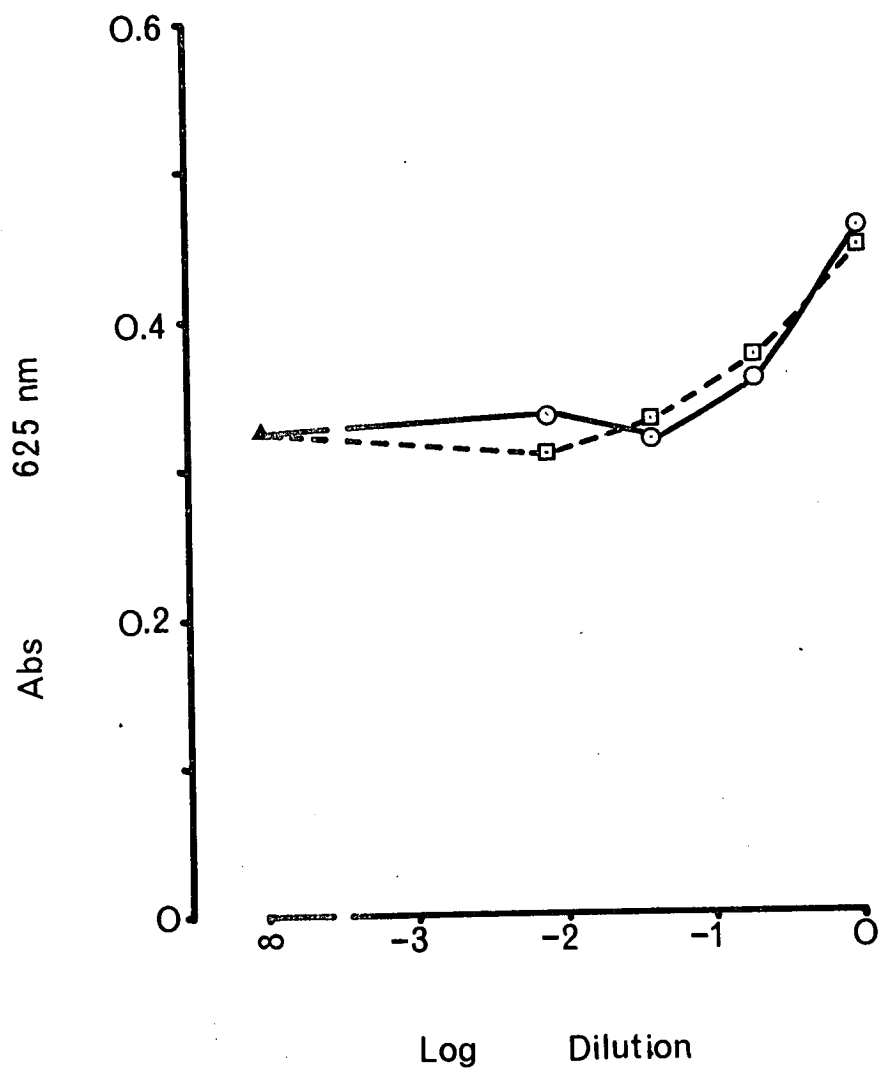
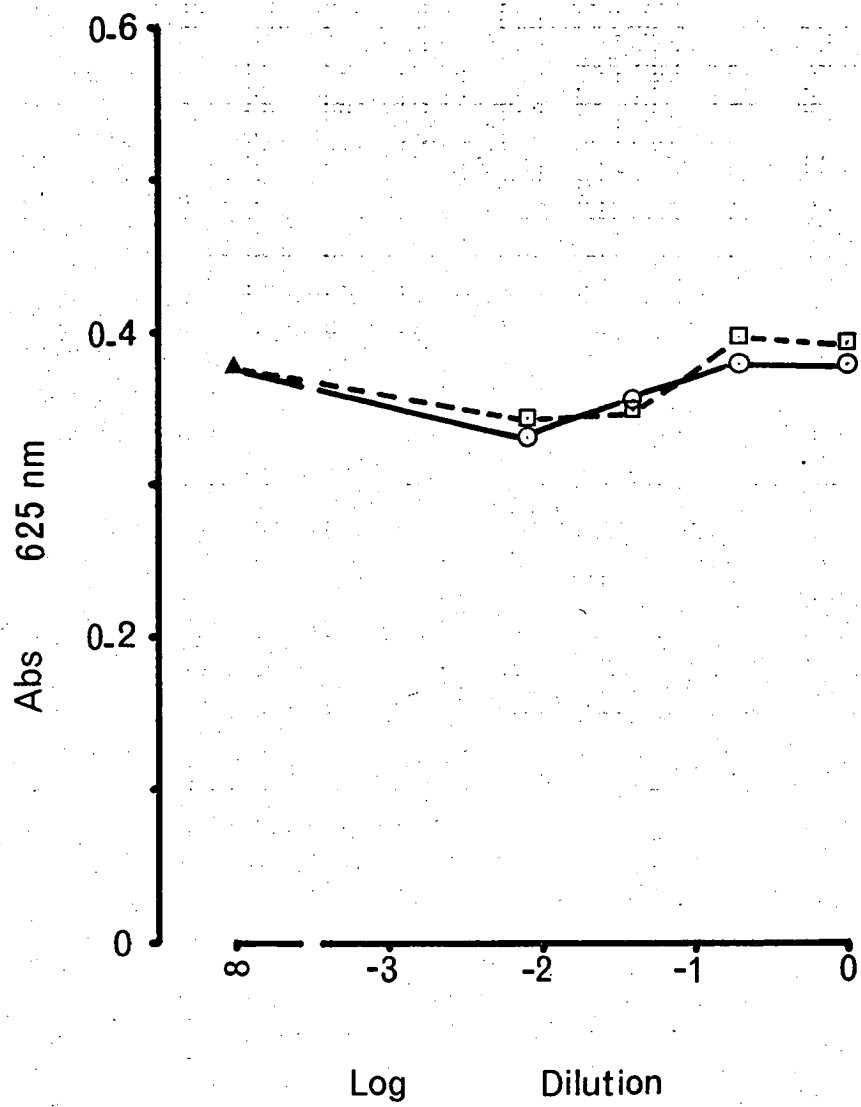


Figure 46

Relation between gibberellin A₃-like activity in mature tobacco leaf extracts (plotted \log_{10} of purified extract dilutions) and α -amylase activity in barley endosperm pieces (free sugars liberated developed in anthrone reagent and measured at 625 nm wavelength).

Standard error of points plotted = 0.0265 (see Appendix 35)

- (○——○) - Extracts from healthy tobacco plants
- (□ - - - - □) - Extracts from virus-infected plants
- (▲) - Sterile water control



versus the bioassay response to 2.5×10^{-8} gm/ml GA3 (Figure 47). The nature of the response varied with the concentration of gibberellic acid. A number of GA3 concentrations were tested in the bioassay against ABA standards and tissue extract dilutions. GA3 concentration of 2.5×10^{-8} gm/ml was found to give the most suitable linear response over the range of dilutions of tissue extracts tested.

Dose/response curves for healthy and infected tissue extracts, chromatogrammed twice in a toluene:ethyl acetate:acetic acid solvent system are presented in Figure 48. Both healthy and infected tissue extract curves are parallel and exhibit the same form as the standard ABA dose/response curves. In estimating the ABA ratio of healthy : infected tissue extracts, the absorbance figures for the $1/20$ dilution of each extract were used (see Appendix 37). The differences in absorbance 625 nm units between healthy and infected extracts at the above dilution and the 2.5×10^{-8} GA3 control line is 0.30 and 0.10 respectively. From the standard ABA/response curve the following concentrations of abscisic acid were estimated:

Healthy tissue extract - 8.92×10^{-8} gm Equivalents ABA/ml

Infected tissue extract - 3.55×10^{-8} gm Equivalents ABA/ml

The ABA ratio of healthy : infected tissue extract is 2.5 : 1. In extracts from mature leaves, there was more than twice the level of abscisic acid in healthy tissues compared with infected tissues. To further verify the nature of the ABA-like growth substance and its relative concentrations in healthy and virus-infected tissues, tissue extracts from mature leaves were purified by TLC in two different solvent systems, ethyl acetate:chloroform:acetic acid and toluene:ethyl acetate:acetic acid. Dose/response curves for the relevant TLC plate zone are presented in Figure 49. Again both curves paralleled each other and the ABA standard dose/response curve. Using the absorbance 625 nm figures for the 1 : 50 extract dilutions (see Appendix 38) the ABA ratio of healthy : infected

Figure 47

Relation between \log_{10} abscisic acid concentration (gm/ml) and α -amylase activity induced by 2.5×10^{-8} gm/ml GA3 in barley endosperm pieces (free sugars liberated by amylase developed with anthrone reagent and measured at 625 nm wavelength).

Standard error of plotted points = 0.0416 (see Appendix 36)

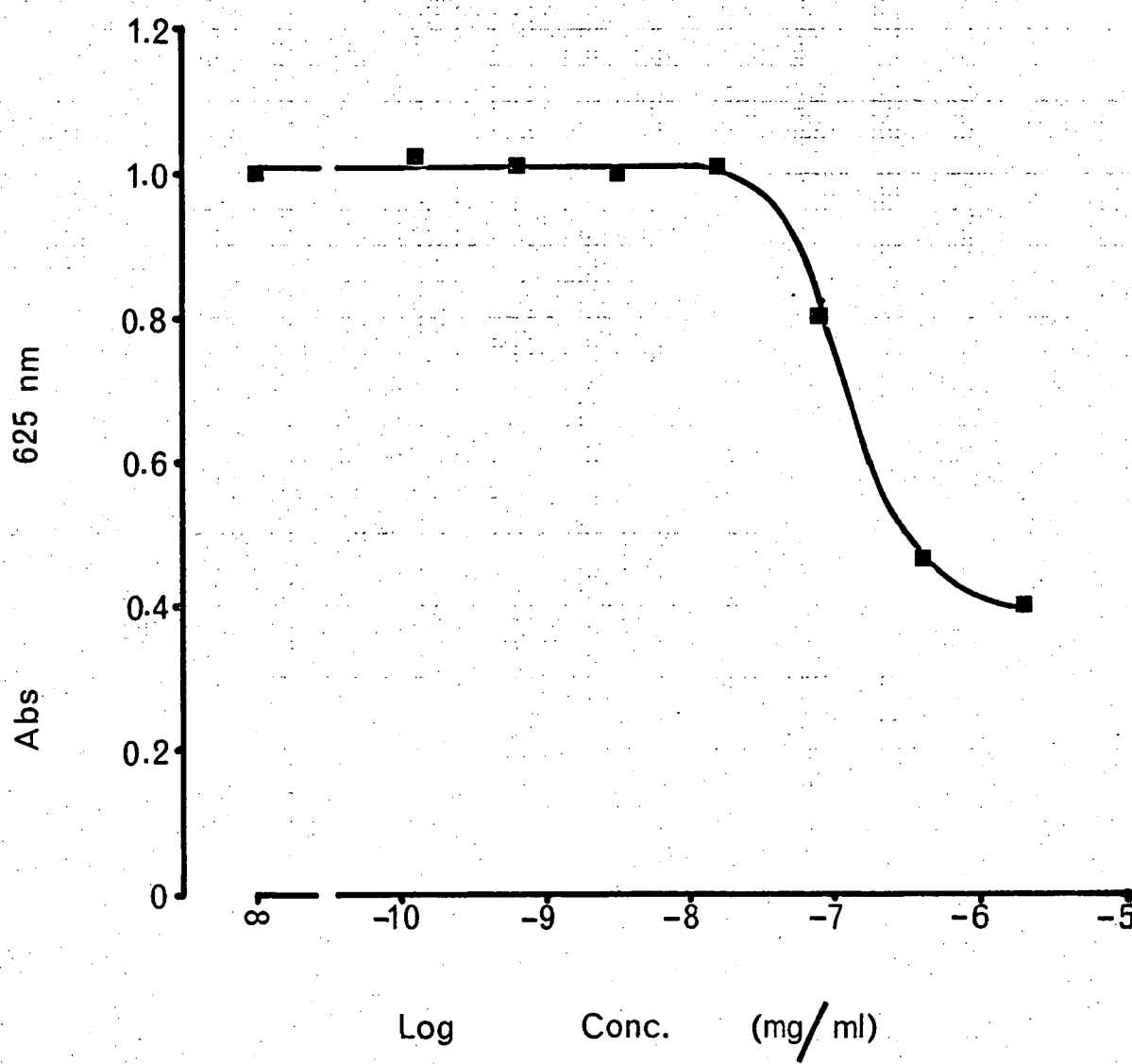


Figure 48

Relation between abscisic acid-like activity in mature tobacco leaf tissues (plotted as \log_{10} of purified extract dilutions) and GA₃-induced α -amylase activity in barley endosperm pieces (sugars liberated by amylase developed with anthrone reagent and measured at 625 nm wavelength). Leaf extracts purified on TLC plates developed in toluene: ethyl acetate:acetic acid solvent system.

Standard error of plotted points = 0.0507 (see Appendix 37)

(○——○) - Extracts from healthy tobacco plants

(□----□) - Extracts from virus-infected plants

(▲) - 2.5×10^{-8} gm/ml GA₃ control

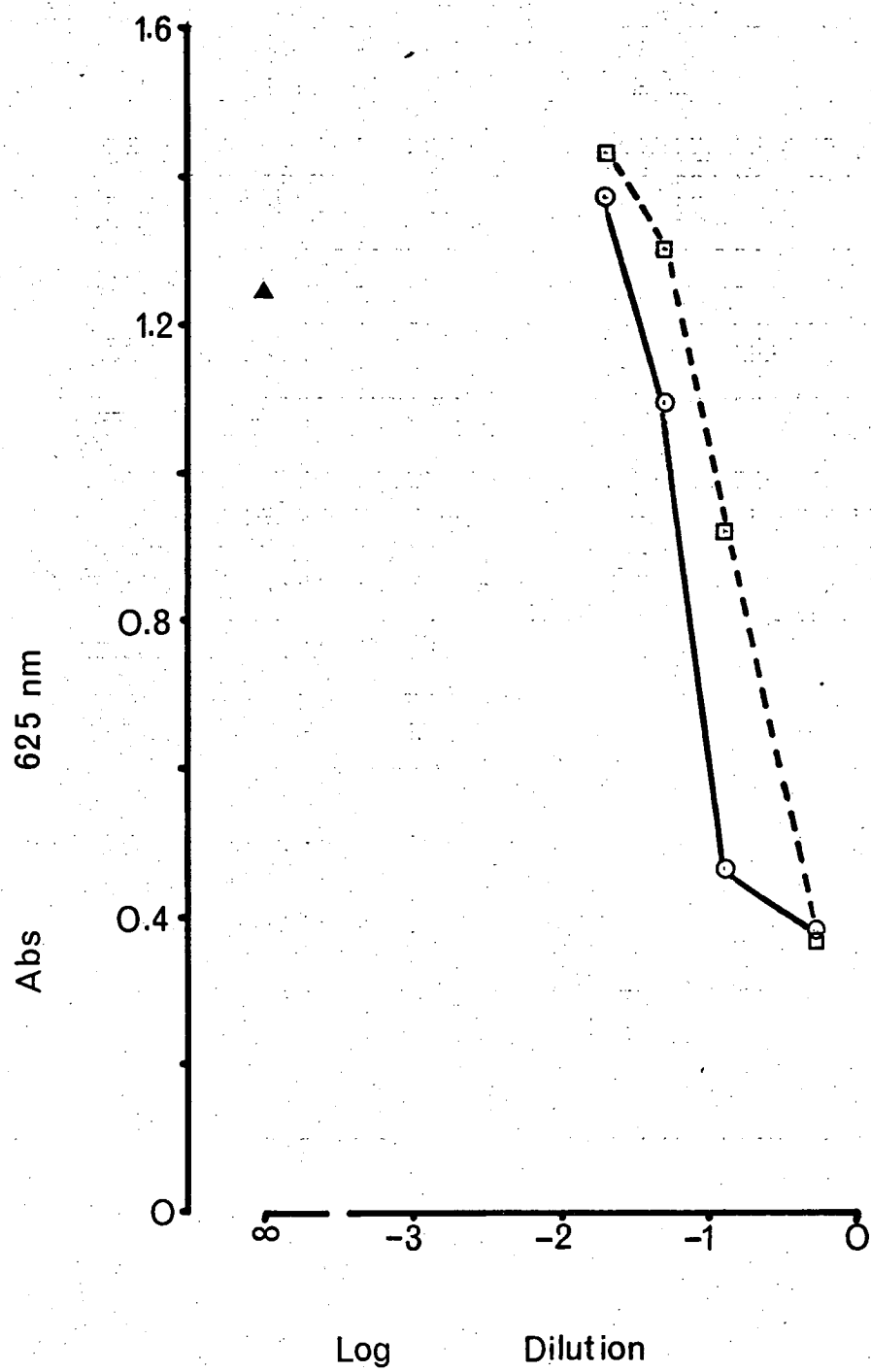


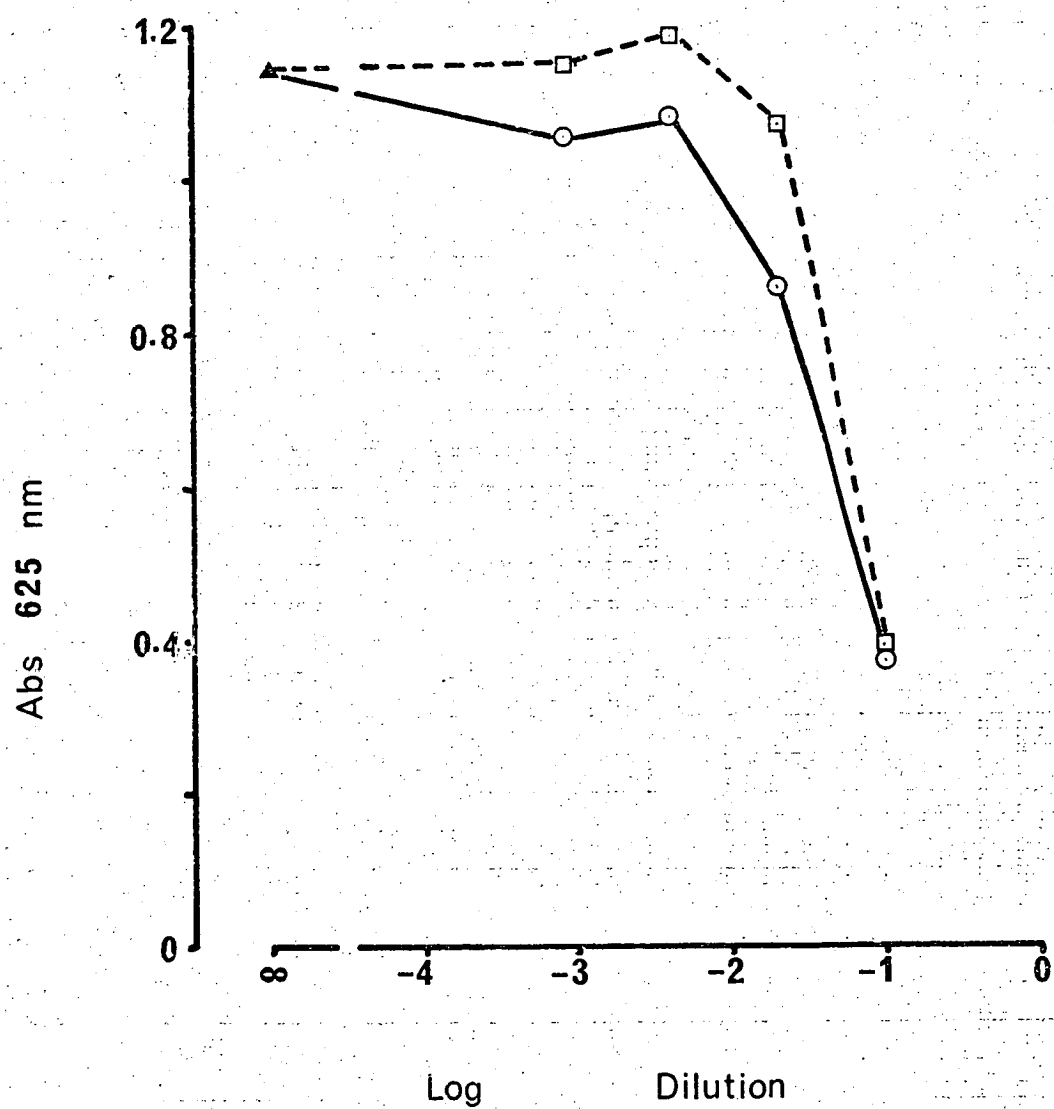
Figure 49

Abscisic acid-like compound from tobacco leaves purified on TLC plates developed in ethyl acetate:chloroform:acetic acid solvent system and further purified on TLC-plates developed in toluene:ethyl acetate:acetic acid solvent system.

Graph represents relation between abscisic acid-like activity in mature tobacco leaves (plotted as \log_{10} purified extract dilutions) and GA3-induced α -amylase activity in barley endosperm pieces (free sugars liberated developed with anthrone reagent and measured at 625 nm wavelength).

Standard error of plotted points = 0.0388 (see Appendix 38)

- (○——○) - Extracts from healthy tobacco plants
- (□----□) - Extracts from virus-infected plants
- (▲) - 2.5×10^{-8} gm/ml GA3 control



leaf tissue extracts was 2.24 : 1. This confirmed the results obtained from a single solvent system extract purification.

The Rf positions of the ABA-like growth inhibitor in two different solvent systems and its dose/response characteristics in the barley endosperm bioassay suggest that this particular inhibitor is probably abscisic acid.

3. Cytokinin-like Activity in Extracts from Healthy and Virus-Infected Plant Tissues

A number of bioassays were tested for their suitability with cytokinins in tobacco leaf tissue extracts. Much of the earlier work involved using the tobacco pith callus bioassay. However, there were several reasons for abandoning this technique as a bioassay for tissue extract cytokinins. An incubation period of 3-4 weeks restricted the number of extracts that could be tested. Stringent aseptic conditions of culture had to be maintained to avoid fungal and bacterial growths in culture. Although the bioassay is among the most sensitive for cytokinins, the final volume of culture medium per assay dish and the degree of replication required, resulted in high final dilutions of each tissue extract. Tobacco pith calluses were very sensitive to other plant constituents and traces of chromatography solvents in thin layer chromatography plate zones. Sterilization of the final culture media may also have reduced the activity of extracted, endogenous cytokinins.

Although the methods are not reported here, two other cytokinin bioassays were briefly tested. These were the barley root growth inhibition bioassay as reported by van Onckelen and Verbeek (1971) and Verbeek *et al.* (1969) and the radish cotyledon expansion bioassay as reported by Letham (1967). The barley root growth inhibition bioassay was discounted because the large assay medium volume required per test, together with replication and dilution of plants extracts, resulted in excessive final dilution values of the partially purified extracts. Also a high

statistical variability was associated with the bioassay. The radish cotyledon expansion bioassay was rejected because the lower limit of sensitivity was too high (0.01 ppm kinetin) to detect cytokinins in tobacco leaf extracts.

The bioassay finally adopted for measuring cytokinin concentrations was the *Amaranthus*-betacyanin pigment production bioassay. Final assay volumes (2 ml per assay dish) allowed for an adequate dilution series and replication per test extract. The bioassay displayed some sensitivity to concentrated plant constituents and solvent traces in the final purified extracts, however, such inhibitions were readily overcome by diluting the final extracts. The sensitivity of this bioassay was at least equivalent to the tobacco pith callus bioassay. The bioassay is more sensitive to naturally occurring cytokinins such as zeatin and its derivatives and 6-benzyl adenine than the synthetic hormone, kinetin (Biddington and Thomas, 1973). The short incubation time for the bioassay (18-20 hours) allowed the use of non-aseptic techniques during extraction and setting up of the bioassay and also minimized the effects of interactions from other hormones that could have been present in the extracts. A standard response curve for kinetin-induced betacyanin pigment production by *Amaranthus* explants is presented in Figure 50.

(a) Cytokinin-like activity in young leaf and shoot extracts

Extracts from healthy and infected tissues were separated on Kieselgel G60 TLC plates in isopropanol:ammonia:water (10:1:1, $v/v/v$). Bioassay of all TLC plate zones revealed two major zones of activity. A slow-migrating zone of activity at R_f 0-0.2 and a faster-migrating zone of activity at R_f 0.5-0.8.

Cytokinin-like activity at both R_f ranges was greater in tissue extracts from virus-infected plants for both the n-butanol soluble fraction (Figure 51) and the water soluble fraction (Figure 52). The higher cytokinin activity of infected tissue extracts as separated and purified by

Figure 50

Relation between \log_{10} kinetin concentration (gm/ml) and betacyanin production by *Amaranthus* explants (measured as Abs. 543 - Abs. 620 nm).

Standard error of plotted points = 0.0112 (see Appendix 39).

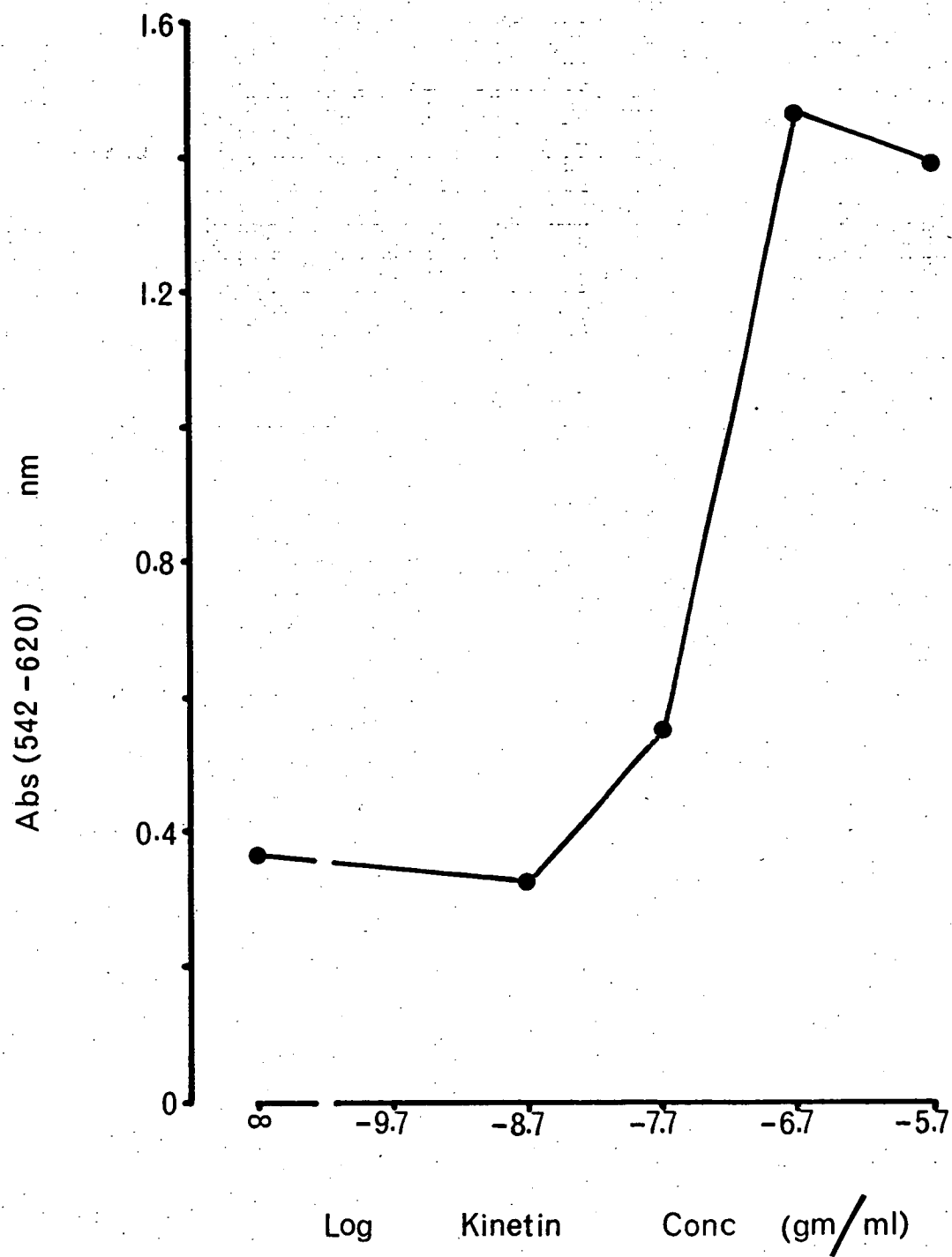


Figure 51

Cytokinin activity in n-butanol soluble fraction of extracts from young leaf and meristem tissues.

Relation between TLC plate zone and betacyanin production by *Amaranthus* explants (Abs. 542 nm - 620 nm).

For statistical analysis and actual value of points plotted see Appendix 40.

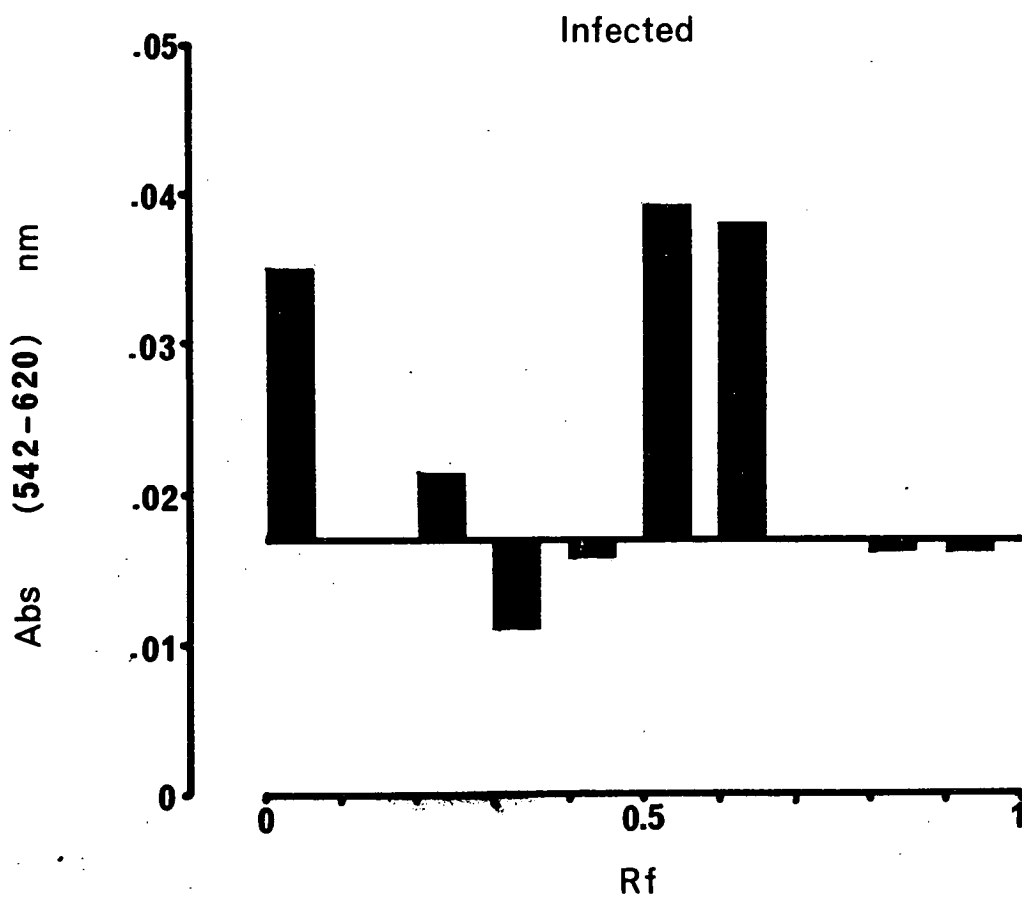
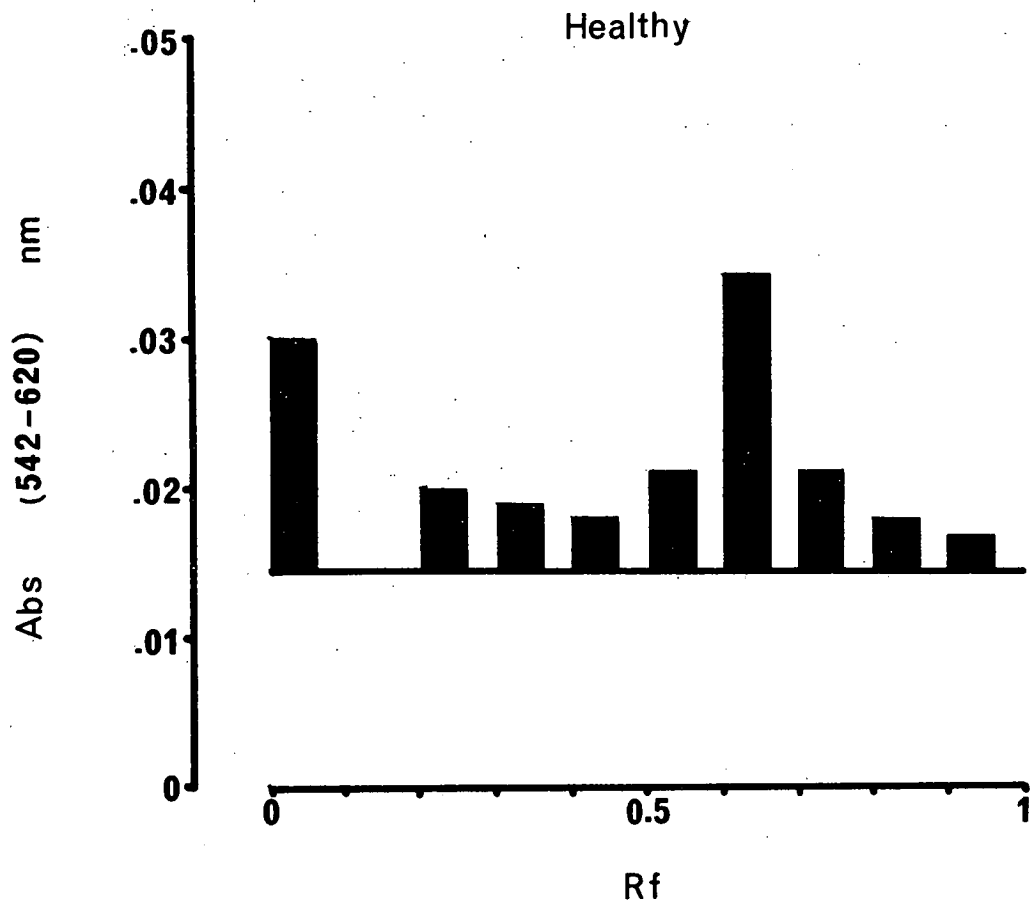
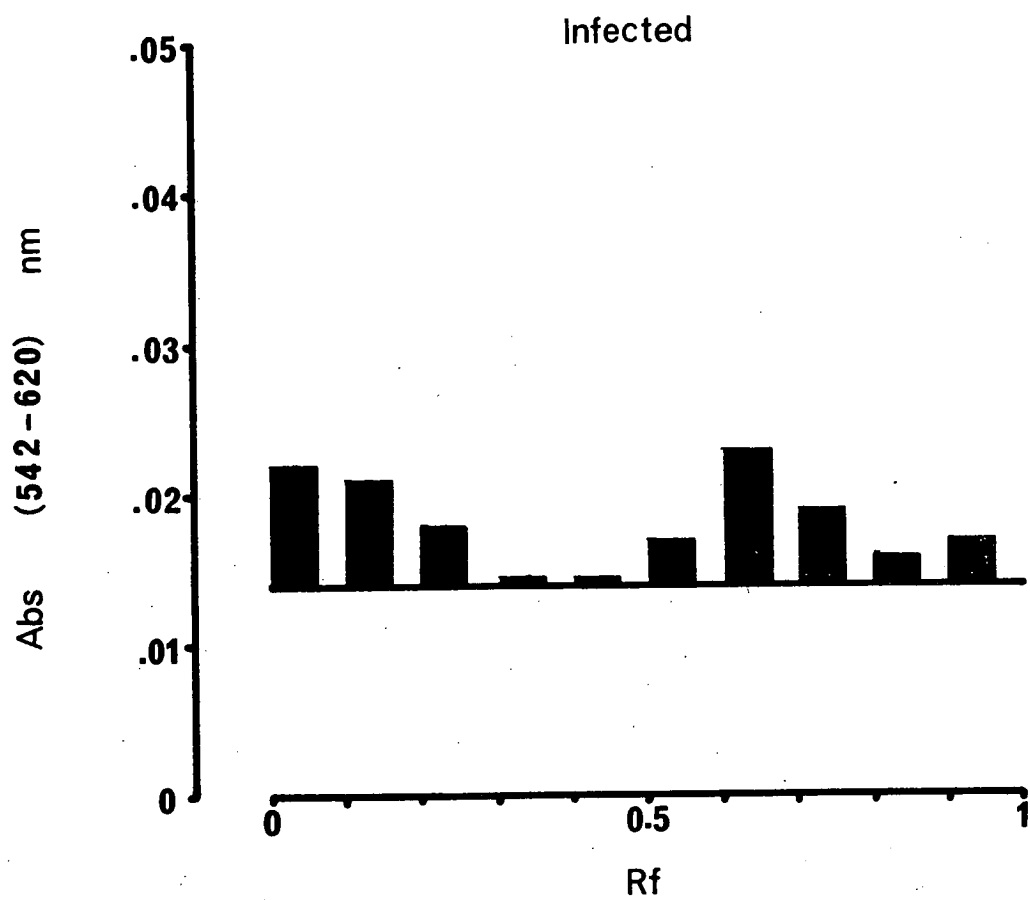
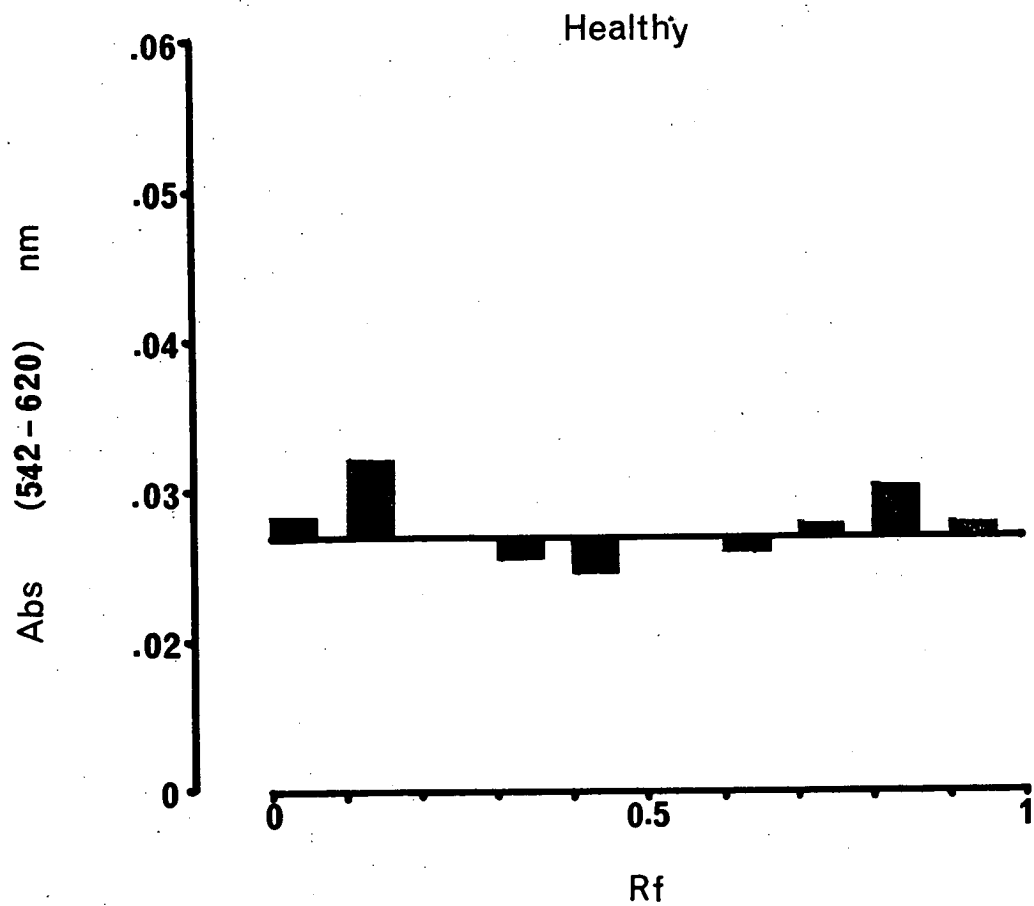


Figure 52

Cytokinin activity in water soluble fraction of extracts from young leaf and meristem tissues. Relation between TIC-plate zone and betacyanin production by *Amaranthus* explants (Abs. 542 nm - Abs. 620 nm).

For statistical analysis and actual value of points plotted see Appendix 41.



TLC was verified from dose/response curves of the n-butanol soluble fractions from both healthy and virus-infected tissue extracts (Figure 53). Both healthy and infected tissue extracts produced a curved response over the dilution range tested. The ratio, infected tissue extract : healthy tissue extract, of cytokinin-like activity, was calculated from the kinetin response curve using the $1/25$ extract dilution data (see Appendix 42). The ratio of kinetin equivalents (gm/ml) for infected versus healthy extracts was 3.55 : 1.

It can be concluded therefore, that in young tissue extracts from tobacco plants, infected with tobacco mosaic virus, there was a higher level of extractable total cytokinin-like compounds than in comparably aged tissues from uninoculated plants. Components of total extractable cytokinin-like compounds from virus-infected plants, separated on TLC plates, were also more active in the bioassay employed than individual components of uninfected plant extracts.

(b) Cytokinin activity in mature leaf tissue extracts

Cytokinin activity in n-butanol soluble fractions was greater in extracts from virus-infected plants. Higher cytokinin activity was detected at both major zones of activity on TLC plates (Figure 54). A dilution series from the n-butanol soluble extracts, assayed for in the *Amaranthus*-betacyanin production bioassay, also revealed a higher cytokinin activity in infected tissue extracts (Figure 55). The ratio of cytokinin activity (gm equivalents kinetin/ml) for infected versus healthy tissue extracts, was 1.33 : 1. This figure is based on the $1/125$ dilution figures for both healthy and infected tissue extracts. Extracts from virus-infected plants were more inhibitory to the bioassay at the lower dilutions tested and therefore calculations to determine the cytokinin activity ratio were based on the $1/125$ dilution data.

There were no major differences in cytokinin-like activity between the water soluble fractions from mature leaf extracts. There is some

Figure 53

Cytokinin activity in n-butanol soluble fraction of extracts from young leaf and meristem tissues. Relation between \log_{10} extract dilution and betacyanin production by *Amaranthus* explants (Abs. 542 nm - Abs. 620 nm).

Standard error of points plotted = 0.0020 (see Appendix 42).

- (○——○) - Extract from healthy tobacco plants
- (□- - - -□) - Extract from virus-infected plants
- (▲) - Distilled water control

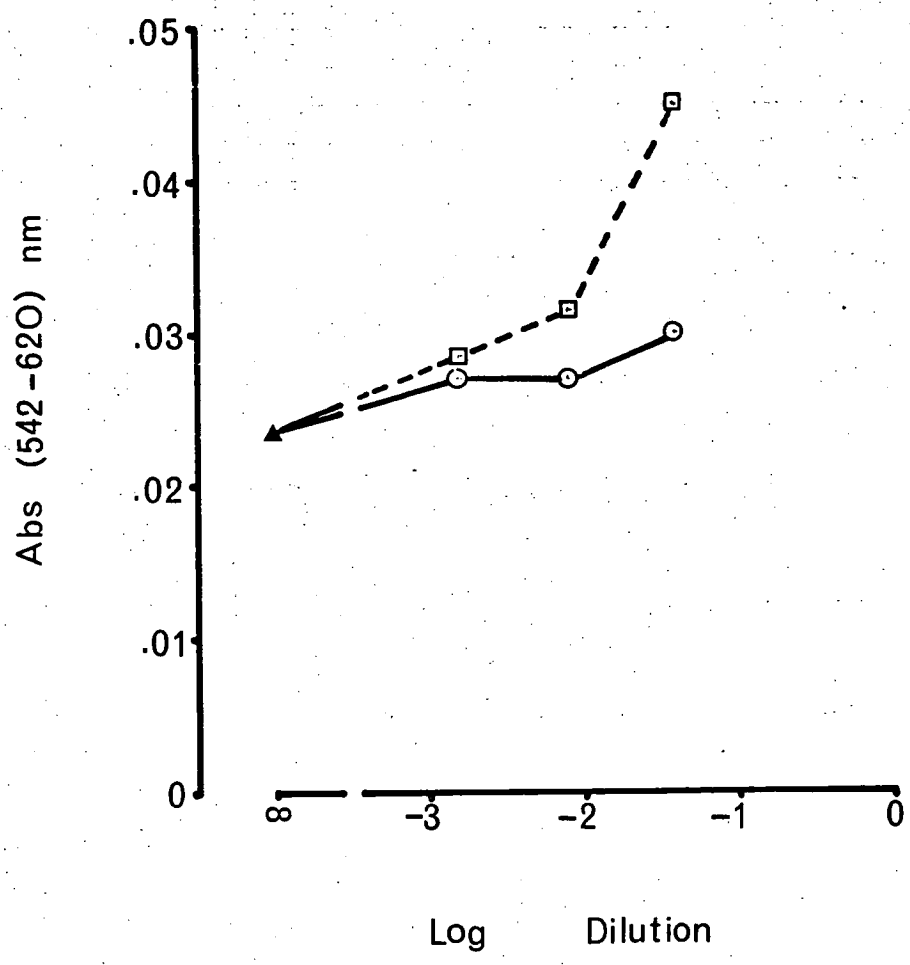


Figure 54

Cytokinin activity in n-butanol soluble fraction of extracts from mature leaves. Relation between TLC-plate zone and betacyanin production by *Amaranthus* explants (Abs. 542 nm - Abs. 620 nm).

For statistical analysis and actual value of points plotted see Appendix 43.

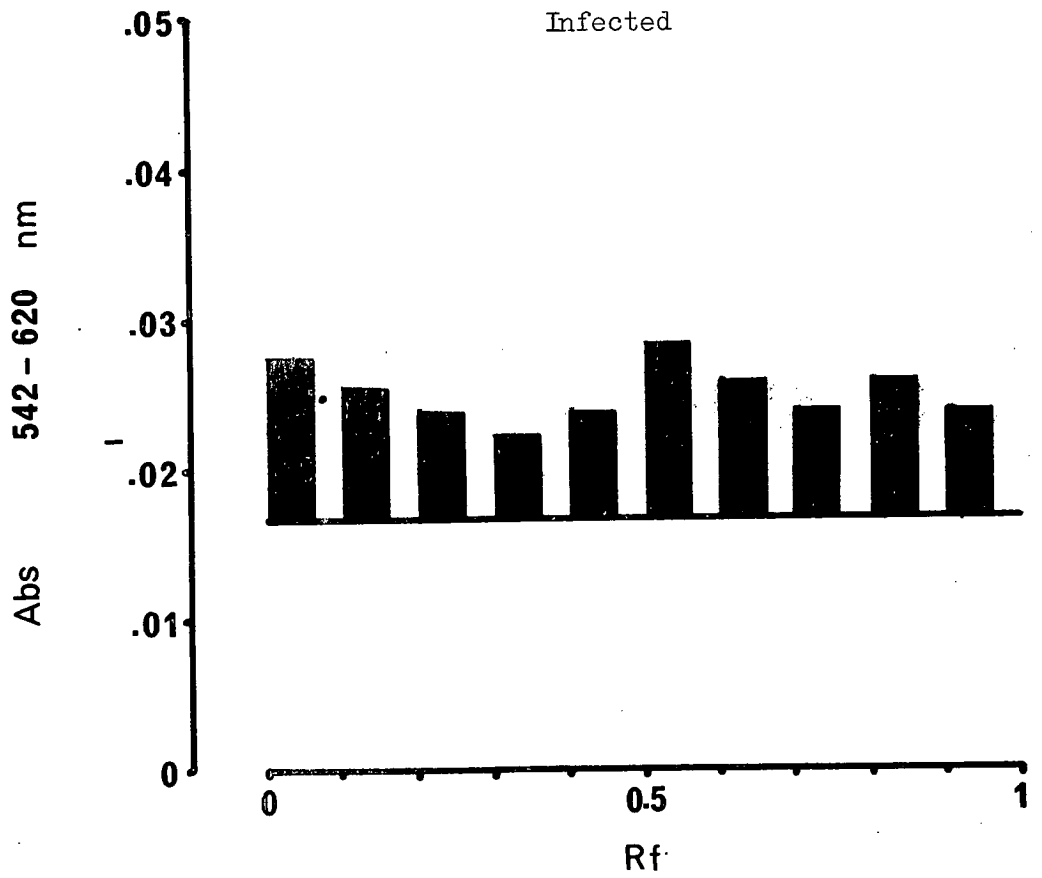
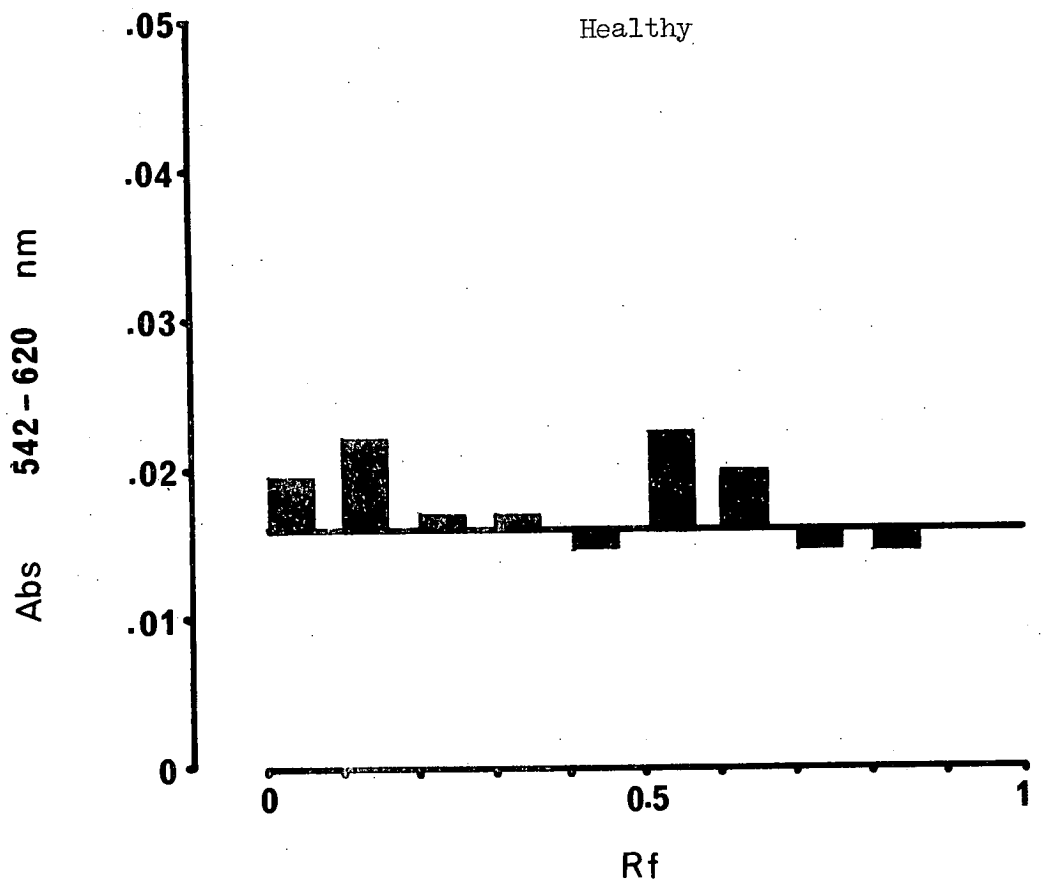
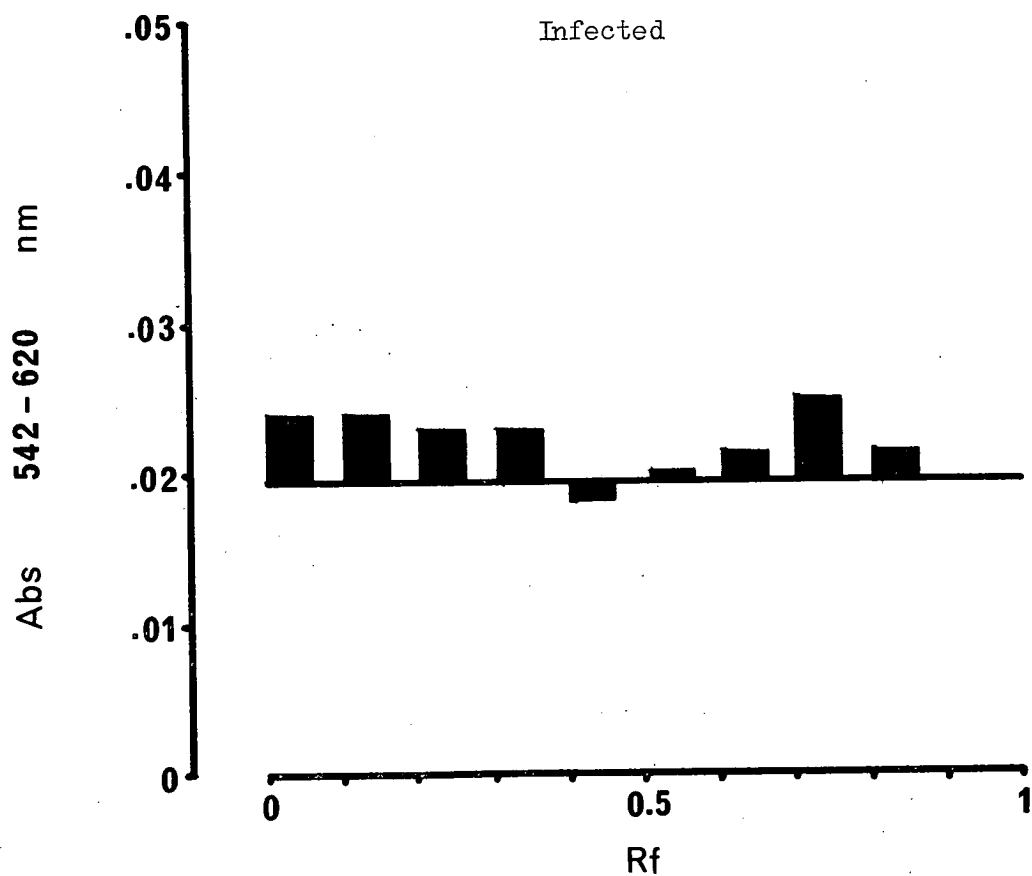
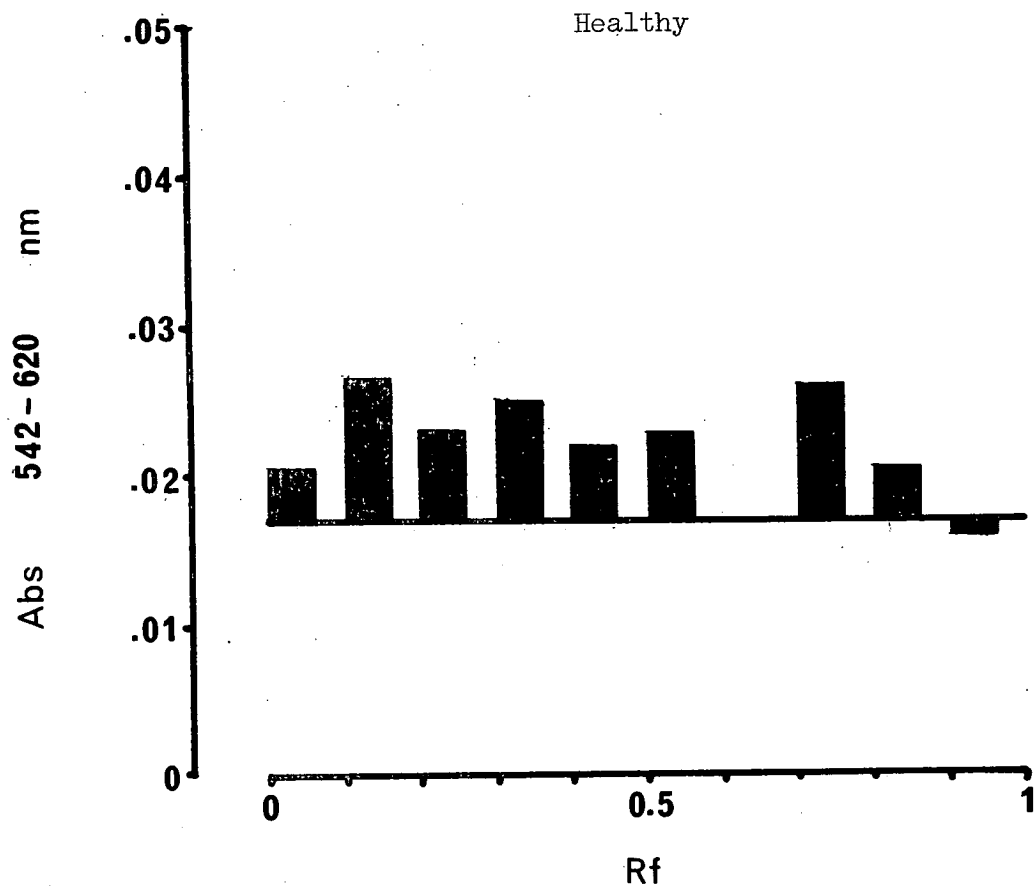


Figure 55

Cytokinin activity in water-soluble fraction of extracts from mature leaves. Relation between TLC-plate zone and betacyanin production by *Amaranthus* explants (Abs. 542 nm - Abs. 620 nm).

For statistical analysis and actual value of points plotted see Appendix 45.



suggestion from the chromatographs of water soluble fractions of a slightly higher cytokinin activity at both low and high Rf values for extracts from healthy tissues (Figure 56). However, based on the extract dilutions/bioassay response curves, there was no difference in total cytokinin activity bioassay response curve for extracts from healthy and between healthy and virus-infected mature leaves (see Figure 57). The failure of water-soluble extracts to induce a dose/response curve was probably a function of low cytokinin activity and inhibitors of plant origin in the concentrated tissue extracts. Dilutions, necessary to eliminate the effect of any inhibitors present, probably lowered cytokinin levels below the sensitivity of the bioassay.

(c) Cytokinin activity of root tissue extracts

As for leaf and stem tissue extracts, root extracts were separated into n-butanol soluble cytokinins and water soluble cytokinins. For both n-butanol fractions and water soluble fractions, the cytokinins of chromatographed extracts did not clearly separate into two major zones of activity. Most of the cytokinin-like activity from the n-butanol soluble fractions, occurred beyond Rf 0.4 (Figure 58). There is some suggestion from the TIC-plate profiles of a higher cytokinin activity in extracts from infected plants. The picture for water soluble fractions from roots is more confusing and no valid conclusions, with respect to virus-induced alterations to patterns of cytokinin activity, can be drawn from these chromatographs (Figure 59).

As no major zones of cytokinin-like activity were found following TIC of root extracts it was not considered necessary to produce dose/response curves for these extracts.

In summary, extracts from leaves and shoots, separated on thin layer chromatography plates, were resolved into two major areas with cytokinin-like activity. Most activity, as determined by the *Amaranthus*-betacyanin pigment production bioassay, occurred at Rf of 0.6 - 0.7. Some activity

Figure 56

Cytokinin activity in n-butanol soluble fraction of extracts from mature leaves. Relation between \log_{10} extract dilutions and betacyanin production by *Amaranthus* explants (Abs. 542 nm - Abs. 620 nm).

Standard error points plotted = 0.0031 (see Appendix 44).

- (○——○) - Extract from healthy tobacco plants
- (□-----□) - Extract from virus-infected plants
- (▲) - Distilled water control

Figure 57

Cytokinin activity in water soluble fraction of extracts from mature leaves. Relation between \log_{10} extract dilutions and betacyanin production by *Amaranthus* explants (Abs. 542 nm - Abs. 620 nm).

Standard error of points plotted = 0.0013 (see Appendix 46).

- (○——○) - Extract from healthy tobacco plants
- (□-----□) - Extract from virus-infected plants
- (▲) - Distilled water control

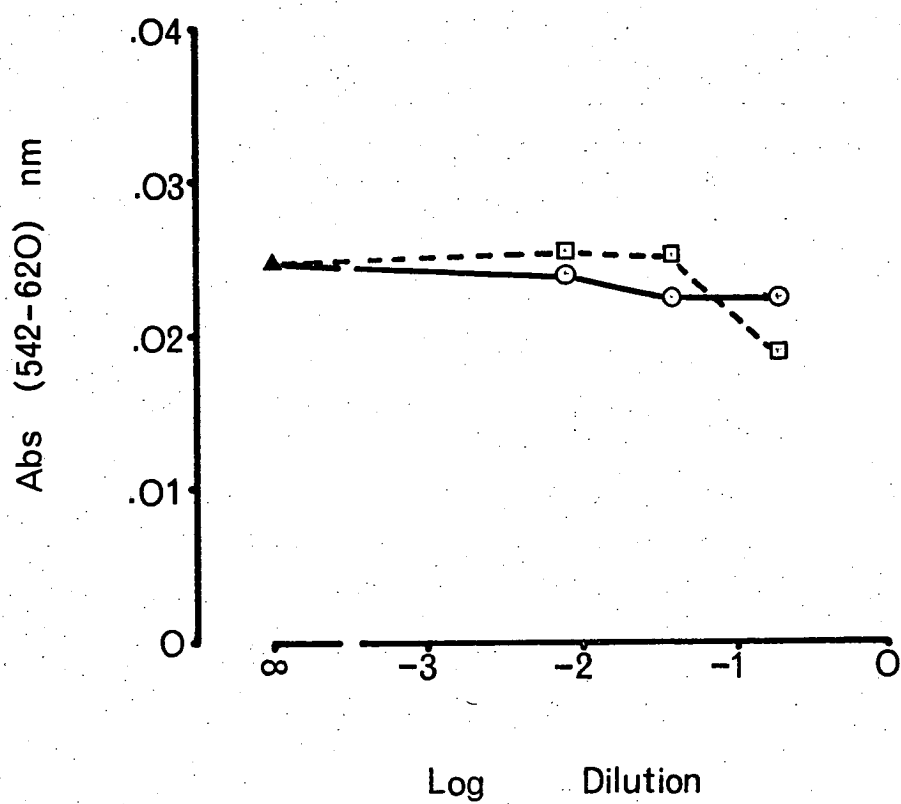
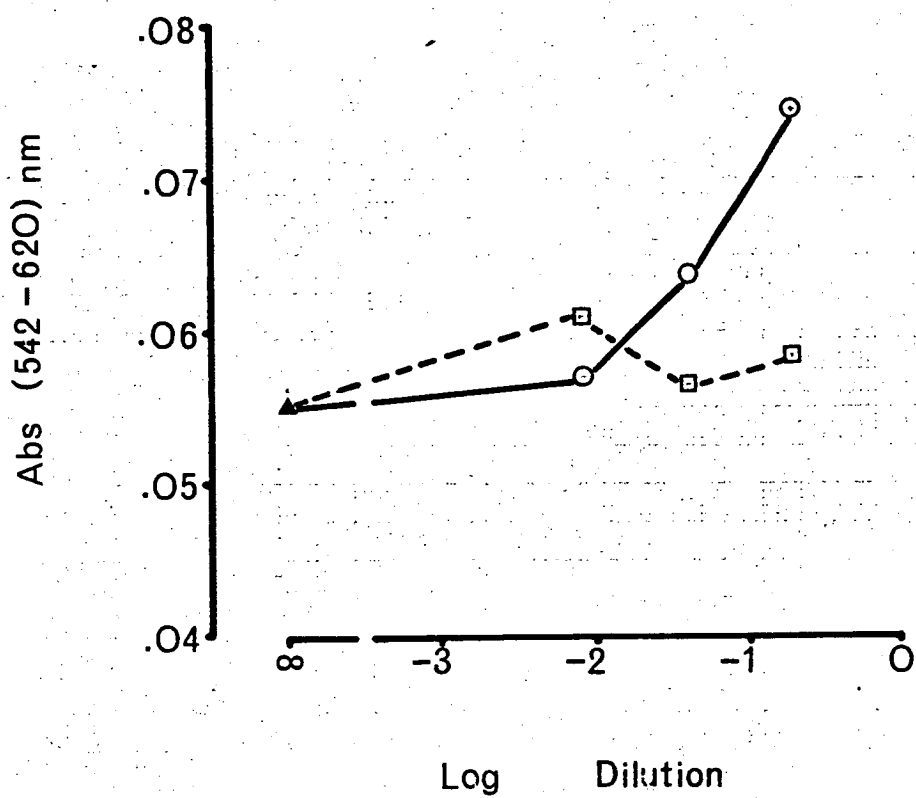


Figure 58

Cytokinin activity in n-butanol soluble fraction from tobacco roots.
Relation between TLC-plate zone and betacyanin production by *Amaranthus*
explants (Abs. 542 nm - Abs. 620 nm).

For statistical analysis and actual value of points plotted see
Appendix 47.

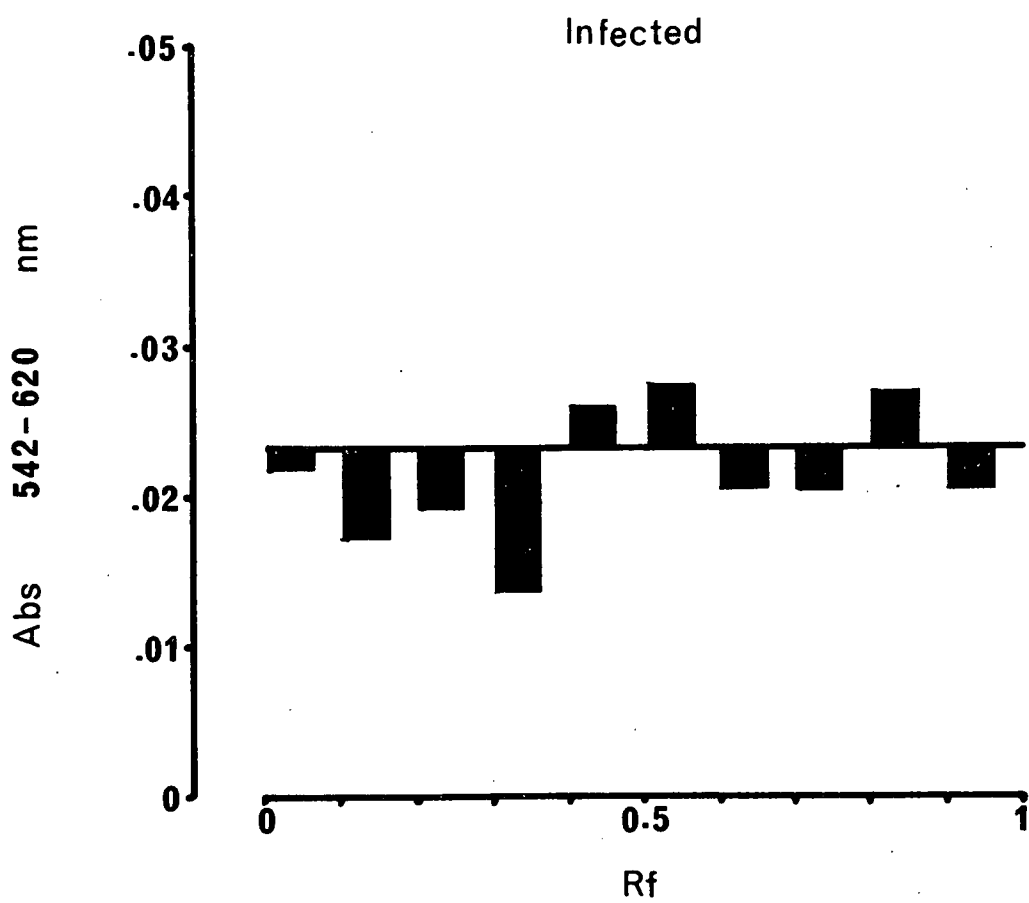
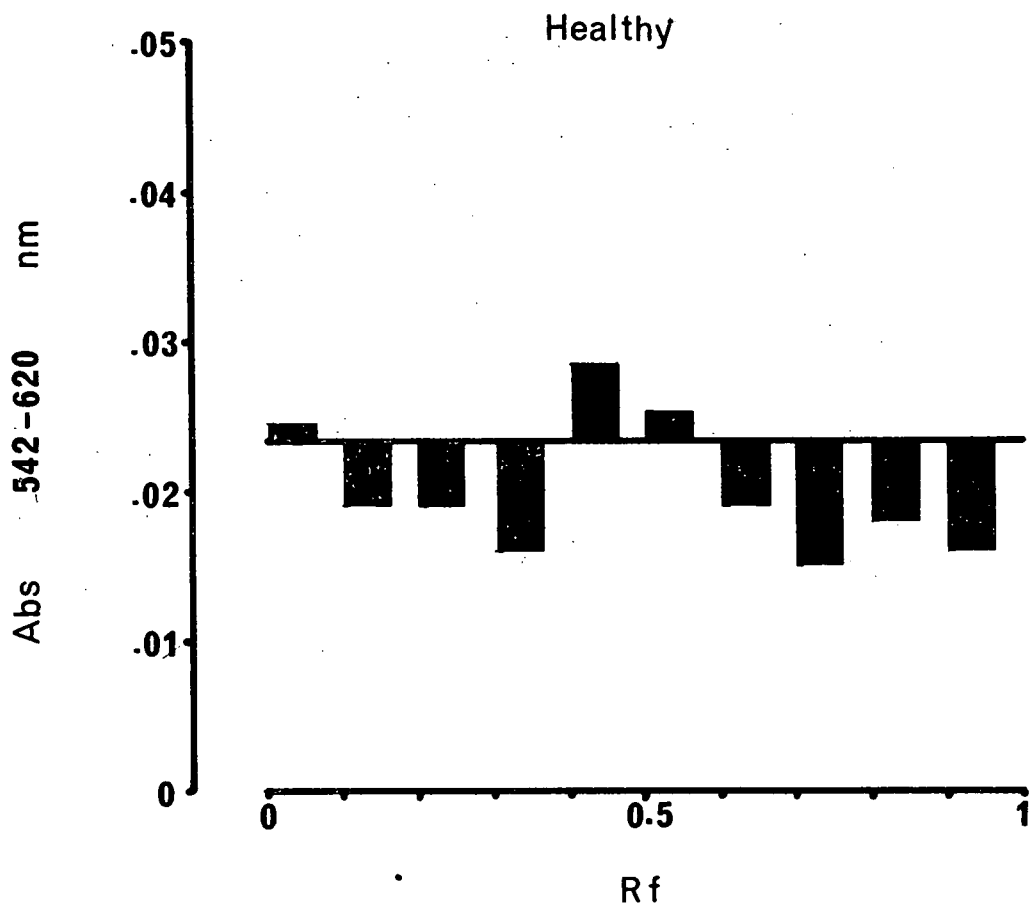
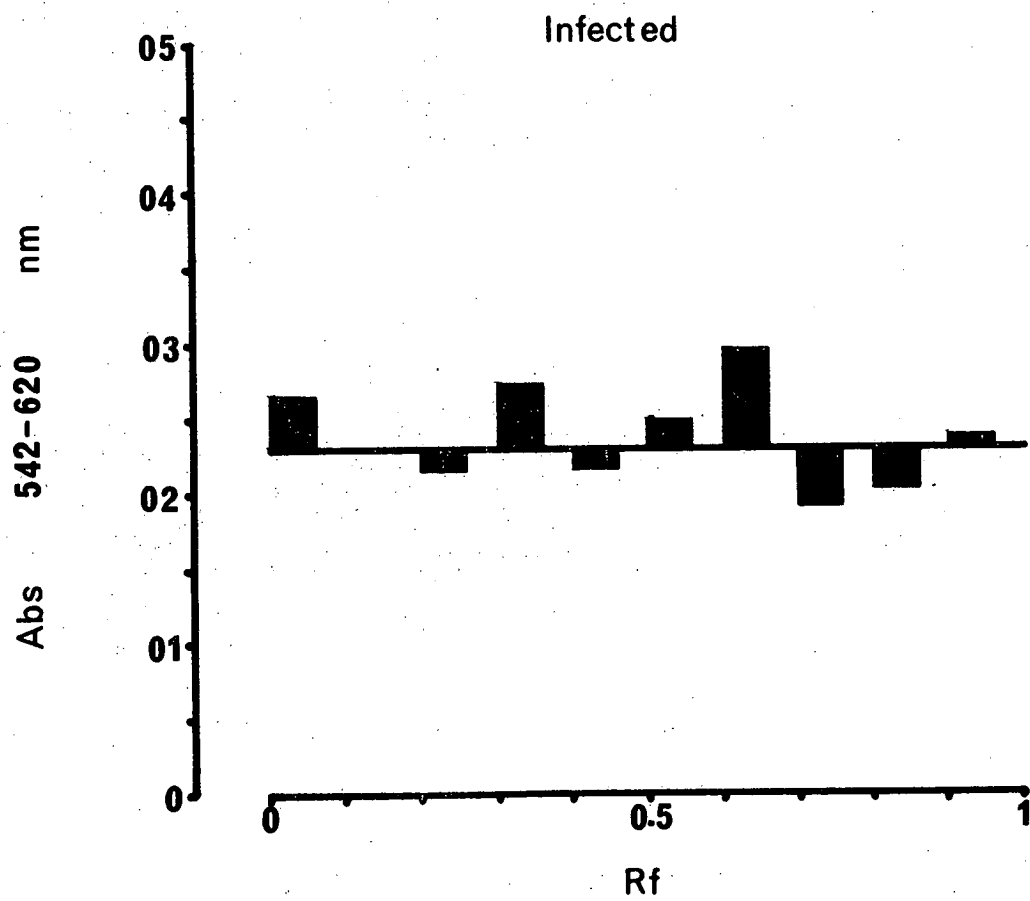
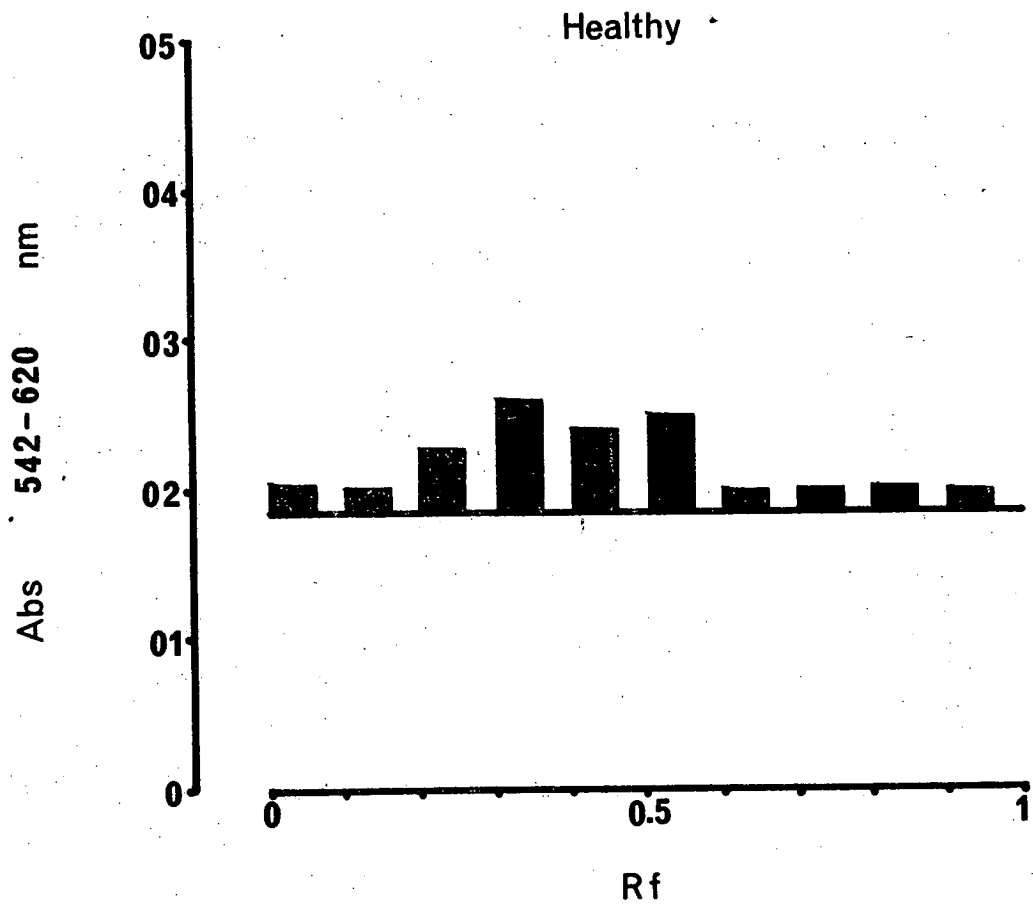


Figure 59

Cytokinin activity in water soluble fraction from tobacco roots.
Relation between TLC-plate zone and betacyanin production by *Amaranthus*
explants (Abs. 542 nm - Abs. 620 nm).

For statistical analysis and actual value of points plotted see
Appendix 48.



also occurred at Rf 0 - 0.2. Both young and mature leaf extracts from infected plants had higher concentrations of n-butanol soluble cytokinin-like compounds compared with similarly aged tissues from uninfected plants. Cytokinin-like compounds at the above Rf values, as resolved on TLC plates, were at a higher level in n-butanol soluble extracts from infected plants than similarly resolved, n-butanol soluble compounds from uninfected plants.

Water soluble compounds with cytokinin-like activity, resolved into two major regions of activity on TLC plates, were at a higher level in young leaf tissues from infected plants compared with similarly aged tissues from uninfected plants. However, in a comparison between mature leaves from infected and uninfected plants both cytokinin types, as separated on TLC plates, were at a higher level in extracts from uninfected plants.

Results for n-butanol soluble and water soluble compounds with cytokinin-like activity, separated by thin layer chromatography, were confirmed by the bioassay response to dilution series of crude n-butanol soluble and water soluble fractions of leaf tissue extracts. Cytokinin-like compounds in tissue extracts from tobacco roots were not resolved in two distinct zones of activity by thin layer chromatography.

The general profile of levels of cytokinin-like compounds, as separated by TLC, were similar for n-butanol soluble and water soluble fractions of a particular leaf age tissue extract. It is possible that much of the activity in the water soluble fractions is due to incomplete partitioning of compounds between aqueous and n-butanol phases. It may be more appropriate to pool n-butanol soluble and aqueous soluble fractions and consider the total extractable cytokinin-like activity. However, as it has been a usual practice to differentiate between n-butanol soluble and water soluble cytokinins and consider them separately, individual results will be considered in the discussion.

4. The Effect of Virus Infection on the Concentration of an Indole Acetic Acid-like Component in Young Leaf and Shoot Tissue Extracts

The barley coleoptile straight growth bioassay was found to be most suitable for auxins when compared with the pea root growth bioassay as reported by Leopold and Guernsey (1953). Both bioassays have poor lower limits of sensitivity to indole acetic acid, relative to bioassays for other growth regulating substances. They were sensitive to concentrated plant constituents and solvent traces in thin layer chromatography plate zones and are sensitive to other hormones. The pea root growth bioassay (tested but not reported here) had the added disadvantage of high statistical variability both within the one bioassay and between bioassays. Provided thin layer chromatography plate zones were diluted beyond the effective range of action of unknown inhibiting substances (about a 1 in 200 dilution for the system employed here) the barley straight growth test was relatively satisfactory.

Crude plant extracts were purified by TLC on Kieselgel G60 in an isopropanol:ammonia:water (10:1:1, V/V) solvent system. A plate zone corresponding to the R_f of indole acetic acid was removed from each plate and tested for auxin-like activity using the barley coleoptile straight growth bioassay. The bioassay response to a concentration range of IAA is presented in Figure 60. The bioassay as used was sensitive to at least 0.01 ppm IAA.

Bioassay response to a five-fold dilution series of each TLC purified plant extract is presented in Figure 61. A negative response was obtained at the lower dilutions tested, with both healthy and virus-infected tissue extracts being similarly effective in inhibiting the bioassay. However, at an extract dilution of 1 : 250, both extracts gave a positive response in the bioassay. Using the 1 : 250 dilution data for each extract (see Appendix 49) a ratio of IAA-like activity for virus-infected versus healthy tissue extracts was obtained. The ratio, in

Figure 60

Relation between \log_{10} indole acetic acid concentration (ppm) and barley coleoptile length (mm).

Standard error of points plotted = 0.1602 (see Appendix 49).

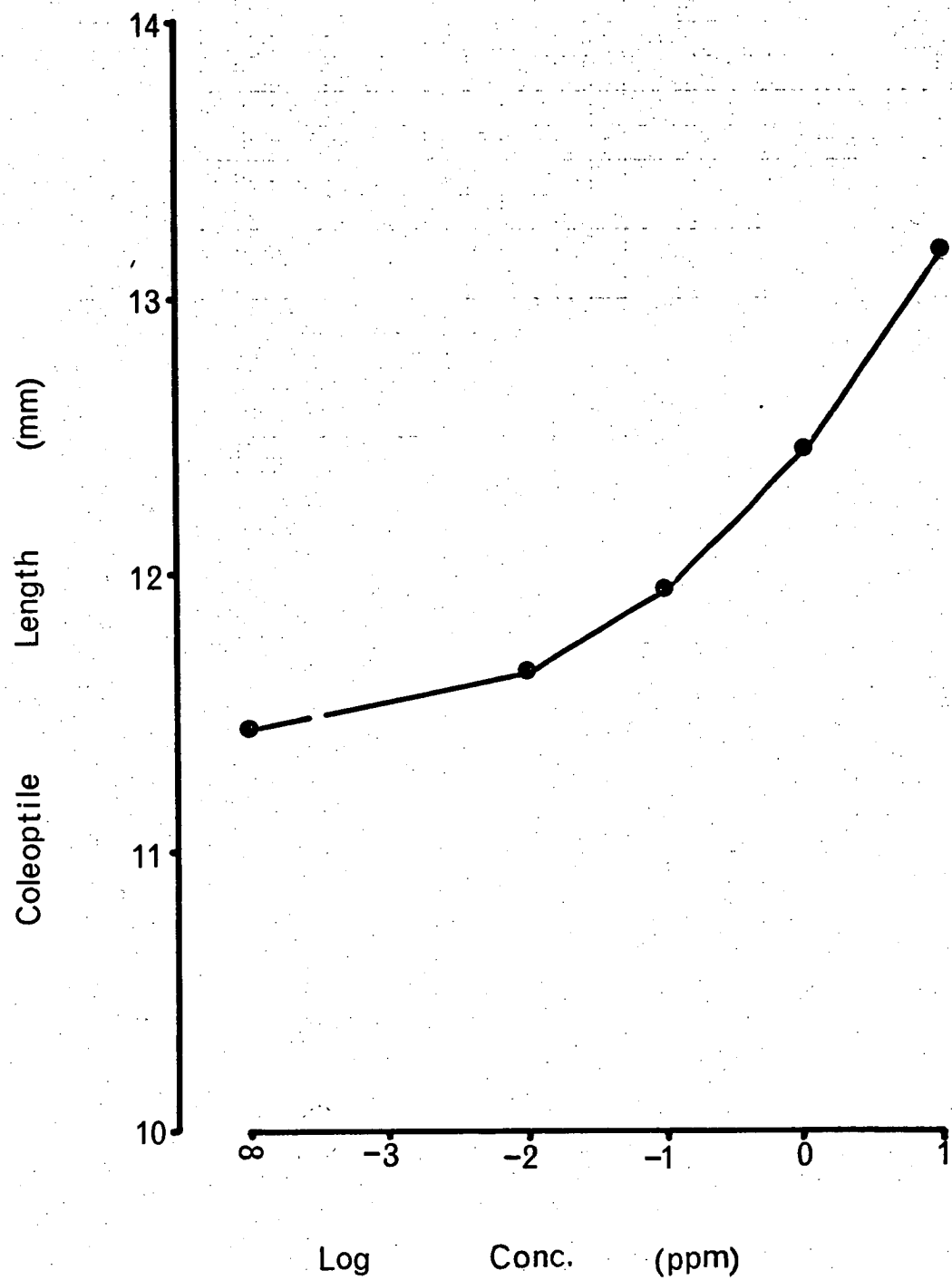
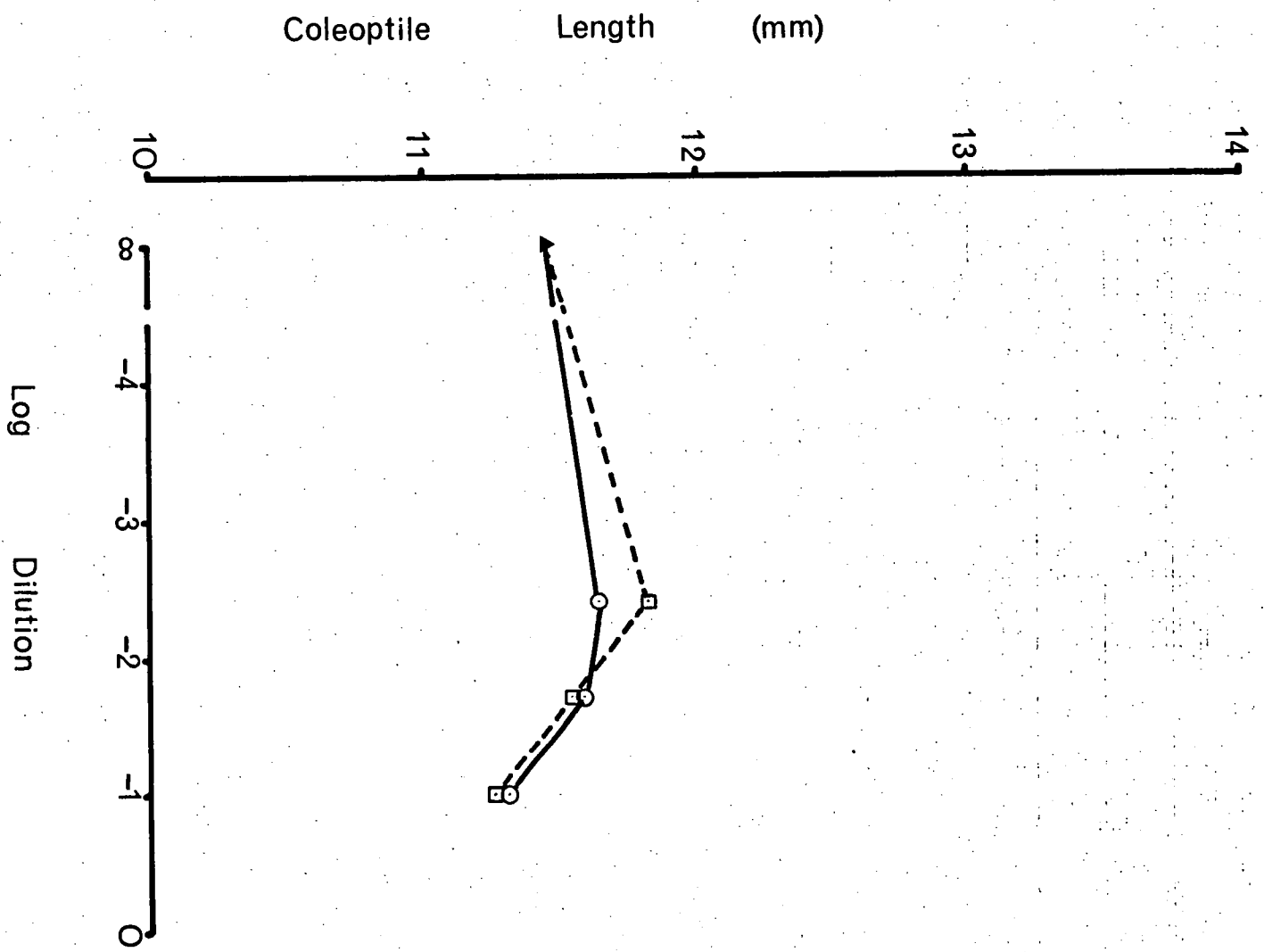


Figure 61

Indole acetic acid-like activity in purified extracts from young leaf and meristem tissues. Relation between \log_{10} extract dilution and barley coleoptile length (mm).

Standard error of points plotted = 0.1602 (see Appendix 49).

- (○——○) - Extract from healthy tobacco plants
- (□-----□) - Extract from virus-infected plants
- (▲) - Distilled water control



terms of ppm IAA equivalents/ml, was 3.55 : 1 (Infected : healthy).

Results for auxin-like activity in tissue extracts would have been more conclusive if the dose/response curves for the different tissue extracts had paralleled the dose/response curve for pure IAA. However, further extract dilution would probably have reduced the auxin content to a level below the sensitivity of the bioassay. A more desirable dose/response curve for the tissue extracts, over the dilutions employed, could only have been achieved by using a lengthier purification procedure.

SECTION III

VIRUS-HOST

ULTRASTRUCTURAL INTERACTIONS

INTRODUCTION

Fine structural detail of virus-infected plant cells has only been possible since the use of aldehyde and osmium fixatives. Unique to all virus-infected cells is the presence of virus particles, usually in some aggregated form. Amorphous inclusion bodies or X-bodies are also associated with a number of virus diseases. With diseases of the mosaic type, the most consistently reported structurally defective host organelle is the chloroplast. Virus effects on chloroplast structure vary with the particular virus and the strain present. The severity of mosaic symptoms induced in tobacco by the U1 strain of tobacco mosaic virus, varies with the age of the tissue. The chief purpose of this section is to determine to what extent the pattern of biochemical changes are associated with structural changes in cell organelles, in diseased tissues of different ages. The other objective of this section is to confirm the virus-free nature of dark green island tissue in the mosaic and compare these tissues structurally with virus-infected and healthy tissues.

MATERIALS & METHODS

1. Tissue Preparation

Leaf tissue squares, 5 mm square, were dissected from tobacco leaves. To facilitate fixing and embedding of tissues, the edge of each tissue piece was cut into 1 mm wide strips, giving a "comb" effect. All tissues were fixed immediately following dissection.

(a) Araldite-embedded tissues

Tissues were infiltrated under vacuum and fixed for 1 hour in 2-6 percent glutaraldehyde in 0.1 M cacodylate-HCl buffer, pH 7.2. Fixative was washed from the tissue squares with four changes of fresh buffer and two changes of distilled water. Following fixation in a 1 percent aqueous solution of osmium tetroxide for 1 hour, tissues were washed with several changes of water to remove excess osmium then stained in 0.5 percent aqueous uranyl acetate for 2 hours. Tissues were dehydrated in a graded alcohol series (30, 50, 60, 70, 80, 90, 95, 97.5, 100 percent alcohol, V/V) allowing at least 15 minutes in each alcohol dilution. Two changes of absolute alcohol were followed by two changes of epoxy propane. Tissue pieces in glass vials were soaked for 24 hours in a 1 : 1 mixture of epoxy propane and araldite (V/V). Epoxy propane was allowed to evaporate off by uncapping the vials and standing for 24 hours at room temperature. Tissues were transferred to fresh araldite and infiltrated for 2 days at room temperature. Araldite was polymerized at 60°C for 2 days. (For composition of araldite mixture used, see Appendix 50).

(b) Glycol methacrylate embedded tissues

The method used was essentially that reported by Leduc and Bernhard (1967). Tissues were fixed with 6 percent glutaraldehyde in 0.1 M phosphate buffer, pH 7.2, for 1 hour following vacuum infiltration. Glutaraldehyde was rinsed from the sections with several washings of distilled water. Dehydration was achieved in a graded concentration series of glycol methacrylate in water with 20 minutes in each of 60, 80, 90 and 97

percent ($\frac{V}{V}$) glycol methacrylate and 20 minutes in unrepolymerized embedding mixture. Tissues were then infiltrated overnight with prepolymer. Embedding medium used was 7 parts of 97 percent glycol methacrylate in distilled water and 3 parts of n-butyl methacrylate containing 2 percent ($\frac{W}{V}$) benzoyl peroxide (10 percent paste). Prepolymer was formed from embedding medium by heating sufficient medium to just cover the bottom of a conical flask until small bubbles just appeared, then rapidly cooling the flask and contents by plunging into a beaker of ice water. The final prepolymer had a viscosity similar to treacle.

Sections in prepolymer were transferred to gelatin capsules and polymerized under long wavelength ultraviolet light for 24 hours at 2°C.

2. Sectioning and Post-Staining Techniques

All sectioning was done with an LKB ultramicrotome, using glass knives. Araldite sections were pre-trimmed with a razor blade. Glycol methacrylate-embedded tissues, due to their brittleness, were trimmed by filing. All sections were mounted on 200 mesh copper grids, coated with collodion/carbon films and post stained in 0.5 percent aqueous uranyl acetate and Reynold's lead citrate (for composition see Appendix 51). Grids were placed, section side down, on droplets of water for 2-3 minutes, then transferred to droplets of uranyl acetate for 10 minutes. Grids were washed with water, placed on droplets of lead citrate for 3 minutes and immediately washed in a stream of distilled water. Grids were blotted and air-dried.

Sections were examined with either an AEI EM6B or a Philips EM 201 electron microscope.

RESULTS & OBSERVATIONS

1. Chloroplast Structure and General Cellular Organization as a Function of Leaf Tissue Age

(a) Very young leaf tissues

Typical cell structure for leaves about 1 cm long (leaf position 2 from the stem apex) is presented in Plate 15 and Plate 16. Crystalline virus inclusion bodies, though neither large nor numerous, were present in leaves at this very young age (Plate 15). Apart from the presence or absence of virus inclusion bodies, there was very little difference in ultrastructure between healthy and infected cells in leaf tissues of this age. Chloroplasts of healthy and infected tissues were undeveloped with poorly differentiated grana and stoma lamellae. Many chloroplasts of healthy and infected tissues were characterized by a densely stained region, probably lipoid in composition.

Virus-induced cell structural abnormalities became more pronounced in leaves at leaf position 3 from the stem apex (leaves 2-3 cm long). At this age, cells within the leaf were still at an active stage of cell division (Plate 22). Chloroplast abnormalities, most pronounced in infected tissues of this age, were associated with the earliest visible differentiation between green and yellow island tissues of the mosaic.

Large accumulations of virus particles, mostly as crystalline virus inclusions, were regularly present in virus-infected cells from yellow areas of leaf mosaics (Plates 17, 18). Although crystalline inclusions were numerous and occupied much of the cell volume, virus particles were only loosely organized within the aggregates with their long axes roughly parallel.

Chloroplasts in tissues with virus accumulations displayed obvious differences in internal structure compared with chloroplasts in cells from virus-free green tissues of infected leaves and leaf cells from healthy plants.

Many chloroplasts of virus-infected cells had a densely stained region near their centres (Plates 17, 18, 19), probably prolamellar bodies and resembled in appearance the degenerate chloroplasts in leaf epidermis cells of similarly aged healthy tissues (Plate 20). Plastids, present in epidermal cells of young leaves, seldom developed so that the mature leaf epidermis was generally devoid of chloroplasts. Grana development was generally poorer in chloroplasts associated with yellow, virus-infected leaf tissues. In comparison with chloroplasts in virus-containing cells, chloroplasts of virus-free, green island tissues (Plate 21) and chloroplasts in leaves from uninfected plants had better developed grana systems and a general absence of the dense staining or prolamella bodies.

A difference in starch granule size between healthy cell and infected cell chloroplasts was also most obvious in leaf tissues of this age. Chloroplasts in cells containing virus particles generally had larger starch granules (Plates 17, 18, 24) than chloroplasts in cells of green, virus-free tissues (Plate 21) or healthy control tissues (Plates 23, 25).

Another most obvious feature of virus-containing cells in leaves 2-3 cm long was the presence of X-bodies in the cell cytoplasm (Plates 26, 27). In very young leaf tissues such bodies were mostly composed of tubular, dense-staining structures more or less randomly organized and often adjacent to cell nuclei.

Plate 15

Section through virus-infected tobacco leaf from leaf position 2 from the stem apex (leaf about 1 cm long). Tissue fixed in glutaraldehyde, embedded in glycol methacrylate and post stained with uranyl acetate/Reynold's lead citrate. Note the negative staining of the nuclear membrane and outer plastid membranes.

(v = virus inclusion, pl = plastid, sb = starch body, dsb = dense staining body, n = nucleus, nm = nuclear membrane)

Magnification 14,300 X



Plate 16

Section through a healthy tobacco leaf at leaf position 2 from the stem apex (leaf 1 cm long). Section fixed in glutaraldehyde, embedded in glycol methacrylate and post stained with uranyl acetate/Reynold's lead citrate. Note the negative staining membranes of the nucleus and plastids. Plastids contain a dense staining body (prolamella body) and well developed starch bodies.

(pl = plastids, sb = starch body, dsb = dense staining body, n = nucleus, nm = nuclear membrane)

Magnification 5,950 X



Plate 17

Section through a virus-infected leaf at leaf position 3 from the stem apex (leaf 2 cm long). Tissues fixed in glutaraldehyde/osmium tetroxide, stained with aqueous uranyl acetate, embedded in araldite and post-stained with uranyl acetate/Reynold's lead citrate. Note the numerous inclusions of virus particles and the poorly developed plastids.

(er = endoplasmic reticulum, pl = plastids, m = mitochondria, n = nucleus, nm = nuclear membrane, dsb = dense staining body, sb = starch body, ps = plasmodesmata, va = vacuole, v = virus inclusion)

Magnification 9,520 X



Plate 18

Section through a virus-infected tobacco leaf at leaf position 3 from the stem apex (leaf 2 cm long). Section fixed in glutaraldehyde/osmium tetroxide, stained with aqueous uranyl acetate, embedded in araldite and post-stained with uranyl acetate/Reynolds lead citrate. Note the massive inclusions of virus particles and the poorly developed plastids.

(pl = plastids, dsb = dense staining body, n = nucleus, v = virus inclusions, ps = plasmodesmata)

Magnification 13,160 X



Plate 19

Plastids in virus-infected tobacco leaf cells of leaves at leaf position 3 from the stem apex. Sections fixed in glutaraldehyde/osmium tetroxide, pre-stained with uranyl acetate, embedded in araldite and post-stained with uranyl acetate/Reynold's lead citrate. Note plastids with poorly developed stroma lamellae and grana and large starch bodies and dense staining bodies (pro-lamella bodies).

(sb = starch body, dsb = dense staining body, v = virus inclusion)

Magnification 21,200 X

Plate 20

Section through the epidermis of a healthy tobacco leaf at leaf position 3 from the stem apex. Section fixed in glutaraldehyde/osmium tetroxide, pre-stained with aqueous uranyl acetate, embedded in araldite and post-stained with uranyl acetate/Reynold's lead citrate. Note the poorly developed plastids with large starch bodies and dense staining bodies.

(pl = plastids)

Magnification 10,380 X

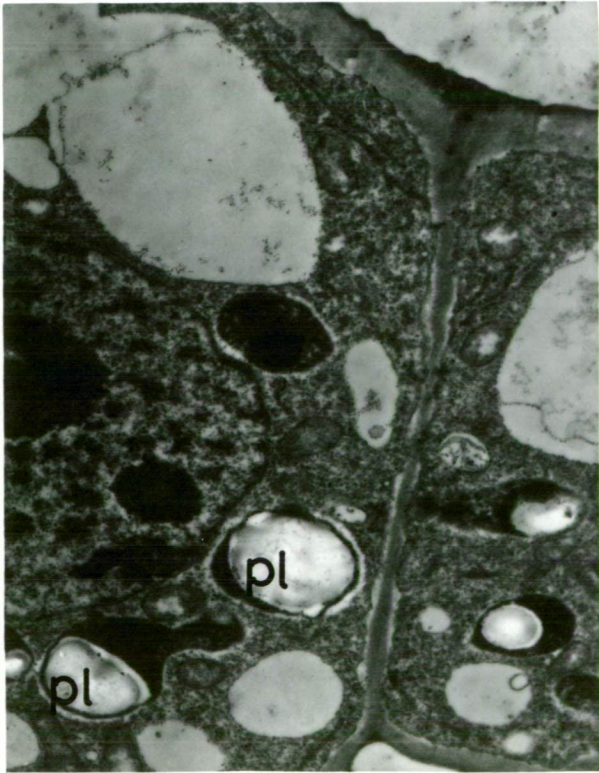
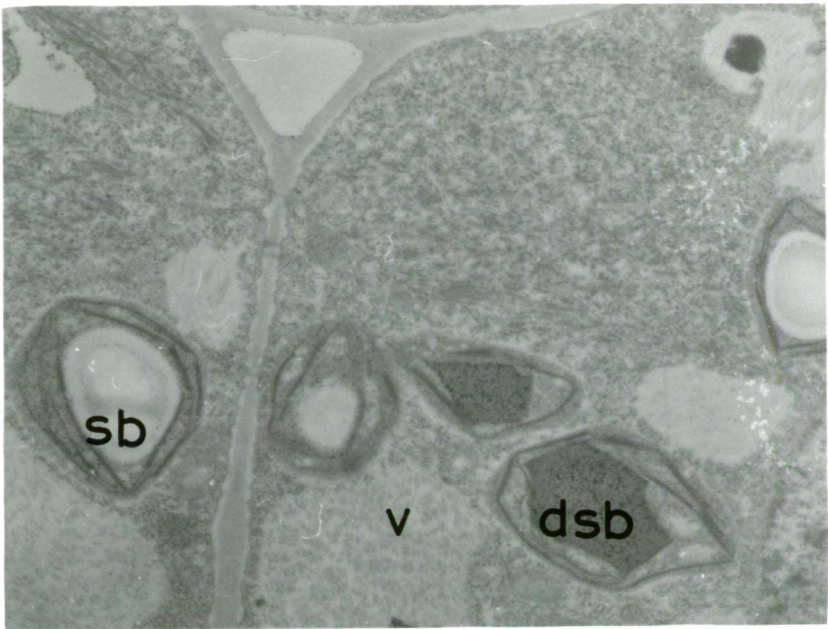


Plate 21

Section through dark green island tissue from a virus-infected leaf at leaf position 3 from the stem apex. Section fixed in glutaraldehyde/osmium tetroxide, pre-stained with aqueous uranyl acetate, embedded in araldite and post-stained with uranyl acetate/Reynold's lead citrate. Note the absence of virus inclusions and the well developed plastids containing stroma lamellae and grana. Plastids also contain only small starch bodies (lightly staining bodies). Very few plastids have a pro-lamella body.

(n = nucleus, pl = plastid, ps = plasmodesmata, va = vacuole)

Magnification 3,570 X

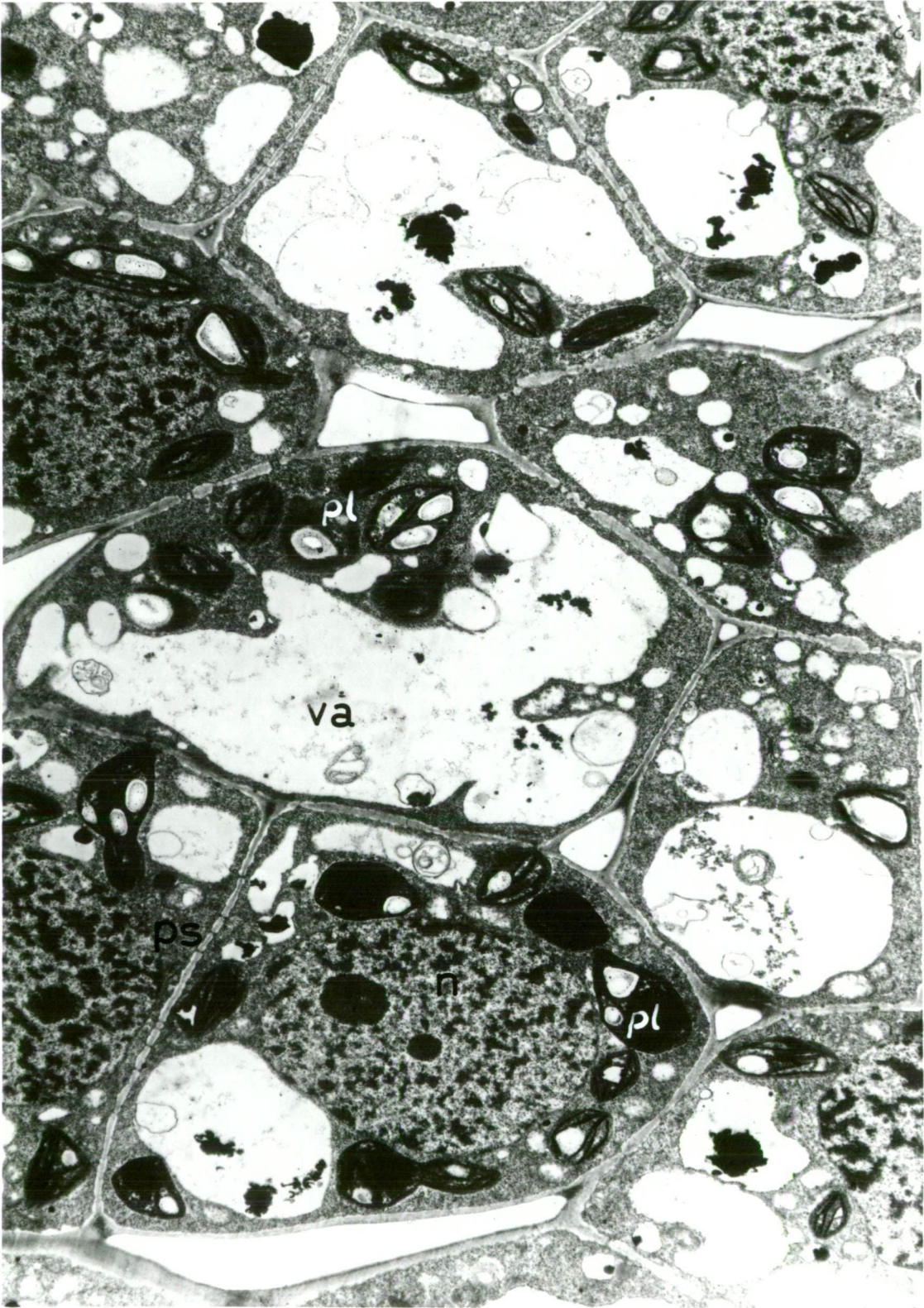


Plate 22

Section through a healthy tobacco leaf at leaf position 3 from the stem apex (leaf 2 cm long). Tissue fixed in glutaraldehyde/osmium tetroxide, pre-stained with aqueous uranyl acetate, embedded in araldite and post-stained with uranyl acetate/Reynold's lead citrate. Note the cell, upper left of the plate, which is in an active state of cell division with an absence of a nuclear membrane and chromatin material scattered throughout the cytoplasm. Cells are connected to each other via numerous plasmodesmata. Plastids are generally well developed with a small starch granule and very little pro-lamella body (dense staining body within plastids).

(ch = chromosome, er = endoplasmic reticulum, n = nucleus, nm = nuclear membrane, m = mitochondrion, pl = plastid, ps = plasmodesmata, va = vacuole)

Magnification 9,520 X

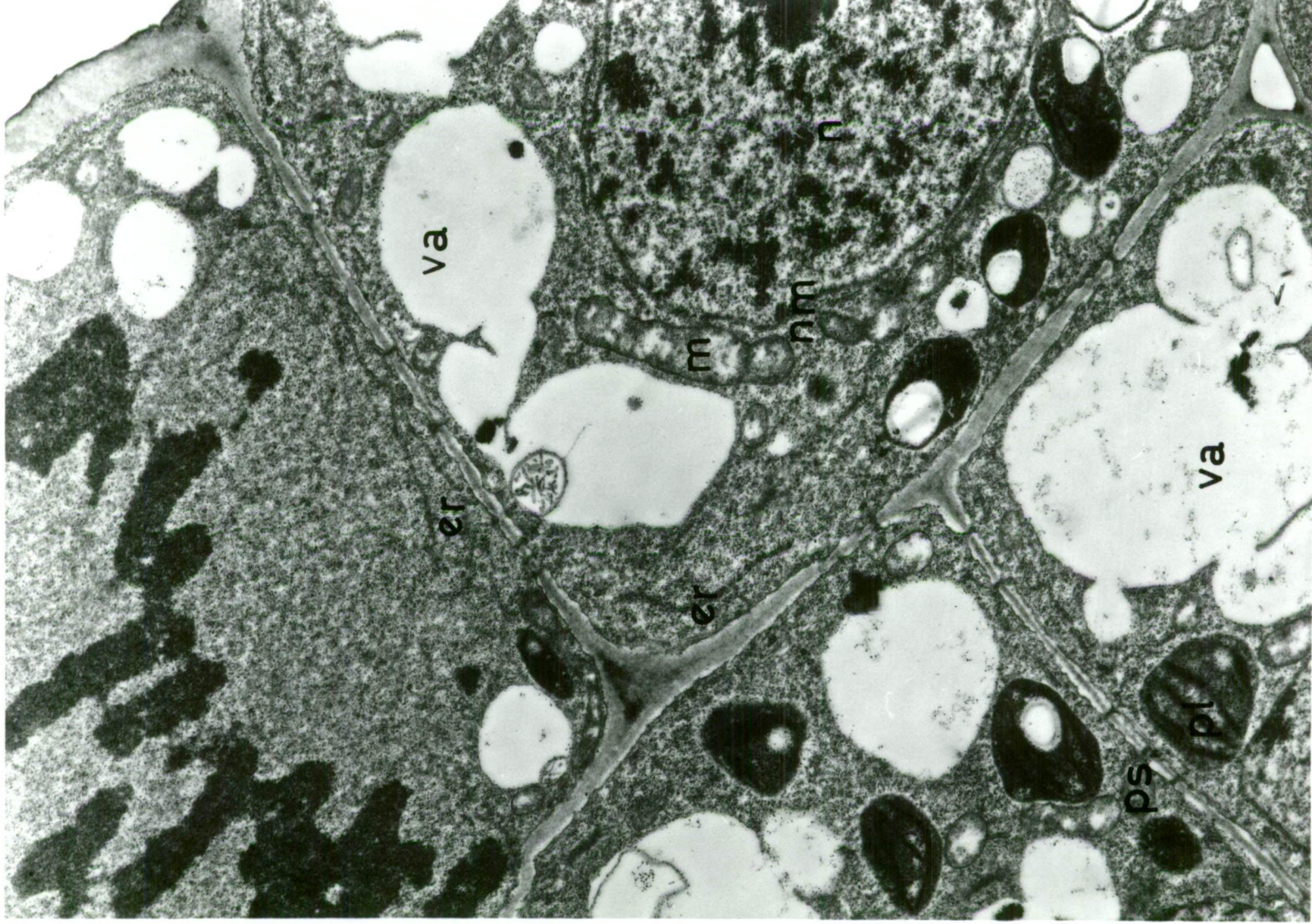


Plate 23

Section through a healthy tobacco leaf (leaf position 3 from the stem apex). Tissue fixed in glutaraldehyde/osmium tetroxide, pre-stained with aqueous uranyl acetate, embedded in araldite and post-stained with uranyl acetate/Reynold's lead citrate. Note the well developed plastids with small starch granules (light staining bodies) and an absence of pro-lamella bodies (dense staining bodies).

(m = mitochondrion, n = nucleus, pl = plastid)

Magnification 13,160 X

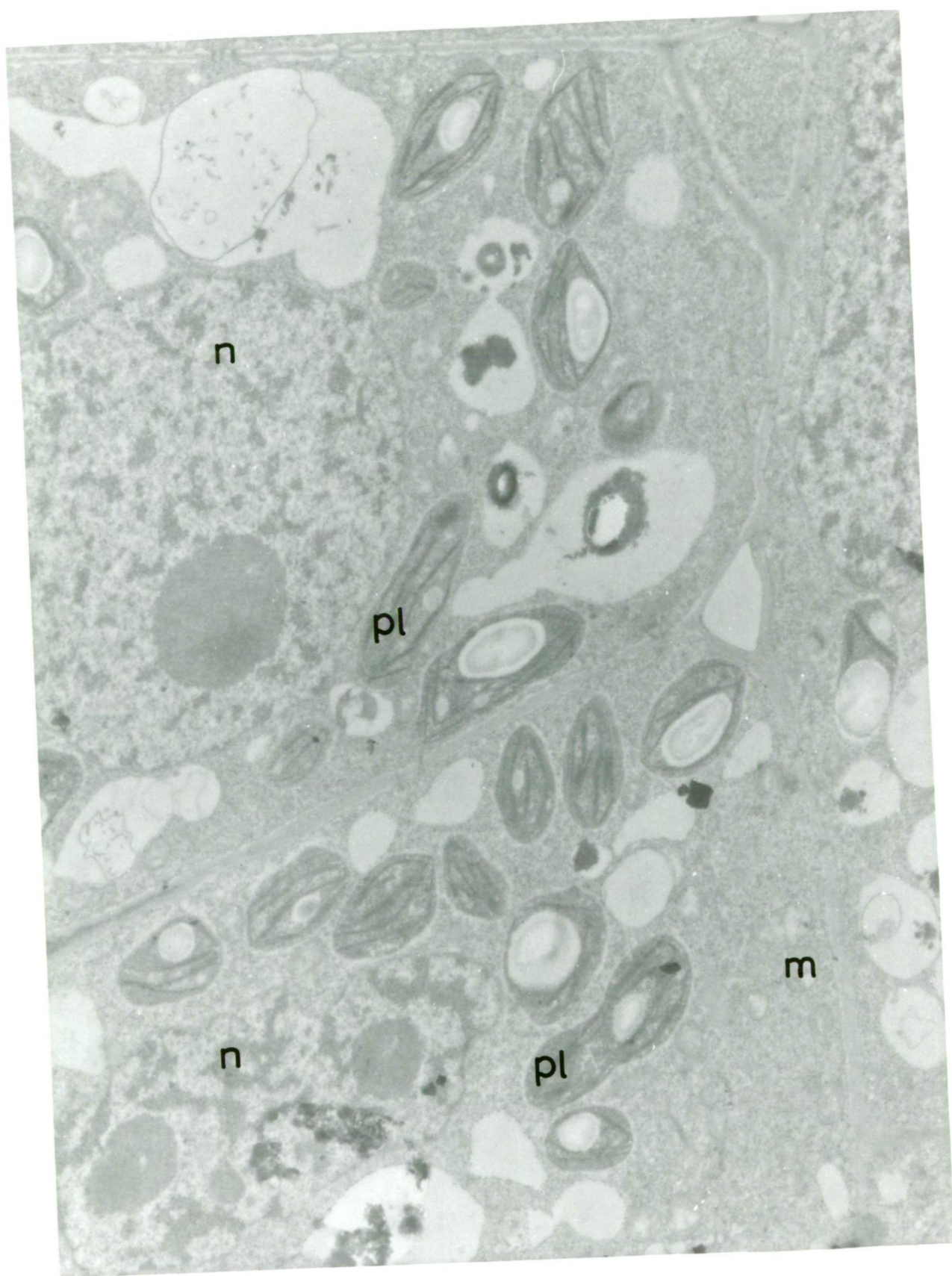


Plate 24

Section through virus-infected tobacco leaf (leaf position 3 from the stem apex). Tissues of both Plate 24 and Plate 25 fixed in glutaraldehyde, embedded in glycol methacrylate and post-stained with uranyl acetate/Reynold's lead citrate. Note the negative contrast of outer membranes of cell organelles and nuclei. Plastids show poorly developed stroma lamellae, little grana and relatively large starch bodies.

(n = nucleus, pl = plastids, v = virus inclusion, x = X-body)

Magnification 6,120 X

Plate 25

Section through a healthy tobacco leaf (leaf position 3 from the stem apex). Plastids show well developed stroma lamellae, rudimentary grana and relatively small starch bodies.

(n = nucleus, pl = plastid)

Magnification 6,120 X

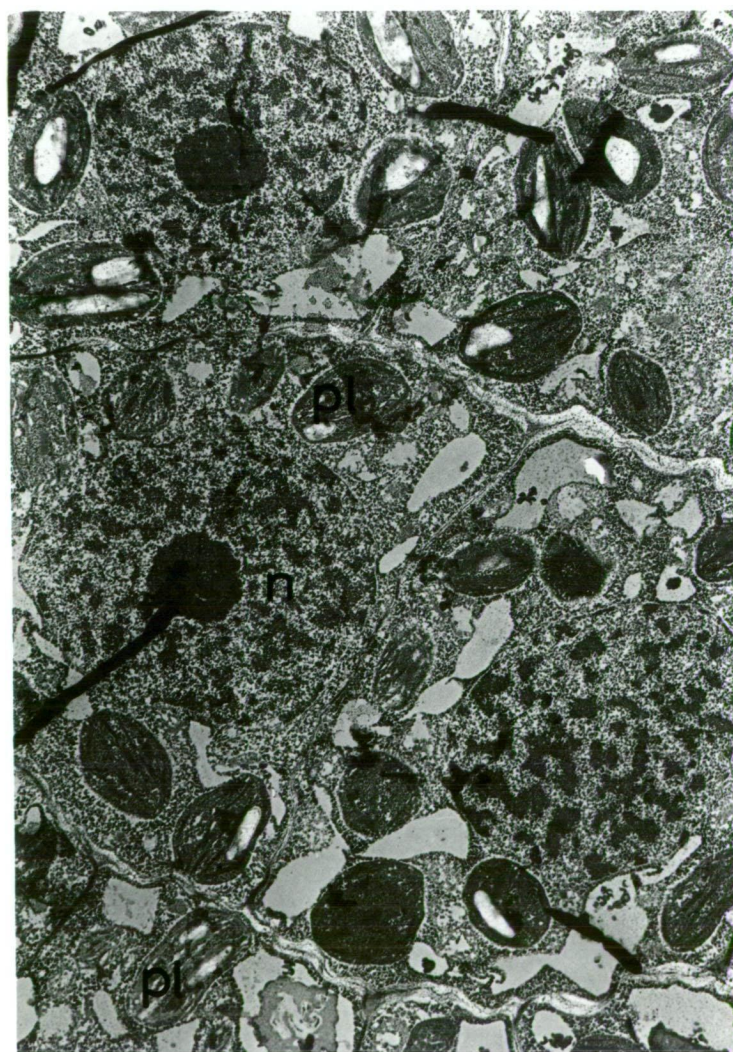
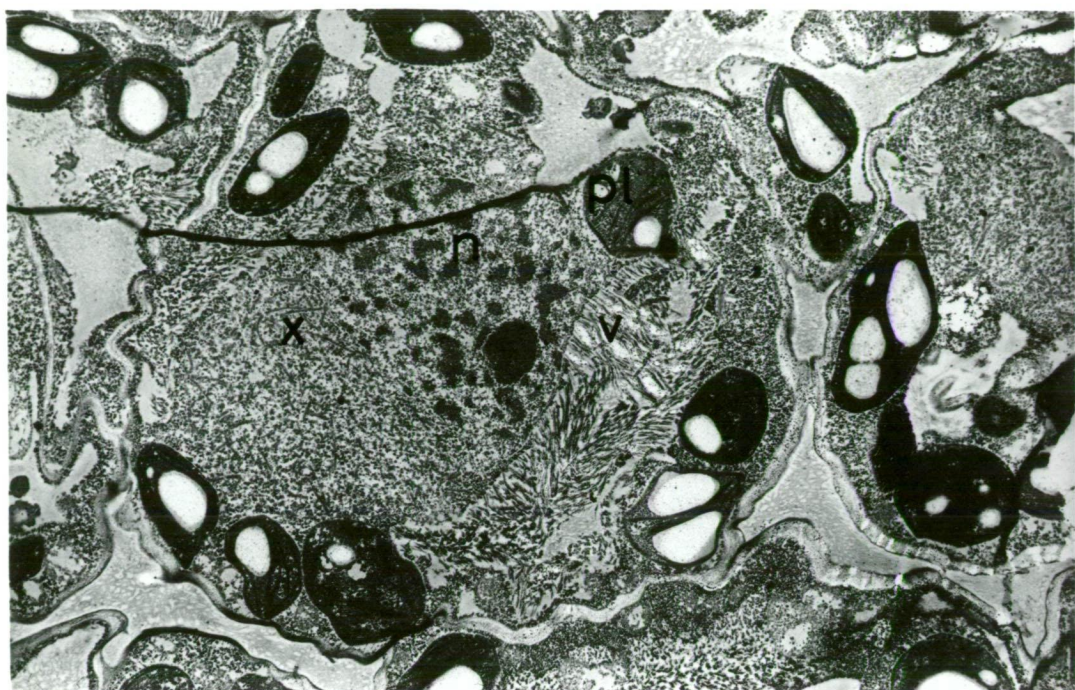


Plate 26

X-body in a virus-infected tobacco leaf cell (leaf position 3 from the stem apex). Tissue fixed in glutaraldehyde, embedded in glycol methacrylate and post-stained with uranyl acetate/Reynold's lead citrate. Note the dense staining tubules of the X-body and the proximity of the X-body relative to the nucleus.

(n = nucleus, nm = nuclear membrane, v = virus inclusion, x = X-body)

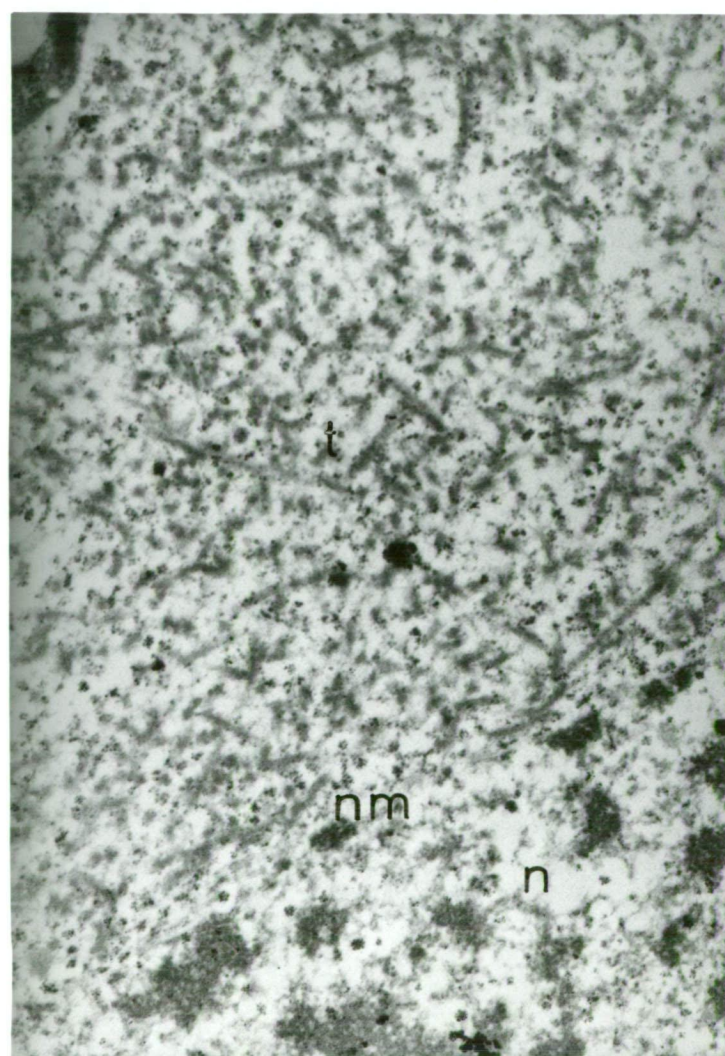
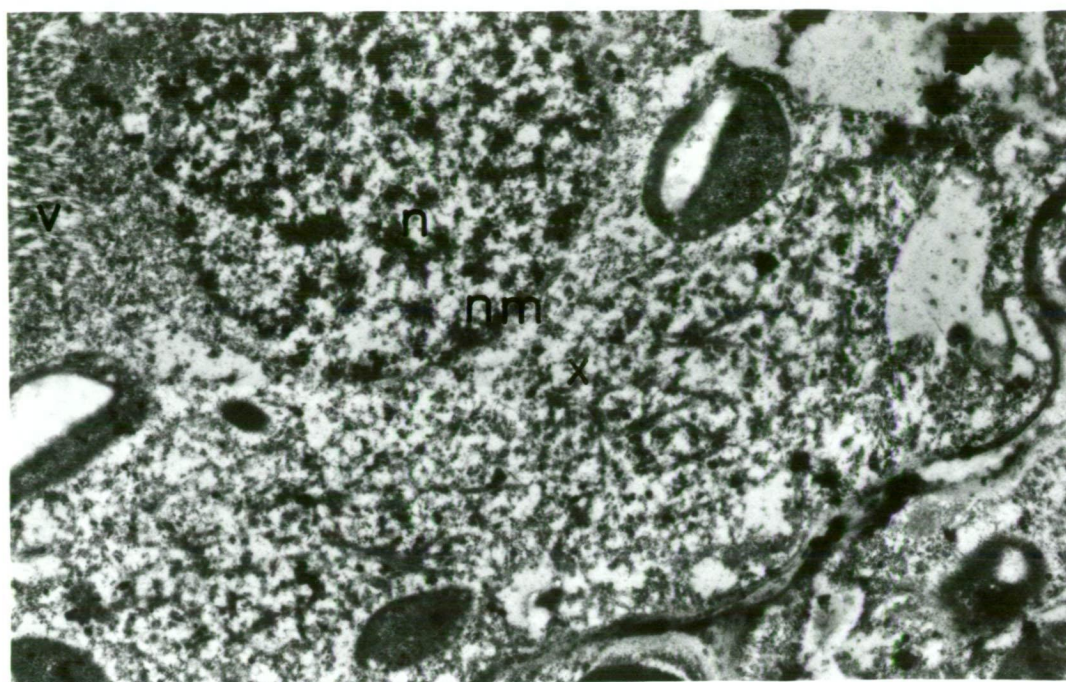
Magnification 10,380 X

Plate 27

X-body in a virus-infected tobacco leaf cell (leaf position 3 from the stem apex). Tissue prepared as for above. The X-body consists mostly of dense staining tubular components arranged more or less randomly and in fairly close association with the cell nucleus.

(n = nucleus, nm = nuclear membrane, t = tubules)

Magnification 26,100 X



(b) Immature leaf tissue

Leaves at leaf position 6 from the stem apex, which included leaves 13-16 cm long (that is about half the length of fully expanded leaves) were designated immature leaf tissues. Immature leaves from infected plants were clearly differentiated into light green and dark green island tissues. Sections across the border between light green and dark green areas of the mosaic pattern confirmed that cells of dark green island tissues, although adjacent to virus-containing cells of light green island tissues, were devoid of virus particles and X-bodies (Plate 28). Cells of dark green island tissues (Plate 31) had the ultrastructural appearance of leaf cells from uninfected leaves of a comparable age (Plate 32). There was no evidence for physical isolation of cells at the border between light green and dark green islands. Adjacent cells from adjoining tissues were connected by normal-appearing plasmodesmata (Plates 29, 30).

Chloroplasts from light green island tissues (Plate 36) and dark green island tissues (Plate 35) of virus-infected leaves at leaf position 6 from the stem apex and chloroplasts from healthy control tissues (Plates 33, 34) of a similar chronological age were similar with respect to shape and internal development of grana, stroma lamellae and starch granule size.

X-bodies, present in virus-containing cells from light green island tissues, were characterized by dense-staining tubules, small crystalline virus inclusions and free virus particles. Such bodies were usually in close proximity to the nucleus and surrounded by crystalline virus inclusions and various cellular organelles (see Plate 37).

Plate 28

Section across the border between light green and dark green island tissues from a virus-infected tobacco leaf (leaf position 6 from the stem apex - leaf 13 cm long). Tissue fixed in glutaraldehyde/osmium tetroxide, pre-stained with aqueous uranyl acetate, embedded in araldite and post-stained with uranyl acetate/Reynold's lead citrate. The cell at the upper right is a dark green island tissue cell. Note the absence of virus from this cell. The cell at lower left is a light green island tissue cell. Note the massive crystalline inclusions of virus in the cell cytoplasm. Plastids in both cells are similar with respect to shape, development of stroma lamellae and grana and starch body size.

(n = nucleus, v = virus inclusion, va = vacuole)

Magnification 5,950 X

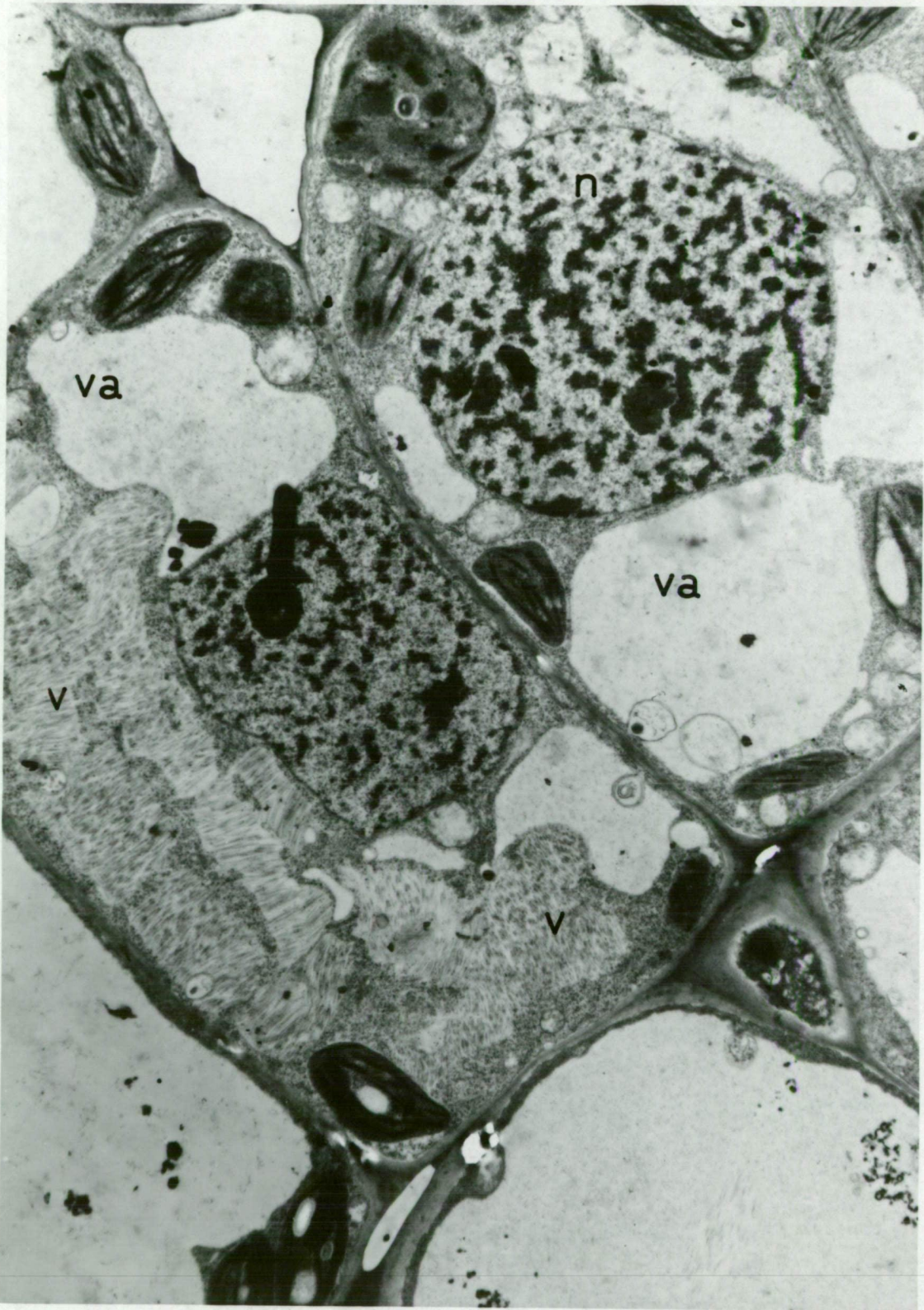


Plate 29

Cell wall boundary between a cell from dark green island tissue (upper left) and a cell from light green island tissue (lower right). Tissue fixed in glutaraldehyde/osmium tetroxide, pre-stained with aqueous uranyl acetate, embedded in araldite and post-stained with uranyl acetate/Reynold's lead citrate. Note the plasmodesmata connections between the two cells.

(v = virus inclusion, x = X-body)

Magnification 27,680 X

Plate 30

Cell wall boundary between a virus-free and virus-containing cell from adjoining light green and dark green islands of infected leaf tissue. Tissues prepared as above. Virus-free cell on the right and virus-infected cell on the left. Note the abundance of plasmodesmata connections between the cells.

(ps = plasmodesmata, v = virus inclusion, va = vacuole)

Magnification 10,380 X

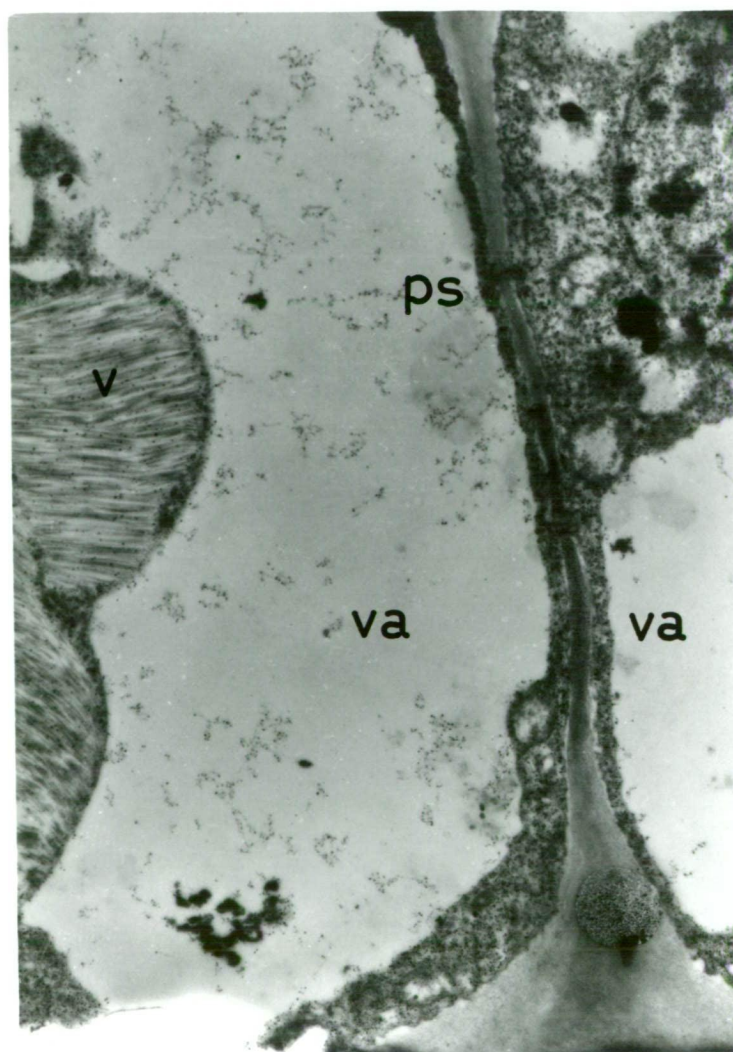
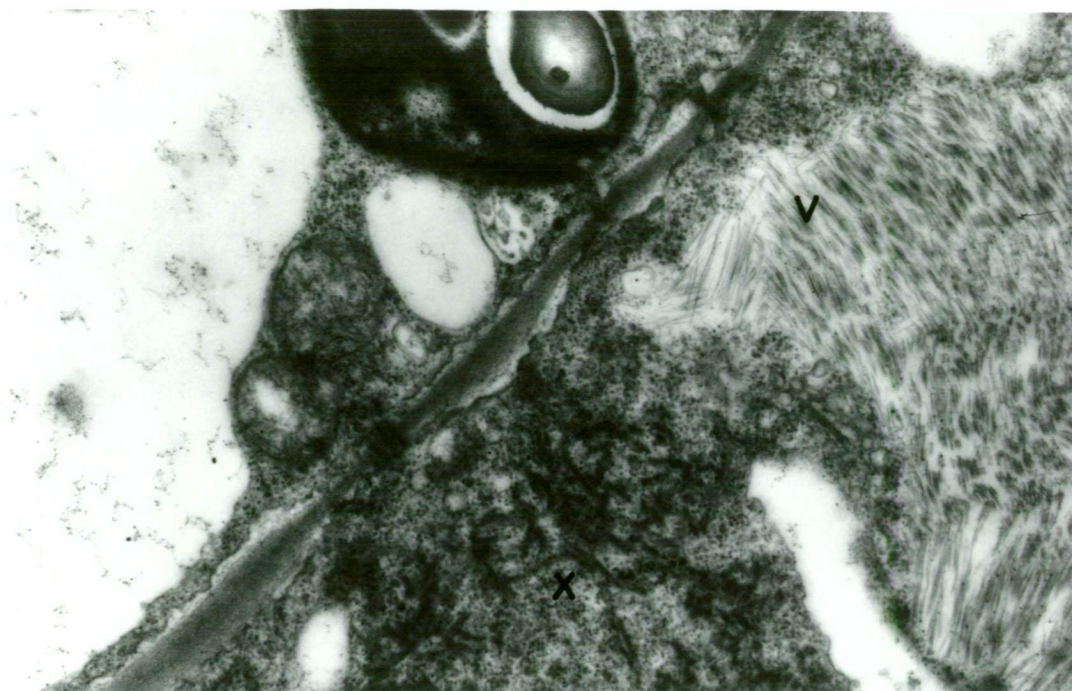


Plate 31

Section through dark green island tissue from a virus-infected tobacco leaf (leaf position 6 from the stem apex). Tissue fixed in glutaraldehyde/osmium tetroxide, pre-stained with uranyl acetate, embedded in araldite and post-stained with uranyl acetate/Reynold's lead citrate. Note the complete absence of virus and X-bodies.

(n = nucleus, pl = plastid, va = vacuole)

Magnification 5,950 X

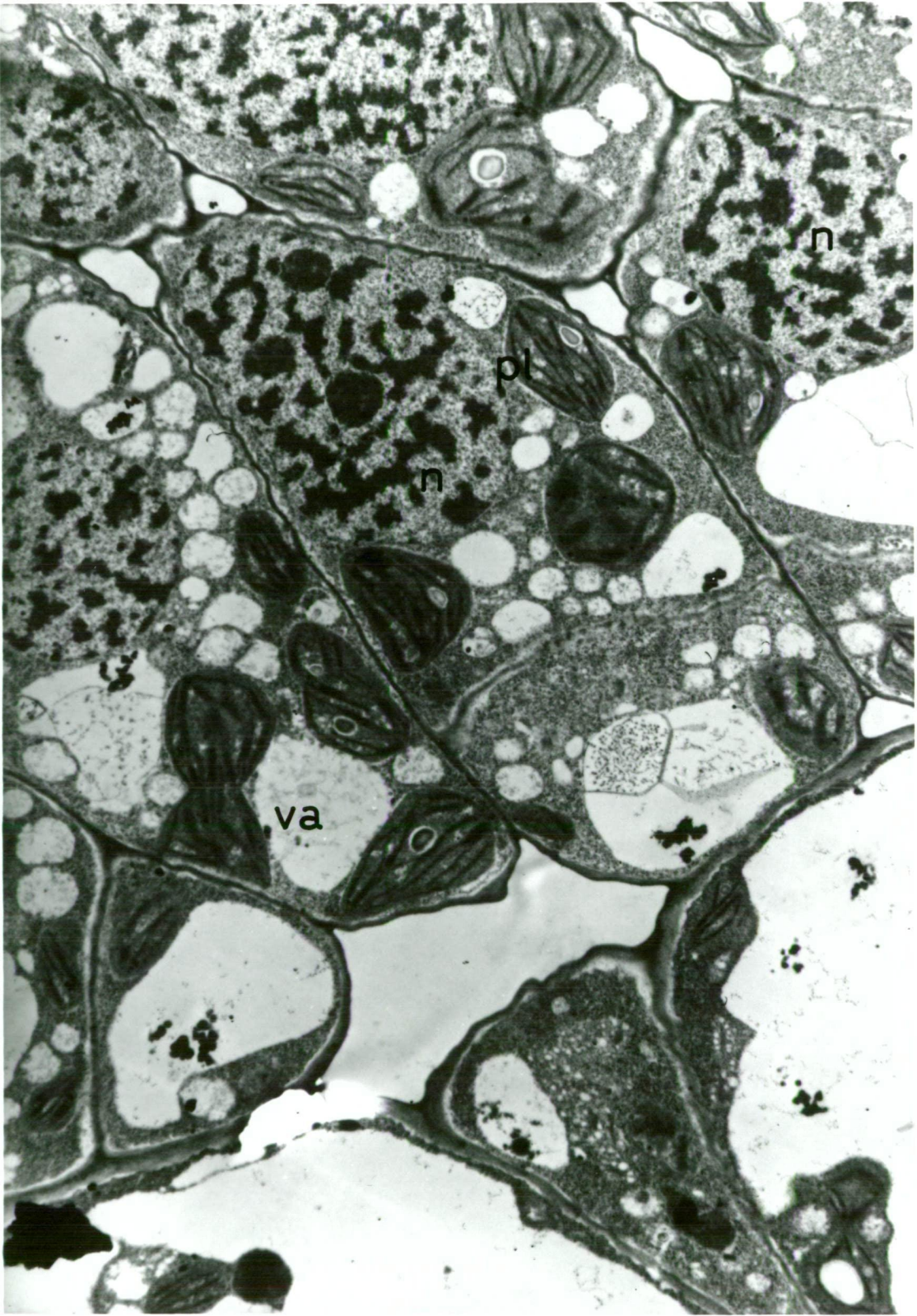


Plate 32

Section through a healthy tobacco leaf (leaf position 6 from the stem apex). Tissue fixed in glutaraldehyde/osmium tetroxide, pre-stained with aqueous uranyl acetate, embedded in araldite and post-stained with uranyl acetate/Reynold's lead citrate.

(n = nucleus, pl = plastid, va = vacuole)

Magnification 6,460 X

Plate 33

Chloroplasts in leaf cells of a healthy tobacco plant (leaf position 6 from the stem apex). Tissue fixed in glutaraldehyde/osmium tetroxide, pre-stained with aqueous uranyl acetate, embedded in araldite and post-stained in uranyl acetate/Reynold's lead citrate.

(m = mitochondrion, n = nucleus, pl = plastid, sb = starch body, va = vacuole)

Magnification 14,840 X

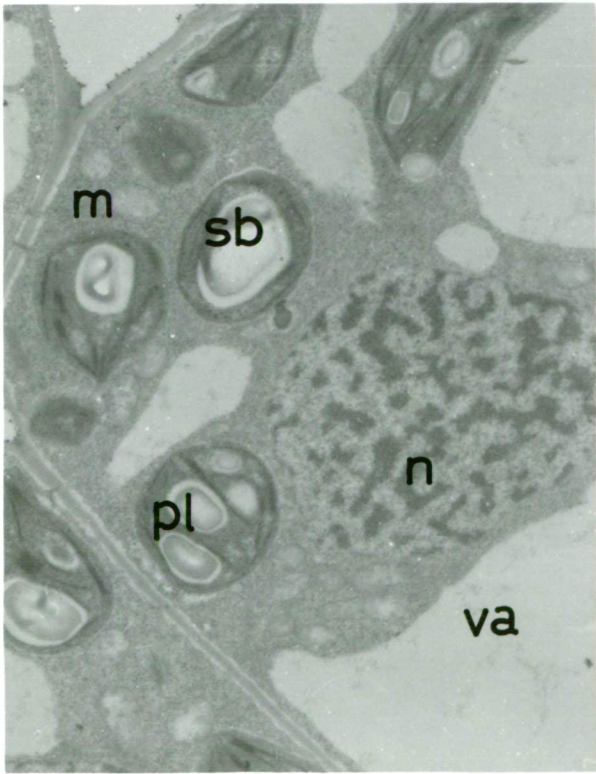
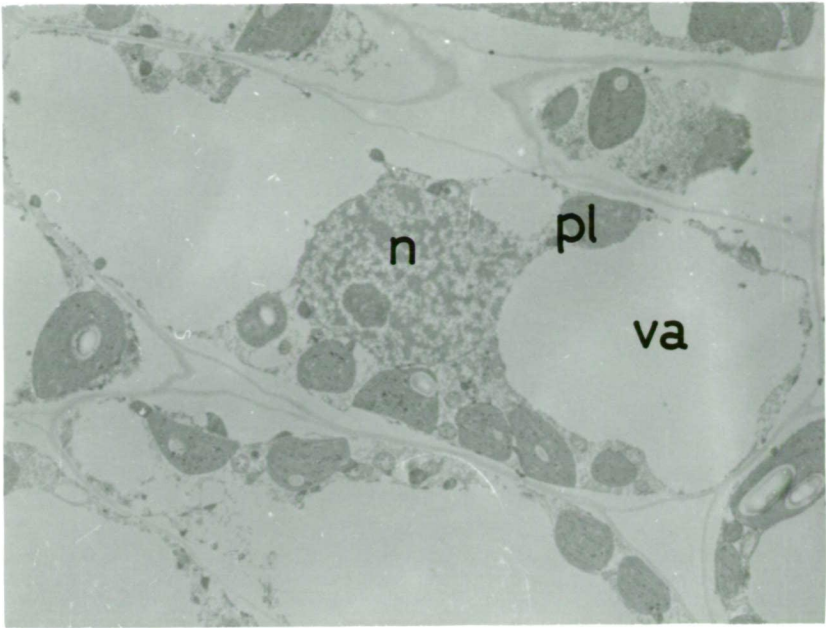


Plate 34

Chloroplasts in healthy tobacco leaf cells (leaf position 6 from the stem apex). Plates 34, 35 and 36 represent tissues fixed in glutaraldehyde/osmium tetroxide, pre-stained with aqueous uranyl acetate, embedded in araldite and post-stained with uranyl acetate/Reynold's lead citrate.

Magnification 9,980 X

Plate 35

Chloroplasts in dark green island tissue cells of virus-infected leaves of tobacco (leaf position 6 from the stem apex).

Magnification 8,000 X

Plate 36

Chloroplasts in light green island tissue cells of virus-infected tobacco leaves (leaf position 6 from the stem apex).

(m = mitochondrion, va = vacuole)

Magnification 19,300 X

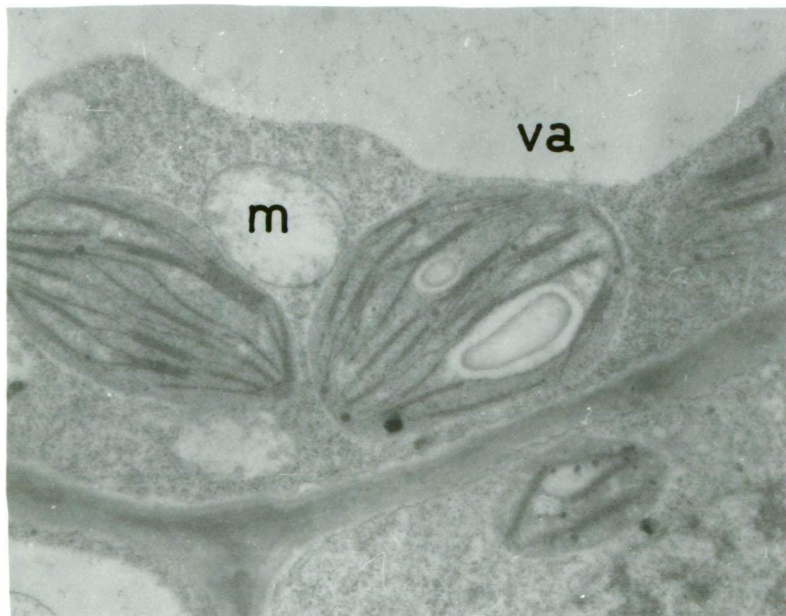
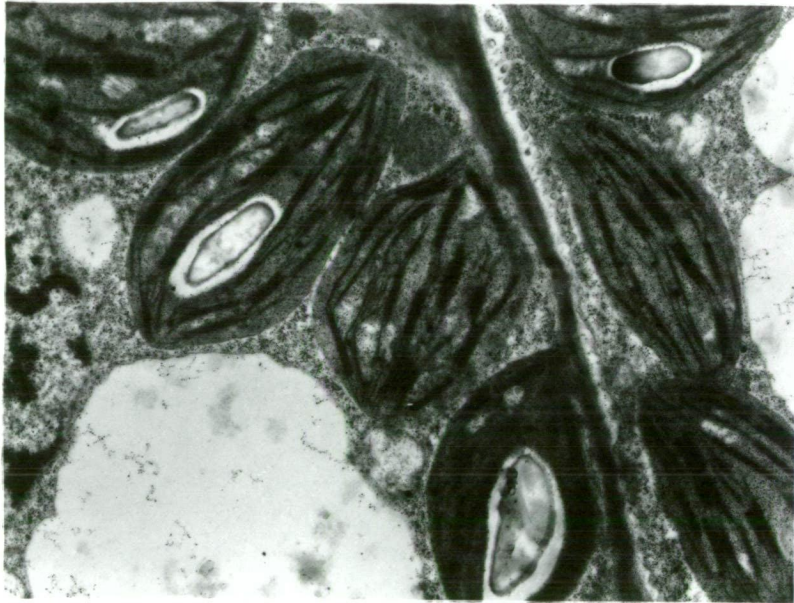
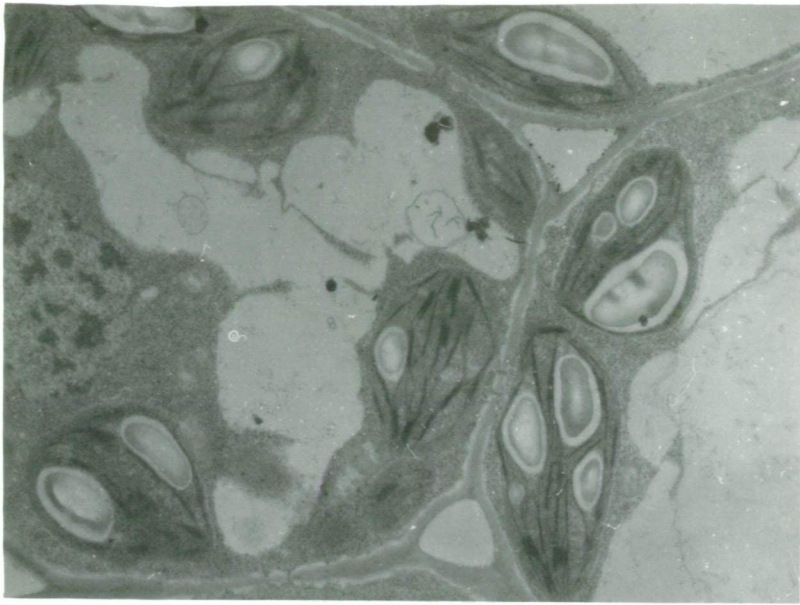
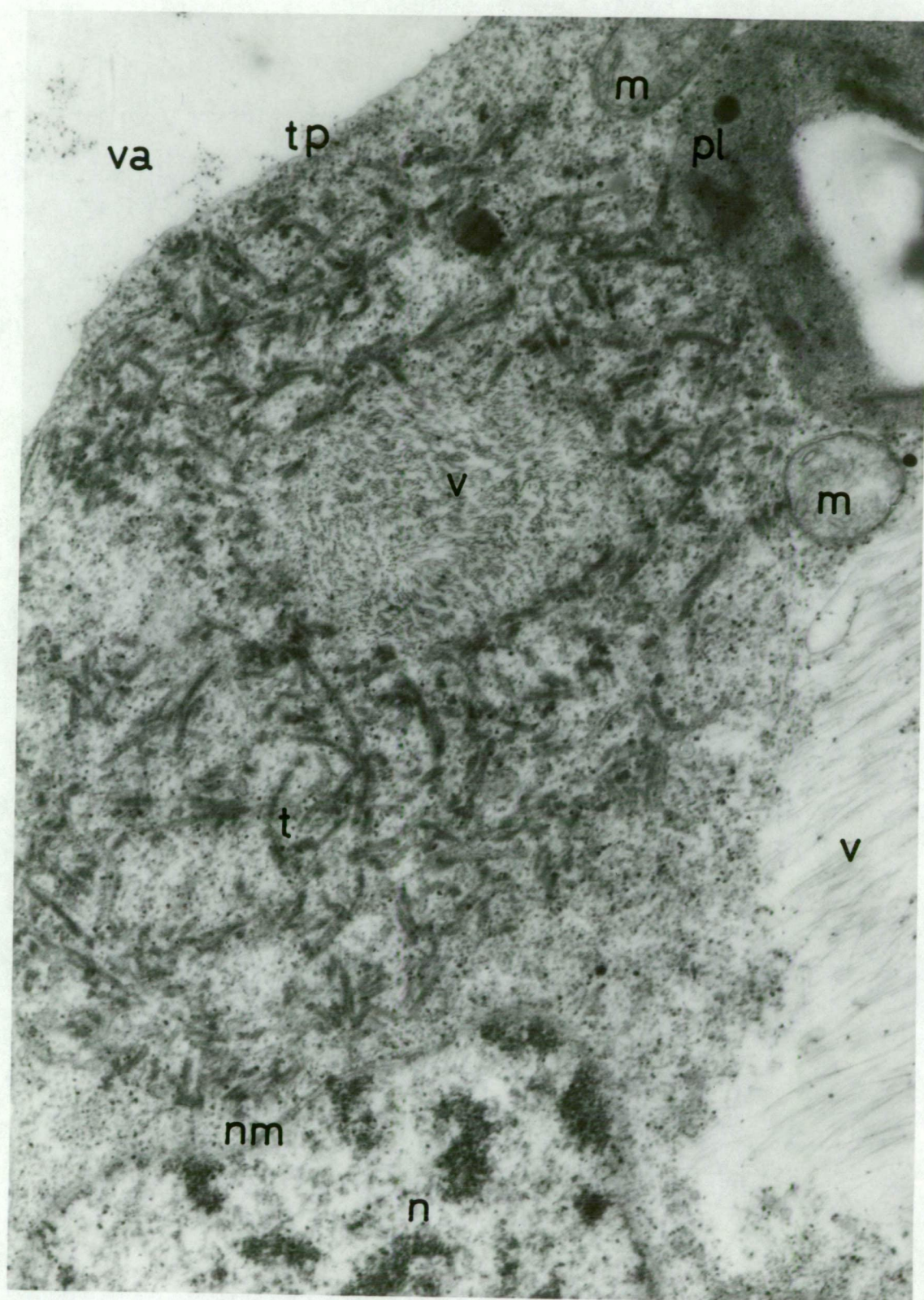


Plate 37

X-body in a virus-infected leaf cell of tobacco (leaf position 6 from the stem apex). Tissue fixed in glutaraldehyde/osmium tetroxide, pre-stained with aqueous uranyl acetate, embedded in araldite, post-stained with uranyl acetate/Reynold's lead citrate. Note the randomly organized tubular structures in the X-body and the presence of a virus crystalline inclusion within the X-body. The X-body is also in the vicinity of the cell nucleus.

(m = mitochondrion, n = nucleus, nm = nuclear membrane, pl = plastid, t = tubular components, tp = tonoplast, v = virus inclusion, va = vacuole)

Magnification 30,940 X



(c) Mature leaf tissues

By the time leaves had reached full expansion size (usually about leaf position 14 from the stem apex) chloroplasts had begun to show signs of structural degeneration. However, chloroplasts in cells of light green island tissues (Plates 38, 40) did not show the same degree of disorganization that was evident in chloroplasts of comparably aged healthy tissues (Plates 39, 41). Chloroplasts of healthy tissues contained more osmophilic globules (Plate 39) and displayed greater disorganization of the stroma lamellae (Plate 41).

Plate 38

Section through a mature, virus-infected leaf (leaf position 14 from the stem apex). Plates 38 and 39 represent tissues fixed in glutaraldehyde/osmium tetroxide, pre-stained with aqueous uranyl acetate, embedded in araldite and post-stained with uranyl acetate/Reynold's lead citrate.

(n = nucleus, pl = plastid, va = vacuole)

Magnification 6,460 X

Plate 39

Section through cells of a mature, healthy tobacco leaf (leaf position 14 from the stem apex). Note the numerous osmophilic globules (dark-staining globules) within the chloroplasts.

(va = vacuole)

Magnification 6,460 X

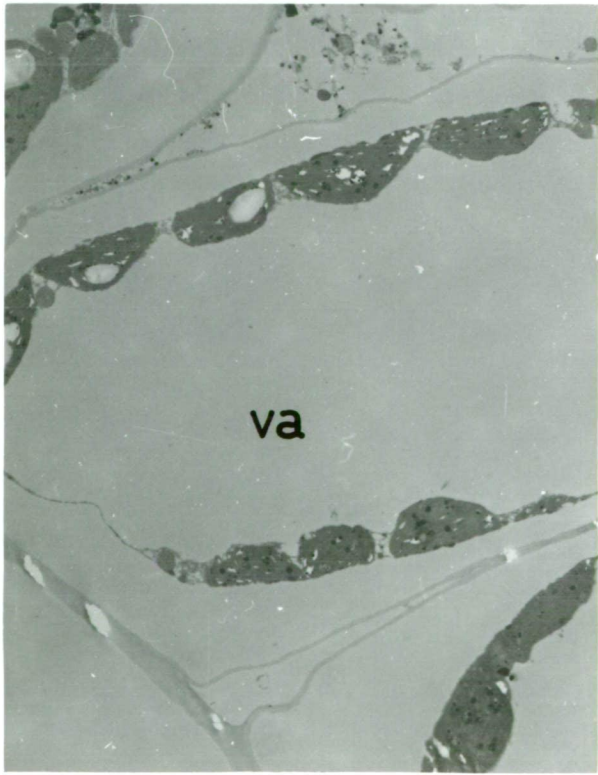
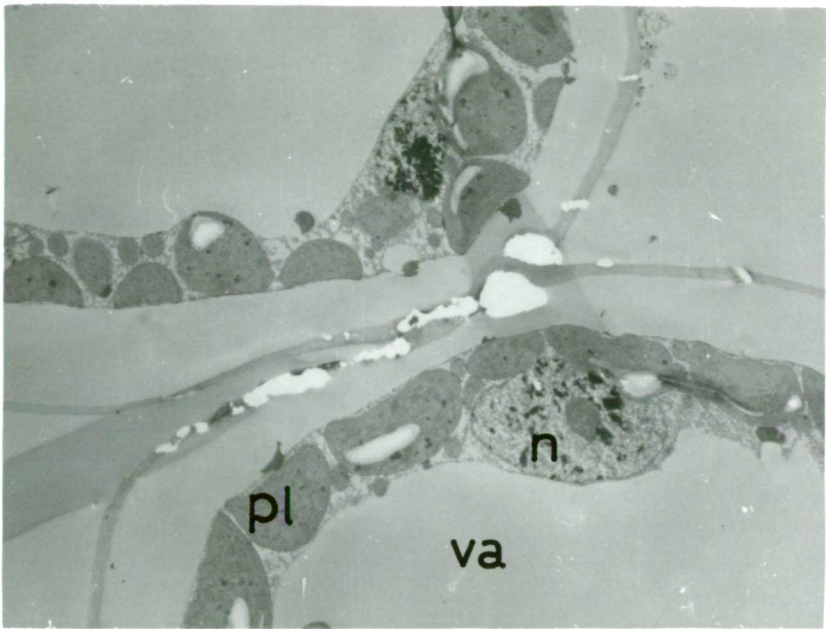


Plate 40

Chloroplasts in a mature leaf cell of virus-infected tobacco (leaf position 14 from the stem apex). Plates 40 and 41 represent tissues fixed in glutaraldehyde/osmium tetroxide, pre-stained with aqueous uranyl acetate, embedded in araldite, and post-stained with uranyl acetate/Reynold's lead citrate. Note the presence of well developed stroma lamellae and grana.

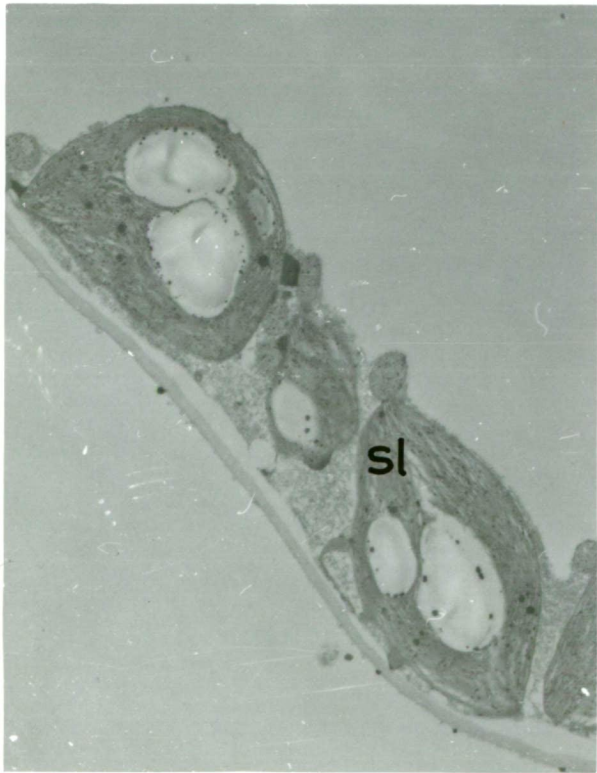
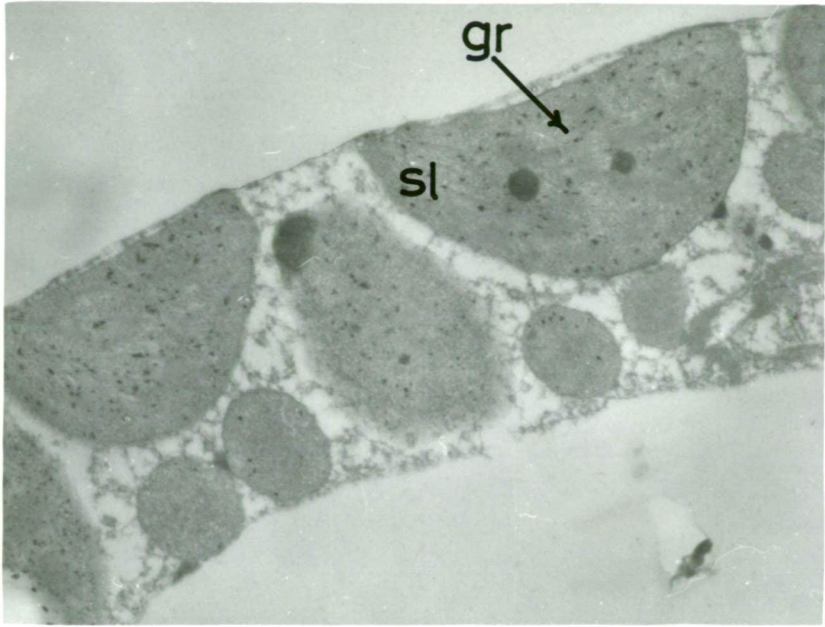
(gr = grana, sl = stroma lamella)

Magnification 29,000 X

Plate 41

Chloroplasts in a mature leaf cell of healthy tobacco (leaf position 14 from the stem apex). Note the disorganized stroma lamellae (sl).

Magnification 14,840 X



(d) Senescing leaf tissues

Senescent breakdown of cellular components was more advanced in cells from healthy leaves. Chloroplasts in cells of healthy senescing tissue had very little recognizable internal structure (Plates 43, 45, 46). These chloroplasts had much reduced stroma lamellae and grana and contained numerous globules and very large, degenerate starch granules. On the other hand, chloroplasts in cells from light green island tissues, although showing some signs of structural degeneration, still contained much grana and stroma lamellae. Starch granules gave staining reactions more typical of chloroplasts from less mature tissues.

Plate 42

Section through senescing, virus-infected tobacco leaf cells (leaf position 17 from the stem apex). Plates 42 and 43 represent tissues fixed in glutaraldehyde/osmium tetroxide, pre-stained with aqueous uranyl acetate, embedded in araldite and post-stained with uranyl acetate/Reynold's lead citrate. Note degenerate chloroplasts with large starch bodies and occasional globules.

(gl= globule, sb = starch body, v = virus inclusion)

Magnification 6,920 X

Plate 43

Section through senescing, healthy tobacco leaf cells, (leaf position 17 from the stem apex). Note the chloroplasts with large and degenerate starch bodies and numerous globules.

(gl = globule, sb = starch body)

Magnification 10,380 X

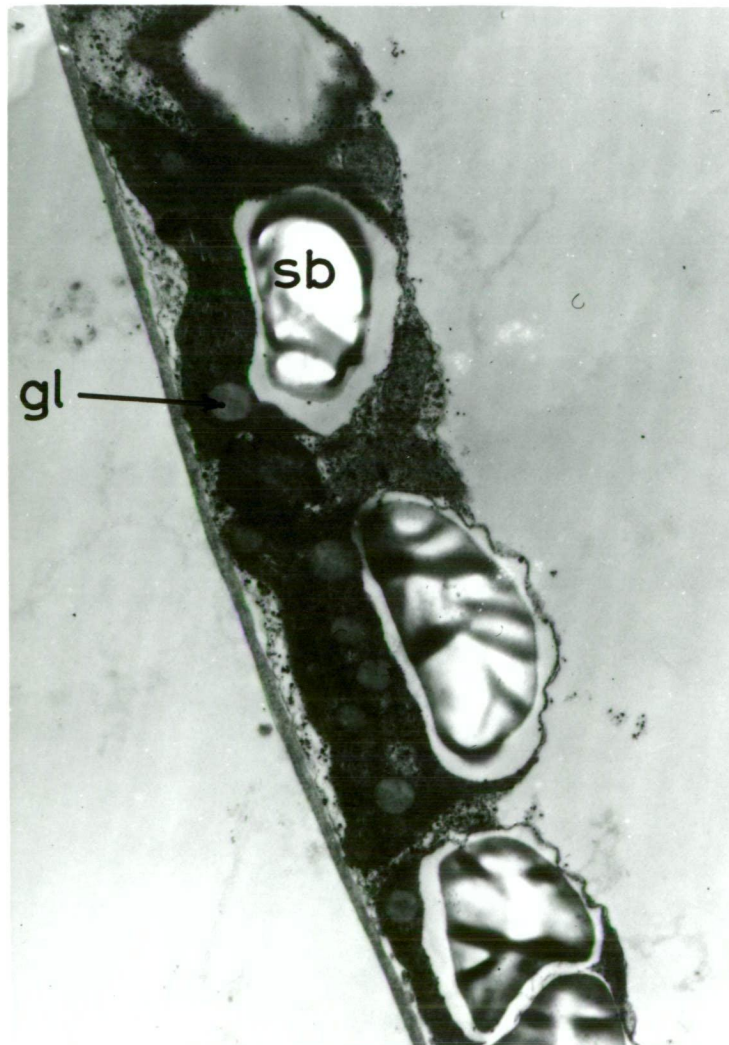
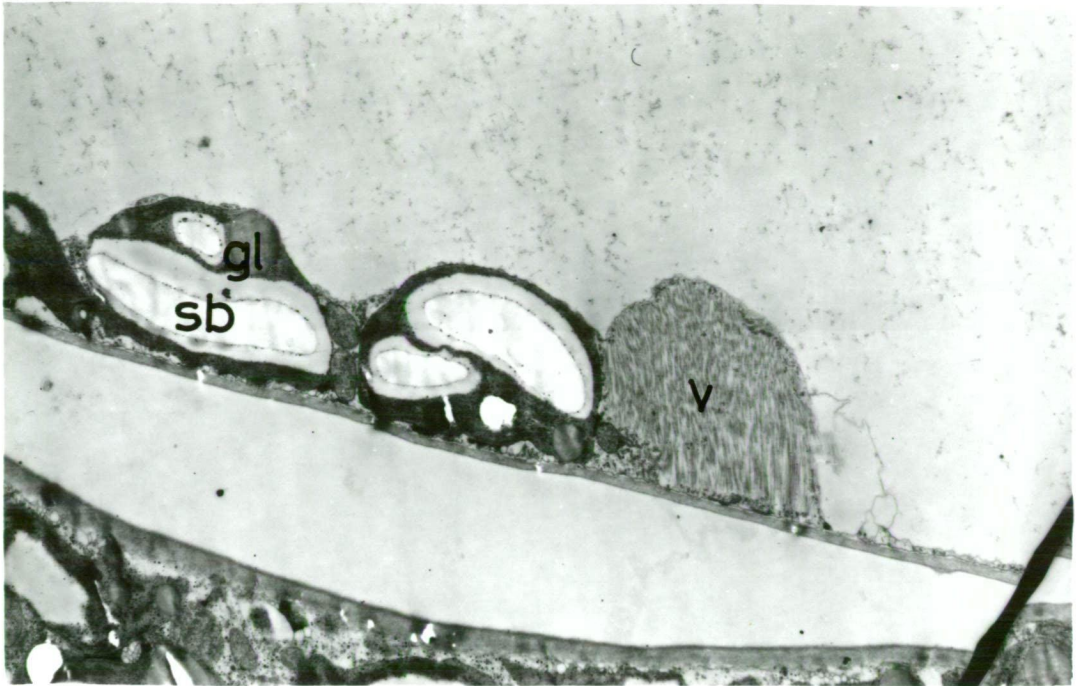


Plate 44

Chloroplasts in senescing, virus-infected, tobacco leaf cells (leaf position 17 from the stem apex). Plates 44, 45 and 46 represent tissues fixed in glutaraldehyde/osmium tetroxide, pre-stained with aqueous uranyl acetate, embedded in araldite and post-stained with uranyl acetate/Reynold's lead citrate. Note the disorganized stroma lamellae and the presence of grana.

(gr = grana, sb = starch body)

Magnification 14,100 X

Plate 45

Chloroplasts in a senescing, healthy tobacco leaf cell (leaf position 17 from the stem apex). Note the lack of organized chloroplast structure and large and degenerate starch bodies. Also note the degenerate mitochondria.

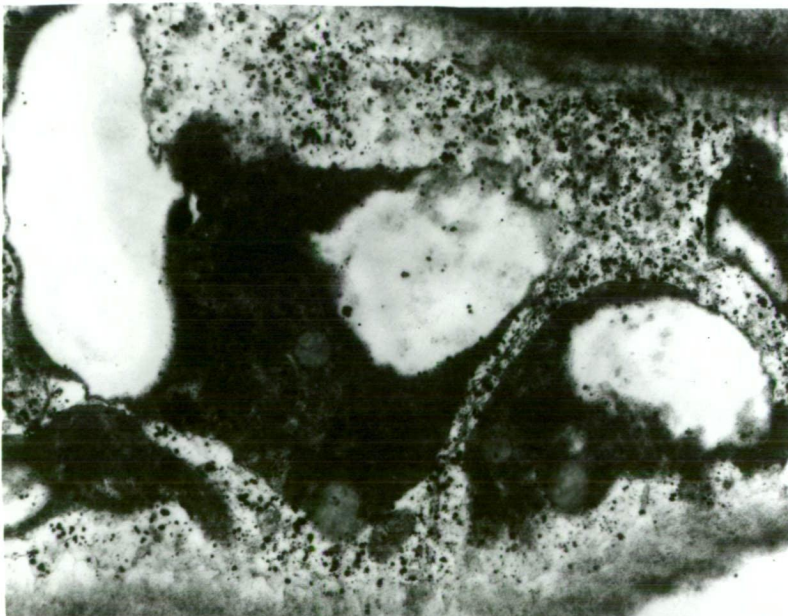
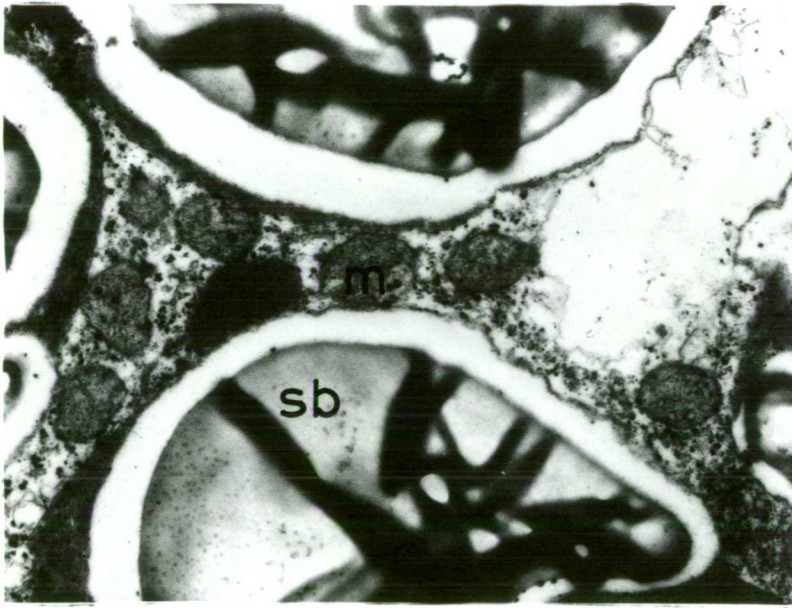
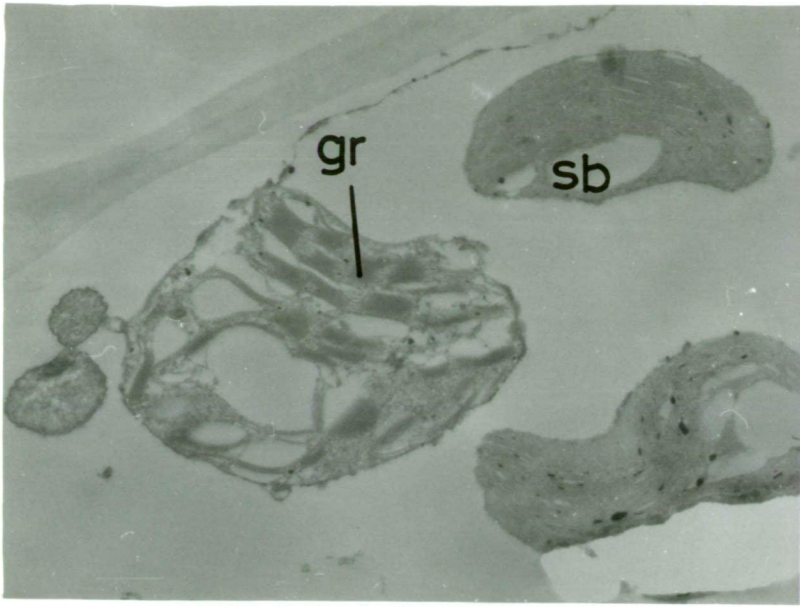
(m = mitochondrion, sb = starch body)

Magnification 16,000 X

Plate 46

Chloroplasts in a senescing, healthy tobacco leaf cell (leaf position 17 from the stem apex). Note the extent of degeneration of plastids.

Magnification 10,000 X



2. Some Miscellaneous Observations of Virus-Infected and Healthy Tobacco Leaf Cells

Single membrane-bound organelles containing a crystalloid core were seen more frequently in virus-containing cells of light green island tissues (Plates 47, 48, 49) than in healthy tissues. The shape and structure of these organelles and their proximity to chloroplasts suggests that they are microbodies as described by Baker *et al.* (1973), Bibby and Dodge (1973), Frederick and Newcomb (1969) and Wrigley (1968). Similar unit-membrane-bound organelles were observed in cells from uninfected tobacco leaves but such bodies rarely contained a crystalloid core.

Other cellular organelles including mitochondria and nuclei appeared to be little affected by virus infection with respect to shape and structure. It was noted however that mitochondria, along with other membrane structures in the cell, were more degenerate in size and structure in cells from uninfected senescing tobacco leaves compared with leaves of a similar chronological age from infected plants (see Plate 45).

Invaginations in the outer chloroplast membrane were also occasionally observed (see Plate 50). Similar chloroplast invaginations were reported by Shalla (1964) who suggested that such invaginations of the outer membrane accounted for some of the reported observations of virus particles within tobacco leaf cell chloroplasts.

Plate 47

Section through a leaf cell of virus-infected tobacco leaf (leaf position 6 from the stem apex). Tissue preparation for Plates 47, 48 49 as previously described for araldite embedding. Note the close association of the microbody with chloroplasts and the crystalloid core of the microbody.

(mb = microbody, n = nucleus, nm = nuclear membrane, pl = plastid, va = vacuole, x = X-body)

Magnification 13,000 X

Plate 48

Microbody in virus-infected tobacco leaf cell (leaf position 8 from the stem apex). Note the single membrane surrounding the organelle and the crystalloid core.

(mb = microbody)

Magnification 60,000 X

Plate 49

Microbody with crystalloid core in a virus-infected leaf cell of tobacco (leaf position 14 from the stem apex).

(m = mitochondrion, mb = microbody, pl = plastid, va = vacuole)

Magnification 19,300 X

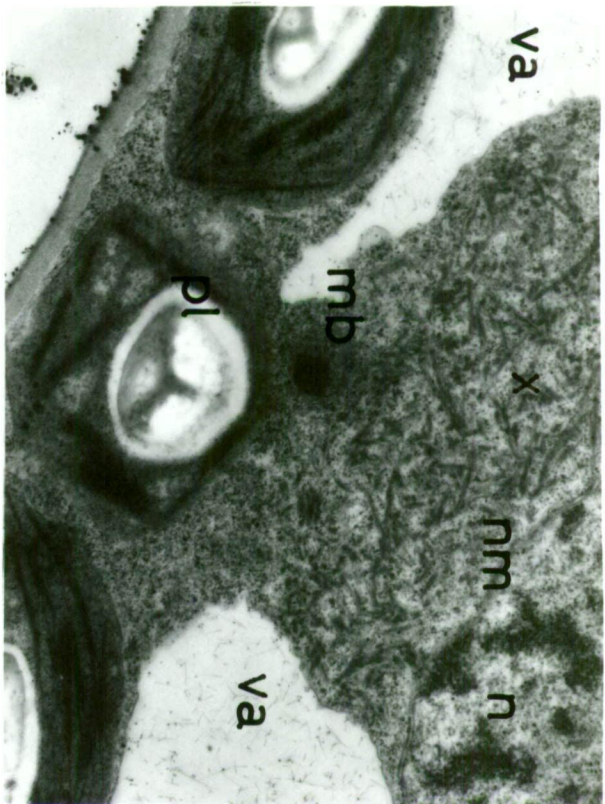
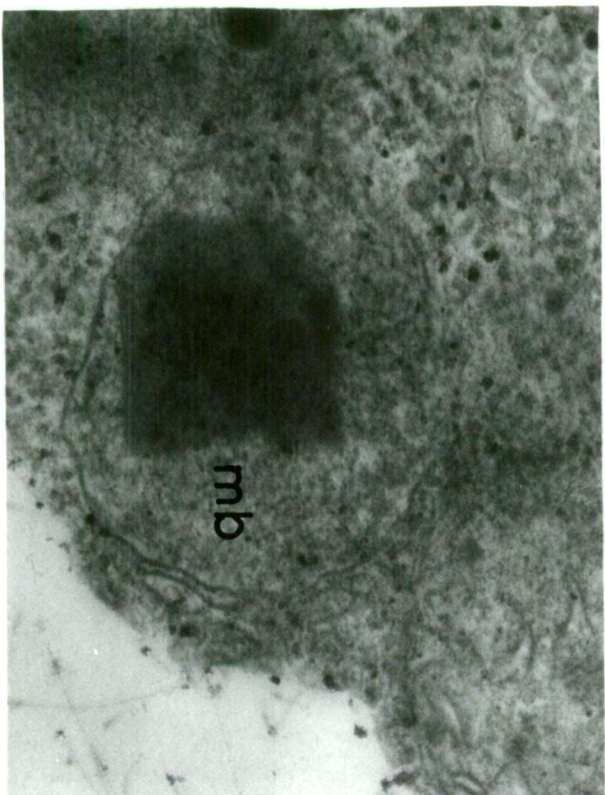
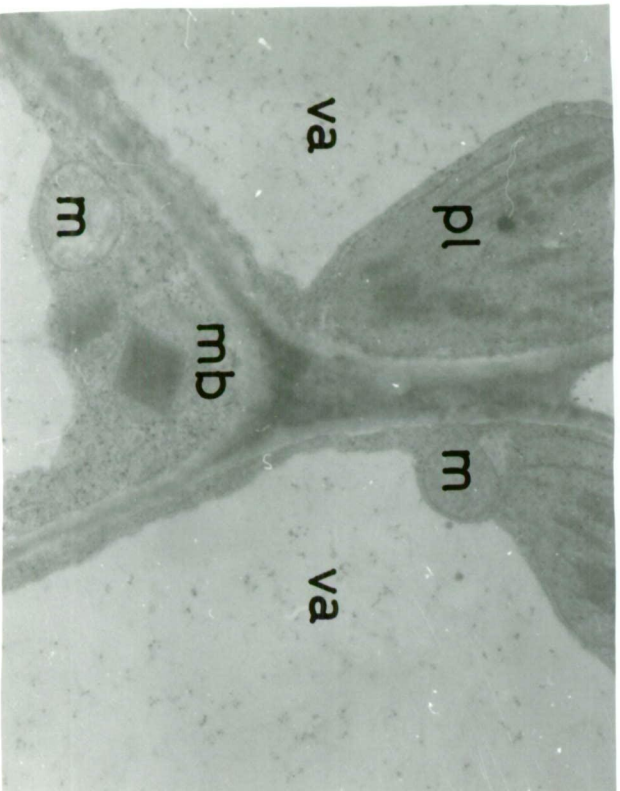
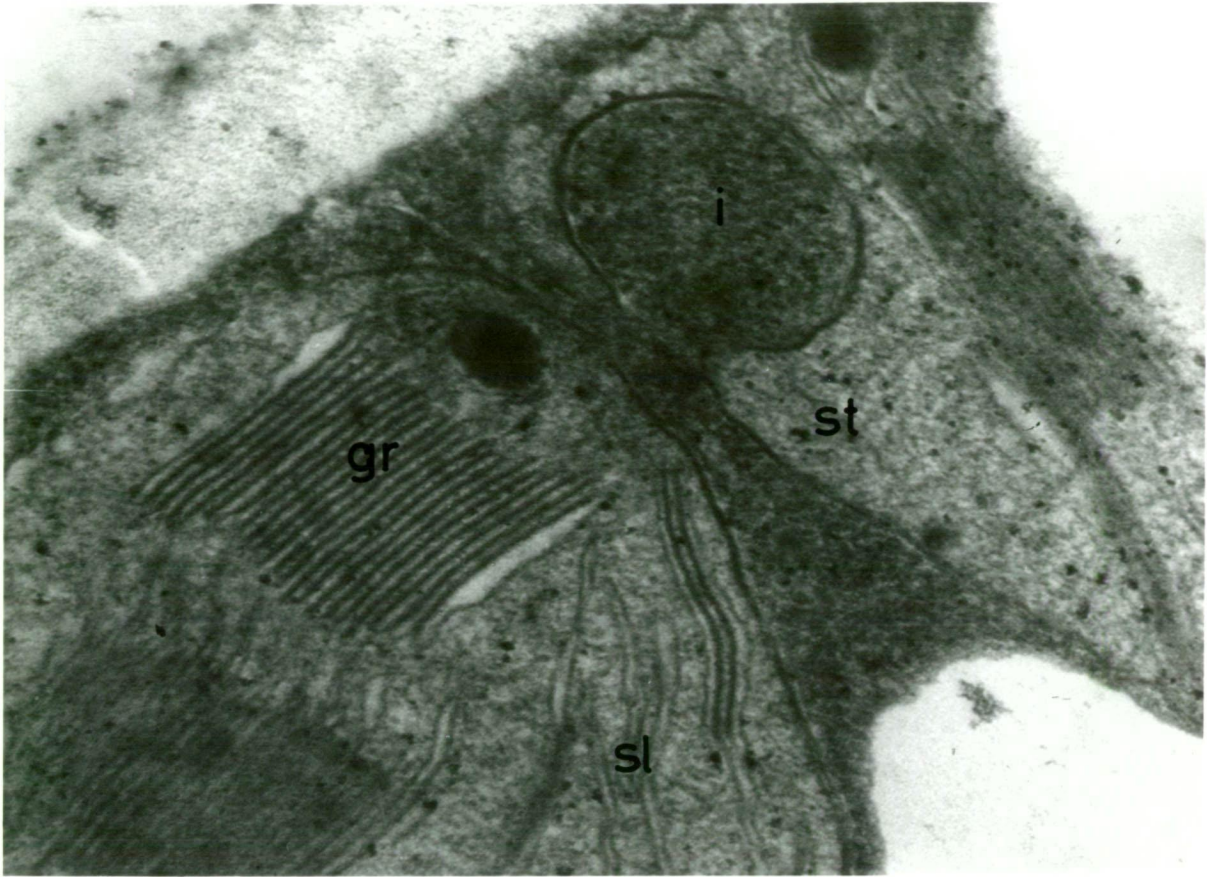


Plate 50

Section through chloroplasts in a cell of dark green island tissue from a virus-infected tobacco plant (leaf position 8 from the stem apex). Note the invagination in the outer membrane of the chloroplast on the right.

(i = invagination, g = grana, sl = stroma lamella, st = stroma)

Magnification 86,500 X



DISCUSSION

Plant virus diseases of the mosaic-type represent a successful interaction between host-cell supported virus synthesis and cellular metabolism. Unsuccessful interactions between invading viruses and host plants, which result in premature host death or limited virus synthesis, have no significance in evolution of virus/host plant combinations and probably represent unsuccessful and incidental associations brought about by man's cultural practices. If a living system is exposed to an environmental stress and it fails to make the necessary physiological and biochemical adjustments, it may either die or fail to reproduce itself. Because of the simple biochemical nature of viruses and their dependence on host cell biosynthetic pathways for reproduction, virus infections can be viewed as internal environmental stresses.

Stunting is often associated with virus infections and for the susceptible tobacco variety Nicotiana tabacum L. var. "Hickory Prior" infected with the U1 strain of tobacco mosaic virus, stunting was an obvious feature of the disease. Plant height, internode length, leaf size and root weight were all reduced in plants showing well developed symptoms. A similar reduction in growth for TMV-infected tobacco plants was reported by Takahashi (1972). The extent to which final plant growth is reduced depends on the age of plants when infection occurred.

The effect of virus infection on subsequent plant growth rate depends on the age of the infection when measurements of growth are taken. The magnitude of the reduction in growth of a leaf, following virus infection depended on the stage of leaf growth development at the time of inoculation. Cell division as a major factor contributing to leaf growth ceases to be important once tobacco leaves reach a length of 3-4 cm. Cell enlargement contributes most to leaf growth beyond this length. No measurable differences in leaf growth rate and final leaf size occurred for any leaves greater than 2 cm long at the time of inoculation. This

confirms the report by Takahashi (1972) that no differences in tobacco leaf shape occurred till 15 days after inoculation with TMV. The greatest reductions in leaf size occurred for those leaves differentiated as leaf primordia, but less than 2 cm long at the time of inoculation. Not only were these leaves greatly reduced in size but they also deviated most from a normal leaf shape. All leaves differentiated subsequent to infection, displayed similar patterns of growth reduction. Reduced plant size can be a function of either reduced cell size, reduced cell numbers or both. Results in Section I suggest that the rate of formation of leaves is greater for virus-infected plants. Takahashi (1972) concluded that virus infection had no effect on the number of leaves formed. These results indicate that the rate of apical mitotic cell division is greater, or at least unaffected in virus-infected plants. The differences in leaf cell size between healthy and virus-infected plants do not seem great enough to account for the differences in final leaf size. Although mesophyll palisade cells were blockier in virus-infected leaves with well developed mosaic patterns, the number of cells per unit leaf area were the same for virus-infected and healthy leaves of a similar chronological age. It must be pointed out that assessments on leaf cell size were only conducted on leaf tissues displaying classic mosaic symptoms. Reduced cell size may have contributed to the gross reductions in leaf size for those leaves that were differentiated but small at the time of inoculation. As neither final cell size nor rate of apical mitotic cell divisions seemed to be affected in leaves with well defined mosaic symptoms, the only explanation for reduced leaf size and probably reduced plant size is a reduction in the rate of sub-apical mitotic cell divisions. Bailiss (1970b) considered that the most important feature contributing to reduced plant growth for tomato infected with aspermy virus, was a reduction in sub-apical mitotic activity. Reports also suggest that patterns of mosaic symptom development are established during the period of

cell division. Doke (1971) concluded that cell division and induced chloroplast abnormalities were the major factors in producing a mosaic disease. This confirmed a report by Reid and Matthews (1966) who considered that the mosaic pattern was determined by events taking place in leaves in which cell division was taking place. The abnormal shape of some leaves on TMV-infected tobacco plants has been attributed to the absence of, or reduced activity of the marginal meristems of leaf primordia (Tepfer and Chessin, 1959).

Virus infectivity assays of tissue extracts from leaves of different chronological age revealed that the maximum rate of virus synthesis occurred in those leaves younger than leaf position 3 from the stem apex. This was confirmed by the large accumulations of virus that were observed in thin sections of infected leaf cells from leaf tissues less than 2 cm long. Cells in an active state of division were also observed in leaf tissues of this age. Esau and Gill (1969) observed that differentiating mesophyll cells of tobacco divided in the presence of large accumulations of TMV. Virus particles have also been detected in the apices of infected plants (Roberts *et al.*, 1970; Faed and Matthews, 1972). It is proposed therefore that high rates of virus synthesis in actively dividing sub-apical cells and leaf primordia reduces the rate of cell division and that reduced cell numbers rather than reduced cell size is the major factor contributing to reduced size of virus-infected tobacco plants.

Reduced rates of cell division and cell expansion if it occurs, are probably the direct expression of virus-induced metabolic disturbances in cells supporting virus synthesis. Virus diseases of the mosaic type result in two distinct leaf tissue types that have been referred to, both here and in the literature, as dark green island tissue and light green island tissue. Previous reports established that virus was concentrated in light green island tissues and that dark green island tissues were relatively free of virus (Reid and Matthews, 1966; Chalcroft and

Matthews, 1967; Atkinson and Matthews, 1970). Virus infectivity studies and observations on cell ultrastructure reported here confirmed that cells in the dark green islands of infected leaves contained little virus and were structurally identical with cells from healthy control tissues of the same chronological age. Because of the two distinct tissue types of mosaic-diseased plants, a comparison can be made between virus-infected and virus-free tissues within the one plant organ. Changes in metabolic activities for the comparison dark green island tissue versus healthy control tissue provides information on the indirect biochemical responses of the plant to infection. The more direct effects of virus multiplication on cellular metabolism are assessed from biochemical changes occurring in light green island tissues compared with dark green islands and healthy control tissues.

Together with reduced plant size, reduced photosynthetic pigments are the most obvious characteristics of plants with mosaic virus diseases. Photosynthesis is the primary metabolic function of plant leaves and the translocation of products of photosynthetic carbon dioxide fixation controls the amount of growth made by roots and shoots. Reduced photosynthetic rate has been reported with diseases of the mosaic type, whether measured as CO_2 uptake (Owen, 1957) or Hill reaction rate (Rubin and Ladygina, 1972). A reduction in photosynthetic pigment levels is obvious from the nature of the disease. Measured chlorophyll "a" levels in diseased and healthy tissues confirmed previous reports of reduced chlorophyll levels accompanying diseases of the mosaic type. High levels of chlorophyll "a" in virus-free tissues of the mosaic, compared with healthy control tissues, suggests that virus infection indirectly enhances either chlorophyll "a" synthesis or chloroplast numbers. The ratios of chlorophyll "a" levels to chlorophyll "b" levels, for the comparisons uninfected leaf tissues versus light green island and dark green island leaf tissues from infected plants, have a similar relative relationship (dark

green island tissue > leaf tissue from uninoculated plants > light green island tissue) to chlorophyll "a" levels, within any leaf age comparison. Such a similarity would occur if chlorophyll "a" synthesis and not chlorophyll "b" synthesis was affected by infection.

Activity of the carbon dioxide fixing enzyme ribulose 1,5-diphosphate carboxylase was higher in leaves from infected plants. However, the comparison between light green island and dark green island tissues indicates that some reduction of enzyme activity is associated with cells supporting virus synthesis. There is a net increase in enzyme activity in light green island tissues relative to healthy control tissue of a similar chronological age. Generally, virus infections have been reported to bring about a net decrease in the activity of RuDP carboxylase (Pratt, 1967; Oxelfelt, 1971). However, these reports mostly concerned the changes which occurred immediately following inoculation, whereas the results reported here refer to enzyme activities in tissues with well established infections. Magyarosy *et al.* (1973) found that squash mosaic virus infections had no effect on RuDP carboxylase activity.

The results for chlorophyll "a" and RuDP carboxylase suggest that the control of synthesis of these two chloroplast components are independent of each other. Sakano and Wildman (1973) reported that RuDP carboxylase activity in etiolated tobacco shoots was similar to the activity in normal green tobacco leaves. Their results also suggest that the suppressing effects of virus infection on chloroplast function may be more specific than a general inactivation of chloroplast activity. If it is assumed that photosynthetic rate is reduced in light green island tissues of infected leaves, then the level of chlorophyll "a" is probably an important limiting factor. Photosynthetic pigments are a component of the photosystems in photosynthesis. By transferring electrons from water, the photosystems generate ATP and reduced pyridine nucleotide phosphates (NADPH₂). The latter is essential for CO₂ fixation via the Calvin cycle.

Tobacco mosaic virus infection of tobacco has been shown to have its greatest effect on photosynthesis by suppressing non-cyclic electron flow and hence ultimately NADPH_2 generation. It would appear that the rate limiting step of carbon dioxide fixation in TMV-infected tobacco plants is NADPH_2 availability.

Ultrastructural observations in chloroplasts from young leaf tissues indicates that virus replication interferes with chloroplast development. Reduced photosynthetic pigment in young, virus-containing cells was associated with reduced stroma lamellae and grana. As well as evidence for suppressed chloroplast function and development in young, infected leaf cells, it cannot be discounted that reduced chloroplast numbers contribute to the measured reductions of photosynthetic pigment and RuDP carboxylase activity. For leaves older than those at leaf position 6 from the stem apex (that is leaves greater than half fully grown) no ultrastructural differences were detected between chloroplasts from healthy, light green island and dark green island leaf tissues. The level of chlorophyll "a" increased in infected leaves as the tissues matured but only exceeded the levels in comparably aged healthy leaves when those tissues were into biochemical senescence. Reduced levels of chlorophyll "a" for infected leaves between leaf position 6 from the stem apex and full expansion size may reflect differences in chloroplast numbers per cell.

Although tissues supporting virus synthesis have a reduced potential for photosynthesis, this may be compensated for to some extent by the very high potential for photosynthesis in dark green island tissues of the same leaf. Both photosynthetic pigment content and RuDP carboxylase activity were higher in these tissues compared with healthy leaf tissues of a similar chronological age.

The mode of action of suppression of chloroplast function and development in young infected cells is difficult to define from the results reported here. Actinomycin D treatment of tobacco leaves has been shown

to produce similar symptoms to virus infection (Hirai and Wildman, 1967). It was suggested that the antibiotic blocked access of mRNA to specific sites on host cell DNA and that this action was similar to that of virus. Partial repression of the genetic mechanism of the chloroplast was also suggested by Pratt (1967) and Hirai and Wildman (1969). The lack of convincing evidence for a direct involvement of chloroplasts in virus synthesis indicates that virus replication interferes with cell genetic control over chloroplast development and action. Eighty six nuclear genes that control chloroplast development have been identified in barley (von Wettstein et al., 1971). Although it is generally accepted that chloroplast DNA codes for chlorophyll synthesis, nuclear genes have been identified that control the insertion of chlorophyll into photosynthetic membranes (von Wettstein et al., 1971). The chloroplast enzyme RuDP carboxylase has two sub-unit components, one of which is coded for by chloroplast DNA and the other by nuclear DNA (Kawashima and Wildman, 1971; von Wettstein et al., 1971; Singh and Wildman, 1973; Alscher et al., 1974; Roy and Jagendorf, 1974). There is evidence for the synthesis of proteins and nucleic acids of chloroplast ribosomal sub-units on 80S, cytoplasmic ribosomes (Spencer et al., 1971; Kloppstech and Schweiger, 1974) and it has also been suggested that chloroplast DNA-dependent RNA polymerase is synthesized on cytoplasmic ribosomes (Kloppstech and Schweiger, 1974). There is ample opportunity for factors external to the chloroplast to impede normal chloroplast function and development. Chloroplasts appear to be particularly sensitive to environmental stresses. Gerola and Dassu (1960) reported that under conditions of nutrient starvation, loss of chloroplast colour occurred accompanied by the appearance of large starch grains and disappearance of lamellae. This description fits very closely the observed ultrastructural characteristics of chloroplasts in young, virus-infected leaf tissues. Suppressed chloroplast development in young, virus-infected cells may simply reflect nutrient starvation within the

cell through rechanneling of metabolites towards virus synthesis.

The profile of leaf tissue age versus nitrate reductase activity for healthy and virus-infected tissues closely followed the chlorophyll "a" level/leaf tissue age profile. Nitrate reductase activity was reduced in tissues supporting virus synthesis. Nitrate reductase is linked, indirectly, to chloroplast function by its association with nitrite reductase (Magalhaes *et al.*, 1973). The nitrate/nitrite reductase system is coupled to photosynthesis through its requirement for NADPH_2 (Magalhaes *et al.*, 1973). Therefore, both nitrite reductase and CO_2 fixation via the Calvin cycle compete directly for NADPH_2 . There is also evidence that nitrate reductase synthesis competes with the chloroplast system protein synthesis for ATP (Knypl, 1973). It has been established (Rubin and Ladygina, 1972), earlier in this section, that the photosystems and their NADPH_2 generating capacity are affected by virus infection. Reduced nitrate reductase activity in infected tissues is probably a direct reflection of reduced chloroplast function and numbers.

As pointed out in the introduction to Section II, catalase is a major enzyme constituent of microbody localized photorespiration. This enzyme was greatly reduced in activity in leaves supporting virus synthesis. The activity of enzymes of photorespiration have been correlated with the level of chlorophyll synthesis (Kuczmak and Tolbert, 1962; Dézsi and Farkas, 1964) and it is tempting to conclude that the activity of catalase is a consequence of reduced chloroplast activity. However, catalase activity remained low in virus-infected tissues as they matured, whereas chloroplast function increased. More recent evidence suggests that activation of photorespiration is independent of the chloroplast system. Feierabend and Beevers (1971) demonstrated that although all enzymes of photorespiration increased in activity when exposed to light, the effect of light on microbody enzymes was independent of chlorophyll formation or the concomitant development of functional chloroplasts. Virus-infected

tissues were observed to have a higher incidence of microbodies with crystalloid cores. Such para crystalline cores, developed by reorganization and compaction of matrix material, have been shown to contain catalase (Vigil, 1973a). Catalase isolated in this form may be biologically less active.

As catalase is important in photorespiration, it may be inferred that photorespiration rate in tissues supporting virus synthesis is greatly reduced. The importance of photorespiration in intermediary metabolism of leaf cells is supported by the loss of carbon dioxide during the course of glycolate oxidation (Vigil, 1973a). Such a CO_2 loss would greatly affect photosynthetic efficiency of plants with high activities of microbody enzymes. Vigil (1973a) pointed out that it was not surprising that the synthesis and oxidation of glycolate in light, as part of photorespiration, severely limited growth and crop productivity. Most tropical plants (C_4 pathway plants) do not have photorespiration accompanying photosynthesis in the same cell and are more efficient producers of dry matter (Vigil, 1973a). Tobacco leaves on the other hand have been shown to have a high activity of glycolate oxidase (Moss, 1967). If a plant cell is to maintain a reduced level of metabolism and synthesis in the presence of large accumulations of virus, it becomes necessary to conserve against carbon losses. This is partly achieved in tobacco leaf cells infected with TMV by reducing photorespiration rate.

The other major loss of CO_2 by cells is through "dark" respiration or "mitochondrial" respiration. From respiration the cell generates ATP at the expense of carbon either fixed in photosynthesis or obtained from translocation. Systemic infections, between the period of inoculation and symptom appearance and virus diseases of the local lesion type generally result in respiration increases (see literature review). From the few reports where advanced systemic infections were analysed, respiration rates were found to be lower in infected plants (Owen, 1955, 1956; Merrett,

1960; Orlob and Army, 1961; Takahashi and Hirai, 1964).

Cytochrome-C oxidase activity was greatly reduced in leaf tissues supporting virus synthesis, especially in younger tissues. Enzyme activity in virus-free areas of infected leaves was less compared with similarly aged healthy tissue but greater than adjoining light-green island tissues. As cytochrome-C oxidase is the terminal enzyme of respiratory chain phosphorylation, its activity represents "dark" respiration rate. The reduced respiration rate of dark green island tissues may be associated with the higher photosynthetic potential of these tissues. By eliminating most other factors, Mangat et al. (1973) concluded that "dark" respiration rate, in photosynthetic tissues, was controlled by the amount of photosynthetically produced ATP. The measured activities of two other mitochondrial enzymes, NADH oxidase and glutamate dehydrogenase, suggests that mitochondrial activity in general is reduced in cells supporting virus synthesis. Rubin and Ladygina (1972) reported losses of mitochondrial ATP and reduced inorganic phosphate uptake by tobacco leaf cell mitochondria following infection with TMV. Virus infection may also reduce respiration rate by reducing oxidative phosphorylation which is directly coupled to the terminal electron transport system of the respiratory chain. Oxidative phosphorylation becomes a rate limiting step when ADP is reduced. Low ADP and ATP levels have been recorded for TMV-infected tobacco plants (Sunderland and Merrett, 1964; Rubin and Ladygina, 1972). High respiration rates are usually associated with plant cells involved in transport or manufacture and release of assimilates. Reduced respiration rate of virus-infected tissues may also imply a reduced translocation rate of carbohydrates. In cells supporting virus synthesis, more carbon is made available for virus synthesis and essential cellular metabolism by reducing losses incurred through photorespiration, respiration and probably translocation. Reduced photosynthesis and respiration in infected cells may also be effective in restraining virus synthesis as such

cells have a reduced energy budget because of a lower potential for ATP generation. As well as being a precursor of nucleic acid synthesis, ATP is also involved in protein synthesis.

The major pathways of carbohydrate metabolism in the cell, as assessed from the activities of key enzymes, were little affected by virus infection. Embden-Meyerhof-Parnas pathway activity, as indicated by the activity of phosphoglucosomerase, was similar for virus-infected, virus-free dark green island and healthy control tissues for all leaf age comparisons. There was some suggestion from the activity of glucose-6-phosphate dehydrogenase in the various tissue types that the pentose phosphate pathway of carbohydrate metabolism was stimulated in virus-infected tissues. The difference in enzyme activity between healthy and virus-infected leaf tissue was most pronounced for leaves that had just reached maturity. This difference in activity may be due to a rapid decline in activity in mature healthy leaves rather than a stimulation of activity in infected leaves.

The response of alcohol dehydrogenase activity, the terminal enzyme of glycolysis in plants, to virus infection depends on the age of tissue analysed. In young leaf tissues, virus infection suppressed enzyme activity whereas in mature tissues, enzyme activity was higher with infection.

The general conclusion that can be reached on carbohydrate metabolism in tobacco is that the major pathways of metabolism are not reduced in plants with well established infections. Because respiration is reduced in virus-infected leaves it must be assumed that a greater proportion of carbohydrates moving through these pathways are directed into other pathways such as amino acid synthesis. Kennedy and Laetsch (1973) have shown that the final products of CO_2 fixation depends on leaf age. Young to mature leaves fixed CO_2 primarily into organic and amino acids. Senescent leaves showed a quantitative shift of primary products towards phosphorylated compounds. Virus synthesis makes heavy demands on nucleic acid and protein synthesis in infected cells. By maintaining normal rates

of carbohydrate metabolism, conserving cell carbon by reducing losses through photorespiration, "dark" respiration and translocation and by converting intermediates of the major pathways of carbohydrate metabolism to amino acids, virus-infected cells would be better able to support both virus synthesis and biosynthesis essential to cell survival.

The full role of hydrolitic enzymes in plant cells is not altogether clear. As well as being involved in the intermediary metabolism of carbohydrates, nucleic acids, nucleotides and phosphoproteins it has also been suggested that they are involved in mobilization of nutrient reserves (Figier, 1968; Sauter, 1972; Wilson, 1973), chloroplast development (Mlodzianowski, 1972), cell division (Wilson, 1973) and senescence (De Leo and Sacher, 1970). Most acid hydrolases are localized within lysosomes although some have been shown to be associated with other membrane components of the cell. ATPase is generally considered to be associated with the endoplasmic reticulum. Specific acid phosphates implicated in sugar transport have been demonstrated in association with the endoplasmic reticulum, golgi apparatus and plasmallema (Figier, 1968). Specific acid phosphatases in tobacco have also been detected in the cell wall fraction (Suzuki and Sato, 1973).

Acid hydrolase activity was generally higher in leaf tissues from virus-infected plants. Increases in specific hydrolytic enzyme activities, as a consequence of virus infection, were also reported by Wolffgang and Keck (1958), Diener (1961), Randles (1968) and Reddy and Stahmann (1970). Enzyme activities reported here were greatest in tissues supporting virus synthesis and lowest in healthy control tissues of a similar age. Increased hydrolase activity in both tissue types of virus-infected leaves again suggests that these tissues have higher rates of carbohydrate turnover and protein and nucleic acid synthesis.

Peroxidases have been extensively studied in relation to virus-infected tissues although little is understood of their role in

intermediary cellular metabolism. The enzyme is located mainly in the cytoplasm with some activity in the chloroplast and mitochondrial fraction (Frederick and Newcomb, 1969). Both increased peroxidase activity and increased numbers of isoenzymes of peroxidase have been reported for virus-infected tissues (Vager, 1955; Orlob and Arny, 1961; Farkas and Stahmann, 1966; Bates and Chant, 1969; Chant and Bates, 1970; van Loon and Geelen, 1971). Increases in the number of isoenzymes of peroxidase, following virus infection, have been shown to be due to stabilization of isoenzymes usually only associated with immature healthy tissues and/or earlier appearance of isoenzymes usually associated with mature healthy tissues (Novacky and Hampton, 1968; Solymosy et al., 1967; Esanu and Dumitrescu, 1971). Peroxidase activity in TMV-infected tobacco leaf tissue, as reported in Section II, confirmed the above reports. Highest enzyme activity was associated with virus-containing tissues while the activity in dark green island tissues was intermediary between the activities in light green islands and healthy control tissue of a similar age.

There is some suggestion from the literature that peroxidase may be involved in auxin metabolism. Raa (1970) reported that peroxidase had the ability to act as an indole acetic acid oxidase and catalyze the oxidative degradation of IAA in vitro. It was postulated that the enzyme could play a role in the regulation of IAA concentration in higher plants. One could postulate that this could lead to growth abnormalities. Gove and Hoyle (1974) similarly found that all peroxidase isoenzymes of horse radish and yellow birch had IAA-oxidase activity.

As well as interacting with specific pathways of cellular metabolism, virus infection has two major effects on overall cellular metabolism. Metabolism was generally suppressed in young leaf tissues supporting active virus synthesis, whereas infection prolonged active cellular metabolism and delayed biochemical senescence once leaves matured. For the

comparison light green island tissue versus healthy control tissue of a similar chronological age, cytochrome-C oxidase, glutamate dehydrogenase, NADH oxidase, chlorophyll "a" and alcohol dehydrogenase were greatly reduced in young virus-infected tissues but higher in mature, infected tissues. Leaf tissues appear to recover from the suppressing effects of virus synthesis as they mature. This is supported by observations of leaf cell ultrastructure changes as leaf tissues mature. Chloroplasts, in particular, displayed signs of developmental suppression in young, virus-infected leaf cells. However, by the time leaves had reached half their full size, there were no obvious structural differences between chloroplasts in virus-infected and healthy leaf cells.

Many biochemical systems decline in activity as healthy tobacco leaves mature. Enzymes associated with carbohydrate metabolism (glucose-6-phosphate dehydrogenase, alcohol dehydrogenase), enzymes localized within mitochondria (cytochrome-C oxidase, glutamate dehydrogenase, NADH-oxidase), chlorophyll "a" level, chlorophyll a : b ratio and nitrate reductase activity declined in healthy leaf tissues once leaves reached maturity (full leaf expansion). Chlorophyll concentration is a particularly sensitive indicator of biological senescence. Holden (1973) pointed out that chlorophyll "a" was destroyed more rapidly than chlorophyll "b" in detached, senescing leaves, leading to a decrease in the chlorophyll a : b ratio. Decline in the chlorophyll a : b ratio is typical of over-mature tobacco leaves (Whitefield and Rowan, 1974). Leaf tissue from virus-infected plants, of a similar chronological age to over-mature healthy leaf tissue, were typified by unaltered or increased activities for glucose-6-phosphate dehydrogenase, alcohol dehydrogenase, cytochrome-C oxidase, glutamate dehydrogenase and NADH oxidase, whereas chlorophyll "a" level and chlorophyll a : b ratio showed low rates of decline. Hydrolytic enzymes had similar profiles of tissue extract age versus enzyme activity for both virus-infected and healthy leaf tissues of similar chronological ages

except that enzyme activities were generally greater in virus-infected leaf tissue extracts. In the past, high activities of hydrolytic enzymes have been associated with senescence, however it is now generally accepted that senescence is either associated with enzyme release from lysosomes (Butler, 1967; Berjak and Villiers, 1972) or new enzyme synthesis independent of lysosomal enzyme synthesis (Abeles *et al.*, 1968; De Leo and Sacher, 1970; Matile and Winklenbach, 1971; Martin and Thimann, 1972).

Different stages of leaf development for virus-infected and healthy leaves of a similar chronological age could account for the differences in metabolic activity between these leaves as they matured. However, measurements of leaf growth reported in Section I indicate that leaves of the same chronological age, on healthy and virus-infected plants, reach full leaf expansion size at the same time, suggesting that these leaves are at a similar stage of growth development. Further support for a virus infection interaction with the onset of leaf senescence is provided from ultrastructural observations of cells in over-mature leaves. Senescence in healthy tobacco leaf cells was associated with obvious chloroplast degradation. Disorganization and loss of stroma lamellae and grana, numerous large osmophilic globules and large atypical starch granules were generally characteristic of these chloroplasts. Disorganized and disrupted tonoplast, plasmallema and endoplasmic reticulum, reduced cytoplasmic staining, presumably through loss of ribosomes and degenerate mitochondria were also typical of senescing leaf cells from uninfected tobacco plants. Degeneration of structure in cells from similarly aged virus-infected tobacco leaves was less pronounced. Chloroplasts had some organized stroma lamellae, recognizable grana, fewer osmophilic globules and normal-looking starch granules. Cell cytoplasm was better stained and membrane systems were more intact. It is concluded therefore, on the basis of biochemical analysis and ultrastructural observations, that mature leaf tissues from virus-infected and healthy tobacco plants, while of a

similar chronological age are not at the same physiological and biochemical stage.

The delaying of senescence in virus-infected plants suggests that plants respond to infection, by alterations in the balance of mechanisms that control overall growth and biosynthesis. Hormones are basic regulators of plant growth, development and biosynthesis. Metabolism of virus-free tissues from infected leaves, compared with similarly aged healthy control leaf tissue, further suggests that the indirect effects of virus infection on host plant metabolism are mediated through a shift in the balance of endogenous plant growth regulators. The level of chlorophyll "a" and the activities of ribulose 1,5-diphosphate carboxylase, glucose-6-phosphate dehydrogenase and alcohol dehydrogenase were much higher in dark green island tissues from infected leaves. The delay in flower initiation and appearance of obvious inflorescences with virus infection also suggests an interaction between virus infection and host hormone synthesis.

All major classes of plant growth regulators were assayed in tissue extracts from virus-infected and uninfected tobacco plants. Gibberellic acid was the only hormone assayed that showed no change in activity with virus infection. Generally, the growth promoting hormones, cytokinin and auxin, were more active in young tissue extracts from virus-infected plants. In mature leaf tissue extracts, n-butanol soluble cytokinins were greater in activity and the growth inhibitor, abscisic acid was less in activity for extracts from virus-infected plants. On the results obtained gibberellin A₃-like activity in extracts from young leaf tissues was not affected by infection while the activity in mature tissue extracts was too low to be detected in the bioassay.

The onset of leaf senescence is usually associated with declines in auxin, gibberellins and cytokinins and an increase in abscisic acid (Beevers, 1968; Addicott, 1968; Addicott and Lyon, 1969). Addicott and Lyon (1969) considered the two major biochemical roles of abscisic acid

to be the inhibition of gibberellin-induced synthesis of hydrolytic enzymes and the promotion of biochemical changes at senescence and abscission. That is, the shift from mature, stable physiology to the degenerate changes associated with shifts in proteins and levels of enzyme activities. Absciscic acid has also been shown to reduce the rate of photosynthesis (Mittelheuser and van Steveninck, 1971) where its greatest effect was shown to be on reducing ribulose 1,5-diphosphate carboxylase activity (Poskuta et al., 1972). The high activity of hydrolase enzymes in light green and dark green island tissues from infected leaves may be an expression of an increased gibberellin to absciscic acid ratio. Gibberellic acid-enhanced synthesis of hydrolytic enzymes has been reported by Chrispeels and Varner (1966b), Ram Chandra and Duynstee (1968) and Jones (1973). Absciscic acid competitively interacts with gibberellic acid to reduce its effective control over hydrolase enzyme synthesis (Chrispeels and Varner, 1966a, 1967; Varner and Johri, 1968; Wright, 1968; Barton et al., 1973; Sequeira, 1973).

Reduced activity of absciscic acid in mature leaves from virus-infected plants would be sufficient to account for delayed biochemical leaf senescence. The effectiveness of reduced absciscic acid activity in infected leaves is further enhanced however, by a higher n-butanol soluble cytokinin activity compared with similarly aged uninfected leaves. It has been well reported that cytokinins delay the onset of senescence (Anderson and Rowen, 1968; Beevers, 1968; Fletcher et al., 1968; Osborne, 1968; Kende, 1971; van Staden, 1973; Richmond and Vonshak, 1974). Although cytokinin action has been reported to reduce hydrolytic enzyme activity (Kende, 1971; Wyen et al., 1972) this action appears to be restricted to specific enzymes (Wyen et al., 1972). The effectiveness of cytokinins in delaying senescence is probably through inhibiting the synthesis of specific catabolic enzymes which normally only appear in over-mature tissues (Abeles et al., 1968; Anderson and Rowan, 1968; Martin and Thimann,

1972). Cytokinins may also act to retard leaf senescence by maintaining the integrity of cell membrane systems. Schaeffer and Sharpe (1971) demonstrated that cytokinins enhanced the synthesis of membrane components as well as preserving methyl groups. Cytokinins were detected in both aqueous and n-butanol extraction fractions of mature tobacco leaves. Bioassay activity of n-butanol soluble cytokinin-like compounds in mature leaf extracts from infected plants, was higher compared with a similar fraction from mature leaves of uninfected plants. Using an identical extraction procedure to the one employed here, van Staden (1973) identified free bases and/or nucleosides in the n-butanol soluble fraction whereas the water soluble fraction contained mostly nucleotide derivatives. Free bases and nucleoside derivatives are most active in promoting cell division and delaying senescence (van Staden, 1973). It was also pointed out that phosphorylation of free bases and nucleosides reduced their effectiveness as control agents. Cytokinins reported here (see Section II) were resolved into two major zones of activity on thin layer chromatography plates, a slow-migrating zone and a fast-migrating zone (R_f 0.6-0.7). Miller (1965) suggested that a slow migrating zone (on TLC plates) with cytokinin activity, was a monophosphate derivative of the faster-migrating zone. However, it cannot be discounted that the slow-migrating zone of activity in water-soluble fractions may simply reflect incomplete hydrolysis by alkaline phosphatase. The slow-migrating zone and fast-migrating zone of cytokinin-like activity for the n-butanol-soluble fraction of mature leaves increased as a result of infection.

In young tobacco tissues, including immature leaves and meristems, all types of cytokinins were higher in activity for plants with well developed symptoms. As previously mentioned, n-butanol-soluble cytokinins are involved in promoting cell division. This would explain why the rate of cell division in the apical meristem was not reduced with virus infection but may be greater as evidenced from the number of leaves formed

following inoculation. Cytokinins have also been implicated as control mechanisms in the regulation of a number of other cell biochemical systems. Cytokinins stimulate chloroplast and photosynthetic activity by regulating chlorophyll synthesis (Fletcher, Teo and Ali, 1973) and specific photosynthetic enzyme activities (Feierabend, 1969, 1970; Kende, 1971; Shindy et al., 1973; De Boer and Feierabend, 1974; Fletcher et al., 1974). High chlorophyll "a" levels in dark green island tissues of infected leaves, high RuDP carboxylase activity in light green island and dark green island leaf tissues and the rapid recovery of chlorophyll "a" synthesis in virus-containing tissues all point to the possible importance of stimulated cytokinin activity in virus-diseased plants. Synthesis of enzymes of the pentose phosphate pathway of carbohydrate metabolism may be regulated by cytokinins (Feierabend, 1969). Cytokinins may also control translocation (Shindy et al., 1973). The increase in activity of enzymes of the pentose phosphate pathway following virus infection, which is reported in this thesis and by others (e.g. Farkas and Solymosy, 1962; Solymosy and Farkas, 1963; Reddy and Stahmann, 1970), may therefore be due to stimulated synthesis of cytokinins.

The potential for products of CO₂ fixation to be translocated from shoots to roots is greatly reduced in tobacco plants with mosaic virus infections. Reduced rates of photosynthesis and the synthesis of viral protein and nucleic acid in cells supporting virus replication results in a high local demand for carbon compounds. Suppressed root growth in virus-infected plants may simply reflect a reduction in the supply of carbohydrates. Roots are generally considered to be the major site for synthesis of cytokinins and as cytokinins enhance photosynthetic rate, translocation and carbohydrate metabolism, stimulated synthesis of cytokinins is possibly a response to carbohydrate starvation.

The activity of an indole acetic acid (IAA)-like compound, in young tobacco tissue extracts, was also greater in virus-infected plants. High

levels of IAA enhance kinetin stimulation of chloroplast enzyme activity (Feierabend, 1970). A kinetin/IAA interaction has also been suggested for the activation of fast-migrating isoenzymes of peroxidase in tobacco callus cultures (Lee, 1972).

In summary, it has been established that tobacco plants infected with a mosaic-inducing strain of tobacco mosaic virus were characterized by reduced size of both shoots and roots. It was confirmed that the leaf mosaic pattern was made up of two distinct tissue types, light green islands of virus-containing cells and dark green islands of virus-free cells. The greatest rate of virus synthesis occurred in those leaf tissues younger than leaf position 3 from the stem apex. Neither reduced cell size nor rate of apical mitotic cell divisions could account for the measured reductions in plant size and it was suggested that reduced plant size was a function of fewer sub-apical mitotic cell divisions in cells supporting virus synthesis. Although plant and leaf size were reduced in virus-infected plants, delayed flowering and a higher rate of leaf formation (apical mitotic cell divisions) establish a potential for more leaves to be produced prior to flower initiation.

Competition between virus synthesis and cellular metabolism was most pronounced in young leaf tissues, where activities of enzymes associated with respiration, photorespiration and chloroplasts together with chlorophyll "a" level were reduced. With aging, virus-infected cells showed biochemical and ultrastructural signs of recovery and delayed senescence. The high demand for carbon for viral protein and nucleic synthesis and the reduced potential for CO_2 fixation by photosynthesis in virus-infected tissues was compensated for, locally, to some extent by reduced cell demand for carbon by photorespiration and "dark" respiration. The high activity of hydrolytic enzymes in virus-infected leaf tissues, indicated the high rate of cellular metabolism of nucleic acids and proteins accompanying virus infection.

Two important features ensure the survival of plants infected with diseases of the mosaic type; the nature of tissue types in diseased leaves and changes in the balance of endogenous growth regulators. The presence of virus-free tissues in diseases of the mosaic type has survival significance in that the high photosynthetic potential of these tissues probably compensates, to some degree, for the loss in photosynthetic potential of tissues supporting virus synthesis. Higher activities of growth regulating hormones such as cytokinins and auxins and reduced activity of the growth retarding hormone, abscisic acid, were generally characteristic of diseased plants. A high cytokinins to abscisic acid ratio in infected tissues would account for an increased rate of apical mitotic cell division, cell metabolic recovery as tissues matured, delayed onset of senescence, stimulated photosynthetic activity and carbohydrate metabolism and preserved cell membrane integrity. Auxin (indole acetic acid-like compound) has been reported to enhance many of the cytokinin effects. A high gibberellic acid to abscisic acid ratio in infected plants would ensure a potential for activity of hydrolytic enzymes, necessary for the maintenance of a high turnover of nucleic acids and proteins in virus-infected tissues.

B I B L I O G R A P H Y

- Abeles, F.B., Holm, R.E. and Gahagan, H.E. 1968. Abscission: induction of degradative enzymes during aging. "Biochemistry and Physiology of Plant Growth Substances." Ed. Wightman, F. and Setterfield, G. Runge Press Ltd., Canada, 1968. p.1515-1523.
- Addicott, F.T. 1968. Environmental factors in the physiology of abscission. *Plant Physiol.*, 43: 1471-1479.
- _____ and Lyon, J.L. 1969. Physiology of abscisic acid and related substances. *Ann. Rev. Plant Physiol.*, 20: 139-164.
- Allison, R.M. 1953. Effect of leaf roll virus infection on the soluble nitrogen composition of potato tubers. *Nature*, 171: 573.
- Alscher, R., Smith, M.A., Petersen, L., Huffaker, R.C. and Criddle, R.S. 1974. *In vitro* synthesis of the large subunit of ribulose diphosphate carboxylase on 70S chloroplast ribosomes. *Pl. Physiol.*, 1974 Annual Supplement, p. 8, No. 37.
- Anderson, J.W. and Rowan, K.S. 1968. The effect of kinetin on senescence in tobacco-leaf tissue after harvest. "Biochemistry and Physiology of Plant Growth Substances." Ed. Wightman, F. and Setterfield, G. Runge Press Ltd., Canada, 1968. p.1437-1446.
- Andreae, W.A. 1952. Effect of scopoletin on indole acetic acid metabolism. *Nature*, 170: 83-84.
- _____ and Thompson, K.L. 1950. Effect of leaf roll virus on the amino acid composition of potato tubers. *Nature*, 166: 72-73.
- Atkinson, P.H. and Matthews, R.E.F. 1970. On the origin of dark green tissue in tobacco leaves infected with TMV. *Virology*, 40(2): 344-356.
- Bailiss, K.W. 1970a. Infections of cucumber cotyledons by cucumber mosaic virus and the participation of chlorophyllase in the development of chlorotic lesions. *Ann. Bot.*, 34(136): 647-655.
- _____. 1970 b. Gibberellins and early disease syndrome of aspermy virus in tomato (*Lycopersicon esculentum* Mill). *Ann. Bot.*, 32: 543-551.
- _____. 1973. The relationship of gibberellin content to cucumber mosaic virus infection of cucumber. *Physiol. Plant Path.*, 4: 73-79 (1974)
- _____ and Hill, T.A. 1971. Biological assays for gibberellins. *Bot. Rev.*, 37: 437-479.
- Baker, J.E., Anderson, J.D. and Worthington, E.K. 1973. Microbodies and catalase of tomato fruit. *Plant Physiol.* 51 (supplement): 18 (article 94) (1973)
- Barton, K.A. Verbeek, R., Ellis R. and Khan, A.A. 1973. Abscisic acid inhibition of gibberellic acid and cyclic 3'5'-adenosine monophosphate induced α -amylase synthesis. *Physiol. Plant.*, 29: 186-189 (1973)

- Basler, E. and Commoner, B. 1956. The effect of tobacco mosaic virus biosynthesis on the nucleic acid content of tobacco leaf. *Virology*, 2: 13-28.
- Bates, D.C. and Chant, S.R. 1969. Alterations in peroxidase activity and peroxidase isozymes in virus-infected plants. *Ann. appl. Biol.* (1970), 65(1): 105-110.
- Baumeister, G. 1951. Wuchs-und Hemmstoffe in der Knolle und im Kraut gesunder und abbaukranker Kartoffel-pflanzen. *Planta*, 38: 638-741.
- Baur, J.S., Halliwell, R.S. and Langston, R. 1967. Effect of TMV on glucose metabolism in *N. tabacum* var. "Samsun", I. Investigations with ¹⁴C-labelled sugars. *Virology*, 32: 406-412.
- Bawden, F.C. 1956. In "Plant viruses and virus diseases". Waltham, Mass., U.S.A. Published by the Chronica Botanica Co.
- _____. 1964. Plant viruses and virus diseases. Ronald Press Co., New York. IV, 361 pp.
- _____ and Pirie, N.W. 1952. Physiology of virus diseases. *Ann. Rev. Plant Physiol.*, 3: 171-188.
- Bayley, J. and Merrett, M.J. 1969. Adenosine triphosphate concentration in relation to respiration and resistance to infection in tissues infected by virus. *New Phytol.* 68: 257-263.
- Beevers, L. 1968. Growth regulator control of senescence in leaf discs of nasturtium (*Tropaeolum majus*). "Biochemistry and Physiology of Plant Growth Substances." Ed. Wightman, F. and Setterfield, G. Runge Press Ltd., Canada, 1968, p.1417-1435.
- Bell, A.A. 1964. Respiratory metabolism of *Phaseolus vulgaris* infected with alfalfa mosaic and southern bean mosaic viruses. *Phytopath.*, 54: 914-922.
- Bennet-Clark, T.A. and Kefford, N.P. 1953. Chromatography of the growth substances in plant extracts. *Nature*, 171: 645-647.
- Bentley, J.A. and Houseley, S. 1954. Bioassay of plant growth hormones. *Physiol. Plant.*, 7: 405-420.
- Berjak, P. and Villiers, T.A. 1972. Aging in plant embryos. V. Lysis of the cytoplasm in non-viable embryos. *The New Phytologist*, 71(6): 1075-1079 (1972).
- Best, R.J. 1936. Studies on a fluorescent substance present in plants. I. Production of the substance as a result of virus infection and some applications of the phenomenon. *Aust. J. exp. Biol. med. Sci.*, 24: 199-213.
- _____. 1937. On the presence of an "oxidase" in the juice expressed from tomato plants infected with the virus of tomato spotted wilt. *Aust. J. exp. Biol. med. Sci.*, 15: 191-199.
- _____. 1944. Studies on a fluorescent substance present in plants. 2. Isolation of the substance in a pure state and its identification as 6-methoxy-7-hydroxy 1:2 benzo-pyrone. *Aust. J. exp. Biol. med. Sci.*, 22: 251-255.

- Bibby, B.T. and Dodge, J.D. 1973. The ultrastructure and cytochemistry of microbodies in dinoflagellates. *Planta (Berl.)*, 112: 7-16 (1973).
- Biddington, N.L. and Thomas, T.H. 1973. A modified Amaranthus Betacyanin bioassay for the rapid determination of cytokinins in plant extracts. *Planta (Berl.)*, 111: 183-186 (1973).
- Boardman, N.K. and Zaitlin, M. 1958a. Association of TMV with plastids. I. Isolation of virus from chloroplast fraction of diseased leaf homogenates. *Virology*, 6: 743-757.
- _____. 1958b. Association of TMV with plastids. II. Biological significance of a virus as isolated from chloroplast fraction. *Virology*, 6: 758-768.
- Bonner, W.D. 1957. Soluble oxidases and their functions. *Ann. Rev. Pl. Physiol.*, 8: 427-452.
- Borges, Maria de L.V. 1953. Respiratory changes in Brassica chinensis L. due to turnip yellow mosaic virus. *Bull. Soc. portug. Sci. nat.*, Ser 2, 4(19), 2, 270-271.
- Boser, H. 1958. Eirflutss pflanzlicher virosen auf stoffweckselfunktionen des wirtes. II. Aktivitäten einiger fermente des glycolysesystems und des cifronensäure cyclus in gesunden and virosen. Kartoffelklättern and knollen. *Phytopath. Z.*, 33: 197-202.
- _____. 1959. Einfluss pflanzlicher virosen auf stoffweckselfunktionen der wirtes. III. P/O Quotienten und einige fermentaktivitäten in knolle, keim und blatt viroser kartoffelpflanzen. *Phytopath. Z.*, 37: 164-169.
- Bozarth, R.F. and Browning, R.E. 1970. Effect of infection with southern bean mosaic virus and the diurnal cycle on the free nucleotide pool of bean leaves. *Phytopath.*, (1970) 60(5):852-855.
- Bozarth, R.F. and Diener, T.O. 1963. Changes in the concentration of free amino acids and amides induced in tobacco plants by potato virus X and potato virus Y. *Virology*, 21: 188-193.
- Budagyan, E.C., Lozhnikova, V.N., Goldin, M.I. and Chailakhyan, M.K. 1964. On the effect of gibberellin-like substances on tobacco mosaic virus. *Review of Applied Mycology*, 43: 377 (No.2052).
- Buell, M.V., Lowry, O.H., Roberts, N.R., Chang, M.W. and Kappahn, J.I. 1958. The quantitative histochemistry of the brain. V. Enzymes of glucose metabolism. *J. Biol. Chem.*, 232:979-993 (1958).
- Burroughs, R., Goss, J.A. and Sill, W.H. 1966. Alterations in respiration of barley plants infected with brome grass mosaic virus. *Virology*, 29: 580-585.
- Butler, R.D. 1967. The fine structure of senescing cotyledons. *J. Exp. Bot.*, 18: 535-543.

- Chalcroft, J.P. and Matthews, R.E.F. 1967. Role of virus strains and leaf ontogeny in the production of mosaic patterns by Turnip Yellow Mosaic Virus. *Virology*, 33: 659-673.
- Chant, S.R. 1967. Respiration rates and peroxidase activity in virus infected *Phaseolus vulgaris*. *Experientia*, 23: 15.
- _____ and Bates, D.C. 1970. The effect of tobacco mosaic virus and potato virus X on peroxidase activity and peroxidase isozymes in *Nicotiana glutinosa*. *Phytochem.*, 9(11): 2323-2326.
- Chen, S., McMahon, D. and Borgorad, L. 1967. Early effects of illumination on the activity of some photosynthetic enzymes. *Plant Physiol.*, 42: 1-5 (1967).
- Chessin, M. 1957. Growth substances and stunting in virus-infected plants. In: Proceedings Third Conference on Potato Virus Diseases. H. Veenman and Zonen, Wageningen. pp.80-84.
- Chrispeels, M.J. and Varner, J.E. 1966a. Inhibition of gibberellic acid induced formation of α -amylase by Abscisin II. *Nature*, 212: 1066-67.
- _____. 1966b. Gibberellic acid-enhanced synthesis and release of α -amylase and ribonuclease by isolated barley aleurone layers. *Pl. Physiol.*, 42: 398-406 (1967).
- _____. 1967. Hormonal control of enzyme synthesis: On the mode of action of gibberellic acid and abscisin in aleurone layers of barley. *Pl. Physiol.*, 42: 1008-1016.
- Commoner, B. and Dietz, P.M. 1952. Changes in non-protein nitrogen metabolism during tobacco mosaic virus metabolism. *J. Gen. Physiol.*, 35: 847-856.
- Commoner, B. and Nehari, V. 1953. The effects of tobacco mosaic virus synthesis on the free amino acid and amide composition of the host. *J. Gen. Physiol.*, 36: 791-805.
- Commoner, B. and Phyllis, M.D. 1952. Changes in non-protein N during TMV biosynthesis. *J. Gen. Physiol.*, 35: 847-856.
- Commoner, B., Scheiber, D.L. and Dietz, P.M. 1953. Relations between tobacco mosaic virus biosynthesis and the nitrogen metabolism of the host. *J. Gen. Physiol.*, 36: 807-830.
- Coombe, B.G., Cohen, D. and Paleg, L.G. 1966a. Barley endosperm bioassay for gibberellins. I. Parameters of the response system. *Plant Physiol.*, 42: 105-112 (1967).
- _____. 1966b. Barley endosperm bioassay for gibberellins. II. Application of the method. *Plant Physiol.*, 42: 113-119 (1967).
- De Boer, J. and Feierabend, J. 1974. Comparison of the effects of cytokinins on enzyme development in different cell compartments of the shoot organs of rye seedlings. *Z. Pflanzenphysiol.*, Bd. 71: 261-270 (1974).

- De Bruyn, J.W., van Keulen, H.A. and Ferguson, J.H.A. 1968. Rapid method for the simultaneous determination of glucose and fructose using anthrone reagent. *J. Sci. Ed. Agric.*, 19: 597-601.
- De Duve, C. and Baudhuin, P. 1966. Peroxisomes (Microbodies and related particles). *Physiol. Revs.*, 46: 323-357.
- De Leo, P. and Sacher, J.A. 1970. Senescence. Association of synthesis of acid phosphatase with banana ripening. *Pl. Physiol.*, 46: 208-211.
- De Zoeten, G.A., Assink, A.M. and van Kammen, A. 1974. Association of cow pea mosaic virus-induced double-stranded RNA with a cytopathological structure in infected cells. *Virology*, 59: 341-355.
- Dézsai, L. and Farkas, G.L. 1964. Effect of kinetin on enzymes of glycolic acid metabolism in cereal leaves. *Acta biol. Acad. Sci. Hung.* (as cited by Solymosy and Farkas 1964 in *Phytopath. Z.*, 51: 153-161).
- Dickson, B.T. 1922. Studies concerning mosaic diseases. Macdonald Col., McGill Univ., Tech. Bull. 2.
- Diener, T.O. 1961. Virus infection and other factors affecting ribonuclease activity of plant leaves. *Virology*, 14: 177-189.
- _____. 1963. Physiology of virus-infected plants. *Ann. Rev. Phytopath.*, 1: 197-218.
- _____ and Dekker, C.A. 1954. Isolation and identification of L-pipecolic acid from western-X diseases peach leaves. *Phytopath.*, 44: 643-645.
- Doke, N. 1971. Effect of tobacco mosaic virus infection on the greening of etiolated tobacco leaves. *Phytopath. Z.*, 73: 359-364 (1972).
- Dunlap, A.A. 1928. Effects of mosaic upon the chlorophyll content of tobacco. *Phytopath.*, 18: 697-700.
- _____. 1931. Carbohydrate variations accompanying the mosaic disease of tobacco. *Am. J. Bot.*, 18: 328-336.
- Elbertzhagen, H. 1958. Ein Beitrag zum Stickstoff-und Phosphatstoffwechsel mosaikviruskranker Tabakpflanzen. *Phytopath. Z.*, 34: 66-82.
- Elmer, O.H. 1925. Transmissibility and pathological effects of the mosaic disease. *Iowa Agr. Expt. Sta. Res. Bull.* 82.
- Engelbrecht, A.H.P. and Esau, K. 1963. Occurrence of inclusions of beet yellows viruses in chloroplasts. *Virology*, 21: 43-47.
- Engelbrecht, A.H.P. and Weier, T.E. 1963. As cited by Matsui and Yamaguchi, 1966.
- Esanu, V. and Dumitrescu, M. 1971. A comparative study of isoperoxidases of Tobacco as influenced by TMV-infection and genetic constitution. *Acta Phytopathologica*, 6(1-4): 31-35 (1973).

- Esau, K. 1967. Anatomy of plant virus infections. *Ann. Rev. Phytopath.*, 5: 45-76.
- _____ and Cronshaw, J. 1967a. Relation of tobacco mosaic virus to the host cells. *J. Cell Biol.*, 33: 665-678.
- _____. 1967b. Tubular components in cells of healthy and tobacco mosaic virus-infected *Nicotiana*. *Virology*, 33: 26-35.
- Esau, K. and Gill, R.H. 1969. Tobacco mosaic virus in dividing mesophyll cells of *Nicotiana*. *Virology*, 38: 464-472.
- Faed, E.M. and Matthews, R.E.F. 1972. Leaf ontogeny and virus replication in *Brassica pekinensis* infected with turnip yellow mosaic virus. *Virology*, 48: 546-554.
- Farkas, G.L. and Solymosy, F. 1962. Activation of hydrogen and electron transport systems in a virus-infected local-lesion host. *Biochem. Jour.*, 84: 113 p.
- Farkas, G.L. and Stahmann, M.A. 1966. On the nature of changes in peroxidase isoenzymes in bean leaves infected by southern bean mosaic virus. *Phytopath.*, 56: 667-677.
- Feierabend, J. 1969. Der Einfluß von Cytokinen auf die Bildung von Photosyntheseenzymen in Roggenkeimlingen (Influence of cytokinins on the formation of photosynthetic enzymes in rye seedlings). *Planta*, 84: 11.
- _____. 1970. Characterization of cytokinin action on enzyme formation during the development of the photosynthetic apparatus in rye seedlings. "Enzymes of the reductive and oxidative pentose phosphate cycles." *Planta*, 94: 1.
- _____ and Beevers, H. 1971. Developmental studies on microbodies in wheat leaves. I. Conditions influencing enzyme development. *Pl. Physiol.*, 49: 28-32 (1972).
- Figier, J. 1968. Localisation infrastructurale de la phosphomonoesterase acide dans la stipule de *Vicia faba* L. au niveau du nectaire. *Planta (Berl.)*, 83: 60-79.
- Fletcher, R.A., Harvey, B.M.R. and Lu, B.C. 1974. Benzyladenine accelerates chloroplast differentiation and stimulates photosynthetic enzyme activity in cucumber cotyledons. *Pl. Physiol. Ann. Suppl.* 1974. p.71 No.402.
- Fletcher, R.A., Quick, W.A. and Phillips, D.R. 1968. Effect of kinetin on senescence and tobacco mosaic virus infection in leaves of *Nicotiana glutinosa*. "Biochemistry and Physiology of Plant Growth Substances." Ed. by Wightman, F. and Setterfield G. Runge Press Ltd., Canada, 1968. p.1447-1455.
- Fletcher, R.A., Teo, C. and Ali, A. 1973. Stimulation of chlorophyll synthesis in cucumber cotyledons by benzyladenine. *Can. J. Bot.*, 51: 937-939 (1973).
- Ford, R.E. and Tu, J.C. 1968. Relationship between free amino acids and symptom expression in corn infected with maize dwarf mosaic virus or sugar cane mosaic virus. *Phytopath. (abstr.)*, 58(8): 1050.

- Fraser, R.S.S. 1971. Effects of two strains of tobacco mosaic virus on growth and RNA content of tobacco leaves. *Virology*, 47: 261-269 (1972).
- Frederick, S.E. and Newcomb, E.H. 1969. Cytochemical localization of catalase in leaf microbodies (Peroxisomes). *J. Cell. Biol.*, 43: 343-353.
- Fritig, B. and Hirth, L. 1971. Biosynthesis of phenylpropanoids and coumarins in TMV-infected tobacco leaves and tobacco tissue cultures. *Acta Phytopathologica*, Vol.6(1-4): 21-29 (1971).
- Fujisawa and Matsui. 1965. As cited by Matsui and Yamaguchi, 1966.
- Gáborjánvi, R., Balázs, E. and Király, Z. 1971. Ethylene production, tissue senescence and local virus infections. *Acta Phytopathologica*, 6(1-4): 51-55.
- Gerola, F.M., Cristofori, F. and Dassu, G. 1960a. Ricerche sulle infra-structure delle cellule de mesofillo fogliare di piante sane e virosate di tabacco (*Nicotiana tabacum*). A: Piante sane. *Carylogia*, 13: 352-366.
- _____. 1960b. Ricerche sulle infra-structure delle cellule de mesofillo fogliare di piante sane e virosate di tabacco (*Nicotiana tabacum*). B: Piante virosate. *Carylogia*, 13: 367-378.
- Gerola, F.M. and Dassu, G. 1960. Structural changes in tobacco chloroplasts during whitening induced by starvation and recovery. *Carylogia*, 13: 398-410.
- Goeffeau, A. and Bové, J.M. 1965. Virus infection and photosynthesis. I. Increased photophosphorylation by chloroplasts from Chinese cabbage infected with turnip yellow mosaic virus. *Virology*, 27: 243-252.
- Goldin, M.I. and Fedotina, V.L. 1962. Proc. 5th Conf. Czechoslovak Plant Virologists, Prague, 1962. Czechoslovak Acad. Sci.
- Goldstein, B. 1924. Cytological study of living cells of Tobacco plants affected with mosaic disease. *Bull. Torrey Bot. Club*, 51: 261-274.
- _____. 1926. A cytological study of the leaves and growing points of healthy and mosaic diseased Tobacco plants. *Bull. Torrey Bot. Club*, 53: 499-599.
- _____. 1927. The X-bodies in the cells of Dahlia plants affected with mosaic disease and dwarf. *Bull. Torrey Bot. Club*, 54: 285-293.
- Goodman, R.N., Kiraly, Z. and Zaitlin, M. 1967. The Biochemistry and Physiology of Infectious Plant Diseases. Van Nostrand, Princeton, New Jersey.
- Goodman, R.N. and Plurad, S.B. 1971. Ultrastructural changes in tobacco undergoing the hypersensitive reaction caused by plant pathogenic bacteria. *Physiol. Pl. Path.*, 1: 11-15.

- Goodwin, R.H. and Taves, C. 1950. The effect of coumarin derivatives on the growth of *Avena* roots. *Am. J. Bot.*, 37: 224-231.
- Gove, J.P. and Hoyle, M.C. 1974. Peroxidase isoenzymes of horseradish and yellow birch. *Pl. Physiol. Ann. Suppl.* 1974. p.41 No.230.
- Grieve, B.J. 1943. Studies on the physiology of host-parasite relations. 4. Some effects of tomato spotted wilt on growth. *Aust. J. Exp. Biol. med. Sci.*, 21: 89-101.
- Gabanski, M. and Kurstak, R. 1960. Glutamic-acid-alanine transaminase in tobacco leaves infected with TMV. *Experientia, Basel*, 16: 407-408.
- Hall, J.L. and Davie, C.A.M. 1971. Localization of acid hydrolase activity in *Zea mays* L. root tips. *Ann. Bot.*, 35: 849-55.
- Hancock, C.R., Barlow, H.W.B. and Lacey, H.J. 1964. The East Malling coleoptile straight growth test method. *J. Exp. Bot.*, 15: 166-176.
- Harpaz, I. and Applebaum, S.W. 1961. Accumulation of asparagine in maize plants infected with maize rough dwarf virus and its significance in plant virology. *Nature*, 192: 780-781.
- Hatta, T., Nakamoto, T., Takagi, Y. and Ushiyama, R. 1971. Cytological abnormalities of mitochondria induced by infection with cucumber green mottle mosaic virus. *Virology*, 45: 292-297. (1971).
- Hemberg, T. and Larsson, I. 1961. The inhibitor- β complex from resting potato tubers as an inhibitor of α -amylase. *Physiol. Plant.*, 14: 861-867.
- Herold, F., Bergold, G.H. and Weibel, J. 1960. Isolation and E.M. demonstration of virus infecting corn (*Zea mays* L.). *Virology*, 12: 335-347.
- Hibino, H. and Matsui, C. 1965. *Ann. Phytopathol. Soc. Japan* (Abstr.), 30: 93. As cited by Matsui and Yamaguchi, 1966.
- Hirai, A. and Wildman, S.G. 1967. Similarity in symptoms produced in tobacco plants by actinomycin D and TMV. *Virology*, 31: 721-722 (1967).
- _____. 1969. Effect of TMV multiplication on RNA and protein synthesis in tobacco chloroplasts. *Virology*, 38: 73-82.
- Hirata, S. 1954. Studies on the phytohormone in the malformed portion of the diseased plants. I. The relation between the growth rate and the amount of free auxin in the fungus galls and virus-infected plants. *Ann. Phytopathol. Soc. Japan*, 19: 33-38.
- Holden, M. 1973. Chloroplast pigments in plants with the C₄-dicarboxylic acid pathway of photosynthesis. *Photosynthetica* 7(1): 41-49 (1973).

- Holden, M. and Tracey, M.V. 1948. The effect of infection with tobacco mosaic virus on the levels of nitrogen, phosphorus, protease and pectase in tobacco leaves and on their response to fertilizers. *Biochem. J.*, 43: 151-156.
- Horie, S. and Morrison, M. 1963. Cytochrome C oxidase components. *J. Biol. Chem.*, 238: 1855-1860.
- Hršel, I. 1962. The electron-microscope investigation of changes in cytoplasmic structures in leaves of *Cucumis sativa* L. infected with Cucumber virus 4. *Biol. Plant. Acad. Sci. bohemosl.*, 4: 232-238.
- Hull, J. and Koss, E.J. 1958. Responses of healthy, ringspot and yellows infected Montmorency cherry trees to gibberellic acid. *Quart. Bull. Mich. Agr. Exp. Sta.*, 41: 19-23.
- Israel, H.W. and Ross, A.F. 1967. The fine structure of local lesions induced by tobacco mosaic virus in tobacco. *Virology*, 33: 272-286.
- Jensen, S.G. 1968. Factors affecting respiration in barley yellow dwarf virus infected barley. *Phytopath.*, 58: 438-443.
- Johnson, M.S. and Young, R.J. 1969. Fractionation on benzoylated DEAE-cellulose of tRNA from tobacco mosaic virus-infected tobacco leaves. *Virology*, 38: 607-613 (1969).
- Jones, J.P. 1956. Ph.D. Thesis. University of Nebraska, Lincoln, Nebraska.
- Jones, R.L. 1973. Gibberellins: their physiological role. *Ann. Rev. Plant Physiol.*, 24: 571-98 (1973).
- Karasek, S.G. 1963. Changes in free and acetylated amino acids during tobacco mosaic virus multiplication. *Biochim. Biophys. Acta*, 78: 644-648.
- Kassanis, B. and Turner, R.H. 1972. Virus inclusions formed by the PM₂ mutant of TMV. *J. gen. Virol.*, 14(1): 119-122.
- Kato, S. and Misawa, T. 1971. Studies on the infection and the multiplication of plant viruses. IV. Suppression of cellular RNA synthesis by the cucumber mosaic virus-infection. *Ann. Phytopath. Soc. Japan*, 37: 272-282.
- _____. 1974. Studies on the infection and multiplication of plant viruses. VII. The breakdown of chlorophyll in tobacco leaves systemically infected with cucumber mosaic virus. *Ann. Phytopath. Soc. Japan*, 40: 14-21.
- Kawashima, N. and Wildman, S.G. 1971. Studies on fraction 1 protein. IV. Mode of inheritance of primary structure in relation to whether chloroplast or nuclear DNA contains the code for a chloroplast protein. *Biochim. Biophys. Acta*, 262: 42-49 (1972).
- Kefford, N.P. 1959. Some growth regulators of tobacco in relation to the symptoms of the physiological disease "frenching". *J. Exp. Bot.*, 10: 462-467.

- Kende, H. 1971. The Cytokinins. *Int. Rev. Cytology*, 31: 301-338.
- Kennedy, R.A. and Laetsch, W.M. 1973. Relationship between leaf development and primary photosynthetic products in the C₄ plant Portulaca oleracea L. *Planta*, 115(2): 113-124 (1973).
- Kiraly, Z., Hammady, M.E.L. and Pozsar, B.I. 1966. Susceptibility to Tobacco Mosaic Virus in relation to RNA and protein synthesis in tobacco and bean plants. *Phytopath. Z.*, 63(1): 47-63.
- Kiruchi, M. and Yamaguchi, A. 1960. Polyphenol oxidase activity of Nicotiana glutinosa leaves infected with tobacco mosaic virus. *Nature*, 187: 1048-1049.
- Kisaki, T. and Tolbert, N.E. 1968. Glycolate and glyoxylate metabolism by isolated peroxisomes or chloroplasts. *Plant Physiol.*, 44: 242-250 (1969).
- Kitajima, E.W. and Costa, A.S. 1974. Fine structure of leaf tissues of some solanaceous plants infected with Brazilian Eggplant mosaic virus. *Phytopath. Z.*, 79: 289-300 (1974).
- Kloppstech, K. and Schweiger, H.G. 1974. The site of synthesis of chloroplast ribosomal proteins. *Plant Science Letters*, 2: 101-105 (1974).
- Knypl, J.S. 1973. Induction of nitrate reductase by chloramphenicol in detached cucumber cotyledons. *Planta (Berl.)*, 114: 311-321 (1973).
- Kolehmainen, L., Zech, H. and von Wettstein, D. 1965. The structure of cells during tobacco mosaic virus production. Mesophyll cells containing virus crystals. *J. Cell Biol.*, 25: 77-97.
- Kordova, N. Poffenroth, L. and Wilt, J.C. 1972. Lysosomes and the toxicity of Rickettsiales. II. Non-cytocidal interactions of egg-grown C. psittaci 6BC and in vitro macrophages. *Can. J. Microbiol.*, 18(6): 869-873 (1972).
- Krupa, L.R. 1959. Metabolism of oats susceptible to Helminthosporium victoriae and victorin. *Phytopath.*, 49: 587-594.
- Kuczmak, M. and Tolbert, N.E. 1962. Glycolic acid oxidase formation in greening leaves. *Plant Physiol.*, 37: 729-734 (1962).
- Leduc, E.H. and Bernhard, W. 1967. Recent modifications of the glycol methacrylate embedding procedure. *J. Ultrastruct. Res.*, 19: 196-199.
- Lee, P.E. 1964. Electron microscopy of inclusions in plants infected by wheat striate mosaic virus. *Virology*, 23: 145-151.
- Lee, T.T. 1972. Interaction of cytokinin, auxin and Gibberellin on peroxidase isoenzymes in tobacco tissues cultured in vitro. *Can. J. Bot.*, 50(12): 2471-2478.
- Leopold, A.C. and Guernsey, F.S. 1953. Auxin polarity in the *Coleus* plant. *Bot. Gaz.*, 115: 147-154.

- Letham, D.S. 1967. A new cytokinin bioassay and the naturally occurring cytokinin complex. In "Biochemistry of physiology of plant growth substances". Edited by Wightman F. and Setterfield, G. Runge Press Ltd., Ottawa, Canada, p.19-31.
- Magalhães, A.C., Neyra, C.A. and Hageman, R.H. 1973. Nitrite assimilation and amino nitrogen synthesis in isolated spinach chloroplasts. *Plant Physiol.*, 53: 411-415 (1974).
- Magyarosy, A.C., Buchanan, B.B. and Schürmann, P. 1973. Effect of a systemic virus infection on chloroplast function and structure. *Virology*, 55: 426-438 (1973).
- Mangat, B.S., Levin, W.B. and Bidwell, R.G.S. 1973. The extent of dark respiration in illuminated leaves and its control by ATP levels. *Can. J. Bot.*, 52(4): 673-681 (1974).
- Maramorosch, K. 1957. Reversal of virus-caused stunting in plants by gibberellic acid. *Science*, 126: 651-652.
- Martin, C. 1958. Étude comparée de l'activité de la polyphénoloxylase chez le tabac sain et inoculé par une maladie à virus. *Compt. rend. Acad. Sci.*, 246: 2026-2029.
- _____ and Thimann, K.V. 1972. The role of protein synthesis in the senescence of leaves. 1. The formation of protease. *Plant Physiol.*, 49: 64-71 (1972).
- Matile, P.H., Balz, J.P., Semadeni, E.G. and Jost, M. 1965. Isolation of spherosomes with lysosome characteristics from seedlings. *Z. Naturforsch.*, 206: 693-698.
- Matile, P. and Winklenbach, F. 1971. Function of lysosomes and lysosomal enzymes in the senescing corolla of the morning glory (*Ipomoea purpurea*). *J. Exp. Bot.*, 23: 759-771.
- Matsui, C. 1958. Pathological cytology of tobacco leaf infected with tobacco mosaic virus III. *J. Biophysic. Biochem. Cytol.*, 4: 831-832.
- _____. 1959. Fine structures of X-body. *Virology*, 2: 306-313.
- _____ and Yamaguchi, A. 1964a. Electron microscopy of host cells infected with tobacco etch virus. I. Fine structure of leaf cells at later stages of infection. *Virology*, 22: 40-47.
- _____. 1964b. Electron microscopy of host cells infected with tobacco etch virus. II. Fine structure of leaf cells before and after the appearance of external symptoms. *Virology*, 23: 346-353.
- _____. 1966. Some aspects of plant viruses *in situ*. *Adv. Virus Res.*, 12: 127-174.
- Matsumoto, H., Wakiuchi, N. and Takahashi, E. 1971. Changes of some mitochondrial enzyme activities of cucumber leaves during ammonium toxicity. *Physiol. Plant*, 25: 353-357.

- Matthews, R.E.F. 1970. Plant Virology. Academic Press, New York.
- _____. 1973. Induction of diseases by viruses, with special reference to turnip yellow mosaic virus. *Ann. Rev. Phytopath.*, 11: 147-170.
- Merrett, M.J. 1960. The respiration rate of tomato stem tissue infected with tomato aucuba mosaic virus. *Ann. Bot.*, 24: 223-231.
- _____. 1962. Oxidase activity of tissues systemically infected by tobacco mosaic virus. *Physiologia Pl.*, 15: 465-472.
- _____ and Bayley, J. 1969. The respiration of tissues infected by virus. *The Bot. Rev.*, 35(4): 372-392.
- _____ and Sunderland, D.W. 1967. The metabolism of ^{14}C -specifically labelled glucose in leaves showing TMV-induced local necrotic lesions. *Physiologia Pl.*, 20: 593-599.
- Miczynski, K.A. 1961. Studies on the free amino acid composition of tobacco plants infected with potato virus X. *Rev. Appl. Mycol.*, 40: 127.
- Milborrow, B.V. 1967. The identification of (+)-abscisin II ((+)-dormin) in plants and measurements of its concentrations. *Planta*, 76: 93-113.
- Miller, C.O. 1965. Evidence for the natural occurrence of zeatin and derivatives: compounds from maize which promote cell division. *Proc. Natl. Acad. Sci. U.S.*, 54: 1052-1058.
- Milo, Jr, G.E. and Sahai Srivastava, B.I. 1969. Effect of cytokinins on tobacco mosaic virus production in local-lesion and systemic hosts. *Virology*, 38: 26-31 (1969).
- Mittelheuser, C.J. and van Steveninck, R.F.M. 1971. Rapid action of abscisic acid on photosynthesis and stomatal resistance. *Planta*, 97: 83-86 (1971).
- Mlodzianowski, F. 1972. The occurrence of acid phosphatase in the thylakoids of developing plastids in lupin cotyledons. *Z. Pflanzenphysiol.*, 66: 362-365.
- Mohamed, N. and Randles, J.W. 1971. Effects of infection by tomato spotted wilt virus on the chloroplast ribosomal ribonucleic acids of tobacco leaves. *Aust. Pl. Path. Conf.* (1971): 9-5.
- Moss, D.N. 1967. High activity of the glycolic acid oxidase system in tobacco leaves. *Plant Physiol.*, 42(Pt.2): 1463-1464.
- Murray, D.R., Wara-Aswapati, O., Ireland, H.M.M. and Bradbeer, J.W. 1972. The development of activities of some enzymes concerned with glycolate metabolism in greening bean leaves. *J. Exp. Bot.*, 24(78): 175-184 (1973).
- Nagata, T. and Takebe, I. 1971. Plating of isolated tobacco mesophyll protoplasts on agar medium. *Planta (Berl.)*, 99: 12-20.

- Nakagaki, Y. 1971. Effect of kinetin on local lesion formation on detached bean leaves inoculated with tobacco mosaic virus or its nucleic acid. *Ann. Phytopath. Soc. Japan*, 37(4): 307-309.
- Nakata, K. and Hidaka, Z. 1960. *J. Electronmicroscopy (Tokyo)*, 8: 65.
As cited by Matsui and Yamaguchi, 1966.
- _____. 1961. *Ann. Phytopath. Soc. Japan*, 26: 236
(Abstr.). As cited by Matsui and Yamaguchi, 1966.
- Nambiar, K.K.N. and Ramakrishnan, K. 1970. Mitochondrial activity in virus-infected plants. *Sci. Cult.*, 36(8): 466-467.
- Nariani, T.K. 1963. Effects of gibberellic acid on tobacco leaf-curl affected plants. *Indian Phytopathol.*, 16: 101-102.
- Nelson, J.S. and Lynn Wakefield, P. 1972. The quantitative histochemistry of the sympathoadrenal system. I. Enzymes of glycolysis. *J. Histochem. Cytochem.*, 21(2): 184-188 (1973).
- Nour-Eldin, F. 1955. The effect of organic acids on tobacco mosaic virus multiplication. *Phytopath.*, 45: 291.
- Novacky, A. and Hampton, R.E. 1968. Peroxidase isozymes in virus-infected plants. *Phytopath.*, 58: 301-305.
- Nye, T.G. and Hampton, R.E. 1966. Biochemical effects of tobacco etch infection on tobacco leaf tissue. II. Polyphenol oxidase activity in subcellular fractions. *Phytochem.*, 5: 1187-1189.
- Orlob, G.B. and Arny, D.C. 1961. Some metabolic changes accompanying infection by barley yellow dwarf virus. *Phytopath.*, 51: 768-775.
- Ornstein, L. 1964. Disc electrophoresis. I. Background and Theory. *Ann. N.Y. Acad. Sci.*, 121: 321-349.
- Osborne, D.J. 1968. Hormonal mechanisms regulating senescence and abscission. "Biochemistry and Physiology of plant Growth Substances." Ed. Wightman, F. and Setterfield, G. Runge Press, Canada, 1968, p.815-840.
- Owen, P.C. 1955. The respiration of tobacco leaves after systemic infection with tobacco mosaic virus. *Ann. appl. Biol.*, 43: 265-272.
- _____. 1956. The effect of infection with tobacco mosaic virus on the respiration of tobacco leaves of varying ages in the period between inoculation and systemic infection. *Ann. appl. Biol.*, 44: 227-232.
- _____. 1957. The effect of infection with tobacco etch virus on the rates of respiration and photosynthesis of tobacco leaves. *Ann. appl. Biol.*, 45: 327-331.
- _____. 1958. Photosynthesis and respiration rates of leaves of *Nicotiana glutinosa* infected with tobacco mosaic virus and of *N. tabacum* infected with potato virus X. *Ann. appl. Biol.*, 46: 198-204.

- Oxefelt, P. 1971. Development of systemic tobacco mosaic virus infection. II. RNA metabolism in systemically infected leaves. *Phytopath. Z.*, 71: 247-256 (1971).
- Parish, C.L., Zaitlin, M. and Siegel, A. 1965. A study of necrotic lesion formation by tobacco mosaic virus. *Virology*, 26: 413-418.
- Pavillard, J. 1952. Recherches sur la croissance des plantes virosées: Virus et auxines. *Compt. Rend. Acad. Sci.*, 235: 87-88.
- _____. 1954. Proceedings of the second conference on Potato virus diseases, Lisse-Wageningen, 25-29 June, pp.178-183.
- _____ and Beauchamp, C. 1957. La constitution auxinique de tabacs sains ou atteints de maladies à virus: Présence et rôle de la scopolétine. *Compt. Rend. Acad. Sci.*, 244: 1240-1243.
- Peterson, P.D. and McKinney, H.M. 1938. The influence of four mosaic diseases on the plastid pigments and chlorophyllase in tobacco leaves. *Phytopath.*, 28: 329-342.
- Pierpont, W.S. 1968. Cytochrome oxidase and mitochondrial protein in extracts of leaves of *Nicotiana glutinosa* L. infected with tobacco mosaic virus. *J. Exp. Bot.*, 19: 264-275.
- Porter, C.A. 1959. Biochemistry of plant virus infection. *Adv. Virus Res.*, VI: 75-91.
- _____ and Weinstein, L.H. 1957. Biochemical changes induced by thiouracil in cucumber mosaic virus infected and non-infected tobacco plants. *Contr. Boyce Thompson Inst.*, 19: 87-106.
- Poskuta, J., Antoszewski, R. and Faltynowicz, M. 1972. Photosynthesis, photorespiration and respiration of strawberry and maize leaves as influenced by abscisic acid. *Photosynthetica*, 6: 370-374 (1972).
- Pratt, M.J. 1967. Chlorophyll and 18S protein concentrations in the leaves of healthy and virus-infected plants. *Proc. Canadian Path. Soc.*, (31st session) May 31 - June 2, 1967 : 24.
- Raa, J. 1970. Degradation of indol-3yl-acetic acid in homogenates and segments of cabbage roots. *Physiol. Plant.*, 24: 498-505 (1971).
- Ram Chandra, G. and Duynstee, E.E. 1968. Hormonal regulation of nucleic acid metabolism in aleurone cells. "Biochemistry and Physiol Physiology of Plant Growth Substances." Ed. Wightman, F. and Setterfield, G. Runge Press Ltd. Canada, 1968, p.723-746.
- Randall, P.J. 1969. Changes in nitrate and nitrate reductase levels on restoration of molybdenum to molybdenum-deficient plants. *Aust. J. Agr. Res.* 20(4): 635-642 (1969).
- Randles, J.W. 1968. Ribonuclease isozymes in chinese cabbage systemically infected with turnip yellow mosaic virus. *Virology*, 36: 556-563.

- Randles, J.W. 1971. Changes associated with pathogenesis in Nicotiana glutinosa systemically infected with lettuce necrotic yellows virus. Aust. Plant Path. Conf., (1971): 9-1.
- Raymond, S. and Weintraub, L. 1959. Acrylamide gel as a supporting medium for zone electrophoresis. Science, 130: 711.
- Reddi, K.K. 1959. Studies on tobacco leaf ribonuclease. III. Its role in the synthesis of tobacco mosaic virus nucleic acid. Biochim. et Biophys. Acta, 33: 164-169.
- _____. 1964. Studies on the formation of tobacco mosaic virus ribonucleic acid. V. Presence of tobacco mosaic virus in the nucleus of the host cell. Proc. Natl. Acad. Sci. U.S., 52: 397-401.
- Reddy, M.N. and Stahmann, M.A. 1970. Isozyme changes in pea wilt. Phytopath., (Abstr.), 60(9): 1309.
- Reid, M.S. and Matthews, R.E.F. 1966. On the origin of the Mosaic induced by turnip yellow mosaic virus. Virology, 28: 563-570.
- Richmond, A.E. and Vonshak, A. 1974. Effects of light and of kinetin on protein synthesis of isolated chloroplasts from senescing leaves. Pl. Physiol. Ann. Suppl. 1974, p.69, No.392.
- Roberts, D.A., Blodgett, F.M. and Wilkinson, R.E. 1952. Potato virus X: Inoculation of potato varieties tolerant to virus Y. Am. Potato J., 29: 212-220.
- _____, Christie, R.G. and Archer, Jr., M.C. 1970. Infection of apical initials of tobacco shoot meristems by tobacco ring-spot virus. Virology, 42(1): 217-220.
- Ross, A.F. and Williamson, C.E. 1951. Physiologically active emanations from virus-infected plants. Phytopath., 41: 431-438.
- Roy, H. and Jagendorf, A.T. 1974. In vitro synthesis of polypeptides related to the small subunit of ribulose 1,5-diphosphate carboxylase (RuDPase). Pl. Physiol. Ann. Suppl. 1974, p.8 No.38.
- Rubin, B.A. and Ladygina, M.E. 1972. Energy conversion and electron transport in green plants in the course of virus pathogenesis. Acta Phytopathologica, 7(4): 383-393 (1972).
- Rubin, B.A. and Zeleneva, I.V. 1964. On the action of some inhibitors on the respiration of cucumber plants infected with cucumber mosaic virus. Fiziol. Rast., 11: 769-773.
- Rubio, M. 1956. Origin and composition of cell inclusions associated with certain tobacco and crucifer viruses. Phytopath., 46: 553-556.
- _____, and van Slogteren, D.H.M. 1956. Light and electron microscopy of X-bodies associated with broad bean mottle virus and Phaseolus virus 2. Phytopath., 46: 401-402.
- Rubio-Huertos, M. 1962. Light and electron microscopy of inclusion bodies associated with Petunia ringspot virus. Virology, 18: 337-342.

- Rubio-Huertos, M. 1964. Estudio al microscopio óptico y electrónico de un virus aislado de Pisum sativum. Microbiologia esp., 17: 1-13.
- _____ and Hidalgo, F.G. 1964. Ultrathin sections of intranuclear and intracytoplasmic inclusions induced by severe etch virus. Virology, 24: 84-90.
- Russell, S.L. and Kimmins, W.C. 1971. Growth regulators and the effect of barley yellow dwarf virus on barley (Hordeum vulgare L.). Ann. Bot., 35: 1037-1043.
- Ryzhkov, V.L. 1957. Behaviour of metabolites and antimetabolites in a study of propagation of tobacco mosaic virus. Izv. Akad. Nauk. SSSR, ser. Biol., 22: 41-54.
- Sakano, K. and Wildman, S.G. 1973. Lack of direct effect of light on synthesis or specific enzymatic activity of fraction I protein of tobacco leaves. Plant Sci. Letters, 2 (1974): 273-276.
- Sauter, J.J. 1972. Respiratory and phosphatase activity in contact cells of wood rays and their possible role in sugar secretion. Z. Pflanzenphysiol. Bd.67(2): 135-145 (1972).
- Schaeffer, G.W. and Sharpe, Jr., F.T. 1971. Cytokinin function: Increase in Methyl-¹⁴C Metabolism to phosphatidyl choline and a decrease in oxidation to Carbon Dioxide-¹⁴C. Physiol. Plant., 25: 456-460 (1971).
- Schlegel, D.E. 1957. The stimulatory effect of organic acids on Tobacco mosaic virus multiplication. Virology, 4: 135-140.
- Schnarrenberger, C., Oeser, A. and Tolbert, N.E. 1972. "Two isozymes each of glucose-6-phosphate dehydrogenase and 6-phosphogluconate dehydrogenase in Spinach leaves." Archives Biochem. Biophys., 154: 438-448 (1973).
- Schuster, G. 1964. The influence of virus infection and daylength on the concentration of acids of the citric acid cycle in leaves of members of the Solanaceae with different photoperiod sensitivity. Flora Allg. Bot. Zeitung (Jena), 154: 490-506.
- Scotland, C.B., Hagedorn, D.J. and Stahmann, M.A. 1955. Electron microscopy of tobacco mosaic virus in situ. Phytopath., 45: 603-607.
- Selman, I.W., Brierly, M.R., Pegg, G.F. and Hill, T.A. 1961. Changes in the free amino acids and amides in tomato plants inoculated with tomato spotted wilt virus. Ann. appl. Biol., 49: 601-615.
- Semadeni, E.G. 1967. Enzymatische charakterisierung der Lysesomena 0 vivalente (Spharosomen) von Maiskeimlingen. Planta, 72: 91-118 (1967).
- Sembdner, G. and Schreiber, K. 1964. Gibberelline-IV. Über die Gibberelline von Nicotiana tabacum L. Phytochem., 4: 49-56 (1965).

- Sequeira, L. 1973. Hormone metabolism in diseased plants. *Ann. Rev. Plant Physiol.*, 24: 353-380.
- Shalla, T.A. 1959. Relations of tobacco mosaic virus and barley stripe mosaic virus to their host cells as revealed by ultrathin tissue-sectioning for the electron microscope. *Virology*, 7: 193-219.
- _____. 1964. Assembly and aggregation of tobacco mosaic virus in tomato leaflets. *J. Cell Biol.*, 21: 253-264.
- _____ and Shepard, J.F. 1972. The structure and antigenic analysis of amorphous inclusion bodies induced by Potato Virus X. *Virology*, 49: 654-667 (1972).
- Sheffield, F.M.L. 1931. The formation of intracellular inclusions in Solanaceous hosts infected with aucuba mosaic of tomato. *Ann. appl. Biol.*, 18: 471-493.
- _____. 1934. Experiments bearing on the nature of intracellular inclusions in plant virus diseases. *Ann. appl. Biol.*, 21: 430-453.
- Shindy, W.W., Kliwer, W.M. and Weaver, R.J. 1973. Benzyladenine-induced movement of ^{14}C -labelled photosynthate into roots of *Vitis vinifera*. *Plant Physiol.*, 51(2): 345-349 (1973).
- Simons, T.J. and Ross, F. 1971. Metabolic changes associated with systemic induced resistance to tobacco mosaic virus in Samsun NN tobacco. *Phytopath.*, 61(3): 293-300.
- Singh, S. and Wildman, S.G. 1973. Chloroplast DNA codes for the ribulose diphosphate carboxylase catalytic site of Fraction 1 proteins of Nicotiana species. *Mol. Gen. Genetics*, 124(3): 187-196.
- Söding, H. and Funke, H. 1941. Über den Wuchsstoffhaushalt abbaukranker Kartoffeln. *Phytopath. Z.*, 13: 351-368.
- Söding, H., Köhler, E. and Funke, H. 1943. Über den Wuchsstoffgehalt abbaukranker Kartoffelknollen. *Phytopath. Z.*, 14: 427-441.
- Solymosy, F. and Farkas, G.L. 1963. Metabolic characteristics at the enzymatic level of tobacco tissues exhibiting localized acquired resistance to viral infections. *Virology*, 21: 210-221.
- _____. 1964. Effect of virus infection on glycolic acid oxidase in tobacco. *Phytopath. Z.*, 51: 153-161.
- _____ and Kiraly, Z. 1959. Biochemical mechanism of lesion formation in plants. *Nature*, 184: 706.
- Solymosy, F., Szirmai, J., Beczner, L. and Farkas, G.L. 1967. Changes in peroxidase isozyme patterns induced by virus infection. *Virology*, 32: 117-121.
- Sommer, E. 1957. Untersuchungen des Stoffwechsels vergilbungskranker Rüben untermitteldeutschen Verhältnissen. *Z. Zuckerind.*, 7: 387-393.

- Spencer, D., Whitfield, P.R., Bottomley, W. and Wheeler, A.M. 1971. Proteins and nucleic acids synthesized by isolated chloroplasts. In "Autonomy and biogenesis of mitochondria and chloroplasts". North Holland Publishing Co. - Amsterdam - Lond. Ed. by Boardman, Linnane and Smillie.
- Spikes, J.D. and Stout, M. 1955. Photochemical activity of chloroplasts isolated from sugar beet infected with virus yellows. *Science*, 122: 375-376.
- Steadman, J.R. and Sequeria, L. 1969. A growth inhibitor from tobacco and its possible involvement in pathogenesis. *Phytopath.*, 59: 499-503.
- _____. 1970. Absciscic acid in tobacco plants: tentative identification and its relation to stunting induced by *Pseudomonas solanacearum*. *Plant Physiol.*, 45: 691-697.
- Steere, R.L. 1957. Electron microscopy of structural detail in frozen biological specimens. *J. Biophys. Biochem. Cytol.*, 3: 45-60.
- Stein, D.B. 1962. The developmental morphology of *Nicotiana tabacum* "white burley" as influenced by virus infection and gibberellic acid. *Am. J. Bot.*, 49: 437-443.
- Stowe, B.B. and Yamaki, T. 1957. The history and physiological action of the gibberellins. *Ann. Rev. Plant Physiol.*, 8: 181-216.
- Sunderland, D.W. and Merrett, M.J. 1963a. Nicotinamide adenine dinucleotide and nicotinamide adenine dinucleotide phosphate concentrations in leaves of *Nicotiana glutinosa* infected by tobacco mosaic virus. *Nature*, 200: 921.
- _____. 1963b. Nicotinamide dinucleotide, adenosine diphosphate and adenosine triphosphate content of tissues infected by tobacco mosaic virus. *Nature*, 199: 1116-1117.
- _____. 1964. Adenosine diphosphate and adenosine triphosphate concentrations in leaves showing necrotic local virus lesions. *Virology*, 23: 274-276.
- _____. 1965. The respiration of leaves showing necrotic local lesions following infection by tobacco mosaic virus. *Ann. appl. Biol.*, 56: 477-484.
- _____. 1967. Respiration rate, adenosine diphosphate and triphosphate concentrations of leaves showing necrotic local lesions following infection by tobacco mosaic virus. *Physiologia Pl.*, 20: 368-372.
- Suzuki, T. and Sato, S. 1973. Properties of acid phosphatase in the cell wall of tobacco cells cultured in vitro. *Plant and Cell Physiol.*, 14: 585-596 (1973).
- Takahashi, T. 1971. Dehydrogenase activities of the pentose phosphate pathway in tobacco leaf epidermis infected with tobacco mosaic virus. *Phytopath. Z.*, 72(1): 29-33.

- Takahashi, T. 1972. Studies on viral pathogenesis in plant hosts. II. Changes in developmental morphology of tobacco plants infected systemically with tobacco mosaic virus. *Phytopath. Z.*, (1972) 74(1): 37-47.
- _____ and Hirai, T. 1964. Respiratory increase in tobacco leaf epidermis in the early stages of tobacco mosaic virus infection. *Physiologia Pl.*, 17: 63-70.
- _____. 1965. Oxidative and phosphorylative activities of mitochondria from tobacco leaf epidermis infected with tobacco mosaic virus. *Physiol. Pl.*, 18: 219-228.
- _____. 1966. Effect of TMV-infection on amino acid incorporation into isolated mitochondria from tobacco leaves. *Physiol. Pl.*, 19: 888-899.
- Tepfer, S.S. and Chessin, M. 1959. Effects of tobacco mosaic virus on early leaf development in tobacco. *Am. J. Bot.*, 46: 496-509.
- Tien, P. and Tang, P.S. 1963. Oxidative metabolism of glucose in leaf tissue infected with tobacco mosaic virus. *Scientia Sinica*, 12: 565-573.
- Tolbert, N.E., Oeser, A., Kisaki, T., Hageman, R.H. and Yamazaki, R.K. 1968. Peroxisomes from spinach leaves containing enzymes related to glycolate metabolism. *J. Biol. Chem.*, 243(19): 5179-5184.
- Tu, J.C. and Ford, R.E. 1968. Effect of maize dwarf mosaic virus infection on respiration and photosynthesis in corn. *Phytopath.*, 58: 282-284.
- Ushiyama, R. and Matthews, R.E.F. 1971. The significance of chloroplast abnormalities associated with infection by turnip yellow mosaic virus. *Virology*, 42: 293-303 (1970).
- Vager, R.M. 1955. The modifications of the respiratory activity of plant enzymes in virus infection. *Zhur. Obsheh. Biol.*, 16: 298-305.
- Van der Scheer, C. and Groenewegen, J. 1971. Structure in cells of *Vigna unguiculata* infected with cow pea mosaic virus. *Virology*, 46: 493-497.
- Van Kammen, A. and Brouwer, D. 1964. Increase in polyphenol oxidase activity by a local virus infection in uninoculated parts of leaves. *Virology*, 22: 9-14.
- Van Loon, L.C. and Geelen, J.L.M.C. 1971. The relation of polyphenol oxidase and peroxidase to symptom expression in tobacco var. Samsun NN after infection with TMV. *Acta Phytopathologica*, 6(1-4): 9-20 (1971).
- Van Onckelen, H.A. and Verbeek, R. 1971. Isolation and assay of a cytokinin from barley. *Phytochem.*, 11: 1677-1680 (1972).
- Van Staden, J. 1973. Changes in endogenous cytokinin levels during abscission and senescence of *Streptocarpus* leaves. *J. Exp. Bot.*, 24(81): 667-673 (1973).

- Van Staden, J., Webb, D.P. and Wareing, P.F. 1971. The effect of stratification on endogenous cytokinin levels in seeds of Acer Saccharum. Planta (Berl.), 104: 110-114 (1972).
- Van Steveninck, R.F.M. 1959. Factors affecting the abscission of reproductive organs in yellow lupins. II. Endogenous growth substances in virus infected and healthy plants and their effect on abscission. J. Exp. Bot., 10: 367-376.
- Varner, J.E. and Johri, M.M. 1968. Hormonal control of enzyme synthesis. "Biochemistry and Physiology of Plant Growth Substances." Ed. Wightman, F., Setterfield, G. Runge Press Ltd., Canada, 1968. p.793-814.
- Venekamp, J.H. 1959. The influence of some viruses on the concentrations of organic acids in a number of plants. Planteziekten (Neth. J. Pl. Path.), 65: 177-187.
- Verbeek, R., van Ocknelen, H. and Gaspar, T.H. 1969. Effets de l'acide gibbéréllique et de la kinétine sur le développement de l'activité α -amylasique durant la croissance de l'Orge. Physiol. Plant, 22: 1192-1199.
- Verhoyen, M. 1966. Respiration rate of virus infected plant tissue held at two different temperatures. Meded. Rijksfac. Landbouwwenten Schapper Gent., 31: 956-966.
- Vigil, E.L. 1973a. Plant Microbodies. J. Hist. Cytochem., 21(11): 958-962.
- _____. 1973b. Structure and function of plant microbodies. Sub-Cell Biochem. (1973), 2: 237-285.
- Von Wettstein, D., Henningsen, K.W., Boynton, J.E., Kannangara, G.C. and Nielsen, O.F. 1971. The genetic control of chloroplast development in barley. In "Autonomy and biogenesis of mitochondria and chloroplasts". North Holland Publishing Co. - Amsterdam - London. Ed. by Boardman, Linnase and Smillie.
- Watson, M.A. and Watson, D.J. 1951. The effect of infections with beet yellows and beet mosaic virus on the carbohydrate content of sugar beet leaves and on translocation. Ann. appl. Biol., 38: 276-288.
- Wehrmeyer, W. 1957. Darstellung und Strukturordnung eines Tabakmosaikvirus-Einschlusskörpers in der Zelle. Naturwissenschaften, 44: 519-520.
- _____. 1959. Entwicklungsgeschichte, Morphologie und Struktur von Tabakmosaikvirus-Einschlusskörpern unter besonderer Berücksichtigung der fibrillären Formen. Protoplasma, 51: 165-196.
- _____. 1960. Die Bildung "intrazellulärer Stäbe" nach Virusinfektion. Naturwissenschaften, 47: 236-237.
- Weintraub, M. and Hagetli, H.W.J. 1964. Studies on the metabolism of leaves with localized virus infections. Particulate fractions and substrates in TMV-infected N. glutinosa L. Can. J. Bot., 42: 533-540.

- Weintraub, M., Ragetli, H.W. and Dwurazna, M.M. 1964. Studies on the metabolism of leaves with localized virus infection. Mitochondrial activity in tobacco mosaic virus-infected Nicotiana glutinosa L. Can. J. Bot., 42: 541-544.
- Whitehead, T. 1934. The physiology of potato leaf roll. I. On the respiration of healthy and leaf-roll infected potatoes. Ann. appl. Biol., 21: 48-73.
- Whitfield, D.M. and Rowan, K.S. 1974. Changes in the chlorophylls and carotenoids of leaves of Nicotiana tabacum during senescence. Phytochem. (1974), 13: 77-83.
- Whyte, P. and Luckwill, L.C. 1966. A sensitive bioassay for gibberellins based on retardation of leaf senescence in Rumex obtusifolius L. Nature, 210: 1360.
- Wildman, S.G., Cheo, C.C. and Bonner, J. 1949. The proteins of green leaves. III. Evidence of the promotion of tobacco mosaic virus at the expense of a main protein component in tobacco leaf. J. Biol. Chem., 180: 985-1001.
- Wilson, G.L. 1973. A lysosomal concept for plant pathology. Ann. Rev. Phytopath., 11: 247-272 (1973).
- Wiltshire, G.H. 1956a. The effect of darkening on the susceptibility of plants to infection with viruses. I. Relation to changes in some organic acids in the French bean. Ann. appl. Biol., 44: 233-248.
- _____. 1956b. The effect of darkening on the susceptibility of plants to infection with viruses. II. Relation to changes in ascorbic acid content of French bean and tobacco. Ann. appl. Biol., 44: 249-255.
- Wolffgang, H. and Keck, A. 1958. Untersuchungen über den Stoffwechsel viruskranker pflanzen. I. Die Phosphatase-Aktivität in Nicotiana tabacum L. var. Samsun nach Infektion mit TMV. Phytopath. Z., 34: 57-65.
- Woltz, S.S. and Littrell, R.H.. 1968. Production of yellow strap leaf of Chrysanthemum and similar diseases with an antimetabolite produced by Aspergillus wentii. Phytopath., 58: 1476-1480.
- Wright, S.T.C. 1968. Multiple and sequential roles of plant growth regulators. "Biochemistry and Physiology of Plant Growth Substances." Ed. Wightman, F. and Setterfield, G. Runge Press Ltd., Canada, 1968. p.521-542.
- Wrigley, N.G. 1968. The lattice spacing of crystalline catalase as an internal standard of length in electron microscopy. J. Ultrastructure Research, 24: 454-464 (1968).
- Wyen, N.V., Udvardy, J., Bagi, G. and Farkas, G.L. 1972. Hormonal control of nuclease level in excised Avena leaf tissues. J. Exp. Bot., 23: 37-44.
- Wynd, F.L. 1942. Certain enzymatic activities of normal and mosaic infected tobacco leaves. J. Gen. Physiol., 25: 649-661.

- Wynd, F.L. 1943. Metabolic phenomena associated with virus infection in plants. Bot. Rev., 9: 395-465.
- Yamaguchi, A. and Hirai, T. 1956. Nature of virus infection in plants. IV. Dehydrogenase activity of green leaves during the course of virus infection. Virus (Osaka), 6: 1-7.
- _____. 1965. The effect of local infection with tobacco mosaic virus on respiration in leaves of Nicotiana glutinosa. Phytopath., 49: 447-449.
- Yamaguchi, A. and Takahashi, A. 1964. The effect of systemic virus infection on the respiration of leaves. Biochemische probleme der Franken Pflanze, 74: 99-109.
- Zachos, D. 1955. Relation entre l'activité de certains systèmes oxydases et la multiplication, chez la tomate, du virus X de la pomme de terre et du virus de la mosaïque du tabac. Compt. Rend. Acad. Sci. Paris, 240: 2084-2086.
- Zaitlin, M. and Jagendorf, A.T. 1960. Photosynthetic phosphorylation and Hill reaction activities of chloroplasts isolated from plants infected with tobacco mosaic virus. Virology, 12: 477-486.

Personal Communication

Dr. G.V. Hoad, University of Bristol research station, Long Ashton, U.K.

APPENDICES

Appendix 1

Leaf length (cms) measurements for leaves at node position 5 above the original inoculated leaf.

Virus Status	Block No.			Means
	I	II	III	
Healthy Controls	22.0	24.0	19.0	
	25.5	22.0	26.0	
	27.5	24.0	20.0	
	26.0	30.0	21.0	
	24.0	23.0	23.0	23.8
Virus-infected	17.0	22.0	20.0	
	14.0	20.5	17.0	
	22.0	19.0	18.5	
	21.5	20.0	16.5	
	23.0	19.5	16.0	19.1

Analysis of Variance

Source of Variation	d.f.	S.S.	M.S.	F ratio
Virus Status	1	165.65	165.65	24.5**
Blocks	2	46.03	23.01	3.4*
Main Error	2	2.47	1.235	1 N.S.
Within Plots Error	24	162.5	6.77	
Total	29	376.65		

Appendix 2

Leaf length (cms) measurements for leaves at node position 8 above the original inoculated leaf.

Virus Status	Block No.			Means
	I	II	III	
Healthy Controls	18.0	15	13	
	20.5	20	17	
	21	18	19	
	21.5	18	15	
	18	20	13	17.8
Virus-infected	11	13	14.5	
	9	17.5	6.5	
	15	14	12.0	
	18.5	15	13.0	
	19	17	15.5	14

Analysis of Variance

Source of Variation	d.f.	S.S.	M.S.	F ratio
Virus Status	1	106.4	106.4	13.35**
Blocks	2	64.9	32.5	4.08*
Error	26	207.25	7.97	
Total	29	378.55		

Appendix 3

Leaf length (cms) measurements for leaves at node position 10 above the original inoculated leaf.

Virus Status	Block No.			Means
	I	II	III	
Healthy Controls	6	6	1.5	
	7	7	8	
	13	13	3	
	9.5	5	5	
	3.5	10	5	6.8
Virus-infected	2.5	5	10.5	
	1	4.5	2.5	
	4.5	3	2	
	11.5	6.5	1.5	
	11	10	7	5.5

Analysis of Variance

Source of Variation	d.f.	S.S.	M.S.	F ratio
Virus Status	1	12.68	12.68	1.06 N.S.
Blocks	2	36.63	18.31	1.53 N.S.
Error	26	313.44	12.0	
Total	29	362.7		

Appendix 4

Plant height (cms) measurements for healthy and virus-infected plants 5-6 weeks following inoculations.

Virus Status	Block No.			Means
	I	II	III	
Healthy Controls	15	22	10	
	19	19	17	
	33	30	16	
	21	20	16	
	18	20	19	19.5
Virus-infected	9.5	14	9.5	
	6	8.5	6.5	
	15	7	8	
	22	6.5	8	
	14	15	6.5	10.5

Analysis of Variance

Source of Variation	d.f.	S.S.	M.S.	F ratio
Virus Status	1	644	644	29 **
Blocks	2	177	88.5	3.4 *
Error	26	265	21.7	
Total	29	1,386		

Appendix 5

Internode length (cms) for node position 5-6.

Virus Status	Block No.			Means
	I	II	III	
Healthy Controls	2.5	3	3	
	4	4	2	
	5	3	2	
	5.5	3	1.5	
	3	3	3	3.2
Virus-infected	2	3	2	
	0.5	3	1	
	1.5	1.5	1.5	
	3.5	1.5	1.5	
	3	2.0	0.5	1.9

Analysis of Variance

Source of Variation	d.f.	S.S.	M.S.	F ratio
Virus Status	1	12.68	12.68	16 **
Blocks	2	8.33	4.17	5.5 *
Error	26	19.74	0.759	
Total	29	40.75		

Appendix 6

The number of leaves formed after inoculation, counted from the fourth leaf from the apex at time of inoculation.

Virus Status	Block No.			Means
	I	II	III	
Healthy Controls	11	10	10	
	11	11	11	
	12	13	10	
	11	11	11	
	10	11	10	11
Virus-infected	12	12	13	
	11	12	11	
	13	11	11	
	13	12	11	
	13	14	12	12

Analysis of Variance

Source of Variation	d.f.	S.S.	M.S.	F ratio
Virus Status	1	10.83	10.83	14.5 **
Blocks	2	3.30	1.65	2.2 N.S.
Error	26	19.37	0.745	
Total	29	33.50		

Appendix 7

(Mean leaf area approximations) cm²

Days after inoculation	Leaf node position from plant base X										Virus status			
	4		9		12		15		18		21		24	
	H	I	H	I	H	I	H	I	H	I	H	I	H	I
19	47	44	151	28	3.2	2.8								
26	47	44	415	81	81	81								
33			464	99	268	204	40	26						
40			469	101	351	264	202	129	13	x11				
50			469	101	351	264	335	226	175	90				
54							348	237	234	119	48	34		
61							348	237	299	164	150	75	26	28
68									315	188	198	116	91	73
76									322	198	254	148	166	128
82									322	198	256	164	210	164

Appendix 8

Lesion scores for infected leaf tissue of different ages

Leaf Position from Apex	Lesion Numbers per half Leaf for 10 ⁻³ Dilution						Average No. Lesions per half Leaf	Number Lesions per Gram Fresh Weight Material	Log Lesion Numbers
	1	2	3	4	5	6			
0 (Meristem)	0	0	0	0	0	1	0.167	1,427	3.15
1	2	4	2	2	11	7	4.67	9,340	3.97
3	6	9	11	22	9	10	11.17	22,340	4.35
5	5	9	9	12	20	8	10.50	21,000	4.32
7	6	4	7	8	17	18	10.00	20,000	4.30
9	16	7	14	12	4	10	10.50	21,000	4.32
12	9	16	8	15	15	7	11.67	23,340	4.37

Appendix 9

Lesion scores for comparisons of tissues
making up the mosaic and uninfected tissues
of the same age (Leaf Position 8 from Apex).

	Lesion Numbers per half Leaf for 10 ⁻³ Dilution						Average Number Lesions per half Leaf	Number Lesions per Gram Fresh Weight	Log Lesion Number
	1	2	3	4	5	6			
Yellow-Green Mosaic Tissue	16	49	31	30	152	27	50.72	101,440	5.006
Dark Green Mosaic Tissue	0	2	2	0	1	12	3.17	6,352	3.803
Healthy Control Tissue	1	0	0	0	0	0	0.167	334	2.524

Appendix 10

Buffers used in leaf tissue extractions for enzyme analysis and buffers used in electrophoresis.

(a) Acrylamide gel buffer and leaf tissue extraction buffer

tris 38 mM	4.598 g/litre
citric acid 2.5 mM	0.5254 g/litre

(pH 8.7 at 25° C)

(b) Electrophoresis tank buffer

boric acid	7.22 g/litre
sodium tetraborate	15.75 g/litre

(pH 8.8 at 25° C)

Appendix 11

Composition of acrylamide gels used for electrophoresis.

(a) 7.5% Gel

7.5 g acrylamide
0.1875 g NN-methylene bisacrylamide
0.10 ml N,N,N,'N'-tetramethyl ethylene diamine
0.10 g ammonium persulphate

(Make up to 100 ml with tris-citrate buffer)

(b) 8.0% Gel

8.0 g acrylamide
0.20 g N,N-methylene bisacrylamide
0.10 ml N,N,N,'N' -tetramethyl ethylene diamine
0.10 g ammonium persulphate

(Make up to 100 ml with tris-citrate buffer)

(c) 10% Gel

10.0 g acrylamide
0.25 g N,N-methylene bisacrylamide
0.10 ml N,N,N,'N'-tetramethyl ethylene diamine
0.10 g ammonium persulphate

(Make up to 100 ml with tris-citrate buffer)

Appendix 12

Reaction rate data for cytochrome-c-oxidase in extracts from young tobacco leaves (leaf position 6 from the stem apex).

	Reaction Time (mins.)	Abs. 550 nm/g fresh wt.
Healthy	1	0
	1.5	0.224
	2	0.368
	2.5	0.492
	3	0.588
	3.5	0.680
	4	0.760
	4.5	0.824
Infected (light-green island)	5	0.896
	1	0
	1.5	0.152
	2	0.260
	2.5	0.348
	3	0.432
	3.5	0.500
	4	0.568
	4.5	0.636
	5	0.696

Appendix 13

Reaction rate data for cytochrome-C oxidase in extracts from immature tobacco leaves (leaf position 9 from the stem apex).

		Abs. 550 nm/gm fresh wt.			
Virus Status	Reaction Time (min.)	Rep I	Rep II	Rep III	Mean
Healthy	1	0	0	0	0
	1.5	0.220	0.152	0.328	0.233
	2	0.408	0.284	0.592	0.428
	2.5	0.56	0.388	0.76	0.569
	3	0.688	0.496	0.848	0.677
	3.5	0.776	0.592	0.924	0.764
	4	0.86	0.680	0.992	0.844
Infected (light green island)	1	0	0	0	0
	1.5	0.140	0.132	0.128	0.133
	2	0.240	0.228	0.240	0.236
	2.5	0.356	0.316	0.336	0.336
	3	0.428	0.384	0.420	0.411
	3.5	0.500	0.456	0.508	0.488
	4	0.568	0.516	0.588	0.557
Infected (dark green island)	1			0	
	1.5			0.176	
	2			0.320	
	2.5			0.460	
	3			0.596	
	3.5			0.712	
	4			0.816	

Split-Plot Analysis of Variance

Source of Variation	d.f.	S.S.	M.S.	F ratio
Reps	2	0.149106	0.074553	1.2
Virus Status	1	0.39324	0.39324	7.905
Error (a)	2	0.099487	0.049744	
Reaction Time	6	2.25805	0.376341	157 **
T x V	6	0.102888	0.017148	7.163 **
Error (b)	24	0.057453	0.002394	
Total	41	3.060224		

$$SE_{\bar{x}} = 0.0282$$

Appendix 14

Reaction rate data for cytochrome-C oxidase in extracts from mature tobacco leaves (leaf position 10 from the stem apex).

Virus Status	Reaction Time (min.)	Abs. 550 nm/gm fresh wt.		
		Rep I	Rep II	Mean
Healthy	1	0	0	0
	1.5	0.088	0.100	0.094
	2	0.156	0.168	0.162
	2.5	0.220	0.228	0.224
	3	0.284	0.272	0.278
	3.5	0.336	0.324	0.330
	4	0.388	0.376	0.382
	4.5	0.440	0.416	0.428
Infected (light green island)	5	0.488	0.448	0.468
	1	0	0	0
	1.5	0.096	0.120	0.108
	2	0.172	0.184	0.178
	2.5	0.248	0.228	0.238
	3	0.308	0.280	0.294
	3.5	0.364	0.324	0.344
	4	0.416	0.364	0.390
	4.5	0.460	0.404	0.432
	5	0.504	0.436	0.470

(Cont.)

Appendix 14 (cont.)

Virus Status	Reaction Time (min.)	Rep I	Rep II	Mean
Infected (dark green island)	1	0	0	0
	1.5		0.080	
	2		0.140	
	2.5		0.196	
	3		0.240	
	3.5		0.276	
	4		0.356	
	4.5		0.364	
	5		0.404	

Split-Plot Analysis of Variance

Source of Variation	d.f.	S.S.	M.S.	F ratio
Reps	1	0.0025	0.0025	3.686
Virus Status	1	0.00082	0.00082	1.209
Error (a)	1	0.0006782	0.0006782	
Reaction Time	8	0.78322	0.09540	288 **
V x T	8	0.00036	0.000045	1
Error (b)	16	0.0052858	0.00033	
Total	35	0.792864		

$$SE\bar{x} = 0.01285$$

Appendix 15

Reaction rate data for cytochrome-C oxidase in extracts from senescing tobacco leaves (leaf position 11, 12 from the stem apex).

		Abs. 550 nm/gm fresh wt.		
Virus Status	Reaction Time (min.)	Rep I	Rep II	Mean
Healthy	1	0	0	0
	1.5	0.072	0.068	0.070
	2	0.132	0.108	0.120
	2.5	0.184	0.148	0.166
	3	0.236	0.176	0.206
	3.5	0.276	0.208	0.242
	4	0.316	0.236	0.276
	4.5	0.348	0.264	0.306
	5	0.388	0.288	0.338
Infected	1	0	0	0
	1.5	0.132	0.076	0.104
	2	0.228	0.124	0.176
	2.5	0.304	0.168	0.236
	3	0.372	0.204	0.288
	3.5	0.428	0.248	0.338
	4	0.492	0.284	0.388
	4.5	0.540	0.308	0.424
	5	0.584	0.340	0.462

Split-Plot Analysis of Variance

Source of Variation	d.f.	S.S.	M.S.	F ratio
Reps	1	0.08841	0.08841	4.186
Virus Status	1	0.05321	0.05321	2.519
Error (a)	1	0.02112	0.02112	
Reaction Time	8	0.56933	0.07117	35.46 **
T x I	8	0.01376	0.00182	1
Error (b)	16	0.03211	0.0020068	
Total	35	0.77794		

$$SE\bar{x} = 0.03168$$

Appendix 16

Reaction rate data for NADH oxidase in extracts from young, immature and mature-senescent tobacco leaves (leaf position 6, 9 and 11 from the stem apex).

Virus Status	Reaction Time (min.)	Abs. 340 nm/gm fresh wt.		
		(Young)	(Immature)	(Mature-Senescent)
Healthy	1	0	0	0
	1.5	0.072	0.060	0.024
	2	0.116	0.100	0.04
	2.5	0.168	0.132	0.064
	3	0.212	0.172	0.072
	3.5	0.252	0.200	0.096
	4	0.288	0.228	0.112
	4.5	0.320	0.252	0.128
	5	0.352	0.280	0.144
Infected (light green island)	1	0	0	0
	1.5	0.044	0.032	0.032
	2	0.080	0.056	0.064
	2.5	0.108	0.072	0.084
	3	0.140	0.096	0.112
	3.5	0.168	0.112	0.136
	4	0.192	0.128	0.156
	4.5	0.216	0.152	0.180
	5	0.240	0.168	0.208
Infected (dark green island)	1		0	
	1.5		0.036	
	2		0.056	
	2.5		0.080	
	3		0.100	
	3.5		0.124	
	4		0.136	
	4.5		0.152	
	5		0.164	

Appendix 17

Reaction rate data for glutamate dehydrogenase in extracts from young and senescent tobacco leaves (leaf positions 6 and 11-12 from the stem apex).

Virus Status	Reaction Time (min.)	Abs. 340 nm/gm fresh wt.	
		(Young)	(Senescent)
Healthy	1	0	0
	1.5	0.104	0.048
	2	0.204	0.080
	2.5	0.296	0.128
	3	0.388	0.172
	3.5	0.472	0.188
	4	0.548	0.232
Infected (light green island)	1	0	0
	1.5	0.076	0.052
	2	0.140	0.104
	2.5	0.196	0.156
	3	0.264	0.204
	3.5	0.316	0.244
	4	0.388	0.284

Appendix 18

Reaction rate data for glutamate dehydrogenase in extracts from immature tobacco leaves (leaf position 9 from the stem apex).

Abs. 340 nm/gm fresh wt.				
Virus Status	Reaction Time (min.)	Rep I	Rep II	Mean
Healthy	1	0	0	0
	1.5	0.064	0.096	0.080
	2	0.124	0.200	0.162
	2.5	0.172	0.296	0.234
	3	0.212	0.380	0.296
	3.5	0.256	0.480	0.368
	4	0.312	0.560	0.436
Infected (light green island)	1	0	0	0
	1.5	0.088	0.172	0.130
	2	0.172	0.320	0.246
	2.5	0.260	0.472	0.366
	3	0.328	0.608	0.468
	3.5	0.400	0.736	0.568
	4	0.468	0.844	0.656
Infected (dark green island)	1	0	0	0
	1.5	0.064	0.088	0.076
	2	0.120	0.184	0.152
	2.5	0.176	0.248	0.212
	3	0.228	0.352	0.290
	3.5	0.276	0.440	0.358
	4	0.324	0.528	0.426

Split-Plot Analysis of Variance

Source of Variation	d.f.	S.S.	M.S.	F ratio
Reps	1	0.210611	0.210611	19.72 *
Virus Status	2	0.151087	0.075543	7.074
Error (a)	2	0.021359	0.010679	1.937
Reaction Time	6	1.190127	0.198355	36 **
T x V	12	0.055548	0.00463	1
Error (b)	18	0.09923	0.0055127	
Total	41	1.727962		

$$SE\bar{x} = 0.053$$

Appendix 19

Reaction rate data for glutamate dehydrogenase in extracts from mature tobacco leaves (leaf position 10 from the stem apex).

Abs. 340 nm/gm fresh wt.				
Virus Status	Reaction Time (min.)	Rep I	Rep II	Mean
Healthy	1	0	0	0
	1.5	0.048	0.068	0.058
	2	0.088	0.144	0.116
	2.5	0.120	0.212	0.166
	3	0.144	0.280	0.212
	3.5	0.204	0.344	0.274
	4	0.240	0.420	0.330
Infected (light green island)	1	0	0	0
	1.5	0.072	0.164	0.118
	2	0.144	0.324	0.234
	2.5	0.204	0.476	0.340
	3	0.268	0.600	0.434
	3.5	0.328	0.728	0.528
	4	0.388	1.000	0.694

Split-Plot Analysis of Variance

Source of Variation	d.f.	S.S.	M.S.	F ratio
Reps	1	0.225365	0.22536	3.9495
Virus Status	1	0.20298	0.20298	3.557
Error (a)	1	0.05706	0.05706	4.939
Reaction Time	6	0.76461	0.12743	11.03
T x V	6	0.09111	0.01519	1.315
Error (b)	12	0.13864	0.011553	
Total	27	1.47976		

$$SE\bar{x} = 0.076$$

Appendix 20

Reaction rates for phosphoglucosomerase in tobacco leaf tissue extracts.

Virus Status/ Leaf Position from Apex		mg Equivalents/gm Fresh wt. Leaf Tissue/45 min.			
		Rep I	Rep II	Rep III	Mean
Healthy	4	2.0	2.9	2.9	2.6
	8	3.6	3.5	4.1	3.74
	12	2.4	0.5	3.6	2.16
Light green Island	4	1.9	2.5	4.1	2.86
	8	2.9	4.1	4.5	3.84
Dark green Island	8	3.9	3.9	3.8	3.86

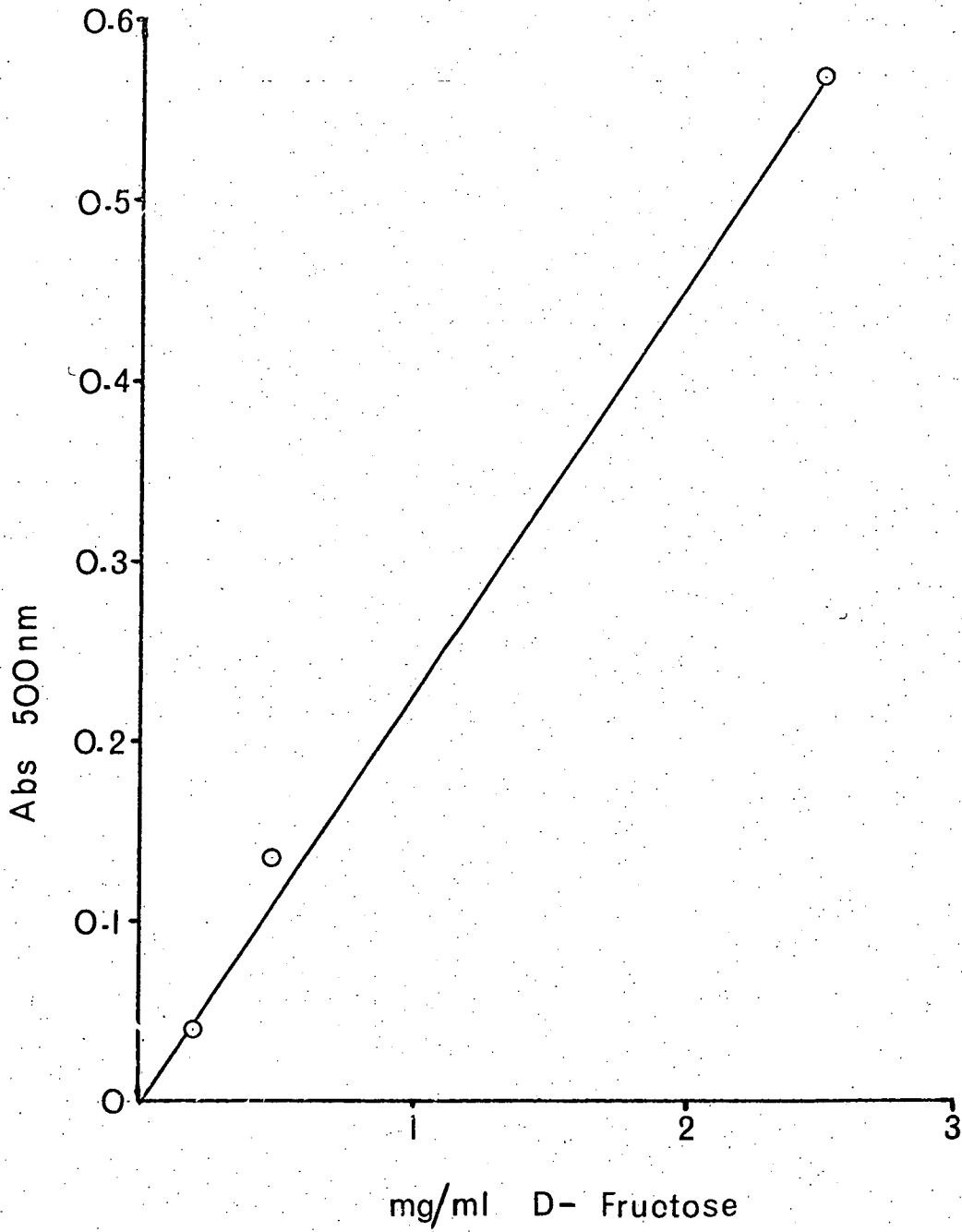
Analysis of Variance

Source of Variation	d.f.	S.S.	M.S.	F ratio
Reps	2	3.974	1.987	3.524 N.S.
Virus Status/Leaf Age	5	8.063	1.613	2.86 N.S.
Error	10	5.639	0.524	
Total	17	17.676		

$$SE\bar{x} = 0.418$$

Appendix 21

Standard curve of fructose concentration versus absorbance 500 nm.



Appendix 22

Reaction rate data for glucose-6-phosphate dehydrogenase in extracts from young tobacco leaves (leaf position 6 from the stem apex).

		Abs. 340 nm/gm fresh wt.		
Virus Status	Reaction Time (min.)	Rep I	Rep II	Mean
Healthy	1	0	0	0
	2	0.0264	0.0188	0.0226
	3	0.0396	0.0316	0.0356
	4	0.044	0.0444	0.0442
	5	0.044	0.0508	0.0476
	6	0.044	0.064	0.054
	7	0.0484	0.0704	0.0594
Infected (light green island)	1	0	0	0
	2	0.016	0.016	0.016
	3	0.032	0.064	0.048
	4	0.0396	0.064	0.0518
	5	0.0396	0.08	0.0598
	6	0.044	0.08	0.062
Infected (dark green island)	1	0	0	0
	2	0.0176	0.012	0.0148
	3	0.0484	0.044	0.0462
	4	0.062	0.072	0.067
	5	0.0708	0.072	0.0714
	6	0.0752	0.088	0.0816
	7	0.0800	0.104	0.092

Split-Plot Analysis of Variance

Source of Variation	d.f.	S.S.	M.S.	F ratio
Reps	1	0.0016145	0.0016145	2.895
Virus Status	2	0.001736	0.000868	1
Error (a)	2	0.00112	0.0005577	
Reaction Time	6	0.026267	0.004378	39 **
T x V	12	0.00151	0.000126	1
Error (b)	18	0.00204	0.0001132	
Total	41	0.0342854		

$$SE\bar{x} = 0.00752$$

Appendix 23

Reaction rate data for glucose-6-phosphate dehydrogenase in extracts from mature tobacco leaves (leaf position 9 from the stem apex).

		Abs. 340 nm/gm fresh wt.		
Virus Status	Reaction Time (min.)	Rep I	Rep II	Mean
Healthy	1	0	0	0
	2	0.0176	0	0.0088
	3	0.0176	0.016	0.0168
	4	0.0264	0.032	0.0292
	5	0.0308	0.064	0.0474
	6	0.0352	0.064	0.0496
	7	0.0352	0.064	0.0496
Infected (light green island)	1	0	0	0
	2	0.0176	0.032	0.0248
	3	0.0308	0.056	0.0434
	4	0.0396	0.068	0.0538
	5	0.0484	0.08	0.0642
	6	0.0528	0.08	0.0664
	7	0.062	0.092	0.077
Infected (dark green island)	1	0	0	0
	2	0.0088	0.020	0.0144
	3	0.0264	0.040	0.0332
	4	0.0352	0.06	0.0476
	5	0.0352	0.092	0.0636
	6	0.0396	0.10	0.0698
	7	0.0396	0.112	0.0758

Split-Plot Analysis of Variance

Source of Variation	d.f.	S.S.	M.S.	F ratio
Reps	1	0.0053314	0.0053314	11.377
Virus Status	2	0.0026361	0.001318	2.8126
Error (a)	2	0.0009373	0.0004686	
Reaction Time	6	0.023045	0.0038408	17.51
T x V	12	0.0007925	0.000066	1
Error (b)	18	0.0039478	0.0002193	
Total	41	0.0366901		

$$SE\bar{x} = 0.0111$$

Appendix 24

Reaction rate data for alcohol dehydrogenase in extracts from young tobacco leaves (leaf position 6 from the stem apex).

Virus Status	Reaction Time (min.)	Abs. 340 nm/gm fresh wt.		
		Rep I	Rep II	Mean
Healthy	1	0	0	0
	2	0.0088	0.008	0.0084
	3	0.02	0.012	0.016
	4	0.032	0.02	0.026
	5	0.044	0.028	0.036
	6	0.053	0.034	0.0435
	7	0.062	0.038	0.05
Infected (light green island)	1	0	0	0
	2	0.008	0.008	0.008
	3	0.008	0	0.004
	4	0.016	0.008	0.012
	5	0.016	0.014	0.015
	6	0.016	0.014	0.015
	7	0.016	0.018	0.017
Infected (dark green island)	1	0	0	0
	2	0.006	0.0048	0.0054
	3	0.020	0.0072	0.0136
	4	0.032	0.0096	0.0208
	5	0.032	0.0142	0.0231
	6	0.032	0.0166	0.0243
	7	0.040	0.0192	0.0296

Split-Plot Analysis of Variance

Source of Variation	d.f.	S.S.	M.S.	F ratio
Reps	1	0.0008428	0.0008428	8.6976
Virus Status	2	0.0017079	0.0008539	8.8122
Error (a)	2	0.0001938	0.0000969	3.1158
Reaction Time	6	0.0049495	0.0008249	26.5
T x V	12	0.0010671	0.0000889	2.859
Error (b)	18	0.0005609	0.0000311	2
Total	41	0.009322		

$$SE\bar{x} = 0.003937$$

Appendix 25

Reaction rate data for alcohol dehydrogenase in extracts from mature tobacco leaves (leaf position 9 from the stem apex).

		Abs. 340 nm/gm fresh wt.		
Virus Status	Reaction Time (min.)	Rep I	Rep II	Mean
Healthy	1	0	0	0
	2	0.0102	0	0.0051
	3	0.0102	0.006	0.0081
	4	0.0128	0.012	0.0124
	5	0.0128	0.018	0.0154
	6	0.0154	0.018	0.0167
	7	0.0284	0.024	0.0262
Infected (light green island)	1	0	0	0
	2	0.018	0.004	0.011
	3	0.03	0.01	0.02
	4	0.048	0.012	0.03
	5	0.068	0.016	0.042
	6	0.074	0.02	0.047
	7	0.08	0.024	0.052
Infected (dark green island)	1	0	0	0
	2	0.026	0.008	0.017
	3	0.036	0.014	0.025
	4	0.052	0.022	0.037
	5	0.08	0.022	0.051
	6	0.106	0.028	0.067
	7	0.114	0.036	0.075

Split-Plot Analysis of Variance

Source of Variation	d.f.	S.S.	M.S.	F ratio
Reps	1	0.006633	0.006633	4.452
Virus Status	2	0.005165	0.00258	1.732
Error (a)	2	0.00298	0.00149	
Reaction Time	6	0.01304	0.00201	8.204
T x V	12	0.00224	0.000187	1
Error (b)	18	0.00442	0.000245	
Total	41	0.0334762		

$$SE\bar{x} = 0.011$$

Appendix 26

Catalase Intensity Ratings

Virus Status	Node Position	Intensity Rating		Total Ratings
		Rf 0.11	Rf 0.17	
Healthy	4	2		2
	5	3		3
	7	5	5	10
	10	5	5	10
	12	5		5
Infected + Virus-Free	5	4		4
Infected	7		2	2
	10		1	
Virus-Free (Infected)	7	5	5	10
	10	4	4	8

Appendix 27

Peroxidase Intensity Ratings

		Intensity Ratings				Total Ratings
Virus Status	Node Position	Rf -0.1	Rf -0.16	Rf 0.56	Rf 0.65	
Healthy	5	3	1		2	6
	7	2	1	0.5		3.5
	10	1	0.5	1		2.5
	12	0.5	0.5	4	4	9
Infected	5	5	2	1	3	11
	7	5	0.5	1	2	8.5
	10	5	0.5	4	4	13.5
Virus-Free (Infected)	5	4	2		2	8
	7	3	1	0.5	1	5.5
	10	3	0.5	2	2	7.5

Appendix 28

Acid Phosphatase Intensity Ratings

Virus Status	Node Position	Intensity Ratings								Total Ratings
		Rf 0.05	Rf 0.09	Rf 0.13	Rf 0.23	Rf 0.32	Rf 0.47	Rf 0.55	Rf 0.62	
Healthy	5	1		1	3	2	0.5	0.25	0.25	8
	7	0.25		0.25	3	2	0.5	0.25		6.25
	10			0.5	3	1	0.5	0.25	0.25	5.5
	12				0.25	1				1.25
Infected	5	3	3	1	4	2	2	0.25		15.25
	7	0.5	1	1	3	2	1	0.5	0.25	9.25
	10	0.25	0.25	0.25	5	2	0.25	0.25	0.25	8.5
Virus-Free (Infected)	5	5	5	2	5	2	3	0.25	0.25	22.5
	7		1	0.5	2	2	1	0.5	0.25	7.25
	10		1	1	4	2	1	1	0.25	10.25

Appendix 29

RNAase Intensity Ratings

Virus Status	Node Position	Intensity Ratings			Total Ratings
		Rf 0.2	Rf 0.84	Rf 0.87	
Healthy	5	3	2	2	7
	7	3	0.25	1	4.25
	10	3	0.5	1	4.5
	12	2	0.5	1	3.5
Infected	5	5	1	3	9
	7	5	1	3	9
	10	4	1	3	8
Virus-Free (Infected)	5	4	0.5	3	7.5
	7	4	0.5	2	6.5
	10	4	0.5	2	6.5

Appendix 30

 α -Amylase Intensity Ratings

Virus Status	Node Position	Intensity Ratings			Total Ratings
		Rf 0.08	Rf 0.23	Rf 0.49	
Healthy	4		2	0.25	2.25
	5	1	2	0.5	3.5
	7		1	0.5	1.5
	10		2	0.5	2.5
	12		3	2	5
Infected + Virus Free	5	3	1	0.5	4.5
Infected	7	2	2	2	6
	10		5	2	7
Virus-Free (Infected)	7	0.5	1	0.5	2
	10		3	2	5

Appendix 31

Esterase Intensity Ratings

Virus Status	Node Position	Rf -0.225	Rf -0.18	Rf -0.12	Rf 0.05
Healthy	5	2	3	0.5	2
	7	4	4	3	4
	10	1	1	4	3
	12	2		4	1
Infected	5	1	3		4
	7	0.5	2	2	5
	10	2	3	3	4
Virus-Free (Infected)	5	1	3	1	3
	7	1	2	2	4
	10	2	2	4	4

(Cont.)

Appendix 31 (Cont.)

Esterase Intensity Ratings

Virus Status	Node Position	Rf 0.16	Rf 0.23	Rf 0.28	Rf 0.37	Rf 0.41
Healthy	5	3	1	0.25	1	
	7	3	0.25	2	2	
	10	2	0.25	1	2	
	12	0.25		0.5	1	
Infected	5	3	1	0.25	1	
	7	3	0.25	1	3	
	10	2	0.25	2	3	0.5
Virus-Free (Infected)	5	3	0.5	1	1	
	7	3	0.25	1	2	
	10	2		2	3	

(Cont.)

Appendix 31 (Cont.)

Esterase Intensity Ratings

Virus Status	Node Position	Rf 0.5	Rf 0.55	Rf 0.68	Rf 0.74	Rf 0.8
Healthy	5	1	0.25	1		
	7	1	0.5	1	1	1
	10	0.5		0.5	0.5	0.5
	12			0.25	0.25	0.5
Infected	5	0.5	1	1	0.25	
	7	1	1	1	0.5	
	10	1		1	1	0.5
Virus-Free (Infected)	5	0.5	0.5	1	0.25	
	7	0.5	0.5	1	0.5	0.5
	10	1		1	0.5	1

Appendix 32

Plating medium for tobacco pith callus culture.

Major Elements (mg/litre)

NH_4NO_3	825
KNO_3	950
$\text{CaCl}_2 \cdot 2\text{H}_2\text{O}$	220
$\text{MgSO}_4 \cdot 7\text{H}_2\text{O}$	1233
KH_2PO_4	680
$\text{Na}_2\text{-EDTA}$	37.3
$\text{FeSO}_4 \cdot 7\text{H}_2\text{O}$	27.8

Minor Elements (mg/litre)

H_3BO_3	6.2
$\text{MnSO}_4 \cdot 4\text{H}_2\text{O}$	22.3
$\text{ZnSO}_4 \cdot 4\text{H}_2\text{O}$	8.6
KI	0.83
$\text{Na}_2\text{MoO}_4 \cdot 2\text{H}_2\text{O}$	0.25
$\text{CuSO}_4 \cdot 5\text{H}_2\text{O}$	0.025
$\text{CoSO}_4 \cdot 7\text{H}_2\text{O}$	0.030

Organics

Sucrose	10 g/litre
meso-inositol	100 mg/litre
Thiamine-HCl	1 mg/litre
D-Mannitol	0.7 M

Final pH adjusted to 5.8 with KOH before autoclaving.

Appendix 33

Average response of the barley endosperm bioassay to a concentration range of GA₃.

Abs. 625 nm of Independent Bioassays							
GA ₃ Concentration (gm/ml)	I	II	III	IV	V	VI	Mean
Control	0.150	0.213	0.182	0.370	0.428	0.339	0.281
10 ⁻¹¹	0.161	0.227	0.172	0.343	0.417	0.312	0.272
10 ⁻¹⁰	0.237	0.240	0.185	0.415	0.460	0.394	0.322
10 ⁻⁹	0.580	0.466	0.301	0.498	0.547	0.605	0.500
10 ⁻⁸	0.957	0.882	0.653	0.759	0.921	0.996	0.862
10 ⁻⁷	1.126	0.904	0.771	1.081	1.090	1.095	1.011

Analysis of Variance

Source of Variation	d.f.	S.S.	M.S.	F ratio
Bioassay	5	0.2897	0.0579	10.5 **
GA ₃ Conc.	5	3.0824	0.6165	111 **
Error	25	0.1384	0.0055	
Total	35	3.5105		

$$SE_{\bar{x}} = 0.0526$$

95% Confidence Limits of points plotted on graph = ± 0.108

Appendix 34

GA3-like activity of a TLC plate zone for young leaf tissue extract.

Extract Dilution	Absorbance 625 nm				
	I	II	III	IV	Mean
Control	0.297	0.299	0.344	0.362	0.326
Healthy $1/_{125}$	0.237	0.385	0.429	0.295	0.337
Healthy $1/_{25}$	0.278	0.224	0.310	0.459	0.318
Healthy $1/_{5}$	0.321	0.352	0.438	0.323	0.359
Healthy 1	0.534	0.364	0.527	0.420	0.461
Infected $1/_{125}$	0.274	0.349	0.220	0.392	0.309
Infected $1/_{25}$	0.325	0.282	0.359	0.364	0.333
Infected $1/_{5}$	0.369	0.392	0.380	0.362	0.376
Infected 1	0.385	0.516	0.372	0.520	0.448
GA3 (10^{-9} gm/ml)	0.469	0.491	0.648	0.577	0.546

Analysis of Variance

Source of Variation	d.f.	S.S.	M.S.	F ratio
Reps	3	0.024416	0.00814	1.77
Extract Dilutions	9	0.22175	0.02464	5.373 **
Error	27	0.123813	0.00459	
Total	39	0.36998		

$$SE_{\bar{x}} = 0.0677$$

$$SE_{Ex} = 0.0338$$

95% Confidence Limits for points plotted on graph = ± 0.069

Appendix 35

GA3-like activity of a TLC plate zone for mature leaf tissue extract.

Extract Dilution	Absorbance 625 nm			Mean
	I	II	III	
Control	0.367	0.395	0.359	0.374
Healthy 1	0.385	0.337	0.417	0.380
Healthy $1/5$	0.359	0.374	0.406	0.380
Healthy $1/25$	0.398	0.310	0.340	0.349
Healthy $1/125$	0.314	0.380	0.299	0.331
Infected 1	0.435	0.337	0.409	0.394
Infected $1/5$	0.444	0.444	0.303	0.397
Infected $1/25$	0.359	0.352	0.357	0.356
Infected $1/125$	0.340	0.301	0.392	0.344

Analysis of Variance

Source of Variation	d.f.	S.S.	M.S.	F ratio
Reps	2	0.001708	0.00085	1
Extract Dilutions	8	0.01266	0.00158	1
Error	16	0.03372	0.002108	
Total	26	0.048087		

SE = 0.0459

SE_x = 0.0265

95% Confidence Limits of points plotted on graph = \pm 0.056

Appendix 36

Response of the barley endosperm bioassay to a dilution series of abscisic acid.

ABA Concentration (mg/ml)	Absorbance 625 nm				
	I	II	III	IV	Mean
GA3 Control	0.857	1.073	1.005	1.073	1.002
2×10^{-6}	0.444	0.409	0.359	0.380	0.398
4×10^{-7}	0.367	0.417	0.573	0.472	0.457
8×10^{-8}	0.847	0.821	0.740	0.778	0.797
1.6×10^{-8}	1.106	1.053	1.023	0.849	1.008
3.2×10^{-9}	0.991	1.073	0.941	0.950	0.989
6.4×10^{-10}	1.009	1.168	0.877	0.982	1.009
1.28×10^{-10}	0.945	1.045	1.020	1.094	1.026

Analysis of Variance

Source of Variation	d.f.	S.S.	M.S.	F ratio
Reps	3	0.02339	0.007796	1.13 N.S.
ABA Concentrations	7	1.93308	0.27615	40 **
Error	21	0.144912	0.0069	
Total	31	2.10138		

SE = 0.0831

SE_x = 0.0416

95% Confidence Limits of points plotted on graph = \pm 0.086

Appendix 37

ABA-like activity of a TLC plate zone (Rf 0.15-0.30) following two separations of mature leaf extract in TEA solvent.

Extract Dilution	Absorbance 625 nm			
	I	II	III	Mean
GA3 Control	1.153	1.301	1.276	1.243
Healthy $1/2$	0.387	0.362	0.400	0.383
Healthy $1/8$	0.426	0.523	0.451	0.467
Healthy $1/20$	0.982	1.305	0.991	1.093
Healthy $1/50$	1.409	1.420	1.278	1.369
Infected $1/2$	0.485	0.382	0.233	0.367
Infected $1/8$	0.890	0.909	0.956	0.918
Infected $1/20$	1.438	1.301	1.158	1.299
Infected $1/50$	1.472	1.444	1.372	1.429
Sterile Water Control	0.450	0.450	0.352	0.417

Analysis of Variance

Source of Variation	d.f.	S.S.	M.S.	F ratio
Reps	2	0.04495	0.02248	2.91 N.S.
Plate Zone Dilutions	9	5.3614	0.5957	77 **
Error	18	0.138915	0.007718	
Total	29	5.5453		

SE = 0.0878
SE \bar{x} = 0.0507

95% Confidence Limits of points plotted on graph = \pm 0.106

Appendix 38

ABA-like activity, following separation in pure solvent systems, in mature leaf tissue extracts.

Extract Dilution	Absorbance 625 nm			
	I	II	III	Mean
GA3 Control	1.183	1.221	1.012	1.139
Healthy $1/10$	0.312	0.429	0.364	0.368
Healthy $1/50$	0.903	0.877	0.799	0.860
Healthy $1/250$	1.138	1.073	1.042	1.084
Healthy $1/1250$	1.124	1.074	1.102	1.100
Infected $1/10$	0.367	0.498	0.253	0.373
Infected $1/50$	1.027	1.042	1.138	1.069
Infected $1/250$	1.183	1.216	1.153	1.184
Infected $1/1250$	1.183	1.098	1.173	1.151

Analysis of Variance

Source of Variation	d.f.	S.S.	M.S.	F ratio
Reps	2	0.01468	0.00743	1.643
Plate Zone Dilutions	8	2.5798	0.3225	71 **
Error	16	0.07234	0.00452	
Total	26	2.66697		

$$SE_{\bar{}} = 0.0672$$

$$SE_{Ex} = 0.0388$$

95% Confidence Limits of points plotted on graph = ± 0.082

Appendix 39

Standard response curve data for kinetin induced betacyanin production by Amaranthus caudatus explants.

Kinetin Concentration (gm/ml)	Betacyanin Level [Abs. (542-620) nm]		Mean Abs. (542-620) nm
	I	II	
0	0.042	0.032	0.037
2×10^{-9}	0.034	0.031	0.033
2×10^{-8}	0.047	0.063	0.055
2×10^{-7}	0.134	0.159	0.147
2×10^{-6}	0.116	0.162	0.139

Analysis of Variance

Source of Variation	d.f.	S.S.	M.S.	F ratio
Reps	1	0.00055	0.00055	2.2 N.S.
Kinetin Concentrations	4	0.02523	0.00631	25 **
Error	4	0.00101	0.00025	
Total	9	0.02678		

$$SE = 0.016$$

$$SE_x = 0.0112$$

05% Confidence Limits for graph points = ± 0.031

Appendix 40

Cytokinin activity of TLC plate zones for n-butanol fraction of young leaf tissue extract.

Absorbance (542-620) nm		
Plate Zone (Rf)	Healthy Extract	Virus Infected Extract
Control	0.0147	0.0173
0 - 0.1	0.0301	0.0350
0.1 - 0.2	0.0145	0.0170
0.2 - 0.3	0.0202	0.0215
0.3 - 0.4	0.0190	0.0111
0.4 - 0.5	0.0179	0.0157
0.5 - 0.6	0.0213	0.0393
0.6 - 0.7	0.0343	0.0381
0.7 - 0.8	0.0213	0.0168
0.8 - 0.9	0.0179	0.0158
0.9 - 1.0	0.0167	0.0158

<u>Analysis of Variance</u>				
Source of Variation	d.f.	S.S.	M.S.	F ratio
Virus Status	1	0.000011	0.000011	0.5
Plate Zone	10	0.00115	0.000115	5.127
Error	10	0.00022	0.000022	
Total	21	0.000224		

SE = 0.0047

Appendix 41

Cytokinin activity of TLC plate zones for the water soluble fraction of young leaf tissue extract.

Absorbance (542-620) nm		
Plate Zone (Rf)	Healthy Extract	Virus Infected Extract
Control	0.0168	0.0137
0 - 0.1	0.0183	0.0218
0.1 - 0.2	0.0223	0.0208
0.2 - 0.3	0.0170	0.0180
0.3 - 0.4	0.0155	0.0144
0.4 - 0.5	0.0144	0.0144
0.5 - 0.6	0.0168	0.0168
0.6 - 0.7	0.0158	0.0228
0.7 - 0.8	0.0180	0.0192
0.8 - 0.9	0.0205	0.0158
0.9 - 1.0	0.0180	0.0169

Analysis of Variance

Source of Variation	d.f.	S.S.	M.S.	F ratio
Plate Zones	10	0.00016	0.000016	3.2
Virus Status	1	0.00000007	0.00000007	1
Error	10	0.00004996	0.000005	
Total	21	0.002099		

SE = 0.0022

Appendix 42

Cytokinin activity of tissue extract dilutions for n-Butanol fraction of young leaf tissue extract.

Extract Dilution	Absorbance (542-620) nm			
	I	II	III	Mean
Control	0.0225	0.0202	0.0283	0.0237
Healthy ¹ / ₂₅	0.0249	0.0321	0.0331	0.0300
Healthy ¹ / ₁₂₅	0.0309	0.0214	0.0283	0.0269
Healthy ¹ / ₆₂₅	0.0296	0.0249	0.0271	0.0272
Infected ¹ / ₂₅	0.0438	0.0395	0.0517	0.0450
Infected ¹ / ₁₂₅	0.0296	0.0274	0.0377	0.0316
Infected ¹ / ₆₂₅	0.0250	0.0250	0.0343	0.0281

Analysis of Variance

Source of Variation	d.f.	S.S.	M.S.	F ratio
Reps	2	0.000187	0.000093	7.96 **
Virus Status	6	0.000864	0.000144	12.29 **
Error	12	0.000141	0.0000117	
Total	20	0.00119		

SE = 0.0034

SE_x = 0.0020

Appendix 43

Cytokinin activity of TLC plate zones for the n-Butanol soluble fraction of mature leaf tissue extract

Absorbance (542-620) nm		
Plate Zone (Rf)	Healthy Extract	Virus Infected Extract
Control	0.0159	0.0168
0 - 0.1	0.0195	0.0275
0.1 - 0.2	0.0222	0.0254
0.2 - 0.3	0.0169	0.0240
0.3 - 0.4	0.0169	0.0227
0.4 - 0.5	0.0145	0.0238
0.5 - 0.6	0.0225	0.0285
0.6 - 0.7	0.0202	0.0261
0.7 - 0.8	0.0146	0.0238
0.8 - 0.9	0.0144	0.0262
0.9 - 1.0	0.0157	0.0239

Analysis of Variance

Source of Variation	d.f.	S.S.	M.S.	F ratio
Plate Zones	10	0.0000965	0.0000097	2.13
Virus Status	1	0.000258	0.000258	57 **
Error	10	0.0000453	0.0000045	
Total	21	0.0004003		

SE = 0.0021

Appendix 44

Cytokinin activity of extract dilutions for the n-butanol soluble fraction of mature leaf tissue extract.

Extract Dilution	Absorbance (542-620) nm			
	I	II	III	Mean
Control	0.0542	0.0572	0.0543	0.0552
Healthy ¹ / ₅	0.0789	0.0718	0.0731	0.0746
Healthy ¹ / ₂₅	0.0697	0.0608	0.0608	0.0638
Healthy ¹ / ₁₂₅	0.0502	0.0649	0.0568	0.0573
Infected ¹ / ₅	0.0529	0.0597	0.0634	0.0587
Infected ¹ / ₂₅	0.0542	0.0645	0.0506	0.0564
Infected ¹ / ₁₂₅	0.0641	0.0607	0.0578	0.0609

Analysis of Variance

Source of Variation	d.f.	S.S.	M.S.	F ratio
Reps	2	0.00004	0.00002	1
Extract Dilution	6	0.000827	0.000138	4.82 *
Error	12	0.000343	0.0000286	
Total	20	0.0012099		

SE = 0.0053

SE_x = 0.0031

Appendix 45

Cytokinin activity of TLC plate zones for the water soluble fraction of mature leaf tissue extract.

Absorbance (542-620) nm		
Plate Zone (Rf)	Healthy Extract	Virus Infected Extract
Control	0.0171	0.0195
0 - 0.1	0.0206	0.0241
0.1 - 0.2	0.0267	0.0241
0.2 - 0.3	0.0230	0.0228
0.3 - 0.4	0.0251	0.0228
0.4 - 0.5	0.0217	0.0181
0.5 - 0.6	0.0227	0.0203
0.6 - 0.7	0.0169	0.0215
0.7 - 0.8	0.0262	0.0249
0.8 - 0.9	0.0205	0.0214
0.9 - 1.0	0.0158	0.0192

Analysis of Variance

Source of Variation	d.f.	S.S.	M.S.	F ratio
Plate Zones	10	0.000126	0.0000126	2.97
Virus Status	1	0.0000003	0.0000003	1
Error	10	0.000042	0.0000042	
Total	21	0.000168		

$$SE = 0.0021$$

Appendix 46

Cytokinin activity of extract dilutions for the water soluble fraction of mature leaf tissue extract.

Extract Dilution	Absorbance (542-620) nm			
	I	II	III	Mean
Control	0.0228	0.0239	0.0275	0.0247
Healthy $1/5$	0.0242	0.0215	0.0219	0.0225
Healthy $1/25$	0.0254	0.0214	0.0203	0.0224
Healthy $1/125$	0.0251	0.0237	0.0230	0.0239
Infected $1/5$	0.0218	0.0169	0.0180	0.0189
Infected $1/25$	0.0238	0.0266	0.0251	0.0252
Infected $1/125$	0.0227	0.0263	0.0275	0.0255

Analysis of Variance

Source of Variation	d.f.	S.S.	M.S.	F ratio
Reps	2	0.0000022	0.0000011	0.2
Extract Dilutions	6	0.000095	0.000016	3.134 *
Error	12	0.0000605	0.00000504	
Total	20	0.000157		

$$SE = 0.0022$$

$$SE_x = 0.0013$$

Appendix 47

Cytokinin activity of TLC plate zones for the n-butanol soluble fraction of root tissue extract.

Plate Zone (Rf)	Absorbance (542-620) nm	
	Healthy Extract	Virus Infected Extract
Control	0.0234	0.0233
0 - 0.1	0.0241	0.0217
0.1 - 0.2	0.0192	0.0169
0.2 - 0.3	0.0191	0.0192
0.3 - 0.4	0.0158	0.0135
0.4 - 0.5	0.0285	0.0262
0.5 - 0.6	0.0252	0.0274
0.6 - 0.7	0.0191	0.0203
0.7 - 0.8	0.0146	0.0203
0.8 - 0.9	0.0180	0.0273
0.9 - 1.0	0.0158	0.0204

Analysis of Variance

Source of Variation	d.f.	S.S.	M.S.	F ratio
Plate Zones	10	0.000547	0.000055	7.24
Virus Status	1	0.0000085	0.0000085	1.12
Error	10	0.0000755	0.00000755	
Total	21	0.00063		

SE = 0.0027

Appendix 48

Cytokinin activity of TLC plate zones for the water soluble fraction of root tissue extract.

Absorbance (542-620) nm		
Plate Zone (Rf)	Healthy Extract	Virus Infected Extract
Control	0.0184	0.0233
0 - 0.1	0.0205	0.0266
0.1 - 0.2	0.0202	0.0227
0.2 - 0.3	0.0227	0.0215
0.3 - 0.4	0.0260	0.0274
0.4 - 0.5	0.0238	0.0215
0.5 - 0.6	0.0249	0.0250
0.6 - 0.7	0.0202	0.0296
0.7 - 0.8	0.0202	0.0191
0.8 - 0.9	0.0203	0.0202
0.9 - 1.0	0.0202	0.0237

<u>Analysis of Variance</u>				
Source of Variation	d.f.	S.S.	M.S.	F ratio
Plate Zones	10	0.000179	0.0000179	2.77
Virus Status	1	0.0000245	0.0000245	3.97
Error	10	0.0000645	0.0000065	
Total	21	0.000268		

SE = 0.0025

Appendix 49

Response of the barley coleoptile straight growth bioassay to standard solutions of IAA and chromatogrammed young tissue extracts.

IAA Concentrations (mg/ml) and Plant Extract Dilutions	Mean Coleoptile Length (mm) per dish		
	I	II	Mean
Zero Control	11.58	11.32	11.45
0.01 ppm IAA	11.44	11.86	11.65
0.10 ppm IAA	11.62	12.28	11.95
1.00 ppm IAA	12.40	12.51	12.46
10 ppm IAA	12.86	13.49	13.18
Healthy Extract $1/10$	11.31	11.30	11.31
Healthy Extract $1/50$	11.40	11.75	11.58
Healthy Extract $1/250$	11.49	11.79	11.64
Infected Extract $1/10$	10.95	11.57	11.26
Infected Extract $1/50$	11.58	11.49	11.54
Infected Extract $1/250$	11.83	11.81	11.82

Analysis of Variance

Source of Variation	d.f.	S.S.	M.S.	F ratio
Reps	1	0.33382	0.33382	6.504 *
[IAA] and Extract Dil'ns	10	6.34121	0.63412	12.36 **
Error	10	0.51323	0.5132	
Total	21	7.18826		

$$SE_{\bar{x}} = 0.2265$$

$$SE_x = 0.1602$$

95% Confidence Limits of points plotted on graph = ± 0.357

Appendix 50

Araldite Composition

Araldite M	10.8 ml
Araldite HY964 (Hardener)	9.2 ml
DY064 (Accelerator)	0.16 ml
Di-n Butyl phthalate (Plasticiser)	0.75 ml

Mix thoroughly for 5 minutes and store at -20°C until used.

Appendix 51

Reynold's Lead Citrate

In a 50 ml volumetric flask, dissolve 1.33 gm lead nitrate and 1.76 gm sodium citrate into 30 ml freshly boiled and cooled distilled water. Shake intermittently and vigorously for 30 minutes to produce a white precipitate. Add 8.0 ml of 1N sodium hydroxide, dilute to 50 ml with preboiled water and mix until precipitate dissolves. Keep stoppered and discard when a noticeable white precipitate occurs.